**Télécom Paris (ENST)**
**Institut Eurécom**

# THESE

Présentée pour Obtenir le Grade de Docteur
de l'Ecole Nationale Supérieure
des Télécommunications

Spécialité: Communication et Electronique

**Rubén de Francisco Martín**

# Optimisation de la Performance des Systèmes MIMO avec Connaissance Partielle du Canal

Soutenue le 29 Février 2008 devant le jury composé de:

| | |
|---|---|
| Jean-Claude Belfiore | Président |
| Miguel Angel Lagunas Hernández | Rapporteurs |
| Geir E. Øien | |
| Geert Leus | Examinateurs |
| Raymond Knopp | |
| Dirk T.M. Slock | Directeur de Thèse |

**Télécom Paris (ENST)**
**Institut Eurécom**

# THESIS

In Partial Fulfillment of the Requirements
for the Degree of Doctor of Philosophy
from Ecole Nationale Supérieure
des Télécommunications

Specialization: Communication and Electronics

**Rubén de Francisco Martín**

# Performance Optimization of MIMO Systems with Partial Channel State Information

Defended on February 29, 2008 before the committee
composed of:

| | |
|---|---|
| Jean-Claude Belfiore | President |
| Miguel Angel Lagunas Hernández | Rapporteurs |
| Geir E. Øien | |
| Geert Leus | Examiners |
| Raymond Knopp | |
| Dirk T.M. Slock | Thesis supervisor |

# Acknowledgments

I would like to thank Prof. Dirk Slock, my thesis supervisor, for his support and guidance during the years I spent at Institut Eurécom.

I am grateful to Prof. Geert Leus and Prof. Ying-Chang Liang for welcoming me into their research groups, in Delft and Singapore, during the elaboration of this thesis.

I would also like to thank Prof. David Gesbert for his continuous help and guidance.

I will always keep wonderful memories of these past years at Eurécom and my stay in France. I had the chance to meet great colleagues and collaborators, but mostly, great friends.

Lastly, I would like to thank my family and my wife, Anna, for their sincere love and unconditional support, before, during, and after my PhD studies.

February 29, 2008
Ruben de Francisco
Sophia Antipolis

# Abstract

Multiple-input multiple-output (MIMO) wireless communication systems have the potential to offer high data rates as well as link reliability. Over the past years, MIMO systems have been regarded as firm candidates for future mobile communication standards, both in single user and multiuser modes of operation. The feasibility of these systems in future standards depends in great measure on the ability to provide high rates with a reduced amount of channel state information at the transmitter (CSIT), due to limited resource availability on the feedback link. This thesis addresses the problem of optimizing MIMO wireless communication systems with partial CSIT. On the one hand, we focus on how to design methods for obtaining CSIT, identifying what types of CSIT are relevant. On the other hand, we propose techniques to exploit the available sources of CSIT to optimize the system performance.

In the first part, point-to-point MIMO channels are considered for the purpose of error rate minimization. Linear precoding techniques are proposed to enhance the performance of space-time coded (STC) MIMO systems, based on statistical information on the MIMO channel. As we show, the performance of such systems can be significantly improved by appropriately combining mean and covariance information.

In the second part of this thesis, we focus on sum-rate performance optimization in MIMO broadcast channels with limited feedback. Low-complexity cross-layer approaches are proposed for systems with joint linear beamforming and multiuser scheduling, optimizing the following parts in the MIMO communications system: linear beamforming techniques, scheduling algorithms, feedback strategies and feedback quantization techniques.

Different feedback models are considered. In a simple scenario where feedback consists of only channel quantization indices, we study the benefits of generating quantization codebooks adapted to the channel statistics, exploiting spatial and temporal correlations. A different feedback model con-

siders separate feedback for channel direction information (CDI) and channel quality information (CQI). In such systems, the users need to estimate the amount of multiuser interference, which is a difficult task since the users can not cooperate. We propose a design framework for scalar CQI feedback design in MIMO broadcast channels, based on an estimate on each user's signal-to-interference-plus-noise ratio (SINR). The proposed scalar feedback encapsulates relevant information, such as the channel gain, the quantization error, the orthogonality constraints between beamforming vectors and the number of active beams. A comparative study between space division multiple access (SDMA) and time division multiple access (TDMA) is provided in different asymptotic regimes, showing the cases in which SDMA becomes more beneficial than TDMA in terms of sum-rate performance and viceversa. In addition, a more realistic system is considered in which each user has a sum rate feedback constraint. In this scenario, the existing tradeoff between multiuser diversity and multiplexing gain is identified, arising from the fact that the available feedback bits need to be shared for CDI and CQI quantization.

The problem of designing linear beamforming techniques for MIMO broadcast channels is also addressed. An iterative optimization method for unitary beamforming is proposed, which achieves linear sum-rate growth with the number of transmit antennas if full CSIT is available. The proposed technique exhibits robustness to channel estimation errors, providing better sum rates than zero-forcing (ZF) beamforming and even minimum mean-square error (MMSE) beamforming as the variance of the estimation error increases. Our work highlights the importance of linear beamforming optimization in limited feedback scenarios. Rather than designing sophisticated feedback schemes, relying on simple linear beamforming techniques, the system performance can be improved by using simple channel quantization strategies combined with optimized linear beamforming techniques robust to CSIT errors.

# Contents

Acknowledgments . . . . . 1
Abstract . . . . . 3
List of Figures . . . . . 9
List of Tables . . . . . 13
Acronyms . . . . . 15
Notation . . . . . 17
Résumé en Français . . . . . 19

**1 Introduction** **43**
1.1 Thesis Overview and Outline . . . . . 44
1.1.1 Point-to-Point MIMO Channels . . . . . 44
1.1.2 MIMO Broadcast Channels . . . . . 45
1.2 Contributions . . . . . 49

**I Point-to-Point MIMO Channels** **51**

**2 Linear Precoding** **53**
2.1 Introduction . . . . . 54
2.2 MIMO Channel Model . . . . . 55
2.3 System Description . . . . . 56
2.4 Partial CSIT Combining Mean and Covariance . . . . . 56
2.5 Linear Precoding for Error Rate Minimization . . . . . 58
2.5.1 Zero Mean Information . . . . . 61
2.5.2 Unit Rank Mean . . . . . 61
2.5.3 Singular Covariance Information . . . . . 62
2.6 Simulation Results . . . . . 63
2.7 Conclusions . . . . . 64
2.A Derivation of Posterior Ditribution . . . . . 66

2.B Proof of Theorem 2.1 . . . . . 66
2.C Proof of Corollary 2.1 . . . . . 67

**II MIMO Broadcast Channels 69**

**3 Joint Linear Beamforming and Multiuser Scheduling 71**
3.1 Introduction . . . . . 72
3.2 System Model . . . . . 74
3.3 Linear Beamforming Techniques . . . . . 76
3.4 Multiuser Scheduling Algorithms . . . . . 77
3.5 Full CSIT Case: A Low-Complexity Approach . . . . . 80
3.5.1 Motivation . . . . . 80
3.5.2 System Assumptions . . . . . 81
3.5.3 Proposed User Selection Algorithms . . . . . 82
3.5.4 Performance Analysis . . . . . 86
3.5.5 Numerical Results . . . . . 89
3.5.6 Discussion . . . . . 91
3.6 Partial CSIT Case: A Low-Complexity Approach . . . . . 91
3.6.1 Motivation . . . . . 91
3.6.2 System Assumptions . . . . . 92
3.6.3 Proposed Algorithm . . . . . 92
3.6.4 Bound on the Multiuser Interference . . . . . 95
3.6.5 Numerical Results . . . . . 96
3.6.6 Discussion . . . . . 97
3.7 Conclusions . . . . . 98
3.A Computation of Multiuser Interference Bounds . . . . . 99

**4 A Design Framework for Scalar Feedback 101**
4.1 Introduction . . . . . 102
4.2 System Model . . . . . 103
4.3 Linear Beamforming with Limited Feedback . . . . . 104
4.4 Scalar Feedback Design . . . . . 106
4.5 Sum-Rate Function . . . . . 111
4.6 Study of Extreme Regimes . . . . . 115
4.6.1 Large Number of Users . . . . . 116
4.6.2 High SNR Regime . . . . . 117
4.6.3 Low SNR Regime . . . . . 119

4.7 Multiuser Diversity - Multiplexing Tradeoff . . . . . 121
4.7.1 Finite Sum Rate Feedback Model . . . . . 122
4.7.2 Problem Formulation . . . . . 124
4.7.3 Simplified Approach: Decoupled Feedback Optimization 126
4.8 Numerical Results . . . . . 127
4.8.1 Effect of Scalar Feedback Quantization . . . . . 130
4.9 Conclusions . . . . . 132
4.A Proof of Proposition 4.1 . . . . . 135
4.B Proof of Theorem 4.1 . . . . . 137

**5 Optimization of Channel Quantization Codebooks 139**
5.1 Introduction . . . . . 140
5.2 System Description . . . . . 142
5.2.1 Linear Beamforming . . . . . 142
5.2.2 User Selection . . . . . 143
5.3 Exploiting Spatial Correlations . . . . . 143
5.3.1 Channel Model . . . . . 143
5.3.2 Codebook Design . . . . . 145
5.3.3 Distortion Measure . . . . . 147
5.3.4 Optimization Procedure . . . . . 148
5.3.5 Practical Considerations . . . . . 148
5.4 Exploiting Temporal Correlations . . . . . 149
5.4.1 Channel Model . . . . . 149
5.4.2 Predictive Vector Quantization . . . . . 149
5.4.3 Codebook Design . . . . . 150
5.4.4 Prediction Function . . . . . 151
5.5 Numerical Results . . . . . 153
5.5.1 Spatially Correlated Channels . . . . . 154
5.5.2 Temporally Correlated Channels . . . . . 155
5.6 Conclusions . . . . . 156

**6 Linear Beamforming Design 157**
6.1 Introduction . . . . . 158
6.2 System Model . . . . . 159
6.2.1 Multi-antenna Receivers . . . . . 160
6.2.2 Single-antenna Receivers . . . . . 160
6.2.3 Imperfect CSIT Model . . . . . 161
6.3 Problem Formulation . . . . . 161

6.3.1 Multi-antenna Receivers . . . . . 161
6.3.2 Single-antenna Receivers . . . . . 163
6.4 Algorithm Description . . . . . 165
6.4.1 Practical Considerations . . . . . 168
6.5 Convergence . . . . . 168
6.6 Complexity Analysis . . . . . 170
6.7 Performance Evaluation . . . . . 172
6.7.1 Case $K = M$, Perfect CSIT . . . . . 172
6.7.2 Case $K = M$, Imperfect CSIT . . . . . 174
6.7.3 Case $K \geq M$, Limited Feedback . . . . . 175
6.8 Conclusions . . . . . 179
6.A Computation of Polynomial Coefficients . . . . . 180

**General Conclusion** **183**

# List of Figures


1 PEP en fonction du SNR pour différents niveaux de CSIT, $\rho = 0.9$ and $\gamma = 40\%$ . . . . . 23

2 Comparaison des résultats analyse-simulation de la borne inférieure sur la somme des débits en utilisant la métrique III, pour $M = 2$ antennes, $K = 15$ utilisateurs, SNR = 10 dB et $B = 1$ bit. . . . . 29

3 Somme des débits obtenue par différentes approches de feedback en fonction du nombre d'utilisateurs, pour $B = 9$ bits, $M = 3$ antennes au transmetteur et SNR = 10 dB. . . . . 30

4 Somme des débits obtenue par différentes approches de feedback en fonction de SNR moyen, pour $B = 9$ bits, $M = 3$ antennes et $K = 10$ utilisateurs. . . . . 31

5 Somme des débits en fonction du nombre d'utilisateurs pour $M = 2$ et SNR = 10 dB. . . . . 32

6 Somme des débits en fonction du nombre d'utilisateurs dans un canal corrélé spatialement, $M = 2$ antennes et SNR = 10 dB. 33

7 Somme des débits en fonction du nombre d'utilisateurs avec un canal corrélé temporellement, $M = 2$ antennes et SNR = 10 dB. 34

8 Somme des débits en fonction du nombre de rotations de plans (itérations de l'algorithme) pour différents nombres d'antennes au transmetteur, $K = M$ utilisateurs et SNR = 10 dB. . . . . 36

9 Somme des débits en fonction du nombre d'antennes $M$ pour $K = M$ utilisateurs et SNR = 10 dB. . . . . 37

10 Somme des débits en fonction de la variance de l'erreur d'estimation du canal pour $M = 4, 8$ antennes, $K = M$ utilisateurs et SNR = 10 dB. . . . . 38

11 Somme des débits en fonction du nombre d'utilisateurs dans un système avec beamforming linéaire et sélection d'utilisateurs, $M = 4$ antennes, SNR = 10 dB, et $B = 10$ bits sur la voie de retour. . . . . 39
12 Somme des débits en fonction de SNR moyen dans un système avec beamforming linéaire et sélection d'utilisateurs, $M = 4$ antennes, $K = 10$ utilisateurs, et $B = 10$ bits sur la voie de retour. . . . . 40

2.1 PEP vs. SNR for different CSIT levels, $\rho = 0.9$ and $\gamma = 40\%$ . 64
2.2 PEP vs. SNR for different CSIT levels, $\rho = 0.9$ and $\gamma = 20\%$ . 65

3.1 Sum rate as a function of the SNR for $M = 2, 4$ transmit antennas and $K = M$ users. . . . . 88
3.2 Sum rate as a function of the number of users for $M = 2$ transmit antennas, and average SNR = 0 dB. . . . . 89
3.3 Sum rate comparison of suboptimal beamforming approaches as a function of the number of users for $M = 2$ transmit antennas, for a) average SNR = 0 dB (below) and b) average SNR = 10 dB (above). . . . . 90
3.4 Sum rate as a function of the number of users for $M = 2$ transmit antennas, and $\sigma_\theta = 0.1\pi$. . . . . 97
3.5 Sum rate as a function of angle spread for $M = 2$ transmit antennas, antenna spacing $d = 0.4\lambda$ and $K = 100$ users. . . . . 98

4.1 Approximated lower bound on the sum rate using Metric I versus the alignment ($\cos\theta_k$) for $M = 4$ antennas, variable number of active beams $M_o$, orthogonality factor $\epsilon = 0.1$ and SNR = 10 dB. . . . . 112
4.2 Sum-rate function using Metric I versus orthogonality factor $\epsilon$ and number of active beams $M_o$, for $K = 35$ users, SNR = 10 dB and $B = 1$ bit. . . . . 115
4.3 Comparison of analytical and simulated lower bounds on the sum rate using Metric III, for $M = 2$ antennas, $K = 15$ users, SNR = 10 dB and $B = 1$ bit. . . . . 116
4.4 Simulated lower bound on the sum rate using Metric III as a function of the orthogonality factor $\epsilon$ for large $K$. . . . . 118
4.5 Finite sum rate feedback model. . . . . 123

4.6 Comparison of simulated lower bound on the sum rate using Metric III, and actual sum rates obtained with second step of feedback and full CSIT. $M = 2$ antennas, $K = 10$ users, SNR $= 20$ dB and $B = 1$ bit. . . . . 128
4.7 Sum rate achieved by different feedback approaches as a function of the number of users, for $B = 9$ bits, $M = 3$ transmit antennas and average SNR = 10 dB. . . . . 129
4.8 Sum rate achieved by different feedback approaches versus average SNR, for $B = 9$ bits, $M = 3$ transmit antennas and $K = 10$ users. . . . . 130
4.9 Sum rate vs. number of users for $M = 2$ and SNR = 10 dB. . 131
4.10 Sum rate vs. number of users for $M = 2$ and SNR = 20 dB. . 132
4.11 Sum rate vs. number of users in a system with optimal $B_1/B_2$ balancing for different SNR values. . . . . 133

5.1 Broadcast channel model with mobile stations (MS) surrounded by local scatterers grouped in clusters, located in different mean angles of departure (AoD) with respect to uniform linear array (ULA) broadside. . . . . 146
5.2 Sum rate for different number of users in a spatially correlated channel, $M = 2$ transmit antennas and SNR = 10 dB. . . . . 153
5.3 Sum rate for different SNR values in a spatially correlated channel, $M = 2$ transmit antennas and $K = 10$ users. . . . . 154
5.4 Sum rate for different number of users in a temporally correlated channel, $M = 2$ transmit antennas and SNR = 10 dB. . 155

6.1 Sum rate as a function of the number of plane rotations (algorithm iterations) for different number of transmit antennas, $K = M$ users and average SNR = 10 dB. . . . . 169
6.2 Convergence of unitary beamforming matrix for different number of transmit antennas. . . . . 171
6.3 Sum rate as a function of the number of antennas $M$ for $K = M$ users and average SNR = 10 dB. . . . . 173
6.4 Sum rate as a function of the average SNR for $M = 8$ transmit antennas and $K = M$ users. . . . . 174
6.5 Sum rate as a function of the channel estimation error variance for $M = 4, 8$ transmit antennas, $K = M$ users and average SNR = 10 dB. . . . . 175

6.6 Sum rate as a function of the number of users in a system with joint beamforming and user scheduling, $M = 4$ transmit antennas, SNR = 10 dB, and $B = 10$ feedback bits. . . . . 177
6.7 Sum rate as a function of the average SNR in a system with joint beamforming and user scheduling, $M = 4$ transmit antennas, $K = 10$ users, and $B = 10$ feedback bits. . . . . 178

# List of Tables


1 Algorithme de Sélection d'Utilisateurs . . . . . 27
2 Méthode d'Optimisation Itérative pour Beamforming Unitaire 35

3.1 Outline of G-SUS Algorithm . . . . . 78
3.2 Outline of G-US Algorithm . . . . . 79
3.3 Outline of Scheduling Algorithm A . . . . . 83
3.4 Outline of Scheduling Algorithm B . . . . . 85
3.5 Outline of Proposed Low-Complexity Approach . . . . . 94

4.1 Outline of Scheduling Algorithm with Variable Number of Active Beams . . . . . 106

5.1 Parameters of Broadcast Channel Model . . . . . 144

6.1 Outline of the Unitary Beamforming Optimization Procedure . 165
6.2 Auxiliary Variables for the Computation of Polynomial Coefficients . . . . . 181

# Acronyms

Here are the main acronyms used in this dissertation. The meaning of an acronym is usually indicated once, when it first occurs in the text.

| | |
|---|---|
| AoD | Angle of Departure |
| AWGN | Additive White Gaussian Noise |
| BER | Bit Error Rate |
| BS | Base Station |
| cdf | cumulative distribution function |
| CSI | Channel State Information |
| CSIR | Channel State Information at Receiver |
| CSIT | Channel State Information at Transmitter |
| CSR | Capacity Scaling Ratio |
| DPC | Dirty-Paper Coding |
| i.i.d. | independent and identically distributed |
| ISI | Inter Symbol Interference |
| FER | Frame Error Rate |
| LF-OSDMA | Limited Feedback Orthogonal Space Division Multiple Access |
| LOS | Line of Sight |
| LU | Lower-Upper |
| TxMF | Transmit Matched Filter |
| MIMO | Multiple-Input Multiple-Output |
| ML | Maximum Likelihood |
| MMSE | Minimum Mean-Square Error |
| MS | Mobile Station |
| NR | Newton-Raphson |
| OLBF | Orthogonal Linear Beamforming |
| OSDMA | Orthogonal Space Division Multiple Access |
| PAS | Power Angular Spread |

| | |
|---|---|
| pdf | probability density function |
| PEP | Pairwise Error Probability |
| PSD | Positive Semidefinite |
| QD | Quotient-Difference |
| QoS | Quality of Service |
| RBF | Random Beamforming |
| SDMA | Space Division Multiple Access |
| SINR | Signal-to-Interference-plus-Noise Ratio |
| SISO | Single-Input Single-Output |
| SNR | Signal-to-Noise Ratio |
| ST | Space-Time |
| STC | Space-Time Code |
| TDMA | Time Division Multiple Access |
| UT | User Terminal |
| ZF | Zero Forcing |

# Notation

Here is a list of the main notations and symbols used in this document. We have tried to keep consistent notations throughout the document, but some symbols have different definitions depending on when they occur in the text.

| | |
|---|---|
| $\mathbb{C}$ | Set of complex numbers |
| $x$ | Scalar variable |
| $\mathbf{x}$ | Vector variable |
| $\mathbf{X}$ | Matrix variable |
| $\lvert x \rvert$ | Amplitude of scalar $x$ |
| $\angle(x)$ | Phase of scalar $x$ |
| $\lVert \mathbf{x} \rVert$ | Euclidean norm of the vector $\mathbf{x}$ |
| $\lVert \mathbf{X} \rVert_F$ | Frobenius norm of the matrix $\mathbf{X}$ |
| $\angle(\mathbf{x}, \mathbf{y})$ | Angle between vectors $\mathbf{x}$ and $\mathbf{y}$ |
| $\mathbf{0}$ | All-zero vector |
| $\mathbf{I}_m$ | Identity matrix of dimension $m \times m$ |
| $(\cdot)^*$ | Complex conjugate operator |
| $(\cdot)^T$ | Transpose operator |
| $(\cdot)^H$ | Hermitian transpose operator |
| $\otimes$ | Kronecker product |
| $\mathrm{tr}(\cdot)$ | Trace operator |
| $\det(\mathbf{X})$ | Determinant of the matrix $\mathbf{X}$ |
| $diag(\mathbf{X})$ | Diagonal matrix of the diagonal elements of the matrix $\mathbf{X}$ |
| $vect(\mathbf{X})$ | Vectorization of the matrix $\mathbf{X}$ |
| $\mathbb{E}(\cdot)$ | Expectation operator |
| $\mathcal{Q}(\cdot)$ | Scalar quantization function |
| $I(X;Y)$ | Mutual information between random variables $X$ and $Y$ |
| $M$ | Number of transmit antennas |
| $N$ | Number of receive antennas |
| $M_o$ | Number of active beams |

| | |
|---|---|
| $\epsilon$ | Orthogonality factor |
| $P$ | Total transmit power |
| $\sigma^2$ | AWGN noise variance |
| $K$ | Number of user terminals |
| $B$ | Number of feedback bits per user |
| $\mathcal{S}$ | User set |
| $\mathcal{G}$ | Set of all possible subsets of user sets |
| $L$ | Number of multipath components |
| $d$ | Antenna spacing at the base station |
| $\lambda$ | Wavelength |
| $\sigma_\theta$ | Angular spread |
| $f_D$ | Doppler spread |
| $T_f$ | Frame length |

# Résumé

Les systèmes de communication multi-antennaires à émission et réception (MIMO) sans fil ont le potentiel d'offrir hauts débits et fiabilité. La faisabilité de cette technologie dans des systèmes de communication mobiles dépend dans une large mesure de la capacité à offrir des débits élevés avec une quantité réduite de connaissance du canal à l'émetteur (CSIT), car la disponibilité des ressources sur la voie de retour est limitée. Cette thèse traite du problème de l'optimisation des systèmes MIMO avec CSIT partielle. D'une part, nous fournissons des méthodes pour obtenir CSIT. D'autre part, nous proposons des techniques pour exploiter les sources de CSIT afin d'optimiser la performance du système.

Dans la première partie, les systèmes MIMO mono-utilisateur sont considérés dans le but de minimiser le taux d'erreur. Des techniques de précodage linéaire sont proposées pour améliorer le fonctionnement des systèmes MIMO avec codage spatio temporel (STC), en combinant des informations sur la moyenne et la covariance du canal. Dans la deuxième partie de cette thèse, nous nous concentrons sur la maximisation de la somme totale des débits sur la voie descendante des systèmes MIMO multi-utilisateur, avec débit limité sur la voie de retour. Nous proposons des algorithmes inter-couche à complexité réduite pour les systèmes avec beamforming linéaire et sélection d'utilisateurs, en optimisant les parties suivantes dans un système de communication MIMO: techniques de beamforming linéaire, algorithmes de sélection d'utilisateurs, informations à transmettre sur la voie de retour et stratégies de quantification.

Différents modèles sont considérés pour la voie de retour (feedback). Dans un scénario où les utilisateurs n'envoyent que des indices de quantification du canal, nous étudions les avantages de la génération des quantificateurs adaptés à la statistique du canal, afin d'exploiter les corrélations spatiales et temporelles. Un autre modèle considère le feedback séparé pour l'information

de direction du canal (CDI) et l'information de qualité du canal (CQI). Dans ces systèmes, les utilisateurs ont besoin d'estimer le montant d'interférence inter-utilisateur, ce qui est une tâche difficile puisque les utilisateurs ne peuvent pas coopérer. Nous proposons un cadre de conception pour CQI dans les systèmes MIMO multi-utilisateur, basé sur l'estimation du rapport signal à interférence plus bruit (SINR). Dans ce cadre, une étude comparative entre multiplexage spatial des utilisateurs (SDMA: space division multiple access) et multiplexage temporel (TDMA: time division multiple access) est présentée dans différents régimes asymptotiques. En outre, dans les systèmes où les bits envoyés sur la voie de retour doivent être partagés pour quantification de CDI et CQI, nous présentons le compromis entre la diversité multi-utilisateur et le gain de multiplexage.

Le problème de la conception des techniques de beamforming linéaire pour systèmes MIMO multi-utilisateur est également abordé. Une méthode d'opti-
misation itérative pour beamforming linéaire unitaire est proposée, robuste aux erreurs d'estimation du canal. La technique proposée permet d'améliorer la performance des émetteurs basés sur le critère de forçage à zéro (ZF), et même avec un critère de minimisation de l'erreur quadratique moyenne (MMSE) si la variance de l'erreur d'estimation augmente. Notre travail montre l'importance de l'optimisation du transmetteur quand le débit sur la voie de retour est limité. Plutôt que de concevoir des systèmes complexes de feedback, en s'appuyant sur des techniques de transmission simples, la performance du système peut être améliorée en utilisant un beamforming linéaire optimisé et des stratégies simples de quantification du canal.

## Chapitre 1: Introduction

La croissance rapide des services sur IP sans fil a eu une importante influence sur l'évolution des standards de communications mobiles au cours des dernières années. La troisième et quatrième génération de systèmes de communication mobiles fournissent services de communication orientée paquets, qui sont plus tolérants aux délais que les services vocaux traditionnels mais ont besoin de très haut débit. L'efficacité spectrale des systèmes sans fil peut être considérablement améliorée par les technologies MIMO, en exploitant la dimension spatiale en plus des dimensions temps et fréquence exploitées dans les systèmes SISO. Les systèmes MIMO ont reçu une attention considérable,

car ils offrent fiabilité et communication haut débit.

Dans le cas du MIMO point à point, plusieurs antennes peuvent exploiter la diversité de l'espace-temps en utilisant le codage spatio-temporel (STC), fournissant des taux d'erreur très faibles en l'absence de connaissance du canal à l'émetteur. Si un certain degré de CSIT est disponible, ces connaissances peuvent être utilisées afin d'améliorer le taux de transfert des données avec multiplexage spatial, transmettant des flux de données indépendants. Dans un système cellulaire multi-utilisateur avec des antennes multiples sur la station de base, CSIT peut être utilisé pour communiquer avec plusieurs utilisateurs en même temps par multiplexage spatial, dans le but de maximiser la somme totale des débits.

La connaissance du canal au récepteur (CSIR) peut être facilement obtenue grâce aux symboles pilotes émis depuis la station de base. D'autre part, l'obtention de CSIT est une tâche complexe qui nécessite l'exploitation de la réciprocité â la station de base ou l'utilisation de la voie de retour. Ainsi, toute source de CSIT partiel, instantané ou statistique, doit être exploitée dans le but d'optimiser la performance du système. Cette thèse traite du problème de l'optimisation de la performance des systèmes MIMO avec CSIT partiel, en fournissant des solutions pratiques aux problèmes actuels et futurs dans les réseaux sans fil MIMO mono et multi-utilisateur.

Dans la première partie de cette thèse, nous nous concentrons sur la conception de techniques de précodage linéaire pour les canaux MIMO point à point. Ces précodeurs utilisent des informations statistiques pour améliorer la performance du système et ils peuvent être concaténées avec STC, offrant ainsi une solution flexible et robuste. Nous considérons la moyenne et la covariance du canal comme CSIT partiel, car ils peuvent refléter différents scénarios pratiques.

Dans la deuxième partie, nous abordons le problème de la maximisation de la somme totale des débits sur la voie descendante pour les systèmes MIMO multi-utilisateur. Nous nous concentrons sur l'optimisation des aspects suivants au niveau PHY/MAC: les techniques de beamforming linéaire multi-utilisateur ou beamforming (formation de faisceaux), algorithmes de sélection d'utilisateurs, informations à transmettre sur la voie de retour et stratégies de quantification. Toutefois, l'optimisation conjointe de l'ensemble de ces éléments est assez compliquée. Lors de l'optimisation de ces réseaux, nous nous posons les questions suivantes:

- Quelles informations doivent être envoyées sur la voie de retour afin

de concevoir des précodeurs linéaires et d'exploiter la diversité multi-utilisateur?

- Comment quantifier les informations sur la voie de retour avec débit limitê disponible en vue d'optimiser la performance du système?
- Comment concevoir des algorithmes de sélection d'utilisateurs à complexité réduite pour exploiter la diversité multi-utilisateur?
- Comment concevoir des techniques robustes de beamforming linéaire avec un débit réduit sur la voie de retour?
- Pouvons-nous trouver des solutions conjointes à ces problèmes?

## Chapitre 2: Systèmes MIMO mono-utilisateur avec précodage linéaire

Dans ce premier chapitre, nous examinons différents cas de CSIT partial basés sur la moyenne et la covariance du canal MIMO point à point. D'une part nous considérons le cas avec moyenne et covariance à priori (ou la distribution à priori du canal est Ricean), et d'autre part le cas avec moyenne et covariance à posteriori (approche Bayésienne basée sur l'estimation du canal et la covariance à priori ).

En outre, plusieurs cas particuliers d'intérêt pratique sont étudiés, à savoir: le cas avec moyenne nulle, le cas où la moyenne est de rang unitaire et le cas avec matrice de covariance singulière.

Dans les systèmes sans fil pratiques, des séquences ou des symboles pilotes sont intégrés dans le signal transmis pour permettre l'estimation de canal au récepteur.

La connaissance du canal à l'émetteur permet l'amélioration du débit dans les systèmes sans fil. Un moyen d'obtenir CSIT est l'utilisation de la voie de retour, en envoyant l'estimation du canal obtenue au récepteur. Puisque la bande de fréquences disponible est limitée, toutes les informations statistiques sur le canal devraient être prises en compte.

Afin d'exploiter CSIT partial dans les systèmes MIMO point à point, la plupart des études actuelles avec précodage exploitent des informations sur la moyenne ou la covariance séparément. La combinaison des deux peut améliorer l'exploitation de la connaissance du canal. Dans notre travail,

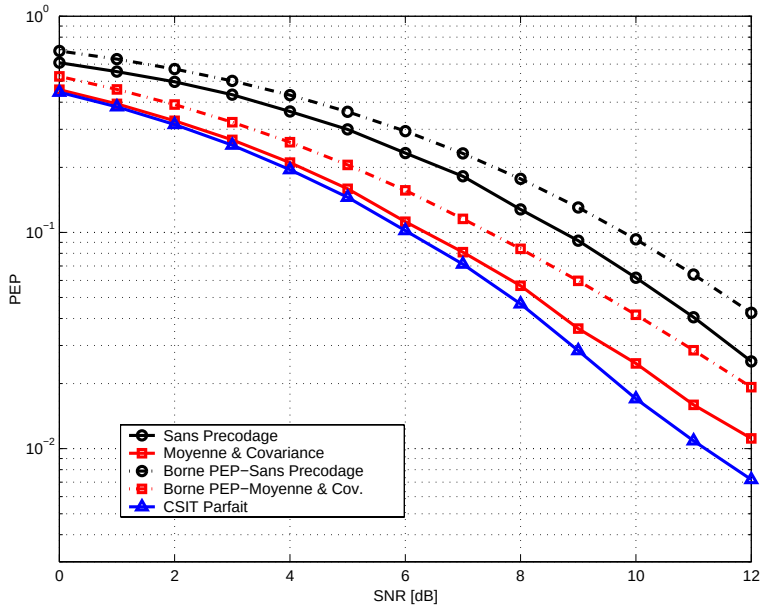


Figure 1: PEP en fonction du SNR pour différents niveaux de CSIT, $\rho = 0.9$ and $\gamma = 40\%$

nous présentons différentes techniques pour combiner les informations sur la moyenne et la covariance dans le but d'optimiser le taux d'erreur dans les systèmes MIMO mono-utilisateur.

Nous considérons un système où l'émetteur encode les bits en utilisant le codage spatio-temporel. Un mot codé $\mathbf{C}$ est de dimension $M \times T$, où $T$ est la longueur de bloc. Avant la transmission, les mots ST codés sont précodés avec la matrice de précodage de dimension $M \times M$.

Nous dérivons une stratégie de précodage optimale pour la minimisation du taux d'erreur dans les systèmes MIMO, qui combine moyenne et covariance. La performance du système est mesurée en termes de probabilité d'erreur par paires (PEP), définie comme la probabilité de choisir le plus proche mot erroné $\mathbf{C}^j$ au lieu de $\mathbf{C}^i$, moyennée sur la distribution (à priori ou à posteriori) du canal. En appliquant la borne de Chernoff, nous trouvons le précodeur linéaire qui minimise une borne supérieure sur la PEP moyenne.

La Figure 1 montre le gain de performance que l'on peut obtenir par rapport à un système non-précodé en combinant les informations sur la moyenne

et la covariance. La contribution de la moyenne à la puissance totale du canal est dénotée par $\gamma$, et $\rho$ est le facteur de correlation. Nous pouvons observer une amélioration remarquable de jusqu'à environ 2.5 dB SNR pour une PEP fixée. Dans ce cas particulier, la performance est proche de celle obtenue par un précodeur optimale avec CSIT parfait.

## Chapitre 3: Systèmes MIMO multi-utilisateur avec beamforming linéaire et sélection d'utilisateurs

Les systèmes MIMO peuvent améliorer l'efficacité spectrale, en exploitant les degrés de liberté créés par de multiples antennes. La capacité dans les scénarios multi-utilisateur peut être renforcée grâce au multiplexage spatial, en transmettant à plusieurs utilisateurs simultanément avec SDMA, plutôt qu'en maximisant la capacité de chaque lien mono-utilisateur. Il a été démontré récemment que la somme-capacité des canaux MIMO est atteinte par codage 'papier sale' (DPC, dirty paper coding) [1]. Toutefois, l'applicabilité de DPC est limitée en raison de sa complexité et de la nécessité de CSIT parfait.

Une alternative prometteuse pour la liaison descendante des systèmes MIMO à faible complexité est le beamforming linéaire. Par opposition à DPC, le beamforming ne réalise aucune pré-soustraction d'interférence, et donc l'interférence multi-utilisateur est traitée comme du bruit. Le problème de trouver les vecteurs de beamforming optimal est un problème d'optimisation non-convexe, et la solution optimale pour une liaison descendante avec $K$ utilisateurs ne peut être donnée que par recherche exhaustive. Evidemment, la complexité de ce problème devient extrêmement élevée pour très grand $K$. Par conséquent, nous nous concentrons plutôt sur les stratégies suboptimaux de beamforming linéaire qui, combinées avec des algorithmes de sélection d'utilisateurs afin d'exploiter la diversité multi-utilisateur, atteignent des sommes de débits élevés.

Dans les systèmes MIMO multi-utilisateur, le gain de capacité est fortement lié à la disponibilité de CSIT. Si une station de base avec $M$ antennes de transmission, en communication avec $K$ récepteurs mono-antennaires, a un CSIT parfait, un gain de multiplexage $\min(M, K)$ peut être atteint. S'il n'y a pas de CSIT, le gain de multiplexage s'effondre à 1. Donc, il

est particulièrement intéressant d'identifier quel type de CSIT partiel peut être transmis à la station de base en vue d'atteindre des débits de données raisonnablement proche de l'optimum.

Une technique populaire avec très faible taux de feedback est celle de beamforming aléatoire (RBF)[2], où $M$ vecteurs orthonormaux aléatoires sont générés et le meilleur utilisateur (celui avec le plus haut SINR) sur chaque faisceau est sélectionné. En exploitant la diversité multi-utilisateur, il est démontré que la croissance optimale de la capacité est de $M \log \log K$ pour $K \to \infty$. D'autres techniques populaires de beamforming sont basés sur le critère de forçage à zéro (ZF), et sur le critère de minimisation de l'erreur quadratique moyen (MMSE).

Pour illustrer ces défis, les avantages et les inconvénients de ces systèmes, deux approches a complexité reduite sont proposées. Dans la première approche, un scénario avec CSIT parfait est considéré, dans lequel une simple stratégie de sélection d'utilisateurs est combinée avec beamforming linéaire basé sur faisceaux orthogonaux. Cela conduit à une forte réduction de la complexité dans l'étape de sélection d'utilisateurs. Nous montrons que l'algorithme proposé peut réaliser une grande partie de la capacité multi-utilisateur.

Dans la deuxième approche, une solution a complexité réduite est proposée pour un scénario avec feedback limité. Comme nous le montrons, des codebooks simples adaptés à la corrélation spatiale au transmetteur peuvent produire des gains élevés de performance. Le système proposé fournit une performance proche de celle de CSIT parfait, lorsque l'ouverture angulaire multi-antennaire à l'émetteur est assez petite, ce qui rend cette approche particulièrement intéressante pour systèmes sans fil avec station de base élevée. En outre, une borne supérieure sur l'interférence multi-utilisateur est dérivée, basé sur une interprétation géométrique du problème. Cette borne est d'une importance capitale car, comme nous montrons dans le chapitre suivant, elle peut être utilisé pour la conception des mesures de feedback aux fins de la sélection d'utilisateurs.

# Chapitre 4: Un cadre de conception pour la voie de retour

Dans ce chapitre, le beamforming linéaire et la sélection d'utilisateurs sont effectuées dans un système où la voie de retour est limitée, et les utilisateurs ont des codebooks de quantification de direction du canal. Le feedback transmis par chaque utilisateur vers la station de base se compose de l'information de direction du canal (CDI) et l'information de qualité du canal (CQI). Nous présentons un cadre de conception pour le feedback de CQI scalaire dans les systèmes MIMO multi-utilisateur qui généralise des techniques proposées précédemment. Une famille de métriques est présentée, basée sur des différents mesures de SINR, qui sont calculés par les récepteurs et envoyés à la station de base en tant que CQI. Les informations suivantes peuvent être combinées par chaque utilisateur sur les paramètres scalaires de CQI

- Puissance du signal: $P$
- Variance du bruit: $\sigma^2$
- Gain du canal: $\|\mathbf{h}_k\|^2$
- Erreur de quantification: $\sin^2\theta_k$
- Facteur d'orthogonalité: $\epsilon$
- Nombre de faisceaux actifs: $M_o$

Le facteur d'orthogonalité $\epsilon$ indique le degré maximum de non orthogonalité entre deux vecteurs beamforming normalisés.

L'algorithme de sélection d'utilisateurs, basé sur feedback scalaire $\xi_k$ de chaque utilisateur, est présenté dans le Tableau 1 (MS: station mobile, BS: station de base). L'ensemble des utilisateurs sélectionnés est dénoté par $\mathcal{S}$, $\mathbf{w}_i$ est le vecteur beamforming du $i$-ème utilisateur (dans ce cas là aussi égal à la direction du canal quantifié) et $B$ est le nombre de bits dédiés à la quantification de CDI. Le nombre de faisceaux actifs au transmetteur $M_o$ et le facteur d'orthogonalité $\epsilon$ sont des paramètres du système fixés par la station de base qui peuvent être adaptés afin de maximiser la somme des débits.

Table 1: Algorithme de Sélection d'Utilisateurs

**MS**

**Calculer & Envoyer sur la voie de retour**

CQI: $\rightarrow \xi_k$

CDI: $\rightarrow$ Index de quantification $i \in \{1, \ldots, 2^B\}$

**BS**

**Initialiser** $\mathcal{S} = \emptyset$

**Itérer** Pour $i : 1 \ldots M_o$ répéter

**Fixer** $\xi^i_{max} = 0$

**Itérer** Pour $k : 1 \ldots K, k \notin \mathcal{S}$ répéter

Si $\xi_k > \xi^i_{max}$ et $\left|\mathbf{w}_k^H \mathbf{w}_j\right| \leq \epsilon \;\; \forall\, j \in \mathcal{S}$

$\xi_k \rightarrow \xi^i_{max}$ et $k_i = k$

**Selectioner** $k_i \rightarrow \mathcal{S}$

Dans le cadre de conception qu'on propose, toute métrique scalaire peut être décrite comme suit:

$$\xi = \frac{\|\mathbf{h}_k\|^2 \cos^2\theta_k}{\|\mathbf{h}_k\|^2 \left(\alpha \cos^2\theta_k + \beta \sin^2\theta_k + 2\gamma \sin\theta_k \cos\theta_k\right) + \frac{M_o \sigma^2}{P}}. \tag{1}$$

Le numérateur dans l'expression ci-dessus reflète la puissance effective reçue dans un système avec quantification du canal. D'autre part, le dénominateur reflète la puissance du bruit et donne une mesure de l'interférence subie par l'utilisateur, par exemple une borne inférieure ou supérieure, en exploitant la structure de la matrice de beamforming. En choisissant différentes valeurs pour les paramètres $\alpha$, $\beta$, $\gamma$ et $M_o$, la signification de la métrique est modifiée et elle produit différents mesures de SINR.

Nous proposons 4 cas particuliers dans le cadre de conception proposée:

- **Métrique I**: Borne inférieure sur SINR moyen. Fonction de $\epsilon$ et $M_o$.
- **Métrique II**: Borne supérieure sur SINR, avec $\epsilon = 0$ et $M_o = M$ fixés.

- **Métrique III**: Borne inférieure sur SINR. Fonction de $\epsilon$ et $M_o$.
- **Métrique IV**: Borne supérieure sur SINR moyen. Fonction de $M_o$, en fixant $\epsilon = 0$.

Une approximation sur la somme des débits ergodique est fournie pour la famille de métriques proposée. La Figure 2 montre une comparaison entre la fonction somme des débits proposée et les résultats des simulations. Dans cette simulation, la Métrique III a été utilisée, dans un système avec $M = 2$ antennes, $K = 15$ utilisateurs et SNR = 10 dB. La fonction proposée correspond bien aux résultats simulés, même dans des cellules avec un faible nombre d'utilisateurs actifs. Cette fonction est utile pour la conception de systèmes et dans le même temps, elle simplifie grandement l'analyse du système. En effet, une comparaison entre la somme des débits de SDMA et TDMA a été fournie dans différentes situations d'intérêt. En particulier, la performance de SDMA est meilleure que celle de TDMA quand le nombre d'utilisateurs est grand. TDMA offre un meilleur taux que SDMA à haut SNR (cas limité par l'interférence). En outre, nous montrons l'importance d'optimiser le facteur d'orthogonalité $\epsilon$ à bas SNR.

Dans les Figures 3 et 4, nous comparons la somme des débits effectifs obtenue par des systèmes avec préfiltrage adapté au transmetteur et basés sur les différentes métriques proposées (Métriques I, II, III et IV), pour $M = 3$ antennes et $B = 9$ bits. A titre de comparaison, les performances de RBF et préfiltrage adapté avec CSIT parfait sont fournies.

La Figure 3 montre une comparaison des performances en termes de somme des débits en fonction du nombre total d'utilisateurs, dans une cellule avec un nombre d'utilisateurs actifs realiste. Le système basé sur la Métrique I fournit des performances légèrement meilleures que les autres approches. La Figure 4 représente les performances des différents systèmes en fonction de SNR, dans un système avec $K = 10$ utilisateurs. Les systèmes avec Métriques I et II présentent une croissance linéaire de la somme des débits en fonction de la SNR, ce qui correspond à une solution TDMA. Le système qui utilise la Métrique IV bénéficie également d'un nombre variable de faisceaux actifs, bien que fournissant une moins bonne performance que les systèmes avec Métriques I et III.

En outre, l'effet de la quantification scalaire des métriques est étudié dans le cadre d'un système ou la somme totale des bits disponibles sur la voie de retour est finie. D'un côté, la quantification de CDI encourt une perte de gains de multiplexage, et de l'autre, la quantification de CQI provoque une

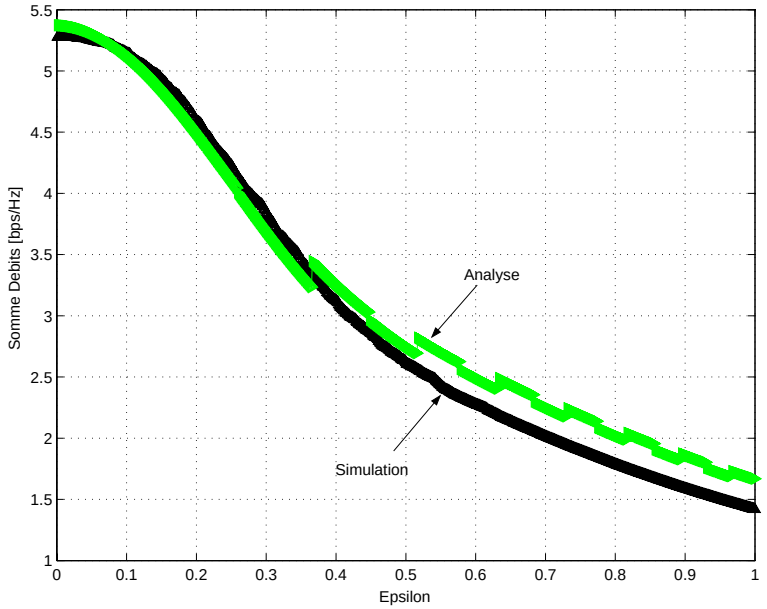


Figure 2: Comparaison des résultats analyse-simulation de la borne inférieure sur la somme des débits en utilisant la métrique III, pour $M = 2$ antennes, $K = 15$ utilisateurs, SNR = 10 dB et $B = 1$ bit.

dégradation de l'exploitation de diversité multi-utilisateur. Donc, dans les systèmes MIMO avec feedback limite, nous identifions un compromis entre la diversité multi-utilisateur et le gain de multiplexage. Nous considérons un système où chaque récepteur a un nombre total de bits disponibles sur la voie de retour $B_{tot}$. De ce montant total de bits, $B_1$ bits sont utilisés pour quantifier le CDI et $B_2$ bits sont utilisés pour la quantification scalaire de CQI, soit $B_{tot} = B_1 + B_2$.

La Figure 5 montre la somme des débits en fonction du nombre d'utilisateurs pour toutes les combinaisons possibles de bits de CDI ($B_1$) et bits de CQI ($B_2$) dans un système avec $B_{tot} = 7$ bits. Comme prévu, il est plus utile d'allouer plus de bits sur CDI dans un système avec un faible nombre d'utilisateurs actifs. D'autre part, quand le nombre d'utilisateurs augmente, il devient plus avantageux d'allouer des bits sur CQI.

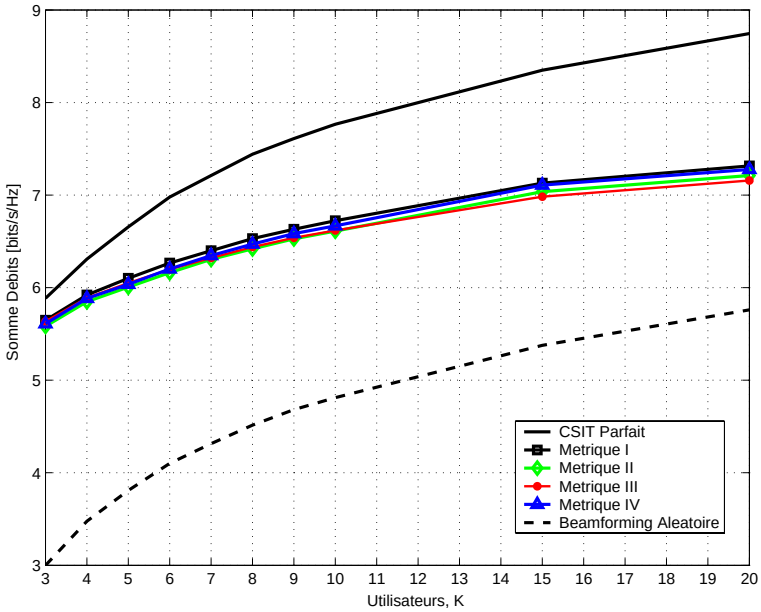


Figure 3: Somme des débits obtenue par différentes approches de feedback en fonction du nombre d'utilisateurs, pour $B = 9$ bits, $M = 3$ antennes au transmetteur et SNR = 10 dB.

# Chapitre 5: Optimisation des quantificateurs du canal

Dans ce chapitre, nous proposons des techniques de quantification de canal pour les systèmes MIMO multi-utilisateur avec voie de retour limitée. Plutôt que de séparer les mesures de CDI et CQI, nous considérons un scénario simple dans lequel chaque utilisateur quantifie directement son vecteur canal. Le compromis entre la diversité multi-utilisateur et le gain de multiplexage introduit dans le chapitre précédent est implicitement optimisé dans les approches proposées, au détriment d'avoir un haut débit sur la voie montante pendant la période initiale dans laquelle les codebooks sont optimisés. Notre objectif consiste à trouver des codebooks de quantification simples qui, dans des scénarios avec corrélation spatiale ou temporelle, fournissent des gains de performances sur les techniques classiques de quantification.

Nous soulignons l'importance des statistiques dans la cellule pour la con-

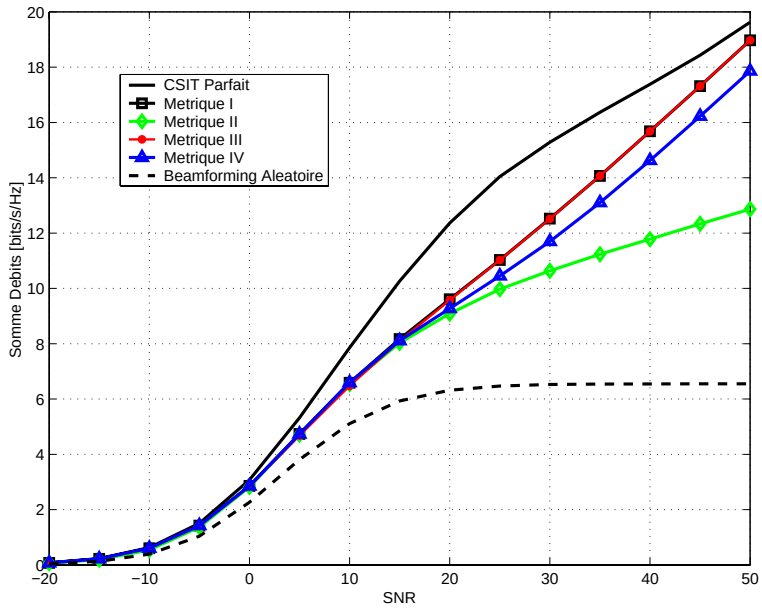


Figure 4: Somme des débits obtenue par différentes approches de feedback en fonction de SNR moyen, pour $B = 9$ bits, $M = 3$ antennes et $K = 10$ utilisateurs.

ception de codebooks dans les canaux MIMO multi-utilisateur. En premier lieu, l'importance d'exploiter les corrélations spatiales est adressée. La distorsion de la somme moyenne des débits dans un système avec beamforming linéaire et sélection d'utilisateurs est minimisé, en exploitant les informations sur la nature macroscopique des canaux. Dans cette première partie, un modèle de canal stochastique non-géométrique est considéré, dans lequel chaque utilisateur peut être atteint par différentes directions spatiales et avec des angles d'ouverture différents.

Sur la base de ce modèle, nous comparons l'approche proposée avec des approches basées sur des codebooks aléatoires afin d'illustrer l'importance d'associer la conception des codebooks aux statistiques de la cellule. L'approche de génération des codebooks est implémentée avec les stratégies de beamforming linéaire avec forçage à zéro et filtre adapté. L'approche LF-OSDMA [3] avec CQI quantifié est simulée; elle généralise le RBF pour les codebooks de taille plus grande que $\log_2 M$. Le codebook de quantification scalaire CQI utilisé pour LF-OSDMA a été conçu avec l'algorithme généralisé Lloyd.

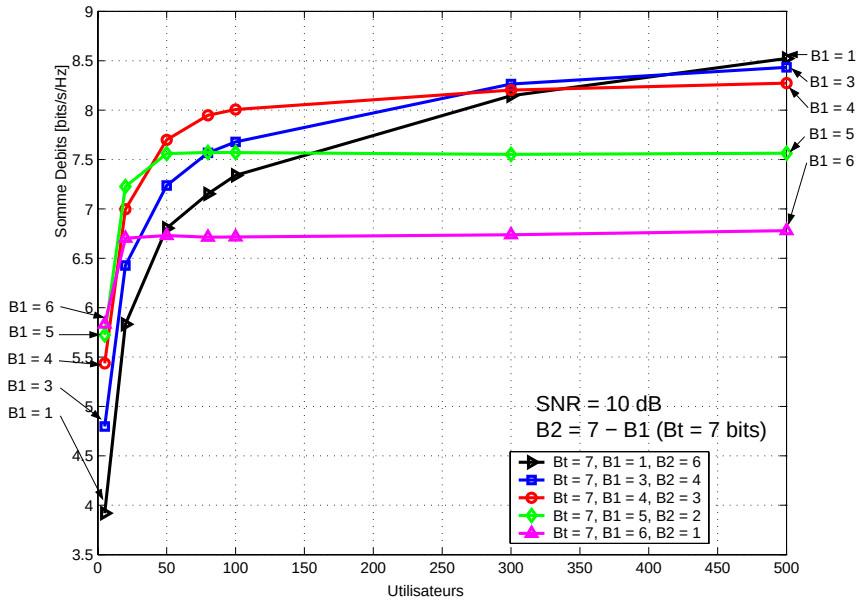


Figure 5: Somme des débits en fonction du nombre d'utilisateurs pour $M = 2$ et SNR = 10 dB.

La Figure 6 représente les performances pour différents nombres d'utilisateurs avec un SNR de 10 dB. Nous voyons que les performances de forçage a zéro et filtre adapté avec un CSI quantifié sont meilleures que celle de LF-OSDMA avec SINR quantifié. L'approche proposée donne de bons résultats particulièrement dans des scénarios avec ouverture angulaire réduite et utilisateurs distribués sur la cellule de manière non-uniforme.

Deuxièmement, nous abordons le problème de l'exploitation des corrélations temporelles dans le système. Nous présentons une approche qui utilise la quantification vectorielle prédictive (PVQ) afin d'exploiter la corrélation entre les réalisations successives du canal dans le but d'améliorer la quantification, et donc d'améliorer la somme des débits. La Figure 7 montre la somme des débits avec PVQ et ZFBF, et celle de LF-OSDMA. La corrélation temporelle est modélisée avec le model de Jake, avec une fréquence Doppler $f_D$ et une longueur de trame $T_f$. L'algorithme prédit le canal sur la base des dernières 3 réalisations du canal. PVQ utilise une simple étape de prédiction afin de supprimer la corrélation entre les canaux précédents et le canal en train d'être quantifié. Ceci permet d'améliorer la performance de l'étape de quantification, comme indiqué dans nos simulations.

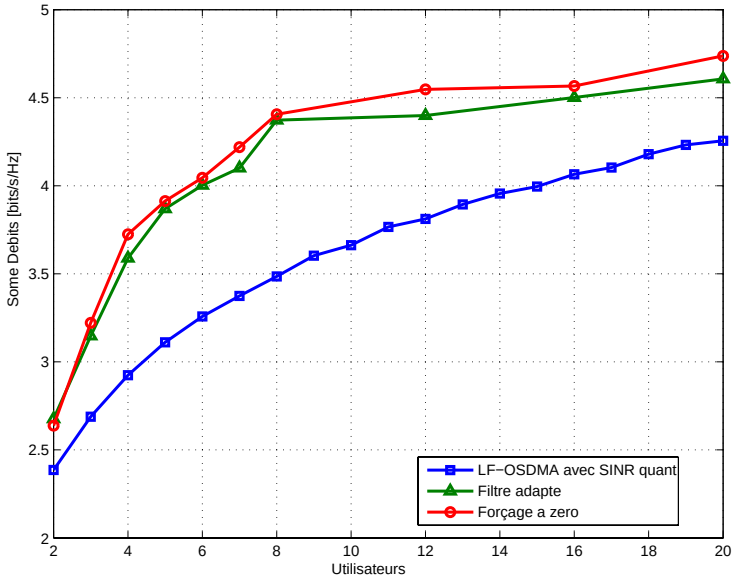


Figure 6: Somme des débits en fonction du nombre d'utilisateurs dans un canal corrélé spatialement, $M = 2$ antennes et SNR = 10 dB.

# Chapitre 6: Optimisation des techniques de beamforming linéaire

Dans ce chapitre, une méthode d'optimisation itérative pour le beamforming unitaire dans les systèmes MIMO multi-utilisateur est proposée, basée sur l'optimisation successive des rotations de Givens. Initialement, nous considérons un système avec CSIT parfait.

La stratégie unitaire proposée cherche l'équilibres entre la puissance et les interférences reçues par chaque utilisateur. À partir d'une matrice unitaire arbitraire initiale $\mathbf{W}^0$, nous proposons un algorithme itératif qui consiste à faire tourner la matrice de beamforming en effectuant des successives optimisations des rotations de Givens jusqu'à ce que la convergence soit atteinte. À la $i$-ème itération, une nouvelle matrice de beamforming unitaire est calculée par rotation de la matrice de $\mathbf{W}^{i-1}$ (calculée à l'itération précédente) dans le plan défini par les vecteurs complexes $(\mathbf{w}_m, \mathbf{w}_n)$, en multipliant à droite par la matrice de rotation de Givens. La matrice de Givens est déterminée

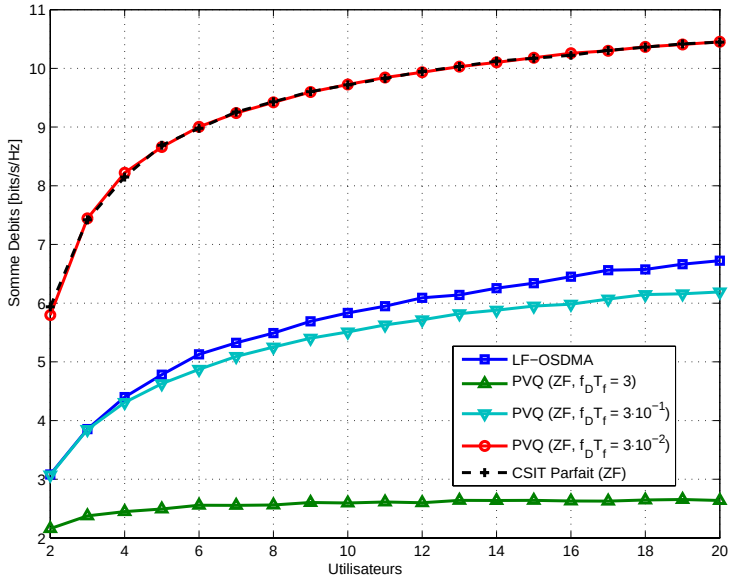


Figure 7: Somme des débits en fonction du nombre d'utilisateurs avec un canal corrélé temporellement, $M = 2$ antennes et SNR = 10 dB.

par les paramètres de rotation $\alpha$ et $\delta$. L'algorithme proposé est présenté dans le Tableau 2. L'ensemble de toutes les paires possibles d'indices $\{m, n\}$ est dénotée $\mathcal{G}$, où les indices sont choisis parmi l'ensemble complet d'indices $\{1, \ldots, M\}$, avec $n > m$. Le nombre de rotations de plans effectuées par l'approche proposée est $N_{PR}$.

La convergence de l'algorithme est illustrée à la Figure 8 pour différents nombres d'antennes de transmission. Dans cette simulation, des rotations de Givens sont effectuées dans tous les paires possibles de vecteurs de beamforming, et un grand nombre de rotations est considéré.

Premièrement, nous comparons la performance de l'approche proposée avec le beamforming ZF et MMSE, dans un scénario où CSIT parfait est disponible et le nombre d'utilisateurs est égal au nombre d'antennes au transmetteur. En outre, nous montrons à titre de référence la performances d'un système qui effectue TDMA, en sélectionnant l'utilisateur avec le plus grand gain du canal. La Figure 9 montre une comparaison en termes de somme des débits en fonction du nombre total d'antennes de transmission $M$, pour SNR

Table 2: Méthode d'Optimisation Itérative pour Beamforming Unitaire

**Initialisation**

- Initialiser la matrice unitaire $\mathbf{W}^0$

$i$**-ème iteration**, $i = 1, \ldots, N_{PR}$

- Choisir une paire d'indices $\{m, n\}$ parmi $\mathcal{G}$
- Trouver les paramètres optimaux de rotation pour le plan $(\mathbf{w}_m, \mathbf{w}_n)$
$$\{\alpha^*, \delta^*\} = \arg\min_{\alpha,\delta} F_{mn}(\alpha, \delta)$$
- Calculer la nouvelle matrice $\mathbf{W}^i = \mathbf{W}^{i-1}\mathbf{R}_{mn}(\alpha^*, \delta^*)$

= 10 dB. Comme prévu, la solution de beamforming MMSE linéaire fournit une croissance linéaire de la somme des débits avec le nombre d'antennes de transmission, tandis que le ZF beamforming s'aplatit. L'algorithme proposé fournit également une croissance linéaire avec $M$, étant proche de beamforming MMSE.

L'impact de la connaissance imparfaite du canal à l'émetteur dans un système avec $K = M$ utilisateurs est aussi étudié. La Figure 10 montre une comparaison de sommes des débits entre l'approche proposée, le beamforming ZF, le beamforming MMSE et TDMA en fonction de la variance de l'erreur d'estimation du canal, pour $M = 4, 8$ antennes et un SNR moyen de 10 dB. L'approche proposée se révèle plus robuste aux erreurs de CSIT quele beamforming ZF ou MMSE. En effet, une petite variance d'erreur suffit pour que l'approche unitaire proposée devienne plus performante que le beamforming MMSE, même pour un grand nombre d'antennes de transmission.

Nous évaluons aussi la technique proposée dans un système MIMO multi-utilisateur avec $K \geq M$ et feedback limité sur la voie de retour. La Figure 11 montre les performances pour différents nombres d'utilisateurs avec SNR de 10 dB, dans un système avec $M = 4$ antennes de transmission et $B = 10$ bits disponibles pour feedback. L'approche proposée utilise une technique de quantification vectorielle à complexité réduite, basée sur la quantification aléatoire des vecteurs avec "pruning", ce qui signifie qu'il doit avoir une distance minimale entre chaque mot du codebook. La performance de l'approche proposée est meilleure que celle de RBF et LF-OSDMA avec feedback quantifié, en particulier dans les systèmes à nombre réduit d'utilisateurs, fournissant des gains de débit proches de 1.5 bps/Hz.

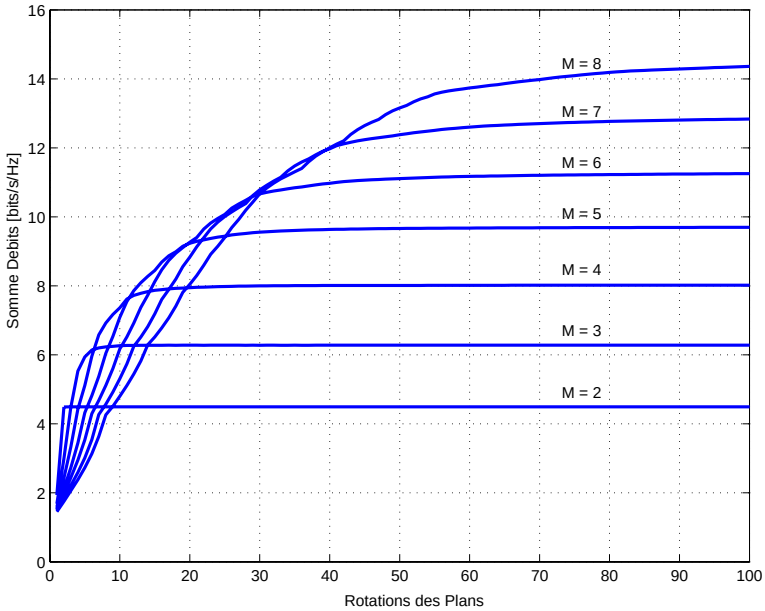


Figure 8: Somme des débits en fonction du nombre de rotations de plans (itérations de l'algorithme) pour différents nombres d'antennes au transmetteur, $K = M$ utilisateurs et SNR = 10 dB.

Dans la Figure 12, la somme des débits est montrée en fonction de SNR moyen dans un système avec $M = 4$ antennes de transmission, $K = 10$ utilisateurs et $B = 10$ bits. Dans le scénario simulé, la technique proposée fournit des gains de performance allant jusqu'à 2-bps/Hz par raport aux autres techniques.

# Conclusion

Dans cette thèse, nous avons mis l'accent sur l'optimisation des performances des systèmes MIMO sans fil avec CSIT partiel. D'une part, nous avons étudié le problème de l'obtention et de la conception de CSIT en systèmes mono et multi-utilisateur, en montrant quelles sources d'information sont nécessaires à l'émetteur. D'autre part, cette thèse a abordé la question de comment exploiter efficacement les sources de CSIT disponibles afin d'améliorer la performance du système.

Dans la première partie de cette thèse, les canaux MIMO point à point

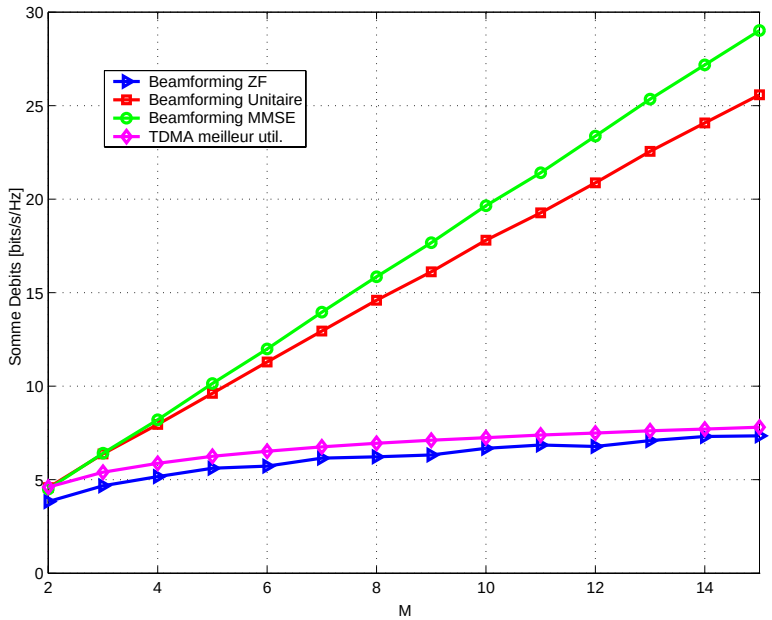


Figure 9: Somme des débits en fonction du nombre d'antennes $M$ pour $K = M$ utilisateurs et SNR = 10 dB.

ont été pris en considération, en soulignant l'importance de CSIT statistique pour la conception de techniques de précodage linéaire. Comme nous l'avons montré, le taux d'erreur d'un système MIMO avec codage spatio-temporel peut être considérablement amélioré, grâce a un précodeur linéaire qui exploite les informations de covariance et moyenne du canal. Afin de fournir une idée claire de la manière dont la moyenne et la covariance doivent être combinées pour obtenir de bonnes performances, différents modèles de canaux MIMO ont été considérés.

La deuxième partie de cette thèse a été consacrée à l'optimisation de la somme des débits dans les systèmes MIMO multi-utilisateur avec ressources limitées sur la voie de retour. Nous avons surtout examiné les systèmes dans lesquels une station de base communique avec un ensemble d'utilisateurs ayant chacun une seule antenne réceptrice. Dans le but de concevoir des techniques pratiques à complexité reduite, nous avons mis l'accent sur les systèmes avec beamforming linéaire et sélection d'utilisateurs. Dans notre travail, nous avons montré l'importance de la conception inter-couche à niveau PHY-MAC, en optimisant les éléments suivants d'un système MIMO

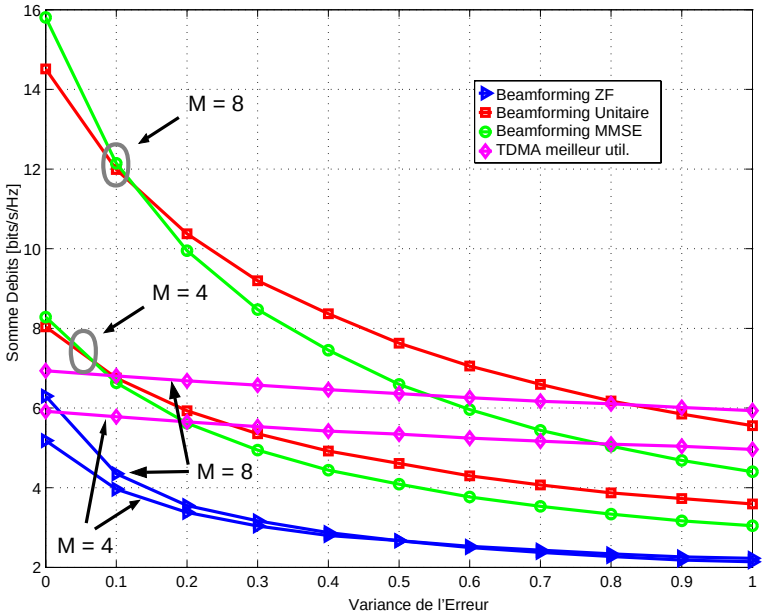


Figure 10: Somme des débits en fonction de la variance de l'erreur d'estimation du canal pour $M = 4, 8$ antennes, $K = M$ utilisateurs et SNR $= 10$ dB.

multi-utilisateur: techniques de beamforming linéaire, algorithmes de sélection d'utilisateurs, informations à transmettre sur la voie de retour et stratégies de quantification.

Un cadre de conception pour la voie de retour des systèmes MIMO multi-utilisateur a été proposé. Un scénario a été envisagé où le feedback pour l'information de direction du canal (CDI) et l'information de qualité du canal (CQI) sont envoyées séparément. Dans ces systèmes, les utilisateurs ont besoin d'estimer l'interférence multi-utilisateur, ce qui est une tâche difficile puisque les utilisateurs ne peuvent pas coopérer. Nous avons proposé une borne sur l'interférence multi-utilisateur qui peut être utilisée dans les métriques scalaires CQI. Cette information est transmise sur la voie de retour pour sélectionner les meilleurs utilisateurs, avec d'autres mesures d'intérêt, tels que le gain du canal, l'erreur de quantification, l'orthogonalité entre les vecteurs de précodage et le nombre de faisceaux actifs. Une étude comparative entre SDMA et TDMA a été fournie dans différents régimes asymptotiques, indiquant les cas dans lesquels SDMA devient plus avantageux que

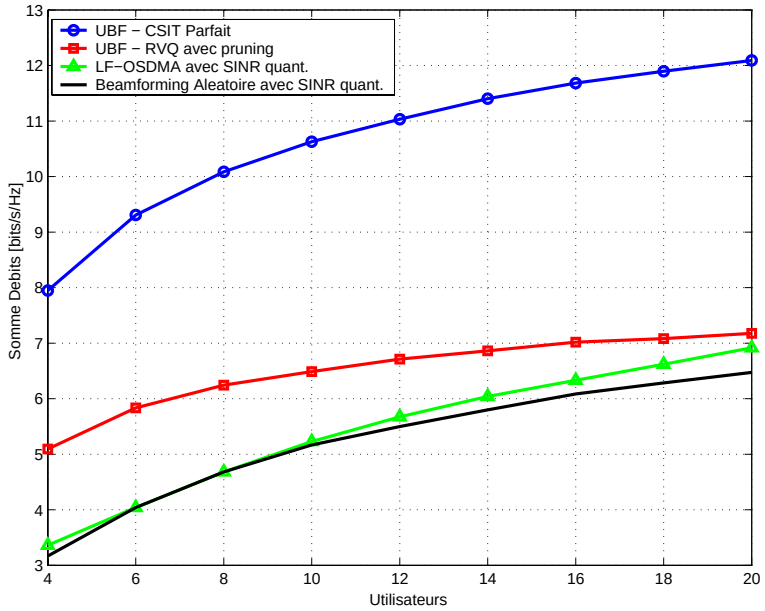


Figure 11: Somme des débits en fonction du nombre d'utilisateurs dans un système avec beamforming linéaire et sélection d'utilisateurs, $M = 4$ antennes, SNR = 10 dB, et $B = 10$ bits sur la voie de retour.

TDMA en termes de somme des débits et vice versa. En particulier, la performance de SDMA surpasse celle de TDMA quand le nombre d'utilisateurs est grand. TDMA offre un meilleur taux que SDMA à haut SNR (cas limité par l'interférence). En outre, l'importance d'optimiser le facteur d'orthogonalité à bas SNR a été démontrée.

Un système plus réaliste a été également examiné dans lequel chaque utilisateur dispose d'une nombre de bits total limité pour CQI et CDI sur la voie de retour. Dans ce scénario, le compromis existant entre la diversité multi-utilisateur et le gain de multiplexage a été identifié, découlant du fait que les bits de feedback disponibles doivent être partagés pour la quantification de CQI et CDI. Le problème de l'optimisation de la distribution de bits pour CQI/CDI a été abordée, ce qui révèle une interaction intéressante entre le nombre d'utilisateurs, la moyenne du rapport signal sur bruit et le nombre de bits de feedback. Alors que dans les systèmes à faible nombre d'utilisateurs la plupart des bits sont alloues à CDI, il devient plus avantageux d'allouer bits à CQI pour un nombre élevé d'utilisateurs. D'autre part, quand le SNR

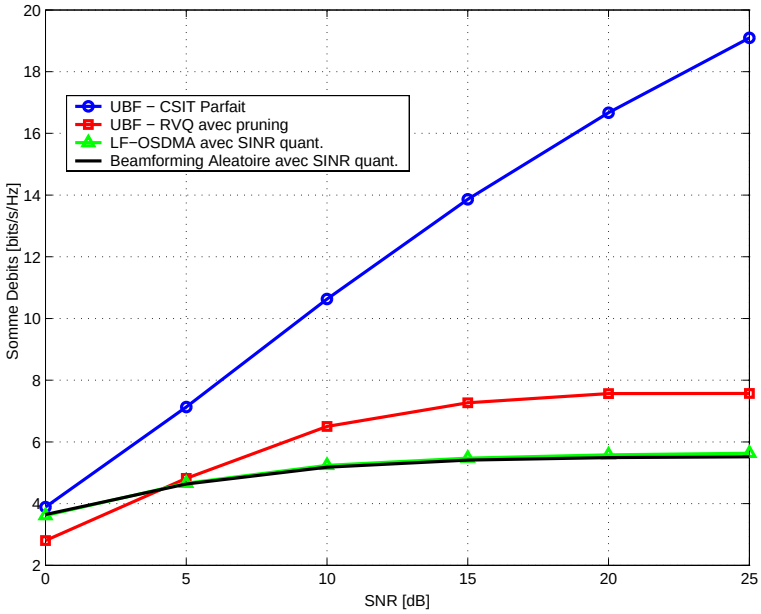


Figure 12: Somme des débits en fonction de SNR moyen dans un système avec beamforming linéaire et sélection d'utilisateurs, $M = 4$ antennes, $K = 10$ utilisateurs, et $B = 10$ bits sur la voie de retour.

moyen augmente, plus de bits devraient être alloués à CDI.

Nous avons aussi abordée le problème de conception des codebooks pour la quantification des canaux MIMO multi-utilisateur, dans les systèmes avec beamforming linéaire et sélection d'utilisateurs. Plutôt que de considérer un cadre séparé pour CQI et CDI, comme étudié dans la partie précédente, un simple cadre a été examiné dans lequel chaque utilisateur quantifie directement son vecteur canal ou l'erreur de prédiction. Des techniques de génération des codebooks ont été proposées, fondées sur l'adéquation entre les codebooks de quantification et les statistiques des canaux, exploitant les corrélations temporelles et spatiales. Nos résultats ont montré que des gains de performance peuvent être atteints en utilisant des codebooks de quantification optimisés en fonction des statistiques dans la cellule.

La conception de techniques optimisées de beamforming a été abordée dans la dernière partie de cette thèse. Une méthode d'optimisation itérative de beamforming unitaire a été proposé, basées sur l'optimisation successive des rotations de Givens. La technique proposée fournit une croissance linéaire

de la somme des débits en fonction du nombre d'antennes de transmission si un CSIT parfait est disponible. En outre, il montre une robustesse aux erreurs d'estimation, en fournissant une somme des débits meilleure que le beamforming ZF et même beamforming MMSE quand la variance de l'erreur d'estimation augmente.

L'approche de beamforming unitaire proposée a été évaluée dans des scénarios multi-utilisateur avec voie de retour à débit limité. Une technique de quantification vectorielle de complexité réduite a été utilisée, basée sur la quantification aléatoire des vecteurs. Notre travail met en évidence l'importance de l'optimisation de beamforming linéaire dans scénarios avec feedback limité. Plutôt que de concevoir des systèmes complexes de feedback, en s'appuyant sur des techniques de transmission simples, la performance du système peut être améliorée en utilisant un beamforming linéaire optimisé et des stratégies simples de quantification du canal.

Tout au long de cette thèse, nous avons insisté sur le fait que l'optimisation conjointe des différentes parties des systèmes de communication MIMO sans fil est nécessaire afin d'offrir de bonnes performances, avec un bas débit sur la voie de retour. Certains aspects d'intérêt pratique pour de tels systèmes de communication ont été optimisés, en considérant principalement des scénarios réalistes avec un nombre raisonnable d'utilisateurs et d'antennes de transmission, et des conditions habituelles de SNR moyen. L'obtention de CSIT dans les systèmes sans fil actuels est coûteuse, car les ressources disponibles sur la voie montante sont limitées. Ainsi, toute source de CSIT, instantanée ou statistique, doit être exploitée à l'émetteur afin d'améliorer la performance du système.

# Chapter 1

# Introduction

The ever increasing growth of IP-based wireless services has dictated the evolution of mobile communication standards over the past years. Third and fourth generation of wireless communication systems support packet-oriented services, which are more delay tolerant than conventional voice services but require very high throughput. The spectral efficiency of wireless systems can be significantly improved by means of multiple-input multiple-output (MIMO) technologies, exploiting the spatial dimension in addition to the time and frequency dimensions exploited in single-input single-output (SISO) systems. MIMO systems have received considerable attention since they provide reliable, high data rate communication. In point-to-point MIMO systems, multiple antennas can exploit the spatio-temporal diversity by means of space-time coding (STC), achieving low error rates in the absence of channel state information at the transmitter (CSIT). If a certain degree of CSIT is available, this knowledge can be utilized in order to improve the data rate through spatial multiplexing, by transmitting independent data streams. In the downlink of a cellular system with multiple antennas at the base station, CSIT can be incorporated to serve users at different locations by means of space division multiple access (SDMA), for the purpose of system throughput maximization.

In practical wireless communication systems, channel state information at the receiver (CSIR) can be easily obtained through training. On the other

hand, obtaining CSIT is a complicated task that requires exploiting channel reciprocity or acquiring feedback from the receiver. Hence, any available source of partial CSIT, instantaneous or statistical, needs to be exploited in order to optimize the system performance. This dissertation addresses the problem of optimizing the performance of MIMO systems with partial CSIT, providing practical solutions to present and future challenges in single user and multiuser MIMO wireless networks. The remainder of this chapter provides a brief overview of this dissertation. In addition, a detailed list of technical contributions is also provided.

## 1.1 Thesis Overview and Outline

This dissertation is composed of two parts. In the first part, comprising Chapter 2, point-to-point MIMO channels are considered for the purpose of error rate minimization in single user scenarios. In the second part, comprising Chapters 3 through 6, the problem of maximizing the sum-rate in MIMO broadcast channels is addressed, providing practical designs for user scheduling algorithms, feedback strategies and transmission schemes. An abstract and introduction is provided at the beginning of each chapter.

### 1.1.1 Point-to-Point MIMO Channels

MIMO systems have received considerable attention in response to the increasing requirements of high throughput in wireless communications. The capacity of point-to-point MIMO channels increases linearly with the minimum of the number of transmit and receive antennas, assuming that the fading coefficients between all antenna pairs are statistically independent and known to the receiver [4], [5]. The spatial diversity provided by MIMO systems can be exploited to reduce the error rate by transmitting the information signal over independently faded branches, or to increase the rate by transmitting independent data streams. It has been shown [6] that there exists a tradeoff between the spatial multiplexing gain

$$r = \lim_{SNR \to \infty} \frac{\mathcal{R}(SNR)}{\log SNR} \tag{1.1}$$

and the diversity gain

$$-d = \lim_{SNR \to \infty} \frac{\log \mathcal{P}_e(SNR)}{\log SNR} \tag{1.2}$$

which are defined in the high signal-to-noise (SNR) regime, given the system rate $\mathcal{R}$ and average error probability $\mathcal{P}_e$. This tradeoff is due to the fact that there is a certain number of degrees of freedom in the MIMO channel that need to be shared in order to achieve diversity or increase the transmission rate. In the absence of CSIT, multiple antennas can exploit the spatial diversity by means of space-time coding, making use of the spatial and temporal dimension [7], [8], [9]. A simple orthogonal space-time block code (O-STBC) was proposed by S. M. Alamouti in [7] for systems with 2 transmit antennas and $N$ receive antennas, which achieves full diversity order of $2N$, which equals the number of independently faded branches. An extension to higher number of transmit antennas was proposed in [8]. If the transmitter has additional channel knowdledge, either instantaneous or statistical, perfect or partial, the performance of such systems can be further improved.

In Chapter 2, the design of simple mechanisms to incorporate partial CSIT at the transmitter side of ST-coded MIMO systems is addressed. The goal consists of designing linear precoders that use statistical information to improve the system performance and that can be concatenated with STC, thus providing a flexible and robust solution. The performance measure of interest in this chapter is the pairwise error probability (PEP) averaged over the channel statistics. As partial CSIT, mean and covariance information are considered, which, as we describe, can reflect different practical scenarios.

### 1.1.2 MIMO Broadcast Channels

The interest in MIMO systems has shifted from point-to-point MIMO channels to MIMO broadcast channels during the last years. As shown in [10], [11], the capacity can be boosted by exploiting the spatial multiplexing capability of transmit antennas, transmitting to multiple users simultaneously over the same bandwidth by means of SDMA, rather than trying to maximize the capacity of a single-user link. If a base station with $M$ transmit antennas communicating with $K$ single-antenna receivers has perfect channel state information (CSIT), a multiplexing gain of $\min(M, K)$ can be achieved. In cellular systems, this is a setting of practical interest, since multiple antennas can be easily deployed at the base station.

It has recently been proven [12] that the capacity region of the MIMO broadcast channel is achieved by dirty paper coding (DPC) [1]. The fundamental idea behind this technique is that when the interference is known non-causally at the transmitter, it is possible to achieve the same capacity

as if there were no interference. However, this technique has two main disadvantages that limit its applicability: a high computational complexity and the need for full CSIT. Hence, it is of particular interest to identify what kind of partial CSIT can be conveyed to the BS and what type of low-complexity transmission techniques can be used in order to achieve sum rates reasonably close to the optimum.

Lack of perfect CSIT in point-to-point MIMO systems simply translates into an offset in the capacity versus SNR curve. The slope is not affected by imperfect channel knowledge and thus the multiplexing gain does not change. However, in MIMO broadcast channels, the level of CSIT critically affects the system performance, and thus feedback design has a greater importance in such systems. This is due to the fact that CSI not only provides better SNR at the receiver side, but also reduces the interference from data intended to other users in the cell. Thus, in a multiuser MIMO environment, co-channel interference must be taken into account for throughput maximization. In a system with $K$ users, the capacity region is characterized by a $K$ dimensional volume. The maximum achievable system throughput is the sum capacity, which is the point in the capacity region that maximizes the sum of all users' information rates. Our goal is to design systems based on partial CSIT that provide sum rates close to the sum capacity while exhibiting reasonable complexity.

A promising low complexity alternative to DPC for the downlink of MIMO systems is linear beamforming. Downlink linear beamforming, although suboptimal, has been shown to achieve a large portion of the DPC capacity, exhibiting the best tradeoff between complexity and performance [13], [14], [15], [16]. In order to achieve the optimal capacity growth of $M \log \log K$ for $K \to \infty$ and single antenna receivers, linear beamforming schemes need to be combined with efficient multiuser scheduling algorithms that exploit multiuser diversity [17]. However, finding the optimal beamforming vectors is a non-convex optimization problem, and the optimal solution for a downlink channel with $K$ users is given by exhaustive search over all possible combinations. Evidently, the complexity of the above problem becomes prohibitively high for large $K$. Thus, we are interested in designing suboptimal linear beamforming techniques that, combined with efficient low-complexity multiuser scheduling algorithms, provide high sum rates.

In realistic scenarios, it is not reasonable to assume that all channel coefficients from each user can be perfectly fed back to the transmitter. Accurate CSIT is difficult to realize in practice, especially in frequency-division duplex

(FDD) systems. Training can be used to obtain channel estimates at the receiver side and thus the assumption of perfect CSIR is reasonable. Methods for obtaining instantaneous CSIT can in general be of two types, by exploiting channel reciprocity (in TDD systems) or by obtaining feedback from the mobile terminals. In reciprocity-based approaches, the CSIT is obtained in the uplink, which in turn is used for downlink transmission. In the latter case, each mobile user obtains estimates of its own channel by using pilot symbols transmitted in the downlink. The users feedback information to the base station by using a dedicated feedback link. Identifying the type of feedback that has to be made available at the base station in order to achieve high sum rates is a critical issue that is addressed in this dissertation.

Based on the above motivations, the second part of this dissertation focuses on systems with joint linear beamforming and multiuser scheduling with limited feedback. In general, a single-cell setting is considered, in which the base station has multiple antennas and each user terminal is equipped with a single antenna receiver. The goal consists of maximizing the sum-rate performance of such systems, while satisfying an average power constraint at the transmitter. At a PHY/MAC level, we focus on the optimization of the following aspects: feedback strategies, feedback quantization techniques, user scheduling algorithms and linear beamforming techniques. However, a joint optimization of all these elements is rather complicated. When optimizing such networks, we address the following issues:

- What *feedback measures* are of importance at the base station in order to design spatial transmission filters and exploit the multiuser diversity?
- How should users perform *feedback quantization* in order to optimize the system performance for a given available feedback rate?
- How should *multiuser scheduling algorithms* be designed in order to exploit multiuser diversity while exhibiting reasonable complexity?
- How to design robust *linear beamforming* techniques in limited feedback scenarios?
- Can we find *joint solutions* to these problems?

Chapter 3 provides a general perspective of the challenges in systems with joint linear beamforming and multiuser scheduling. An overview of these systems is provided, introducing some standard linear beamforming

techniques and multiuser scheduling algorithms. The remainder of the chapter is devoted to low-complexity solutions to the joint linear beamforming and multiuser scheduling problem. Initially, a scenario with perfect CSIT is considered, in which a simple scheduling algorithm and linear beamforming technique based on orthogonal beams are presented. This leads to a dramatic complexity reduction in the multiuser scheduling part with respect to exhaustive user search. In the last part of this chapter, an integral low-complexity solution is proposed in a scenario with limited feedback. As we show, simple codebooks adapted to the transmit spatial correlation can yield large performance gains. In addition, a bound on the multiuser interference experienced by each user is derived, based on a geometric interpretation of the problem. This bound is of practical importance since, as we show in the following chapters, since it can be used for the design of feedback metrics for the purpose of user selection.

In Chapter 4, a design framework for scalar feedback in MIMO broadcast channels is proposed. We consider limited feedback scenarios in which each user conveys channel quality information to the base station for the purpose of user scheduling along with channel direction information. A family of metrics is presented based on bounds on the individual SINRs, which are computed at the receivers and fed back to the base station as channel quality information. Based on this framework, the sum rate of systems with joint linear beamforming, multiuser scheduling and limited fedback is analyzed, in a variety of asymptotic regimes. Particular importance is given to the comparison between time division multiple access (TDMA) and SDMA techniques, due to its timely relevance in the current developments of wireless standards. The effect of quantization on such scalar feedback is also studied, introducing the tradeoff between multiuser diversity and multiplexing gain that arises in scenarios with a finite sum-rate feedback model.

In Chapter 5, an alternative limited feedback model to the one presented in Chapter 4 is considered, in which the users quantize directly their vector channels by using optimized channel quantization codebooks, thus embedding channel direction and quality information in a single codebook. We focus on the design of such quantization codebooks for MIMO broadcast channels, adapting them to arbitrary linear beamforming techniques and multiuser scheduling algorithms. The proposed quantization codebooks exploit spatial and temporal correlations in the system, providing performance increases over non optimized channel quantization techniques.

Chapter 6 addresses the design of linear beamforming techniques for

MIMO broadcast channels. So far, most designs in the literature, and also the schemes considered for future wireless standards, rely on simple beamforming techniques, focusing on the design of accurate and meaningful feedback measures. In this chapter, we highlight the importance of designing linear beamforming techniques robust to noisy CSIT. A linear beamforming technique based on iterative optimization of unitary matrices is proposed, which achieves linear sum-rate growth with the number of transmit antennas and outperforms common linear beamforming techniques under imperfect CSIT conditions. As our results show, the performance of a system with joint linear beamforming and multiuser scheduling in limited feedback scenarios can be improved by optimizing the linear beamformers, combined with simple feedback design and quantization techniques.

Finally, the general conclusions reached in this dissertation are presented, summarizing the main results obtained as well as future challenges of MIMO technologies.

## 1.2 Contributions

The contribution in Chapter 2 is the derivation of linear precoding schemes that minimize an upper bound on the pairwise error probability [18], [19]. Our work generalizes the work presented in [20], by averaging the PEP over a Gaussian distribution - prior or posterior - that can correspond to different scenarios, providing a solution to the general problem and a variety of particular cases.

In Chapter 3, the two main contributions are the low-complexity schemes proposed in [21] and [22], for perfect CSIT and limited feedback, respectively. The former, coined as orthogonal linear beamforming (OLBF), consists of a joint solution for beamforming and scheduling which aims at reducing the complexity of exhaustive-search user selection algorithms, and builds upon the work presented in [2] for limited feedback scenarios. The second part of the chapter proposes a scheme which exploits the spatial correlation at the transmitter in a setting with limited feedback. The users are assigned a fixed channel quantization vector - which is used as beamforming vector - and feed back information regarding the channel strength and quantization error. We derive a useful upper bound on the multiuser interference, which is computed at the base station for the purpose of user selection.

The contributions in Chapter 4 are the result of a number of publications

in the quest for high-performance scalar feedback measures. In Chapter 4, a design framework is proposed [23] that generalizes the work in [24], [25], [26], [27], as well as other scalar measures used in well known approaches such as [2] or [28]. After deriving an approximated cumulative distribution function for the proposed family of metrics and its associated sum rate approximation, our framework enables us to perform simple asymptotic analysis in different regimes, namely: large number of users, high SNR regime and low SNR regime. In addition, a clarifying comparison between TDMA and SDMA is given under different conditions, highlighting the importance of allowing a variable number of active beams at the transmitter. We identify the multiuser diversty vs. multiplexing gain tradeoff arising in scenarios where the total sum of bits for channel direction information and channel quality information - contained in the scalar feedback - is limited [29].

In Chapter 5, new codebook design approaches are proposed [30]. A Monte Carlo approach is used to generate optimized channel quantization codebooks in order to exploit the cell statistics, by minimizing the average sum rate distortion. In the first part, we stress the importance of adapting the codebook to non uniform user distributions. In the second part, predictive vector quantization is used to improve the performance by exploiting temporal correlations.

A novel method for iterative optimization of unitary beamformers is proposed in Chapter 6 [31], [32], based on successive optimization of Givens rotations. A convergence and complexity study is presented, evaluating the performance through simulations in several scenarios. As we show, the proposed technique achieves linear sum-rate increase with the number of transmit antennas and perfect channel knowledge at the transmitter side. More importantly, the proposed unitary beamforming approach proves to be very robust to channel estimation errors. When combined with simple vector quantization techniques for CSI feedback in MIMO broadcast channels, the proposed technique is shown to be well suited for limited feedback scenarios.

Other articles published in parallel during the course of this thesis, which have not been included in this dissertation, are the following. In [33], linear precoders that exploit the covariance information of the MIMO channel are presented, which are combined with spatio-temporal spreading. In the context of WCDMA systems, adaptive complexity equalizers have been proposed in [34].

# Part I

# Point-to-Point MIMO Channels

# Chapter 2

# Linear Precoding

*In this chapter techniques are proposed for combining information about the mean and the covariance of the channel for the purpose of MIMO transmission in point-to-point systems. Partial channel state information at the transmitter (CSIT) is typically used in MIMO systems for the design of spatial prefiltering and waterfilling. For the purpose of generating CSIT, the cases of mean or covariance information have generally been solved separately in the literature. A Bayesian approach is presented here incorporating both pieces of information. The proposed Bayesian approach encompasses the existing cases of mean or (transmit) covariance information as special instances. Various cases of mean and covariance information are discussed, including prior mean and covariance (Ricean channel distribution) and posterior mean and covariance (based on a noisy channel estimate and prior covariance information). For a given Gaussian channel distribution (prior or posterior), an optimized linear precoding solution is derived, which minimizes an upper bound on the pairwise error probability in a space-time coded system. In addition, several particular cases of practical interest are studied, namely: zero mean information, unit rank mean and singular covariance information. Simulation results illustrate the performance benefits that can be reached by effectively exploiting the available mean and covariance information in point-to-point MIMO systems.*

## 2.1 Introduction

In practical wireless systems, training sequences or pilot symbols are incorporated in the transmitted signal to allow for channel estimation at the receiver. The density of training data needs to increase as the mobility and the channel variation increases. Nevertheless, even with training data available, the channel estimate can only be of limited quality, and the channel estimation errors reduce the channel capacity. Furthermore, the fact of substituting information symbols by training symbols obviously limits the capacity. Channel knowledge at the transmitter helps improving the system throughput in wireless systems. A means to obtain CSIT consists of feeding back to the transmitter channel estimates obtained at the receiver. Since the bandwidth available is limited, all statistical information about the channel should be taken into account. For instance, a priori information on the channel distribution can be used to yield improved channel estimates, leading to a posterior channel distribution, as we show in this chapter.

The presence of severe correlations has important detrimental effects on the capacity and performance of MIMO systems. In fact, most space-time code designs assume independent Rayleigh fading for each stream, which in practice is not true as shown in [35]. The problem has been addressed by transmitting on the eigen-modes of the transmit antenna correlation matrix [36], which yields better performance and capacity gains. In [37], a prefiltering approach is proposed assuming partial CSIT, where knowledge of the transmit antenna correlations is successfully exploited to improve the pairwise error probability (PEP) of a space-time (ST) coded system.

In order to exploit partial CSIT in point-to-point MIMO systems, most of the current precoding schemes exploit either information about the mean [38] or the covariance [37]. A combination of the two can improve exploitation of channel knowledge by weighting them according to certain criteria. In [20], the combination of mean and covariance information at the transmitter side of a point-to-point MIMO system is considered, for the purpose of PEP minimization. In that work, the transmitter concatenates orthogonal space-time block coding (O-STBC) and linear precoding. The available CSIT is used to design an optimized linear precoder, which adapts the transmitted ST codewords to the channel statistics. However, no closed form solution is provided to the general problem, and the optimal precoder is solved numerically. In our work, we consider a similar scenario, in which the linear precoder is optimized in order to minimize an upper bound on the PEP. Following the

optimization problem formulated in [20], we provide a closed form solution. In addition, several particular cases of practical interest are studied, namely: zero mean information, unit rank mean and singular covariance information. Independently to the work presented herein, similar results were obtained in [39] for non-zero mean channels with transmit correlation. Practical aspects such as the asymptotic PEP reduction at high SNR provided by a mean component can be found in [40].

In our work, we present different techniques to combine mean and covariance information. We show how to exploit both sources of partial CSIT to optimize the error rate in MIMO systems, by performing linear precoding at the transmitter. As we describe, the source of partial CSIT can be of different nature. It may correspond to a Ricean distribution with a line-of-sight (LOS) component, or perhaps to a noisy channel estimate with known noise covariance. In addition, mean and covariance information do not necessary have to correspond to prior distributions, but they can be given by a Bayesian approach, with a certain posterior mean and covariance. To that end, we provide a generalized perspective, in which the system performance is optimized over a Gaussian channel distribution.

## 2.2 MIMO Channel Model

A point-to-point multiple antenna channel is considered, in which a transmitter equipped with $M$ antennas communicates with a receiver that has $N$ antennas. Representing the impulse response between transmit antenna $m$ and receive antenna $n$ as $\mathbf{h}_{nm}$, the MIMO channel is described by the following $N \times M$ matrix

$$\mathbf{H} = \begin{bmatrix} \mathbf{h}_{11} & \mathbf{h}_{12} & \dots & \mathbf{h}_{1M} \\ \mathbf{h}_{21} & \mathbf{h}_{22} & \dots & \mathbf{h}_{2M} \\ \vdots & \vdots & \ddots & \vdots \\ \mathbf{h}_{N1} & \mathbf{h}_{N2} & \dots & \mathbf{h}_{NM} \end{bmatrix} \tag{2.1}$$

A flat-fading MIMO channel is assumed, with random complex Gaussian entries and separable covariance structure. Hence

$$\mathbb{E}\mathbf{H}\mathbf{H}^H = \mathrm{tr}\{C_T\}C_R \tag{2.2}$$

$$\mathbb{E}\mathbf{H}^T\mathbf{H}^* = \mathrm{tr}\{C_R\}C_T \tag{2.3}$$

where $C_R$ and $C_T$ denote the covariance matrix between transmit and receive antenna elements, respectively. The vectorized channel is defined as $\mathbf{h} = vec(\mathbf{H})$, which stacks the columns of $\mathbf{H}$ in a vector of dimension $MN \times 1$. The $MN \times MN$ covariance matrix for the MIMO channel is denoted as $C_{\mathbf{hh}}$, which in our separable model can be factorized as

$$C_{\mathbf{hh}} = C_T \otimes C_R \tag{2.4}$$

where $\otimes$ denotes Kronecker product. In addition, the MIMO channel may have a certain mean, denoted as $m_{\mathbf{H}}$. The vectorized version of dimension $MN \times 1$ is denoted as $m_{\mathbf{h}}$. As a special case, if the MIMO channel has separable mean structure, the vectorized mean can be represented as $m_{\mathbf{h}} = m_T^* \otimes m_R$ and in matrix form as $m_{\mathbf{H}} = m_R m_T^H$.

## 2.3 System Description

The transmitter encodes the information bits into a ST codeword $\mathbf{C}$ of dimension $M \times T$, where $T$ is the block length, i.e. the number of time instants spanned by a ST codeword. A quasi-static scenario is considered, where the MIMO channel is assumed to remain constant during the transmission of a ST codeword. Prior to transmission, the ST codewords are prefiltered with the matrix $\mathbf{W}$ of dimension $M \times M$, which is determined by taking into account mean and covariance information, as we detail in the following sections. The linear precoding uses this statistical information to improve the system performance of the ST coded system, by minimizing pairwise error probability. In the presence of zero-mean additive white Gaussian noise, the received signal is given by

$$\mathbf{Y} = \mathbf{HWC} + \mathbf{V} \tag{2.5}$$

where the noise covariance matrix is $C_{\mathbf{vv}} = \sigma^2 \mathbf{I}_{MN}$. The matrices $\mathbf{Y}$ and $\mathbf{V}$ have dimension $N \times T$. The transmitted data is recovered by means of a Maximum Likelihood (ML) receiver.

## 2.4 Partial CSIT Combining Mean and Covariance

When mean and covariance information are present at the transmitter side, this information can be of different nature. In the presence of a LOS com-

ponent between transmitter and receiver, the MIMO channel may be modeled as Ricean. In this first case of interest, the vectorized channel $\mathbf{h}$ has a prior distribution $\mathbf{h} \sim \mathcal{CN}(m_{\mathbf{h}}, C_{\mathbf{hh}})$, with mean $m_{\mathbf{h}}$ due to the LOS component. The Ricean channel can be modeled as $\mathbf{H} = m_{\mathbf{H}} + C_R^{1/2}\mathbf{H}_w C_T^{H/2}$ with $\mathbf{h}_w = vec(\mathbf{H}_w)$ distributed as $\mathcal{CN}(\mathbf{0}, \mathbf{I}_{MN})$.

A second scenario is the case when mean information corresponds to the channel estimate and perfect covariance information is present at the transmitter. The channel in this case is modeled as Rayleigh with distribution $\mathbf{h} \sim \mathcal{CN}(\mathbf{0}, C_{\mathbf{hh}})$. On the other hand, the channel estimates can be modeled as $\widehat{\mathbf{H}} = \mathbf{H} + \widetilde{\mathbf{H}}$, with $\widetilde{\mathbf{h}} = vec(\widetilde{\mathbf{H}})$ following a distribution $\mathcal{CN}(\mathbf{0}, \sigma^2_{\widetilde{h}}\mathbf{I}_{MN})$, and could be due to a combination of the following sources of error: estimation noise, quantization noise and prediction noise. The combination of mean and covariance information leads to a Gaussian posterior distribution with posterior mean given by

$$\widehat{\widehat{\mathbf{h}}} = (\mathbf{I}_{MN} + \sigma^2_{\widetilde{h}}\, C_T^{-1} \otimes C_R^{-1})^{-1}\widehat{\mathbf{h}} \tag{2.6}$$

and posterior covariance

$$\widehat{C}_{\mathbf{hh}} = (\sigma^{-2}_{\widetilde{h}}\, \mathbf{I}_{MN} + C_T^{-1} \otimes C_R^{-1})^{-1}. \tag{2.7}$$

The expressions for posterior mean and covariance are found by refining the channel estimates $\widehat{\mathbf{H}}$ (mean information), assuming that the statistics of $\mathbf{H}$ and $\widetilde{\mathbf{H}}$ are known, as shown in Appendix 2.A. If only posterior mean is present, it is due to noise-free channel estimation ($\sigma^2_{\widetilde{h}} \to 0$) and thus $\|\widehat{C}_{\mathbf{hh}}\|_F \to 0$. On the other hand, only posterior covariance will be present if $\widehat{\widehat{\mathbf{h}}} = \widehat{\mathbf{h}} = \mathbf{0}$, or if the estimation noise tends to infinity. In addition, if a rich scattering environment is assumed at the receiver side, the covariance at the receiver can be modeled as identity. In this case, the posterior (unvectorized) mean is given by

$$\widehat{\widehat{\mathbf{H}}} = \widehat{\mathbf{H}}(\mathbf{I}_M + \sigma^2_{\widetilde{h}}\, C_T^{-1})^{-1} \tag{2.8}$$

and the posterior covariance

$$\widehat{C}_{\mathbf{hh}} = \widehat{C}_T \otimes \mathbf{I}_N \tag{2.9}$$

with posterior covariance seen from the transmitter

$$\widehat{C}_T = (\sigma^{-2}_{\widetilde{h}}\, \mathbf{I}_M + C_T^{-1})^{-1}. \tag{2.10}$$

In a simplified scenario with noisification of the mean, assume we only have access to $\mathbf{D}\widehat{\widehat{\mathbf{H}}}$ instead of having acess to $\widehat{\widehat{\mathbf{H}}}$ directly, where the elements of the diagonal matrix $\mathbf{D}$ are i.i.d. $\mathcal{CN}(0,1)$. Now the distribution becomes zero mean with transmit side covariance matrix $\widehat{R}_T = \widehat{\widehat{\mathbf{H}}}^H \widehat{\widehat{\mathbf{H}}} + \widehat{C}_T$. Under these circumstances, the mean information falls into the covariance information, and thus the correlation becomes the covariance. Hence, optimal MIMO transmission schemes with partial CSIT for the case of only covariance information will apply for the described model that combines mean and covariance information. If linear prefiltering is carried out at the transmitter side (after the ST encoding stage) to adapt the transmission to the channel knowledge, an optimal prefilter will lead to capacity maximization or typically PEP minimization. If we assume $C_R = \mathbf{I}_N$, the optimal prefilter that maximizes capacity and minimizes PEP pours power along the eigenvectors of the posterior correlation matrix seen from the transmitter, following a waterfilling power allocation policy for minimum PEP [37] and possibly different weighting for the capacity maximization solution [41].

## 2.5 Linear Precoding for Error Rate Minimization

In this section, we derive an optimal precoding strategy for error rate minimization in MIMO systems combining mean and covariance information at the transmitter. The source of mean and covariance information can be either prior or posterior, as described in the previous section. We optimize the performance of the proposed system in terms of PEP averaged over $\mathbf{h}$, prior or posterior, with a distribution $\mathcal{CN}(m_{\mathbf{h}}, C_{\mathbf{hh}})$. We assume identity covariance matrix at the receiver. In the analysis, we follow the work developed by *Jongren et al.* in [20].

The transmitter is supposed to have a codebook containing a finite number of ST codewords. Our goal consists of designing a linear precoder, which minimizes the PEP for the ST encoded system by incorporating statistical knowledge. The PEP is defined as the error probability of choosing the nearest distinct codeword $\mathbf{C}^j$ instead of $\mathbf{C}^i$. The code error matrix can be defined as $\widetilde{\mathbf{E}}(i,j) \doteq \left[\mathbf{C}^i - \mathbf{C}^j\right]$. In practice, the average PEP is limited by the minimum distance code error matrix, given by $\mathbf{E} = \arg\min_{\widetilde{\mathbf{E}}(i,j)} \det\left[\widetilde{\mathbf{E}}(i,j)\widetilde{\mathbf{E}}^H(i,j)\right]$.

The average PEP is given by

$$P(\mathbf{C}^i \to \mathbf{C}^j) = \int P(\mathbf{C}^i \to \mathbf{C}^j|\mathbf{h})p_{\mathbf{h}}(\mathbf{h})d\mathbf{h} \tag{2.11}$$

where the complex Gaussian probability density function (pdf) $p_{\mathbf{h}}(\mathbf{h})$ is

$$p_{\mathbf{h}}(\mathbf{h}) = \frac{e^{-tr\left[(\mathbf{h}-m_{\mathbf{h}})^H C_{\mathbf{hh}}^{-1}(\mathbf{h}-m_{\mathbf{h}})\right]}}{\pi^{MN}\det(C_{\mathbf{hh}})}. \tag{2.12}$$

By applying the Chernoff bound and averaging over the distribution of $\mathbf{h}$, an upper bound on the average PEP is given by

$$P(\mathbf{C}^i \to \mathbf{C}^j) \leq \int e^{-d_{min}^2(\mathbf{C}^i,\mathbf{C}^j)/4} p_{\mathbf{h}}(\mathbf{h})d\mathbf{h}. \tag{2.13}$$

When concatenating the Space-Time encoder at the transmitter with a linear prefilter to exploit partial CSIT, the minimum Euclidean distance is

$$d_{min}^2(\mathbf{C}^i, \mathbf{C}^j) = d^2(\mathbf{E}) = \frac{1}{\sigma^2}\|\mathbf{HWE}\|_F^2 \tag{2.14}$$

where $\mathbf{W}$ is the linear prefilter. Note that the Chernoff bound is a convex function of $\mathbf{W}$, which greatly simplifies the search for an optimal $\mathbf{W}$ matrix. On the other hand, it can be shown that if $\mathbf{EE}^H = \alpha\mathbf{I}$, the PEP is minimized at high SNR for a given optimal prefilter. Thus, the system under consideration has $\mathbf{EE}^H = \alpha\mathbf{I}$, e.g. orthogonal ST block codes [8] (single stream) or ST spreading [42] (full stream). Let $\eta = \frac{\alpha}{4\sigma^2}$ and $\Psi = \mathbf{WW}^H$. Particularizing for the defined scenario, with separable covariance structure and identity covariance matrix at the receiver, the solution to (2.13) is given by

$$P(\mathbf{C}^i \to \mathbf{C}^j) \leq \frac{e^{\mathrm{tr}\left[m_{\mathbf{H}}C_T^{-1}\left((\eta\Psi+C_T^{-1})^{-1}-C_T\right)C_T^{-1}m_{\mathbf{H}}^H\right]}}{\det(\eta\Psi + C_T^{-1})^N\det(C_T)^N}. \tag{2.15}$$

The performance criterion can be expressed logarithmically (neglecting parameter-independent terms) as follows

$$J = \mathrm{tr}\left[m_{\mathbf{H}}C_T^{-1}\left((\eta\Psi + C_T^{-1})^{-1} - C_T\right)C_T^{-1}m_{\mathbf{H}}^H\right] - N\log\det(\eta\Psi + C_T^{-1}) \tag{2.16}$$

By solving the problem above, we obtain the following theorem.

**Theorem 2.1** Assuming a normalized average power constraint, the optimal $\Psi$ that minimizes the performance criterion in (2.16) is given by

$$\Psi = \left\{ \frac{1}{2\mu} \left[ N\mathbf{I}_M + \left( N^2\mathbf{I}_M + \frac{4\mu}{\eta} C_T^{-1} m_{\mathbf{H}}^H m_{\mathbf{H}} C_T^{-1} \right)^{\frac{1}{2}} \right] - \frac{1}{\eta} C_T^{-1} \right\}_+ \tag{2.17}$$

where $\mu$ is the Lagrange multiplier associated with the power constraint and $\{\cdot\}_+$ takes the positive semidefinite (PSD) part[1].

*Proof.* See Appendix 2.B. □

It can be seen straightforwardly from (2.17) that as $\eta$ tends to infinity (i.e. SNR tends to infinity), the optimal $\Psi$ tends to $\Psi = \frac{1}{M}\mathbf{I}_M$, since in this particular case the value of the Lagrange multiplier is $\mu = NM$. This result is equivalent to transmission without CSIT, which shows that as the SNR increases the importance of CSIT gets reduced. Another solution assuming full-rank $\Psi$ is provided in what follows, to have a more intuitive idea of the unequal power-loading policy at the transmitter. We define the eigenvalue decomposition $C_T^{-1} m_{\mathbf{H}}^H m_{\mathbf{H}} C_T^{-1} = \mathbf{U}\Sigma\mathbf{U}^H$ where $\mathbf{U}$ is a unitary matrix and $\Sigma = diag(\sigma_1, \sigma_2, \ldots, \sigma_M)$.

**Corollary 2.1** Assuming the matrix $\Psi$ is full rank, the solution to the optimization problem in (2.16) is given by

$$\Psi = \mathbf{U}\Lambda\mathbf{U}^H - \frac{1}{\eta} C_T^{-1} \tag{2.18}$$

where $\Lambda = diag(\lambda_1, \lambda_2, \ldots, \lambda_M)$. The elements in the matrix of eigenvalues $\Lambda$ are given by

$$\lambda_i = \frac{N + \sqrt{N^2 + 4\frac{\mu\sigma_i}{\eta}}}{2\mu}. \tag{2.19}$$

*Proof.* See Appendix 2.C. □

[1]Note that $\{\cdot\}_+$ is an extension of the scalar function $\max(0, x)$ to matrices. This operation can be done by calculating first the eigenvalue decomposition of the matrix argument, setting al nonnegative eigenvalues to zero, and computing the resulting positive semidefinite matrix.

To obtain the optimal precoder either from (2.17) or (2.18), let the eigenvalue decomposition of $\Psi$ be $\Psi = \mathbf{V}_\Psi \Lambda_\Psi \mathbf{V}_\Psi^H$. Since $\Psi = \mathbf{W}\mathbf{W}^H$, the optimal precoder is $\mathbf{W} = \mathbf{V}_\Psi \Lambda_\Psi^{1/2}$. Thus, the optimal transmission strategy as reflected in the above equations corresponds to transmission along the eigenvectors of a matrix that combines mean and covariance, and a waterfilling power allocation policy. The first and second term in (2.18) are differently weighted depending on the SNR and the covariance information. In the remainder of this section we introduce some particular cases of special interest.

### 2.5.1 Zero Mean Information

When the mean is zero, it can be seen from equation (2.17) that in this case $\Psi$ becomes

$$\Psi = \left\{ \frac{N}{\mu}\mathbf{I}_M - \frac{1}{\eta}C_T^{-1} \right\}_+ . \tag{2.20}$$

The value of the Lagrange multiplier can be analytically expressed as

$$\mu = \frac{NM}{\left[1 + \frac{1}{\eta}tr(C_T^{-1})\right]}. \tag{2.21}$$

It is clear from (2.20) and (2.21) that as the SNR increases the covariance information becomes less important, and $\Psi$ converges to a scaled identity matrix.

### 2.5.2 Unit Rank Mean

A particular case of interest is the case when the mean information has rank one. Since $m_{\mathbf{H}}$ is unit rank, also $C_T^{-1} m_{\mathbf{H}}^H m_{\mathbf{H}} C_T^{-1}$ becomes unit rank. The mean $m_{\mathbf{H}}$ can be represented as a combination of a pair of vectors $s$ and $t$, $m_{\mathbf{H}} = \mathbf{s}\,\mathbf{t}^H$. The solution for $\Psi$ in the case of unit rank mean derived from the full-rank solution in (2.18) is given by

$$\Psi = [u_1 \mathbf{U}_2]\Lambda[u_1 \mathbf{U}_2]^H - \frac{1}{\eta}C_T^{-1} \tag{2.22}$$

where $\Lambda = diag(1 + \frac{tr\left[C_T^{-1}\right]}{\eta}, 0, \ldots, 0)$, $u_1$ is the eigenvector associated with the only non-zero eigenvalue and $\mathbf{U}_2$ are arbitrary vectors chosen such that the matrix $[u_1 \mathbf{U}_2]$ forms an orthonormal basis. It can be seen from (2.22)

that as the SNR increases the solution approaches to beamforming along a single direction, defined by $C_T^{-1} m_{\mathbf{H}}^H m_{\mathbf{H}} C_T^{-1}$, which is a combination of mean and covariance information.

### 2.5.3 Singular Covariance Information

When the covariance information is singular, it can be modeled as follows

$$C_T = \left[X_{/\!/} X_{\perp}\right] \begin{bmatrix} \mathbf{A} & 0 \\ 0 & 0 \end{bmatrix} \left[X_{/\!/} X_{\perp}\right]^H \tag{2.23}$$

where $\perp$ and $/\!/$ represent singular and non-singular parts respectively. Let $\left[m_{\mathbf{H}/\!/} m_{\mathbf{H}\perp}\right] = m_{\mathbf{H}} \left[X_{/\!/} X_{\perp}\right]$ and $C_{T/\!/}$ be the non-singular part of $C_T$. The optimization problem in this case becomes

$$\begin{cases} J = \min\limits_{\Psi} tr \left[ m_{\mathbf{H}/\!/} C_{T/\!/}^{-1} \left(\eta \Psi_{/\!/} + C_{T/\!/}^{-1}\right)^{-1} C_{T/\!/}^{-1} m_{\mathbf{H}/\!/}^H \right] \\ \quad -N \log\det(\eta \Psi_{/\!/} + C_{T/\!/}^{-1}) - \eta tr\left(m_{\mathbf{H}\perp} \Psi_{\perp} m_{\mathbf{H}\perp}^H\right) \\ s.t.\ tr(\Psi_{/\!/} + \Psi_{\perp}) = 1 \end{cases} \tag{2.24}$$

where $\Psi = [\Psi_{/\!/} \Psi_{\perp}]^T$. The objective function $J$ can be divided in two optimization problems $J = J_{/\!/} + J_{\perp}$ minimized separately. The power constraints in both cases have to be adjusted so that $P_{/\!/} + P_{\perp} = 1$. Hence, each minimization problem has a different power constraint associated. The optimization problem for the singular part is given by

$$\begin{cases} J_{\perp} = \min\limits_{\Psi_{\perp}} -\eta tr\left(m_{\mathbf{H}\perp} \Psi_{\perp} m_{\mathbf{H}\perp}^H\right) \\ s.t.\ tr(\Psi_{\perp}) = P_{\perp} \end{cases} \tag{2.25}$$

In order to minimize the objective function in (2.25) subject to the power constraint, we introduce the following eigenvalue decompositions: $m_{\mathbf{H}\perp}^H m_{\mathbf{H}\perp} = \mathbf{V}_{m_\perp} \Lambda_{m_\perp} \mathbf{V}_{m_\perp}^H$ and $\Psi_{\perp} = \mathbf{V}_{\Psi_\perp} \Lambda_{\Psi_\perp} \mathbf{V}_{\Psi_\perp}^H$. By applying the following inequality $tr(AB) \leq \sum_i \lambda_i(A)\lambda_i(B)$, it can be seen that (2.25) is minimized (the trace is maximized) by setting $\mathbf{V}_{\Psi_\perp} = \mathbf{V}_{m_\perp}$. Let $\Lambda_{m_\perp} = diag(\lambda_{m_\perp,1}, \ldots, \lambda_{m_\perp,M})$ and $\Lambda_{\Psi_\perp} = diag(\lambda_{\Psi_\perp,1}, \ldots, \lambda_{\Psi_\perp,M})$ ordered decreasingly. The optimization problem becomes

$$\begin{cases} J_{\perp} = \min\limits_{\lambda_{\Psi_\perp,i}} -\eta \sum\limits_{i=1}^{M} \lambda_{\Psi_\perp,i} \lambda_{m_\perp,i} \\ s.t.\ \sum_{i=1}^{M} \lambda_{\Psi_\perp,i} = P_{\perp} \end{cases} \tag{2.26}$$

Clearly, the function described above is minimized (the summation is maximized) if all the power is transmitted along the strongest eigenvalue, $\lambda_{m_\perp,1}$. Hence, the solution is given by choosing $\lambda_{\Psi_\perp,1} = P_\perp$ and $\lambda_{\Psi_\perp,i} = 0$, $i = 2, 3, \ldots, M$. With this choice, the value of the objective function becomes $J_\perp = -\eta P_\perp \lambda_{m_\perp,1}$. Hence, the precoding solution corresponds to eigenbeamforming in the direction of the eigenvector of $m_{\mathbf{H}\perp}^H m_{\mathbf{H}\perp}$ associated with the largest eigenvalue $\lambda_{m_\perp,1}$. The remaining optimization problem for the non-singular part is given by

$$\begin{cases} J_{/\!/} = \min\limits_{\Psi_{/\!/}} tr\left[m_{\mathbf{H}/\!/} C_{T/\!/}^{-1}\left(\eta\Psi_{/\!/} + C_{T/\!/}^{-1}\right)^{-1} C_{T/\!/}^{-1} m_{\mathbf{H}/\!/}^H\right] \\ \qquad -N\log\det(\eta\Psi_{/\!/} + C_{T/\!/}^{-1}) - \eta P_\perp \lambda_{\perp 1} \\ s.t.\ tr(\Psi_{/\!/}) = P_{/\!/} = 1 - P_\perp \end{cases} \tag{2.27}$$

The solution for this part is equivalent to the general solution with waterfilling shown in (2.17), but with reduced dimension and power constraint due to singularities. On the other hand, an optimal power split solution exits $(P_{/\!/}, P_\perp)$ under certain circumstances such that $J(P_{/\!/}) = J_{/\!/}(P_{/\!/}) + J_\perp(1 - P_{/\!/})$ is minimized. If $J(P_{/\!/})$ has an absolute minimum $P_{/\!/|J_{min}}$, there are three different possibilities. If $0 < P_{/\!/|J_{min}} < 1$, the optimal power for the non-singular part is $P_{/\!/|opt} = P_{/\!/|J_{min}}$ and for the singular part $P_{\perp|opt} = 1 - P_{/\!/|opt}$. The solution is a combination of beamforming (in $\perp$ part) and waterfilling (in $/\!/$ part). If $P_{/\!/|J_{min}} \geq 1$ then $P_{/\!/|opt} = 1$ and $P_{\perp|opt} = 0$, and the solution is given by waterfilling in the non-singular part. Finally, if $P_{/\!/|J_{min}} \leq 0$ then $P_{/\!/|opt} = 0$ and $P_{\perp|opt} = 1$, and the solution is given by beamforming in $m_\perp^H m_\perp$.

## 2.6 Simulation Results

The system considered is 2x2 O-STBC as described in [8] with QPSK modulation. The symbols are transmitted over a channel with an arbitrary mean and a correlation factor $\rho$ (cross-diagonal terms in $C_T$).

Figure 2.1 shows the gain in performance that can be obtained w.r.t. a non-precoded system by combining mean and covariance knowledge. We can observe a remarkable improvement in the simulated range of up to approximately 2.5 dB in SNR decrease for a given PEP. In this particular case, the performance is close to the one achieved by an optimal prefilter with perfect CSIT.

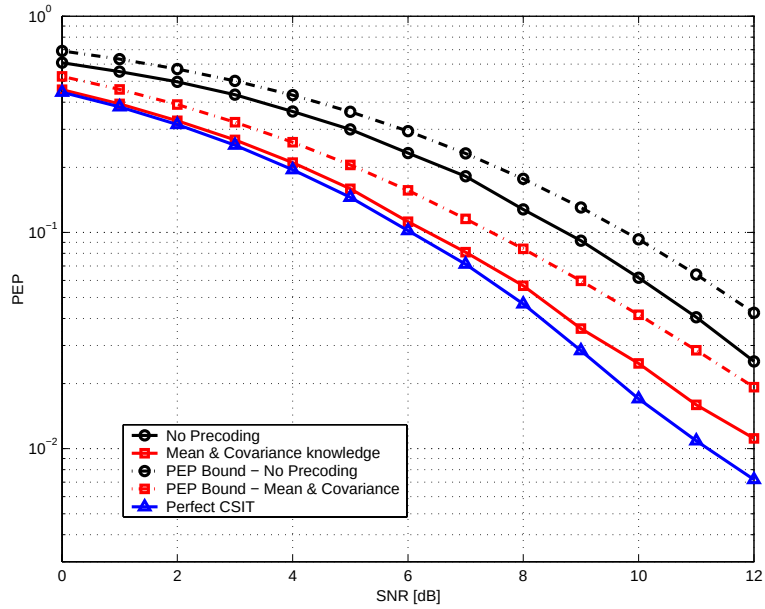


Figure 2.1: PEP vs. SNR for different CSIT levels, $\rho = 0.9$ and $\gamma = 40\%$

In Figure 2.2 we compare the performance of a system with only covariance or mean knowledge at the transmitter and a system with both sources of CSIT. As we have shown, the cases of only mean or covariance CSIT can be considered special instances of a system that combines both. The contribution of the mean to the average channel power is denoted by $\gamma$.

## 2.7 Conclusions

In this chapter, techniques for combining mean and covariance information have been presented. Both sources of information can be either prior (e.g. correlated channel with LOS) or posterior (given by a Bayesian approach). We have provided a general precoding solution for PEP minimization when combining both sources of partial CSIT at the transmitter, and analyzed some cases of special interest. The simulation results have shown how mean and covariance information should be combined in order to exploit the available sources of CSIT in point-to-point MIMO systems.

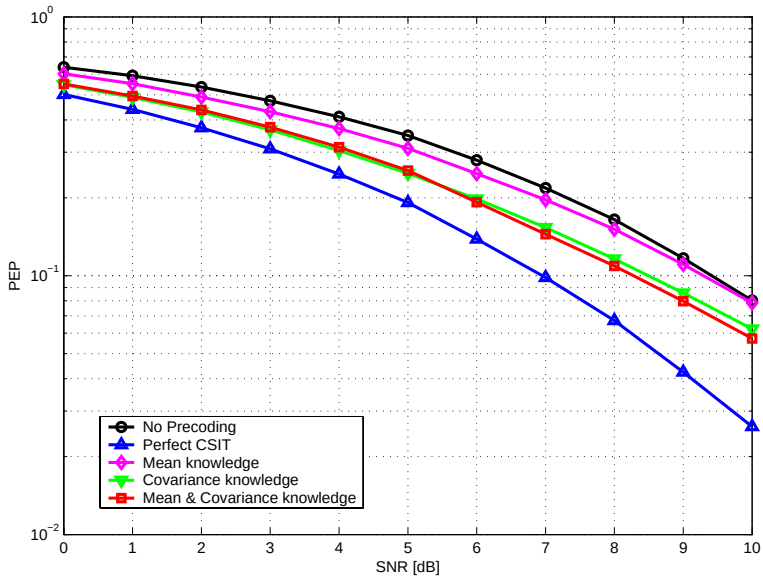


Figure 2.2: PEP vs. SNR for different CSIT levels, $\rho = 0.9$ and $\gamma = 20\%$

# APPENDIX

## 2.A Derivation of Posterior Ditribution

Assuming the additive noise model $\widehat{\mathbf{h}} = \mathbf{h} + \widetilde{\mathbf{h}}$, our goal is to find the posterior distribution of $\mathbf{h}$, given knowledge of the distributions of $\widetilde{\mathbf{h}}$ and $\mathbf{h}$ and perfect knowledge of $\widehat{\mathbf{h}}$. Let $p_{\mathbf{h}}(\mathbf{h})$ and $p_{\widehat{\mathbf{h}}}(\widehat{\mathbf{h}})$ be the probability density functions of $\mathbf{h}$ and $\widehat{\mathbf{h}}$, respectively. We are interested in finding the posterior distribution (or conditional distribution) of $\mathbf{h}$ conditioned on $\widehat{\mathbf{h}}$, denoted as $p_{\mathbf{h}|\widehat{\mathbf{h}}}(\mathbf{h}|\widehat{\mathbf{h}})$, which is completely specified by its mean and covariance since it is a Gaussian process. We define the posterior mean as $\widehat{\widehat{\mathbf{h}}} = \mathbb{E}_{\mathbf{h}|\widehat{\mathbf{h}}}\mathbf{h}$ and the posterior covariance as $\widehat{C}_{\mathbf{hh}} = \mathbb{E}_{\mathbf{h}|\widehat{\mathbf{h}}}\left[\mathbf{h} - \mathbb{E}_{\mathbf{h}|\widehat{\mathbf{h}}}\mathbf{h}\right]\left[\mathbf{h} - \mathbb{E}_{\mathbf{h}|\widehat{\mathbf{h}}}\mathbf{h}\right]^H$.

The posterior mean is calculated as follows

$$\widehat{\widehat{\mathbf{h}}} = m_{\mathbf{h}} + C_{\mathbf{h}\widehat{\mathbf{h}}} C_{\widehat{\mathbf{h}}\widehat{\mathbf{h}}}^{-1}\left(\widehat{\mathbf{h}} - m_{\widehat{\mathbf{h}}}\right) \tag{2.28}$$

where $C_{\mathbf{h}\widehat{\mathbf{h}}} = \mathbb{E}[\mathbf{h} - m_{\mathbf{h}}][\widehat{\mathbf{h}} - m_{\widehat{\mathbf{h}}}]^H$, $C_{\widehat{\mathbf{h}}\mathbf{h}} = \mathbb{E}[\widehat{\mathbf{h}} - m_{\widehat{\mathbf{h}}}][\mathbf{h} - m_{\mathbf{h}}]^H$ and $C_{\widehat{\mathbf{h}}\widehat{\mathbf{h}}} = [\widehat{\mathbf{h}} - m_{\widehat{\mathbf{h}}}][\widehat{\mathbf{h}} - m_{\widehat{\mathbf{h}}}]^H$. The posterior covariance is given by

$$\widehat{C}_{\mathbf{hh}} = C_{\mathbf{hh}} - C_{\mathbf{h}\widehat{\mathbf{h}}} C_{\widehat{\mathbf{h}}\widehat{\mathbf{h}}}^{-1} C_{\widehat{\mathbf{h}}\mathbf{h}}. \tag{2.29}$$

Based on the known distributions of $\mathbf{h}$ and $\widetilde{\mathbf{h}}$ and due to independence between these random processes, we have that $C_{\mathbf{h}\widehat{\mathbf{h}}} = C_{\widehat{\mathbf{h}}\mathbf{h}} = C_{\mathbf{hh}}$ and $C_{\widehat{\mathbf{h}}\widehat{\mathbf{h}}} = C_{\mathbf{hh}} + C_{\widetilde{\mathbf{h}}\widetilde{\mathbf{h}}}$. Substituting the obtained expressions for $C_{\mathbf{h}\widehat{\mathbf{h}}}$, $C_{\widehat{\mathbf{h}}\mathbf{h}}$ and $C_{\widehat{\mathbf{h}}\widehat{\mathbf{h}}}$ into equations (2.28) and (2.29), and after standard matrix manipulations, we obtain the desired result for the posterior mean and covariance.

## 2.B Proof of Theorem 2.1

The optimization problem described in (2.16) can be expressed as

$$\begin{cases} \min\limits_{\Psi} tr\left[m_{\mathbf{H}} C_T^{-1}\left(\eta\Psi + C_T^{-1}\right)^{-1} C_T^{-1} m_{\mathbf{H}}^H\right] - N\log\det(\eta\Psi + C_T^{-1}) \\ s.t.\ tr(\Psi) = 1 \end{cases}$$

The solution is obtained by means of the Karush-Kuhn-Tucker (KKT) conditions. Define the Lagrangian as

$$L(\Psi,\mu) = tr\left[m_{\mathbf{H}} C_T^{-1}\left(\eta\Psi + C_T^{-1}\right)^{-1} C_T^{-1} m_{\mathbf{H}}^H\right] \\ -N\log\det(\eta\Psi + C_T^{-1}) + \mu\ \left[tr(\Psi) - 1\right] \tag{2.30}$$

where $\mu$ is the Lagrange multiplier associated with the equality constraint. Differentiating $L(\Psi,\mu)$ w.r.t. $\Psi$, we get

$$\mu\Phi\Phi - \eta N\Phi - \eta C_T^{-1} m_{\mathbf{H}}^H m_{\mathbf{H}} C_T^{-1} = 0 \tag{2.31}$$

where the change of variable $\Phi = \eta\Psi + C_T^{-1}$ has been used for clarity. The solution for $\Psi$ to the quadratic matrix equation described above is given by

$$\Psi = \left\{\frac{1}{2\mu}\left[N\mathbf{I}_M + \left(N^2\mathbf{I}_M + \frac{4\mu}{\eta} C_T^{-1} m_{\mathbf{H}}^H m_{\mathbf{H}} C_T^{-1}\right)^{\frac{1}{2}}\right] - \frac{1}{\eta} C_T^{-1}\right\}_+$$

where $\{\cdot\}_+$ takes the positive semidefinite (PSD) part.

## 2.C Proof of Corollary 2.1

Introducing the eigenvalue decompositions $C_T^{-1} m_{\mathbf{H}}^H m_{\mathbf{H}} C_T^{-1} = \mathbf{U}\Sigma\mathbf{U}^H$ and $\Psi + \frac{1}{\eta} C_T^{-1} = \mathbf{V}\Lambda\mathbf{V}^H$ in equation (2.30) and eliminating constant terms, the minimization problem becomes

$$\begin{cases} \min\limits_{\Psi} tr\left(\frac{1}{\eta}\Lambda^{-1}\mathbf{V}^H\mathbf{U}\Sigma\mathbf{U}^H\mathbf{V}\right) - N\log\det(\Lambda) \\ s.t.\ tr(\Lambda) = \beta \end{cases}$$

where $\beta = 1 + \frac{1}{\eta} tr\left[C_T^{-1}\right]$ and the properties $tr(AB) = tr(BA)$ and $\mathbf{V}^H\mathbf{V} = \mathbf{I}_M$ have been used. Since the solution we seek assumes $\Psi$ to be PSD, also $\Lambda - \frac{1}{\eta}\mathbf{V}^H C_T^{-1}\mathbf{V}$ is assumed PSD. The optimum $\mathbf{V}$ that minimizes the first term can be chosen as $\mathbf{V} = \mathbf{U}$ [20].
Let $\Sigma = diag(\sigma_1,,\ldots,\sigma_M)$ and $\Lambda = diag(\lambda_1,\ldots,\lambda_M)$. The Lagrangian in this case is given by

$$L(\lambda_i,\mu) = \sum_{i=1}^{M}\left(\frac{1}{\eta}\frac{\sigma_i}{\lambda_i} - N\log\lambda_i\right) + \mu\left(\sum_{i=0}^{M}\lambda_i - \beta\right) \tag{2.32}$$

where $\mu$ is the Lagrange multiplier corresponding to the power constraint. Differentiating $L(\lambda_i, \mu)$ w.r.t. $\lambda_i$, we get

$$\lambda_i = \frac{N + \sqrt{N^2 + 4\frac{\mu\sigma_i}{\eta}}}{2\mu}. \tag{2.33}$$

Thus, the solution for $\Psi$ is given by

$$\Psi = \mathbf{U}\Lambda\mathbf{U}^H - \frac{1}{\eta}C_T^{-1}.$$

# Part II

# MIMO Broadcast Channels

# Chapter 3

# Joint Linear Beamforming and Multiuser Scheduling

*In this chapter, the problem of joint linear beamforming and multiuser scheduling is presented. A brief overview is provided, introducing the most extended linear beamforming techniques and scheduling algorithms in the literature. In order to illustrate the challenges, advantages and disadvantages of such systems, two low-complexity approaches are proposed. In the first approach, a scenario with perfect CSIT is considered, in which a simple multiuser scheduling strategy combined with a linear beamforming technique based on orthogonal beams are presented. This, as we show, leads to a dramatic complexity reduction in the multiuser scheduling stage. In the second approach, a low-complexity solution is proposed for a scenario with limited feedback. As we show, simple codebooks adapted to transmit spatial correlation can yield large performance gains. In addition, a bound on the multiuser interference experienced by each user is derived, based on a geometric interpretation of the problem. This bound is of capital importance since, as we show in the next chapter, it can be used for the design of feedback measures for the purpose of user selection.*

## 3.1 Introduction

MIMO systems can significantly increase the spectral efficiency by exploiting the spatial degrees of freedom created by multiple antennas. The capacity can be boosted by exploiting the spatial multiplexing capability of transmit antennas, transmitting to multiple users simultaneously by means of space division multiple access (SDMA), rather than maximizing the capacity of a single-user link, as shown in [10], [11]. It has recently been proven in [43] that the sum capacity of the MIMO broadcast channel is achieved by dirty paper coding (DPC) [1]. However, the applicability of DPC is limited due to its computational complexity and the need for full CSIT.

A promising low complexity alternative for the downlink of MIMO systems is linear beamforming. As opposed to DPC, linear beamforming does not perform any interference pre-subtraction, and thus multiuser interference is treated as noise. Finding the optimal beamforming vectors is a non-convex optimization problem, and the optimal solution for a downlink channel with $K$ users can only be given by exhaustive search. Evidently, the complexity of this problem becomes prohibitively high for large $K$. Hence, we focus instead on suboptimal linear beamforming strategies which, combined with efficient multiuser scheduling algorithms to exploit the multiuser diversity [17], achieve high sum rates. Downlink linear beamforming has been shown to achieve a large portion of DPC capacity, exhibiting the best tradeoff between complexity and performance [13], [14], [16]. When combined with multiuser scheduling, zero-forcing beamforming [44] has been shown to achieve the same asymptotic sum rate as that of DPC [15].

In point-to-point MIMO systems, the capacity increases linearly with the minimum of the number of transmit/receive antennas, irrespective of the availability of channel state information (CSIT) [4], [5]. In multiuser MIMO systems, the capacity gain is highly dependent on the available CSIT. If a base station with $M$ transmit antennas, communicating with $K$ single-antenna receivers, has perfect CSIT, a multiplexing gain of $\min(M, K)$ can be achieved. The approximation of close to perfect CSI at the receiver (CSIR) is often reasonable; however, this assumption is unrealistic at the transmitter. Recently, it was shown that if the base station has imperfect channel knowledge, the full multiplexing gain is reduced at high SNR [45], whereas if there is complete lack of CSI knowledge, the multiplexing gain collapses to one [46]. Hence, as the broadcast channel's capacity is sensitive to the accuracy of CSIT, it is of particular interest to identify what kind of partial

CSIT can be conveyed to the base station in order to achieve data rates reasonably close to the optimum. In this disertation, we give special interest to this issue, defining and optimizing the feedback that the user terminals need to compute and send to the base station. This feedback must be designed with the purpose of not only yielding good channel estimates for linear beamforming design, but also enabling the base station to perform efficient user selection.

Several limited feedback approaches, imposing a bandwidth constraint on the feedback channel, have been studied in point-to-point MIMO systems [47], [48], [49], [50]. In this context, each user feeds back finite precision (quantized) CSIT on its channel direction by quantizing its normalized channel vector to the closest vector contained in a predetermined codebook. An extension of the limited feedback model for multiple antenna broadcast channels for the case of $K \leq M$ is made in [51], [52]. In [51] it was shown that the feedback load per user must increase approximately linearly with $M$ and the transmit power (in dB), in order to achieve the full multiplexing gain. These schemes rely only on channel direction information and no information on the channel magnitude is provided.

Recently, MIMO broadcast channels with limited feedback and more users than transmit antennas (i.e. $K \geq M$) have attracted particular interest and several joint beamforming and scheduling schemes aiming to maximize the sum rate have been proposed. A popular, very low-rate feedback technique, coined as random beamforming (RBF), is proposed in [2], where $M$ random orthonormal beamforming vectors are generated and the best user on each beam is scheduled. By exploiting multiuser diversity, this scheme is shown to yield the optimal capacity growth of $M \log \log K$ for $K \to \infty$. However, the sum rate of this scheme degrades quickly with decreasing number of users.

A different type of limited feedback approaches considers that each user reports channel direction information (CDI) related to a codebook back to the transmitter, as well as some form of scalar channel quality information (CQI). Several beamforming methods have been investigated, including unitary beamforming [53], transmit matched-filtering [54], and zero-forcing beamforming [54], [55], [26], [56]. Note that in these contributions, the CQI feedback is considered unquantized for analytical simplicity. Considering the more realistic constraint of finite CSI feedback rate, [29] studies the problem of optimal bit rate allocation between CQI and CDI, and the resulting multiuser diversity - multiplexing gain tradeoff in limited feedback MIMO systems. On the other hand, [57] proposes a threshold-based feedback scheme

for SDMA systems under a sum feedback rate constraint.

The benefit of using as CQI a measure related to the signal-to-interference-plus-noise ratio (SINR) was shown in [28]. One challenge of designing feedback metrics is that the SINR measurement depends, among others, on the channel as well as on the number of simultaneously scheduled users. Since user cooperation is not allowed, the number of simultaneous users and the available power for each of them is generally unknown at the mobile. In addition, the feedback metrics must be computed at the user end prior to computation of the beamforming vectors at the transmitter side. Thus, estimation of the multiuser interference at the receiver side is a difficult and critical task. A principal drawback of previous works is that the proposed metrics assume a fixed number of scheduled SDMA users, based on non-achievable SINR upper bounds. Instead, it may be interesting to consider schemes allowing adaptive transition between SDMA and time division multiple access (TDMA) modes, as well as more practical received SINR estimates. This problem is addressed in Chapter 4, in a scenario with separate CDI and CQI feedback. In Chapter 5, a different limited feedback scenario is considered, in which the users quantize directly their vector channels by using optimized channel quantization codebooks, thus embedding channel direction and quality information in a single codebook.

The remainder of this chapter is organized as follows. Initially, an introduction to linear beamforming schemes with perfect CSIT is provided. Common linear beamforming techniques used in the multiuser MIMO literature are formally presented, namely zero-forcing beamforming, minimum mean squared error beamforming and transmit matched filtering. In the following section, the problem of multiuser selection comes into play. Standard user selection algorithms are reviewed, which, together with the linear beamforming techniques previously mentioned, will be often referred to throughout this dissertation. In the last two sections of this chapter, reduced-complexity approaches combining linear beamforming and multiuser scheduling are proposed, first in a scenario with perfect CSIT and next in a more realistic scenario with limited feedback.

## 3.2 System Model

The model here presented describes a generic system model for MIMO broadcast channels, which will be often used throughout this dissertation. User

terminals with a single antenna are in general considered, unless stated otherwise. This is a practical case of interest in current cellular networks, and it also leads to more tractable mathematical problems.

We consider a multiple antenna broadcast channel consisting of $M$ antennas at the transmitter and $K$ single-antenna receivers. We assume that the number of mobiles is greater than or equal to the number of transmit antennas, i.e., $K \geq M$, implying the use of a user selection algorithm. We limit here to the case of linear beamforming where exactly $M$ spatially separated users access the channel simultaneously. However, in practice, the number of scheduled users may be considered less than or equal to the number of transmit antennas, as proposed in next chapter. The received signal $y_k$ of the $k$-th user is mathematically described as

$$y_k = \mathbf{h}_k^H \mathbf{x} + n_k, \qquad k = 1, \ldots, K \tag{3.1}$$

where $\mathbf{x} \in \mathbb{C}^{M\times 1}$ is the transmitted signal, $\mathbf{h}_k \in \mathbb{C}^{M\times 1}$ is the channel vector, and $n_k$ is additive white Gaussian noise at receiver $k$. We assume that $n_k$ is independent and identically distributed (i.i.d.) circularly symmetric complex Gaussian with zero mean and variance $\sigma^2$. The transmitted signal is subject to an average transmit power constraint $P$, i.e., $\mathbb{E}\{\|\mathbf{x}\|^2\} = P$. We consider an homogeneous network where all users have the same average SNR.

An i.i.d. block Rayleigh flat fading channel is considered, whose parameters are considered invariant during each coded block, but are allowed to vary independently from block to block. Let $\mathbf{H} \in \mathbb{C}^{K\times M}$ refer to the concatenation of all channels, $\mathbf{H} = [\mathbf{h}_1\ \mathbf{h}_2 \ldots \mathbf{h}_K]^H$, where the $k$-th row is $\mathbf{h}_k^H$. Define $\mathcal{G}$ as the set of all possible subsets of cardinality $M$ of disjoint indices among the complete set of user indices $\mathcal{Q}^0 = \{1, \ldots, K\}$. Let $\mathcal{S} \in \mathcal{G}$ be one such group of $M$ users selected for transmission at a given time slot. Then $\mathbf{H}(\mathcal{S})$, $\mathbf{W}(\mathcal{S})$, $\mathbf{s}(\mathcal{S})$, $\mathbf{y}(\mathcal{S})$ are the concatenated channel vectors, unit-norm beamforming vectors, unit-variance uncorrelated data symbols and received signals respectively for the set of scheduled users $\mathcal{S}$. When concatenating the beamforming matrix $\mathbf{W}(\mathcal{S})$ prior to transmission, the signal model can be described as follows

$$\mathbf{y}(\mathcal{S}) = \mathbf{H}(\mathcal{S})\mathbf{W}(\mathcal{S})\mathbf{s}(\mathcal{S}) + \mathbf{n} \tag{3.2}$$

The SINR at the $k$-th receiver is

$$SINR_k = \frac{|\mathbf{h}_k^H \mathbf{w}_k|^2}{\sum_{i\in\mathcal{S}, i\neq k} |\mathbf{h}_k^H \mathbf{w}_i|^2 + \sigma^2}. \tag{3.3}$$

We focus on the ergodic sum rate, which means that the capacity is averaged over the fading distribution, and thus the block size does not affect our results. Assuming Gaussian inputs, the ergodic sum rate (SR) is given by

$$SR = \mathbb{E}\left\{\sum_{k\in\mathcal{S}} \log\left[1 + SINR_k\right]\right\} \tag{3.4}$$

## 3.3 Linear Beamforming Techniques

In the following lines, a brief description of the most extended linear beamforming techniques is provided. The beamforming matrices are computed on the basis of the concatenated user channels $\mathbf{H}(\mathcal{S}) = [\mathbf{h}_{k_1} \dots \mathbf{h}_{k_M}]^H$, where the subindex $k_i$ stands for the user index scheduled over the $i$-th beamforming vector. Note that, in the absence of perfect CSIT, the beamfoming matrix $\mathbf{W}$ is instead computed on the basis of the concatenated estimated user channels, denoted as $\widehat{\mathbf{H}}(\mathcal{S}) = \left[\widehat{\mathbf{h}}_{k_1} \dots \widehat{\mathbf{h}}_{k_M}\right]^H$. Special attention has been paid to zero forcing (ZF) beamforming (or channel inversion) techniques in the recent literature [58], extended in [15] to systems with multiuser scheduling. The ZF beamformer is computed as follows

$$\mathbf{W}_{ZF}(\mathcal{S}) = \frac{1}{\lambda}\mathbf{H}(\mathcal{S})^H \left[\mathbf{H}(\mathcal{S})\mathbf{H}(\mathcal{S})^H\right]^{-1} \tag{3.5}$$

where $\lambda = \frac{1}{\sqrt{P}} tr\left[(\mathbf{H}(\mathcal{S})\mathbf{H}(\mathcal{S})^H)^{-1}\right]$. However, a main drawback of this technique is that the sum rate does not scale with the number of antennas. This is due to the large spread in the singular values of the channel matrix, as discussed in [59]. In order to overcome this limitation, minimum mean squared error (MMSE) beamforming (or regularized channel inversion) [59] has been proposed, which regularizes the channel inversion and improves the condition of the inverse, enabling linear capacity growth with the number of transmit antennas. The MMSE beamformer is given by

$$\mathbf{W}_{MMSE}(\mathcal{S}) = \gamma\mathbf{H}(\mathcal{S})^H \left[\mu\mathbf{I} + \mathbf{H}(\mathcal{S})\mathbf{H}(\mathcal{S})^H\right]^{-1} \tag{3.6}$$

where $\gamma$ is chosen such that $tr\left(\mathbf{W}_{MMSE}(\mathcal{S})\mathbf{W}_{MMSE}(\mathcal{S})^H\right) = P$. By fixing $\mu = \frac{M\sigma^2}{P}$, the resulting SINR at each receiver is maximized for large $K$, as shown in [59]. Another linear beamforming technique that will be used in

our work is transmit matched filtering (TxMF), which consists of employing as beamforming vectors the vector channels of the users scheduled for transmission. The beamfoming matrix is computed as follows

$$\mathbf{W}_{MF}(\mathcal{S}) = \mathbf{H}(\mathcal{S})^H. \tag{3.7}$$

## 3.4 Multiuser Scheduling Algorithms

The optimal multiuser scheduling solution can be conceptually given by exhaustive search over all possible user sets. In a system employing exhaustive search, the scheduler selects the set of users that maximize the sum rate as follows

$$\mathcal{S}^* = \arg\max_{\mathcal{S}\in\mathcal{G}} \sum_{k\in\mathcal{S}} \log_2 \left[1 + SINR_k(\mathcal{S})\right] \tag{3.8}$$

where the values $SINR_k(\mathcal{S})$ have to be computed for each user $k$ in each possible set $\mathcal{S}$, given a certain beamforming strategy. In order to avoid the prohibitive complexity of exhaustive search, suboptimal user selection algorithms are often implemented at the transmitter side. In addition, in the presence of imperfect CSIT, other user selection metrics rather than the exact SINR values may be considered instead.

In this chapter, we consider multiuser scheduling algorithms that rely on scalar scheduling metrics to select a set of users for transmission. The scalar metric for the $k$-th user, denoted as $\xi_k$, may be computed either at the base station or at the user terminal. In the latter case, the user feeds back the scheduling metric to the base station. The design of such scalar metrics is treated in detail in the next chapter. These metrics can be combined with different user selection algorithms. As our optimization objective is to maximize the system capacity, the optimum policy under max-sum-rate scheduling is to select $\mathcal{M} \leq M$ users among $K$ users that maximize the sum rate through exhaustive search. In this chapter, for simplicity, we assume that $\mathcal{M} = M$ users are scheduled at a given time slot. As the complexity of such a combinatorial optimization problem is prohibitively high for large $K$, we resort to low-complexity scheduling strategies based on greedy user selection (see e.g. [15], [16], [28]).
In the remainder of this section, a brief overview of standard user selection algorithms found in the literature is provided.

Table 3.1: Outline of G-SUS Algorithm

| | |
|---|---|
| **Step 0** set $\mathcal{S}^* = \emptyset$, $\mathcal{Q}^0 = 1, \ldots, K$ | |
| For $i = 1, 2, \ldots, M$ repeat | |
| **Step 1** | $k_i = \arg \max_{k \in \mathcal{Q}^{i-1}} \xi_k$ |
| **Step 2** | $\mathcal{S}^* = \mathcal{S}^* \cup k_i$ |
| **Step 3** | $\mathcal{Q}^i = \left\{ k \in \mathcal{Q}^{i-1} \mid \ \lvert \mathbf{h}_k^H \mathbf{h}_j \rvert \leq \epsilon \ \forall j \in \mathcal{S}^* \right\}$ |

### G-SUS algorithm

We first review a heuristic scheduling algorithm based on greedy semi-orthogonal user selection (G-SUS) [15], [28]. Using $\xi_k$ and $\mathbf{h}_k$, $k = 1, \ldots, K$, the base station performs user selection to support up to $M$ out of $K$ users at each time slot. Note that, in the case of imperfect CSIT, the estimated (or quantized) user channels are used instead, denoted as $\hat{\mathbf{h}}_k$, $k = 1, \ldots, K$.

The algorithm is outlined in Table 3.1. The first user is selected from the set $\mathcal{Q}^0 = \{1, \ldots, K\}$ of cardinality $|\mathcal{Q}^0| = K$ as the one having the highest channel quality, i.e. $k_1 = \arg\max_{k \in \mathcal{Q}^0} \xi_k$. The $(i+1)$-th user, for $i = 1, \ldots, M-1$, is selected as $k_{i+1} = \arg\max_{k \in \mathcal{Q}^i} \xi_k$ among the user set $\mathcal{Q}^i$ with cardinality $|\mathcal{Q}^i| \leq K$, defined as $\mathcal{Q}^i = \left\{ k \in \mathcal{Q}^{i-1} \mid \ \lvert \mathbf{h}_k^H \mathbf{h}_j \rvert \leq \epsilon \ \forall j \in \mathcal{S}^* \right\}$. The system parameter $\epsilon$ defines the maximum allowed non-orthogonality (maximum correlation) between quantized channels and it is a parameter set in advance. Evidently, if $\epsilon$ is very large, the selected users may cause significant multiuser interference, reducing the system sum rate. Conversely, if $\epsilon$ is too small, the scheduler may not find enough semi-orthogonal users to transmit to.

### G-US algorithm

We generalize here the low-complexity greedy user selection (GUS) scheme [16] for the case of imperfect (or quantized) CSIT. The algorithm here described is envisaged either for a system with perfect CSIT, or a scenario in which each user feeds back its quantized channel direction based on a predetermined codebook and scalar instantaneous feedback $\xi_k$, which are used in turn to perform joint scheduling and beamforming with quantized CSIT. In

Table 3.2: Outline of G-US Algorithm

| | |
|---|---|
| **Step 0** | Set $\mathcal{S}_0 = \emptyset$, $\mathcal{R}(\mathcal{S}_0) = 0$, and $\mathcal{Q}^0 = 1, \ldots, K$ |
| **Step 1** | $k_1 = \arg\max_{k \in \mathcal{Q}^0} \xi_k$ |
| | Set $\mathcal{S}_1 = \mathcal{S}_0 \cup \{k_1\}$ |
| | While $i < M$ repeat |
| | $i \leftarrow i + 1$ |
| **Step 2** | $k_i = \arg \max_{k \in (\mathcal{Q}^0 - \mathcal{S}_{i-1})} \mathcal{R}(\mathcal{S}_{i-1} \cup \{k\})$ |
| **Step 3** | Set $\mathcal{S}_i = \mathcal{S}_{i-1} \cup \{k_i\}$ |
| **Step 4** | if $\mathcal{R}(\mathcal{S}_i) \leq \mathcal{R}(\mathcal{S}_{i-1})$ |
| | finish algorithm and $i \leftarrow i - 1$ |
| **Step 5** | Set $\mathcal{S}^* = \mathcal{S}_i$ and $\mathcal{M} = i$ |

the perfect CSIT case, $\xi_k$ takes on the meaning of the SINR of user $k$, while in the imperfect CSIT case $\xi_k$ corresponds to an estimate on the SINR, e.g. an upper or lower bound on the SINR (refer to Chapter 4 for more details). The algorithm is summarized in Table 3.2, where $\mathcal{R}(\mathcal{S}_i) = \sum_{k \in \mathcal{S}_i} \log_2(1 + \xi_k)$ and $\mathcal{S}_i$ is the set of selected users up to the $i$-th step. The user with the highest estimated rate (equivalently $\xi_k$ metric) among $K$ users is first selected, and at each iteration, a user is added only if the sum rate (based on the estimated SINR) is increased. At each step, it is important to re-process the set of previously selected users (thus, re-calculating the linear beamformers) once a user is added to the set $\mathcal{S}_i$.

A main advantage of G-US compared to G-SUS is that it does not necessarily require the use of the predetermined system parameter $\epsilon$. The value of the orthogonality constraint $\epsilon$ affects the performance of the user selection algorithm. If $\epsilon$ is set too small, the multiuser diversity gain decreases, and the user set $\mathcal{Q}^i$ can be empty before $M$ quasi-orthogonal users are found. The optimal value decreases with $K$, as the probability of finding $M$ semi-orthogonal users among $K$ is larger, however it is difficult to be optimized analytically. Furthermore, since the G-US algorithm re-processes the set of already selected users under the same zero-forcing beamforming optimization when one user is added at each step, its performance can be better or equal to that of G-SUS.

## 3.5 Full CSIT Case: A Low-Complexity Approach

In this section, the problem of joint linear beamforming and scheduling in a MIMO broadcast channel with full CSIT is considered. We show how orthogonal linear beamforming (OLBF) can be efficiently combined with a low-complexity user selection algorithm to achieve a large portion of the multiuser capacity. The use of orthogonal transmission enables the transmitter to calculate exact SINR values during the user selection process. The knowledge of multiuser interference proves to be of particular importance for user scheduling as both the number of users in the cell and the average signal-to-noise ratio (SNR) decrease. The sum capacity of our scheme is characterized in the low-SNR regime, providing analytical results on the performance gain over zero-forcing beamforming (ZFBF).

Simulation results show performance improvements with respect to ZFBF and transmit matched filtering (TxMF) in realistic networks with low to moderate number of users. The proposed algorithm is also compared with the ZFBF scheme with G-US (ZFBF-GUS) introduced in [16]. We show that in systems with low to moderate number of active users, the proposed scheme exhibits sum-rate gains over ZFBF-GUS in the low-SNR regime. However, as the average SNR and number of users increase, suboptimal ZFBF techniques like [16] can provide higher rates. One of our main results is to show that in the regime of low number of users, orthogonal SDMA offers better performance than optimal zero-forcing beamforming. Analytical results are provided and corroborated through numerical simulations.

### 3.5.1 Motivation

In this section, we focus on joint downlink linear beamforming and scheduling with the objective of maximizing the system sum rate. The optimal solution is given by exhaustive search over all possible user sets, as described by (3.8). Combining multiuser scheduling with a particular beamforming strategy, the base station is required to compute the beamformers for each user set $\mathcal{S}$. In addition, the SINR values have to be computed for each possible set $\mathcal{S}$ and user $k$.

In order to avoid exhaustive user search, suboptimal scheduling approaches can be implemented instead, such as greedy user selection algorithms. The

idea behind gredy approaches is to pre-select a reduced number of users according to different criteria, e.g. orthogonality properties as in G-SUS, hence reducing the search space. Once scheduling is performed, the base station computes the beamformers for transmission and is able to determine each user's achievable SINR. The inconvenience of these approaches is that in order to precisely know the SINR of a user, the beamformers have to be computed first, which is in general a computationally complex operation. Hence, suboptimal scheduling techniques rely generally on criteria other than the exact SINR values. In certain scenarios, such as systems with low number of users or in low SNR conditions, precise knowledge of SINR can help to increase the system performance, as we show later on.

We propose a low-complexity user selection technique valid under the constraint of using orthonormal beamforming vectors for transmission. Orthonormal transmission enables calculation of the exact signal-to-interference plus noise ratio (SINR) values during the user selection process in a compact and computationally efficient manner. This SINR expression was introduced as a scalar feedback metric for MIMO broadcast channels with limited feedback [28], [60]. In the case of full channel knowledge and suboptimal user scheduling, the use of orthogonal beamformers provides a precise control on the multiuser interference at the transmitter. In order to improve the system performance, this knowledge proves to be of particular importance for decreasing number of users and average signal-to-noise ratio (SNR). In addition, the exact per-user contribution to the sum rate can be computed at each selection step.

### 3.5.2 System Assumptions

We consider equal power allocation over each transmit beam. Let $\mathcal{P}$ be an $M \times M$ diagonal matrix with entries equal to $\sqrt{P/M}$. Assuming the columns of the beamforming matrix $\mathbf{W}$ are normalized, the system model given in (3.2) can be described as follows

$$\mathbf{y}(\mathcal{S}) = \mathbf{H}(\mathcal{S})\mathbf{W}(\mathcal{S})\mathcal{P}\mathbf{s}(\mathcal{S}) + \mathbf{n}. \tag{3.9}$$

In addition, the use of OLBF and normalized beamforming vectors implies that the matrix $\mathbf{W}(\mathcal{S})$ is unitary, i.e., $\mathbf{W}(\mathcal{S})\mathbf{W}(\mathcal{S})^H = \mathbf{W}(\mathcal{S})^H\mathbf{W}(\mathcal{S}) = \mathbf{I}_M$.

At the $k$-th mobile, the received signal is given by

$$y_k = \sqrt{\frac{P}{M}} \sum_{i \in \mathcal{S}} \mathbf{h}_k^H \mathbf{w}_i s_i + n_k, \qquad k = 1, \ldots, K. \tag{3.10}$$

### 3.5.3 Proposed User Selection Algorithms

In order to avoid the prohibitively high complexity of exhaustive search, we use a low-complexity user selection approach. The base station schedules $M$ among $K$ users for downlink transmission with the purpose of maximizing the sum rate and under the constraint of orthonormal beamforming.

The user selection criterion consists of scheduling the users with the largest SINR values. In order to express each user's SINR, we use the following simplified expression

$$SINR_k = \frac{\|\mathbf{h}_k\|^2 \rho_k^2}{\|\mathbf{h}_k\|^2 (1 - \rho_k^2) + \frac{M\sigma^2}{P}} \tag{3.11}$$

where $\rho_k$ is the alignment between the $k$-th user instantaneous normalized channel vector $\overline{\mathbf{h}}_k = \frac{\mathbf{h}_k}{\|\mathbf{h}_k\|}$ (channel direction) and the corresponding beamforming vector $\mathbf{w}_k$, defined as $\rho_k = \left|\overline{\mathbf{h}}_k^H \mathbf{w}_k\right|$. Note that a similar metric is also reported in [28], [60]. Since the linear beamformers used for transmission are orthonormal, the beamforming vectors $\mathbf{w}_j$, $\forall\ j \neq k$ span the null space of $\mathbf{w}_k$. Hence, as shown in [51], the multiuser interference can be simplified as $I_k = \frac{P}{M} \|\mathbf{h}_k\|^2 (1 - \rho_k^2)$. In next section, we provide a bound for the multiuser diversity, treating the case of orthonormal beamforming vectors as a particular case (see Corollary 3.1).

In what follows, we propose two algorithms with different computational complexity. As we later show through simulations, Algorithm B shows better performance than Algorithm A at the expense of higher processing complexity.

#### Algorithm A

An outline of Algorithm A is provided in Table 3.3. The proposed suboptimal transmission scheme has reduced complexity, in the sense that it has

- Simple beamforming strategy: given $K$ users, only 1 possible transmission set is taken in consideration.
- Reduced user search space: greedy algorithm with linear complexity of order $\mathrm{O}(K)$ is used. Hence, combinatorial search over the entire index set is avoided.

Table 3.3: Outline of Scheduling Algorithm A

**Step 0** Select first scheduled user and beamforming vector

$k_1 = \arg\max_{k \in \mathcal{Q}^0} \|\mathbf{h}_k\|$

$\mathbf{w}_{k_1} = \overline{\mathbf{h}}_{k_1}$

Set $\mathcal{S}^* = \{k_1\}$

**Step 1** Gram-Schmidt orthogonalization

Compute orthonormal basis $\mathbf{W}$ from $\mathbf{w}_{k_1}$

**Step 2** Loop

For $i = 2, \ldots, M$ repeat

**Step 2.1** Set $SINR^i_{max} = 0$

**Step 2.2** Loop

For $k = 1, \ldots, K, k \notin \mathcal{S}^*$ repeat

**Step 2.2.1** Compute $\rho_k = \left|\overline{\mathbf{h}}_k^H \mathbf{W}(i)\right|$

**Step 2.2.2** Compute $SINR_k = \frac{\|\mathbf{h}_k\|^2 \rho_k^2}{\|\mathbf{h}_k\|^2 (1-\rho_k^2) + \frac{M\sigma^2}{P}}$

**Step 2.2.3** If $SINR_k > SINR^i_{max}$

$SINR_k \rightarrow SINR^i_{max}$ and $k_i = k$

**Step 2.3** $k_i \rightarrow \mathcal{S}^*$

Given $M$ possible users to be scheduled out of $K$ active users, the user scheduled on the first beam, denoted as $k_1$, is the one that exhibits the largest channel norm, i.e.,

$$k_1 = \arg\max_{k \in \mathcal{Q}^0} \|\mathbf{h}_k\| \,. \tag{3.12}$$

Once the best user is identified, its beamforming vector is given by

$$\mathbf{w}_{k_1} = \overline{\mathbf{h}}_{k_1} \tag{3.13}$$

so that transmit matched filtering is performed for the first user. Hence, this user observes an alignment of $\rho_{k_1} = 1$, and thus $SINR_{k_1} = \frac{P}{M\sigma^2} \|\mathbf{h}_{k_1}\|^2$, independently of the users scheduled on the remaining beams. Note also that the first user is selected as the best over $K$ users, therefore exploiting all multiuser diversity gain. The remaining $M-1$ beamforming vectors are found by the following procedure. Since orthogonal transmission is to be performed, the already selected vector $\mathbf{w}_{k_1}$ corresponds to a basis vector of the orthonormal basis $\mathbf{W} \in \mathbb{C}^{M\times M}$ to be used for transmission. Hence, the complete set of beamforming vectors can be found by applying the *Gram-Schmidt* orthogonalization method [61]. Let $\mathbf{W}(i)$ be the $i$-th column of the beamforming matrix $\mathbf{W}$ and define $\mathbf{W}(1) = \mathbf{w}_{k_1}$. Once the beamforming vectors are determined, the user scheduled on the $i$-th beam, $i = 2, \ldots, M$, corresponds to the user that maximizes the SINR expression

$$k_i = \arg \max_{k \in \mathcal{Q}^0 - \{k_1, \ldots, k_{i-1}\}} SINR_k \tag{3.14}$$
$$s.t.\ \mathbf{w}_k = \mathbf{W}(i)$$

Note that selection of the $k_i$ user does not affect the expression of $SINR_{k_j}$, for $j \neq i, j =, 2 \ldots, M$, since the beamforming vectors in OLBF are already determined in the first step, and therefore the SINR expression of $k$-th user is only a function of $\mathbf{h}_k$ and $\rho_k$ as equation (3.11) shows. In the selection process, exact SINR values are computed for the given beamforming vectors. This ensures that, even though the transmit directions are fixed (after selecting $k_1$), the exact knowledge of interference will allow to capture a large portion of the sum rate even when the number of users is reduced.

The sum rate of the scheduled user set $\mathcal{S}^* = \{k_1, k_2, \ldots, k_M\}$ is given by

$$R(\mathcal{S}^*) = \sum_{i=1}^{M} \log_2 \left[1 + SINR_{k_i}\right]. \tag{3.15}$$

**Algorithm B**

An outline of Algorithm B is provided in Table 3.4. This algorithm exhibits increased complexity compared to Algorithm A, which can be summarized as follows

- Simple beamforming strategy: given $K$ users, only $K$ possible transmission sets are taken in consideration.
- Reduced user search space: user selection algorithm of complexity of order $\mathrm{O}(K^2)$ (hence, combinatorial search over the entire index set is avoided).

Table 3.4: Outline of Scheduling Algorithm B

**Initialize** Set $\mathcal{S}^* = \emptyset$ and $R(\mathcal{S}^*) = 0$

For $k = 1, \ldots, K$ repeat

**Step 0** Set $k_1 = k$

$\mathbf{w}_{k_1} = \overline{\mathbf{h}}_k$

$\mathcal{S} = \{k_1\}$

**Step 1** Gram-Schmidt orthogonalization

Compute orthonormal basis $\mathbf{W}$ from $\mathbf{w}_{k_1}$

**Step 2** Loop

For $i = 2, \ldots, M$ repeat

**Step 2.1** Set $SINR^i_{max} = 0$

**Step 2.2** Loop

For $j = 1, \ldots, K, j \notin \mathcal{S}$ repeat

**Step 2.2.1** Compute $\rho_j = \left|\overline{\mathbf{h}}_j^H \mathbf{W}(i)\right|$

**Step 2.2.2** Compute $SINR_j = \frac{\|\mathbf{h}_j\|^2 \rho_j^2}{\|\mathbf{h}_j\|^2 (1-\rho_j^2) + \frac{M\sigma^2}{P}}$

**Step 2.2.3** If $SINR_j > SINR^i_{max}$

$SINR_j \rightarrow SINR^i_{max}$ and $k_i = j$

**Step 2.3** $k_i \rightarrow \mathcal{S}$

**Step 3** $R(\mathcal{S}) = \sum_{j \in \mathcal{S}} \log\left[1 + SINR_j\right]$

**Step 4** If $R(\mathcal{S}) > R(\mathcal{S}^*)$, $R(\mathcal{S}) \rightarrow R(\mathcal{S}^*)$ and $\mathcal{S} \rightarrow \mathcal{S}^*$

Hence, Algorithm B also considers a finite set of possible beamformers (thus limiting the complexity) but does not perform a greedy selection procedure.

This algorithm is equivalent to Algorithm A, but instead of selecting the first user as in equation (3.12), all users are considered as possible candidates, i.e., $k_1 = k, k = 1, \ldots, K$. In other words, the procedure described in Algorithm A is performed $K$ times. Each time, a new set of beamforming vectors is computed, given that $\mathbf{w}_{k_1} = \overline{\mathbf{h}}_{k_1}$ changes from user to user, and its corresponding rate is computed by using (3.15). Let $R_m(\mathcal{S})$ denote the sum rate for a user set $\mathcal{S}$ at $m$-th iteration of the algorithm, where $m = 1, \ldots, K$. The set of beamforming vectors $\mathbf{W}(\mathcal{S}^*)$ and scheduled users $\mathcal{S}^*$ are those having the maximum sum rate $R_m(\mathcal{S})$ among the $K$ iterations of the algorithm. Thus the resulting sum rate of Algorithm B is given by

$$R\left(\mathcal{S}^*\right) = \max_{\mathcal{S}, m \in \mathcal{Q}^0} R_m(\mathcal{S}). \tag{3.16}$$

At this point, we should note that here we focus on the region of low to moderate number of users, which is of particular interest in real scenarios. A sum rate analysis of our proposed algorithms for $K \to \infty$ can show that both our schemes achieve asymptotically the optimum sum rate scaling of $M \log \log K$. This is also evident as random opportunistic beamforming [2], which has been shown to achieve the DPC capacity scaling [13], is a pessimistic lower bound on the performance of our scheme.

### 3.5.4 Performance Analysis

In this section, we study the sum rate performance of OLBF (Algorithm A) at low-power regime, and its capacity growth is compared with that of zero-forcing beamforming with equal power allocation. For simplicity, we assume that $K = M$, and thus the results are independent of the user selection strategy. The analytical tool used for the characterization of capacity at asymptotically low SNR was proposed by Verdú [62]. At low SNR, the capacity $C(SNR)$ (in nats/dimension) can be approximated by the second-order Taylor series expansion:

$$C(SNR) = \dot{C}(0)SNR + \frac{\ddot{C}(0)}{2}SNR^2 + o(SNR^2) \tag{3.17}$$

with $\dot{C}(0)$ and $\ddot{C}(0)$, the first and second derivative, respectively, of the function $C(SNR)$ at $SNR = 0$.

The sum capacity of zero-forcing beamforming with equal power allocation $C_{ZFBF}(SNR)$ is given by

$$C_{ZFBF}(SNR) = \mathbb{E}\left\{\sum_{i\in\mathcal{S}} \log\left(1 + \frac{SNR}{M}\left|\gamma_i\right|^2\right)\right\} \tag{3.18}$$

where $\gamma_i = \mathbf{h}_i^H \mathbf{w}_i$ is the effective channel of the $i$-th user, and $\mathbf{w}_i$ the zero-forcing beamformer, corresponding to the $i$-th column of the matrix $\mathbf{W}(\mathcal{S})$. Note that $\left|\gamma_i\right|^2$ is a chi-square random variable with two degrees of freedom for all $i$ (denoted $\chi^2_{(2)}$).

The derivatives of the sum capacity in nats are equal to

$$\dot{C}_{ZFBF}(0) = \mathbb{E}\left\{\left|\gamma_i\right|^2\right\} = 1 \tag{3.19}$$

and

$$\ddot{C}_{ZFBF}(0) = -\frac{\mathbb{E}\left\{\left|\gamma_i\right|^4\right\}}{M}. \tag{3.20}$$

Similarly, when OLBF is used, the sum capacity $C_{OLBF}(SNR)$ is given by

$$C_{OLBF}(SNR) = \mathbb{E}\left\{\log\left(1 + \frac{SNR}{M}\left\|\mathbf{h}_{k_1}\right\|^2\right)\right\}$$

$$+\mathbb{E}\left\{\sum_{i\in\mathcal{S}-\{k_1\}} \log\left(1 + SINR_{k_i}\right)\right\} \tag{3.21}$$

with $\left\|\mathbf{h}_{k_i}\right\|^2 \sim \chi^2_{(2M)}$.

The derivatives of the sum capacity in nats are equal to

$$\dot{C}_{OLBF}(0) = 2 - 1/M \tag{3.22}$$

and

$$\ddot{C}_{OLBF}(0) = -\frac{\mathbb{E}\left\{\left\|\mathbf{h}_k\right\|^4\right\}}{M} + \frac{M-1}{M^2}\mathbb{E}\left\{\left\|\mathbf{h}_k\right\|^4 (1-\rho_k^2)^2\right\}. \tag{3.23}$$

Note that for isotropically distributed channels, $\|\mathbf{h}_k\|$ and $\rho_k$ are independent random variables. As a first-order approximation, as $SNR \to 0$, the capacity grows linearly with SNR, i.e. $C_{ZFBF} \approx SNR$ and $C_{OLBF} \approx$

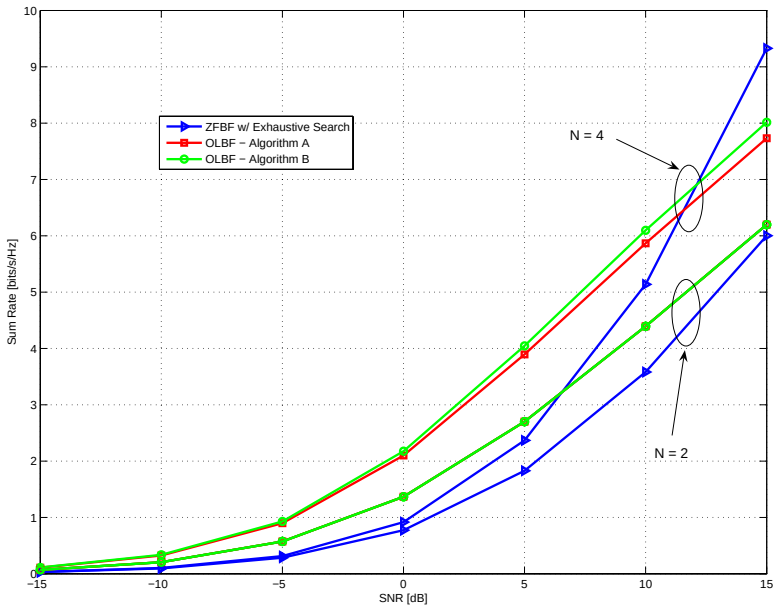


Figure 3.1: Sum rate as a function of the SNR for $M = 2, 4$ transmit antennas and $K = M$ users.

$(2-1/M)SNR$, meaning that the capacity scaling (for fixed $M$) at low SNR satisfies

$$\lim_{SNR\to 0} \frac{C_{ZFBF}(SNR)}{SNR} = 1 \tag{3.24}$$

and

$$\lim_{SNR\to 0} \frac{C_{OLBF}(SNR)}{SNR} = 2 - 1/M. \tag{3.25}$$

By taking the capacity scaling ratio $CSR = \frac{C_{OLBF}(SNR)}{C_{ZFBF}(SNR)}$, we conclude that a system employing OLBF provides at low SNR a gain of $10\log_{10}(\frac{2M-1}{M})$ dB compared to a system based on zero-forcing beamforming, or equivalently, a factor of $CSR = (2M-1)/M$ in rate (nats/s/Hz) for the same power.

Figure 3.1 shows a sum rate comparison between OLBF and ZFBF versus average SNR for $M = 2$ and $M = 4$ transmit antennas. We can observe the consistency of the simulation results with the above analysis, since the sum capacity gap between OLBF and ZFBF increases with the number of transmit antennas (by a factor of $2 - 1/M$) at low SNR.

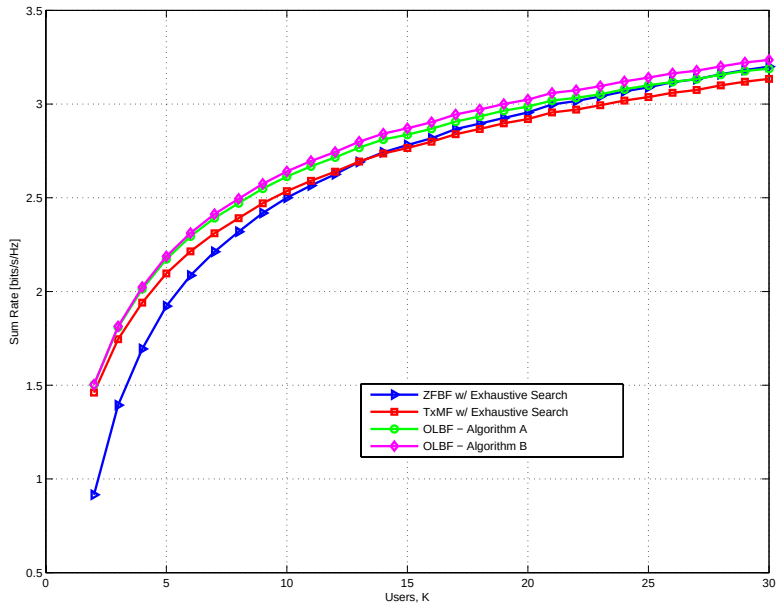


Figure 3.2: Sum rate as a function of the number of users for $M = 2$ transmit antennas, and average SNR = 0 dB.

### 3.5.5 Numerical Results

The performance of the proposed algorithms is evaluated through simulations, for $M = 2$ transmit antennas, comparing the sum rate with three alternative transmission techniques for the MIMO downlink: ZFBF with exhaustive user search, TxMF with exhaustive user search, and ZFBF-GUS [16]. We consider in the simulated ZFBF approaches simple power normalization as described in equation (3.5) instead of optimal power allocation techniques.

Figure 3.2 shows a performance comparison between ZFBF with exhaustive search, TxMF with exhaustive search and the proposed OLBF suboptimal techniques in the low SNR regime. In this scenario, the proposed algorithm outperforms matched filtering for the simulated range of active users. We can observe that the proposed scheme with orthogonal beamforming shows even better performance than zero-forcing where the user selection is performed via exhaustive search. However, as the number of active users in the cell increases, the gap between ZFBF and OLBF becomes smaller.

In Figure 3.3, instead of comparing with optimal scheduling techniques

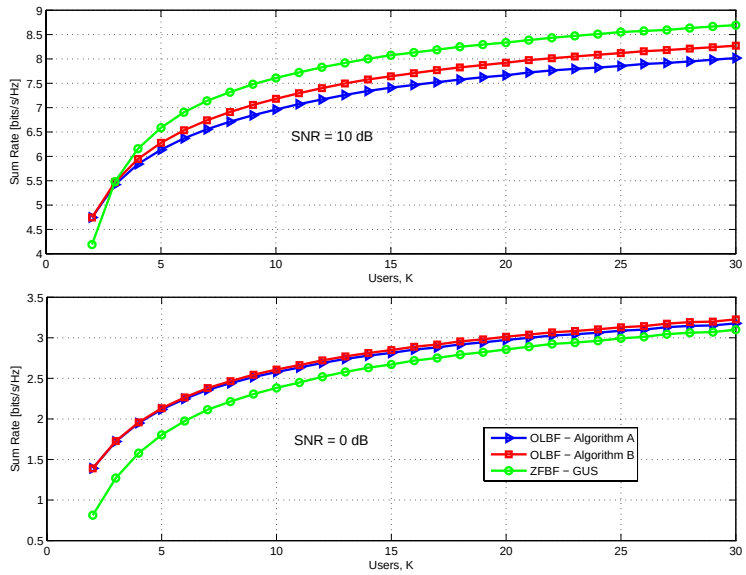


Figure 3.3: Sum rate comparison of suboptimal beamforming approaches as a function of the number of users for $M = 2$ transmit antennas, for a) average SNR = 0 dB (below) and b) average SNR = 10 dB (above).

as done in Figure 3.2, we focus on another suboptimal technique, ZFBF-GUS [16]. It is a fair comparison, since the proposed OLBF approaches and ZFBF-GUS rely on suboptimal scheduling algorithms. However, our proposed scheduling algorithm is computationally much less complex than [16], which involves computation of matrix inversions. We observe that knowledge of the interference exploited during the user selection process is particularly beneficial as the total number of users $K$ and the average SNR decrease. In this region, ZFBF-GUS exhibits a performance degradation. Knowledge of the interference between users that do not have good spatial separability helps to improve the task of the scheduler. Hence, the proposed scheme with joint beamforming and scheduling can effectively select users for transmission in sparse networks where moderate number of users is present, providing good average rates through a low-complexity design. However, as the average SNR increases, ZFBF-GUS can provide higher rates except for the case when the number of transmit antennas equals the number of users.

### 3.5.6 Discussion

In this section, we have shown how orthogonal linear beamforming (OLBF) can be efficiently combined with a low-complexity user selection algorithm to achieve a large portion of the multiuser capacity. The use of orthogonal transmission enables the transmitter to calculate exact SINR values during the user selection process. The proposed suboptimal algorithms provide performance gains with respect to optimal ZFBF and TxMF, as both the number of users in the cell and the average SNR decrease. Sum rate comparison with a ZFBF technique based on greedy user selection further shows the benefits of OLBF in cells with low to moderate number of active users in low SNR environments, highlighting the importance of multiuser interference knowledge for user scheduling.

## 3.6 Partial CSIT Case: A Low-Complexity Approach

The problem of joint scheduling and beamforming for a multiple antenna broadcast channel with partial CSIT is considered. We show how long-term statistical channel knowledge can be efficiently combined with instantaneous low-rate feedback for user selection and linear beamforming. A low complexity algorithm based on an estimate (bound) of the multiuser interference is proposed. Our scheme is shown to exhibit significant throughput gain over opportunistic techniques, approaching the sum rate of full CSIT for small angle spreads.

### 3.6.1 Motivation

The capacity gain of multiuser MIMO systems is highly dependent on the available CSIT. While having full CSI at the receiver can be assumed, this assumption is not reasonable at the transmitter side. In [51], a finite rate feedback model is proposed, in which each receiver quantizes its channel and feeds back a finite number of bits regarding its channel realization based on a codebook. An SDMA extension of opportunistic beamforming [63] using partial CSIT in the form of individual SINR is proposed in [2], achieving optimum capacity scaling for large number of users. However, these schemes do not exploit long-term statistical knowledge of the channel. Combining the

spatial correlation with the channel norm is addressed in [64], however it has not been exploited in an SDMA context. A means to combine instantaneous scalar feedback with statistical CSIT for the sole purpose of user selection is proposed in [65].

Here we make the following key points:

- Statistical CSIT, while causing almost negligible per-slot feedback overhead, can reveal information about the spatial separability of users.
- Scalar feedback can be used at the transmitter to evaluate the quality of the CSIT and estimate the multiuser interference.

Based on the above points we propose a practical low complexity scheme with joint scheduling and beamforming. Each user has a predefined beamforming vector, matched to the principal eigenvector of the channel correlation matrix. In order to achieve full multiuser diversity gain, we propose to feed back the following scalar values: 1) the alignment between the channel and each user's predefined beamforming vector 2) the channel norms. Our method shows a considerable gain over random opportunistic beamforming for angle spread less than 45 degrees, which makes it a practical approach especially for cellular outdoor systems.

### 3.6.2 System Assumptions

As considered in the previous section, equal power allocation over each of the data streams is assumed also here. We consider transmission in a downlink where insufficient scattering around the transmitter makes the MIMO channel spatially correlated. The channel vector is complex Gaussian distributed with zero mean and full-rank correlation matrix $\mathbf{R}_k = \mathbb{E}\{\mathbf{h}_k\mathbf{h}_k^H\}$. We assume that $\mathbf{R}_k$ is perfectly known at both ends of the link, which can be obtained from uplink measurements or using a low-rate feedback channel. The eigendecomposition of the transmit correlation matrix is $\mathbf{R}_k = \mathbf{V}_k\mathbf{\Lambda}_k\mathbf{V}_k^H$, where $\mathbf{\Lambda}_k$ is a diagonal matrix with the eigenvalues of $\mathbf{R}_k$ in descending order and $\mathbf{V}_k = \left[\mathbf{v}_k^1\ \mathbf{v}_k^2 \cdots \mathbf{v}_k^M\right]$ is a unitary matrix with the eigenvectors of $\mathbf{R}_k$.

### 3.6.3 Proposed Algorithm

We propose an algorithm that performs joint scheduling and beamforming in the downlink, based on statistical channel information and limited instantaneous channel feedback. As our optimization criterion is to maximize the

system throughput, it is desirable to schedule a set of $M$ users with large channel gains and mutually orthogonal beamforming vectors. The proposed algorithm is outlined in Table 3.5.

### Feedback Strategy

If the CSIT consists of channel gains and quantized channel directions, the multiuser interference cannot be completely eliminated, resulting to a bounded sum rate even for $K \to \infty$ [24]. Motivated by this fact, in order to achieve full multiuser diversity gain, we propose that each user feeds back the following scalar values: *1)* the alignment between its instantaneous normalized channel vector $\overline{\mathbf{h}}_k$ and a predefined beamforming vector, $\rho_k = \left|\overline{\mathbf{h}}_k^H \mathbf{w}_k\right|$ and *2)* its channel norm $\|\mathbf{h}_k\|^2$.

### User scheduling

If a perfectly orthogonal set of beamforming vectors can be found, the above mentioned instantaneous limited feedback is sufficient to achieve the same asymptotic sum rate as that of DPC. However, in practice, this cannot be fulfilled and the remaining interference cannot be calculated explicitly. Therefore, we derive a bound on the multiuser interference based on the available limited feedback, which is shown in detail in the next section. For user $k$ and index set $\mathcal{S}$, the multiuser interference can be expressed as $I_k(\mathcal{S}) = \sum_{i\in\mathcal{S}, i\neq k} \frac{P}{M} |\mathbf{h}_k^H \mathbf{w}_i|^2 = \frac{P}{M} \|\mathbf{h}_k\|^2 \overline{I}_k(\mathcal{S})$, where $\overline{I}_k(\mathcal{S})$ denotes the interference over the normalized channel $\overline{\mathbf{h}}_k$. Using $\overline{I}_{UB_k}(\mathcal{S})$, the upper bound on $\overline{I}_k(\mathcal{S})$, we have the following lower bound on the SINR:

$$SINR_k^{LB}(\mathcal{S}) = \frac{\frac{P}{M} \|\mathbf{h}_k\|^2 \rho_k^2}{\frac{P}{M} \|\mathbf{h}_k\|^2 \overline{I}_{UB_k}(\mathcal{S}) + \sigma^2}. \tag{3.26}$$

The scheduler is optimized to select the set of users that maximize a lower bound on the SR as follows

$$\mathcal{S}^* = \arg\max_{\mathcal{S}} \sum_{k\in\mathcal{S}} \log\left[1 + SINR_k^{LB}(\mathcal{S})\right]. \tag{3.27}$$

In order to reduce the complexity of the user search, we define a threshold $\mu_{th}$ and consider only users with product $\|\mathbf{h}_k\| \rho_k > \mu_{th}$. This threshold is defined by selecting the top $\mu$ percent values of $\|\mathbf{h}_k\| \rho_k$, and becomes necessary in dense networks where exhaustive search may be prohibitive, even though the computation of (3.27) entails low complexity.

Table 3.5: Outline of Proposed Low-Complexity Approach

| INITIALIZATION | |
|---|---|
| **MS** | |
| Update & Feedback | $\mathbf{w}_k = \mathbf{v}_k^1 \rightarrow$ BS $\forall k = 1, \cdots, K$ |
| **BS** | |
| Compute & Store | $\alpha_k(\mathcal{S})$, $\beta_k(\mathcal{S})$, $\gamma_k(\mathcal{S})$ $\forall k, \mathcal{S}$ (eq. 3.32) |
| AT EACH TIME SLOT | |
| **MS** | |
| Compute & Feedback | $\|\mathbf{h}_k\| \rightarrow$ BS $\quad \forall k = 1, \cdots, K$ |
| | $\rho_k = \left\|\overline{\mathbf{h}}_k^H \mathbf{w}_k\right\| \rightarrow$ BS |
| **BS** | |
| *User selection* | |
| **Step 0** Set $SR_{LB}^* = 0$ and $\mathcal{S}^* = \emptyset$ | |
| For all $\mathcal{S} \in \mathcal{G}$ with $\|\mathbf{h}_k\|\, \rho_k > \mu_{th}$, repeat | |
| **Step 1** Compute | |
| $\overline{I}_{UB_k}(\mathcal{S}) = \rho_k^2 \alpha_k(S) + \left(1-\rho_k^2\right) \beta_k(S) + 2\rho_k \sqrt{1-\rho_k^2}\gamma_k(S)$ | |
| **Step 2** Compute $SINR_k^{LB}(\mathcal{S}) = \frac{\frac{P}{M}\|\mathbf{h}_k\|^2 \rho_k^2}{\frac{P}{M}\|\mathbf{h}_k\|^2 \overline{I}_{UB_k}(\mathcal{S}) + \sigma^2}$ | |
| **Step 3** Compute $SR_{LB} = \sum_{k \in \mathcal{S}} \log\left[1 + SINR_k^{LB}(\mathcal{S})\right]$ | |
| **Step 4** If $SR_{LB} > SR_{LB}^*$, $SR_{LB} \rightarrow SR_{LB}^*$ and $\mathcal{S} \rightarrow \mathcal{S}^*$ | |
| *Beamforming* | |
| Construct beamforming matrix $\mathbf{W}(\mathcal{S})$ | |

### Beamforming Vectors

As a low complexity approach, we consider a system where each user has a preferred beamforming vector known both by the base station and mobile. As shown in [66], for single-user MIMO communications, given a certain user $k$ with correlation matrix $\mathbf{R}_k$ the average rate is maximized by matching the beamforming vector to the principal eigenvector of its correlation matrix, $\mathbf{w}_k = \mathbf{v}_k^1$. Hence, we design each user's beamforming vector according to this strategy. This is equivalent to a system where each user has a trivial - yet practical - codebook with a single codevector (eigen-codebook), which is updated at a very low rate when the transmit correlation changes in time.

### 3.6.4 Bound on the Multiuser Interference

Before deriving the bound on the multiuser interference, we state the following result.

**Lemma 3.1** Let $\mathbf{U}_k \in \mathbb{C}^{M\times(M-1)}$ be an orthonormal basis spanning the null space of $\mathbf{w}_k$. Then,

$$\left\|\overline{\mathbf{h}}_k^H \mathbf{U}_k\right\|^2 = 1 - \rho_k^2 \tag{3.28}$$

*Proof.* Define the orthonormal basis $\mathbf{Z}_k$ of $\mathbb{C}^{M\times M}$ obtained by stacking the column vectors of $\mathbf{U}_k$ and $\mathbf{w}_k$: $\mathbf{Z}_k = [\mathbf{U}_k \mathbf{w}_k]$. Since $\mathbf{Z}_k\mathbf{Z}_k^H = \mathbf{I}$ and $\overline{\mathbf{h}}_k$ has unit power

$$\left\|\overline{\mathbf{h}}_k^H \mathbf{Z}_k\right\|^2 = \overline{\mathbf{h}}_k^H \mathbf{Z}_k\mathbf{Z}_k^H \overline{\mathbf{h}}_k = \overline{\mathbf{h}}_k^H \overline{\mathbf{h}}_k = 1. \tag{3.29}$$

Then, by definition of $\mathbf{Z}_k$ we can separate the power of $\overline{\mathbf{h}}_k$ as follows

$$\left\|\overline{\mathbf{h}}_k^H \mathbf{Z}_k\right\|^2 = \left\|\overline{\mathbf{h}}_k^H \left[\mathbf{U}_k \mathbf{w}_k\right]\right\|^2 = \left\|\overline{\mathbf{h}}_k^H \mathbf{U}_k\right\|^2 + \left|\overline{\mathbf{h}}_k^H \mathbf{w}_k\right|^2 = 1. \tag{3.30}$$

Setting $\left|\overline{\mathbf{h}}_k^H \mathbf{w}_k\right|^2 = \rho_k^2$ and solving the above equation for $\left\|\overline{\mathbf{h}}_k^H \mathbf{U}_k\right\|^2$ we obtain the desired result. □

Define the matrix $\Psi_k(\mathcal{S}) = \sum_{i\in S, i\neq k} \mathbf{w}_i \mathbf{w}_i^H$ and the operator $\lambda_{max}\{\cdot\}$, which returns the largest eigenvalue. We obtain the following result:

**Theorem 3.1** Given an arbitrary set of unit-norm beamforming vectors $\{\mathbf{w}_i, i \in \mathcal{S}\}$, the interference experienced by the $k$-th user can be bounded as follows

$$\begin{aligned} \overline{I}_k(\mathcal{S}) \;&\leq\; \rho_k^2\, \mathbf{w}_k^H \Psi_k(\mathcal{S}) \mathbf{w}_k \\ &+\; (1-\rho_k^2)\, \lambda_{max}\left\{\mathbf{U}_k^H \Psi_k(\mathcal{S}) \mathbf{U}_k\right\} \\ &+\; 2\rho_k \sqrt{1-\rho_k^2}\, \left\|\mathbf{U}_k^H \Psi_k(\mathcal{S}) \mathbf{w}_k\right\| \end{aligned} \tag{3.31}$$

*Proof.* See Appendix 3.A. □

Note that, in the proposed algorithm, when computing the interference bound from (3.31) for each user $k$ and index set $\mathcal{S}$, the following values can be prestored at the BS

$$\begin{cases} \alpha_k(\mathcal{S}) = \mathbf{w}_k^H \Psi_k(\mathcal{S}) \mathbf{w}_k \\ \beta_k(\mathcal{S}) = \lambda_{max}\left\{\mathbf{U}_k^H \Psi_k(\mathcal{S}) \mathbf{U}_k\right\} \\ \gamma_k(\mathcal{S}) = \left\|\mathbf{U}_k^H \Psi_k(\mathcal{S}) \mathbf{w}_k\right\| \end{cases} \tag{3.32}$$

hence not contributing to increase complexity during runtime. As shown in Table 3.5, the initialization procedure is performed before data transmission starts. Afterwards, the quantities $\alpha_k(\mathcal{S})$, $\beta_k(\mathcal{S})$, $\gamma_k(\mathcal{S})$ and $\mathbf{w}_k$ can be updated either when a new user enters the system or periodically, in order to account for variations in the users' long-term statistics. Thus, the upper bound on the multiuser interference involves low computational complexity and can be expressed as

$$\overline{\mathrm{I}}_{UB_k}(\mathcal{S}) = \rho_k^2 \alpha_k(\mathcal{S}) + \left(1-\rho_k^2\right) \beta_k(\mathcal{S}) + 2\rho_k \sqrt{1-\rho_k^2}\gamma_k(\mathcal{S}) \tag{3.33}$$

Consider the following particular cases to have a more intuitive idea of this bound: *(a)* $\rho_k \to 1$, then $\overline{\mathrm{I}}_{UB_k}(\mathcal{S}) \to \rho_k^2 \alpha_k(S)$. In this case, the interference is due to non-orthogonalities between $\mathbf{w}_k$ and the remaining beamforming vectors; *(b)* as the beamforming vectors become orthogonal, i.e. $\left|\mathbf{w}_i^H \mathbf{w}_j\right| \to 0 \ \forall i \neq j \in \mathcal{S}$, then $\alpha_k(\mathcal{S}) \to 0$, $\beta_k(\mathcal{S}) \to 1$, $\gamma_k(\mathcal{S}) \to 0$ and hence $\overline{I}_{UB_k}(\mathcal{S}) \to 1 - \rho_k^2$. Particularly, when perfect orthogonality exists, we can state the following

**Corollary 3.1** Given an orthonormal set of $M$ beamforming vectors in $\mathbb{C}^M$, the interference experienced by user $k \in \mathcal{S}$ is given by

$$\overline{I}_k(\mathcal{S}) = 1 - \rho_k^2. \tag{3.34}$$

*Proof.* Direct consequence of Lemma 3.1 when the interfering beamforming vectors are basis vectors of the null space of $\mathbf{w}_k$. □

Hence, the derived interference bound becomes tighter as the orthogonality between beamforming vectors increases.

### 3.6.5 Numerical Results

At the transmitter side, we consider a uniform linear antenna array (ULA) with antenna spacing $d = 0.4\lambda$, where $\lambda$ is the wavelength (here for a 2GHz system). We assume that the channel evolves according to a specular model where the channel impulse response is a superposition of a finite number of paths. The path gains are assumed to be zero-mean, unit variance complex Gaussian distributed. Each of these paths have a Gaussian distributed angle of incidence with respect to the transmitter broadside. We evaluate our scheme for $M = 2$ antennas and SNR = 10 dB.

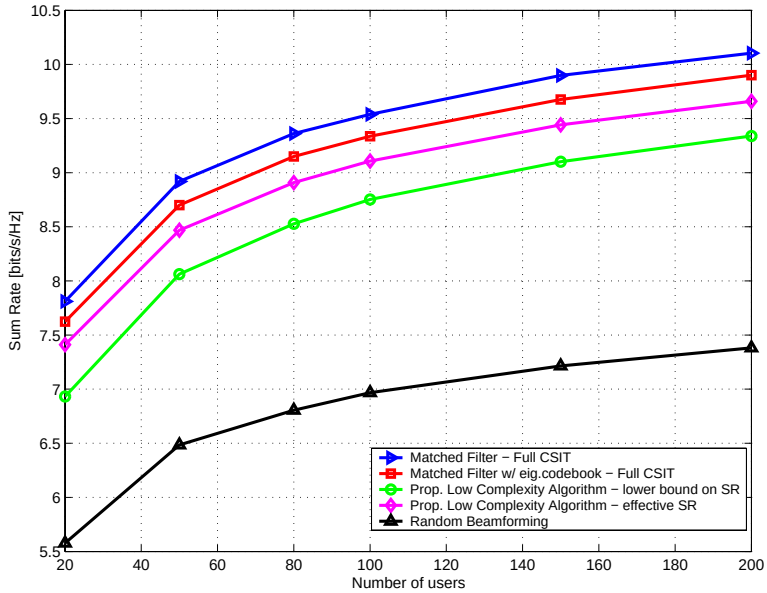


Figure 3.4: Sum rate as a function of the number of users for $M = 2$ transmit antennas, and $\sigma_\theta = 0.1\pi$.

Figure 3.4 and Figure 3.5 show a performance comparison in terms of sum rate for several approaches, as a function of the number of users and the angle spread, respectively. Since the proposed scheme is based on TxMF, we give as a reference the performance of TxMF with perfect CSIT. In order to evaluate the proposed user selection metric based on reduced feedback, we also compare with a scheme that while having the same beamforming strategy (transmission along the principal eigenvector of $\mathbf{R}_k$), uses full CSIT for user scheduling. Our method shows a clear gain over random beamforming [2] for angle spread less than 45 degrees making it a practical approach for cellular outdoor systems.

### 3.6.6 Discussion

We presented a low complexity beamforming/scheduling algorithm for spatially correlated MIMO channels, exploiting statistical channel knowledge combined with limited instantaneous feedback. The proposed scheme exhibits performance close to that of full CSIT when the multipath angular

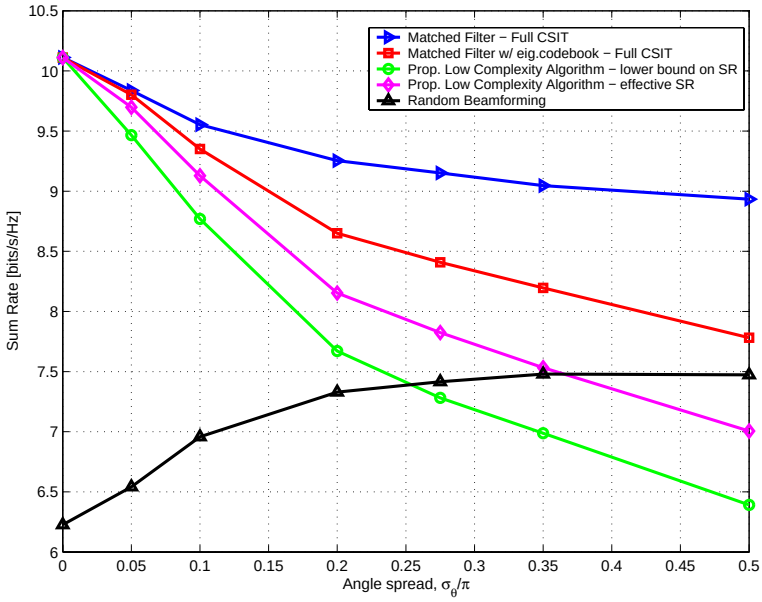


Figure 3.5: Sum rate as a function of angle spread for $M = 2$ transmit antennas, antenna spacing $d = 0.4\lambda$ and $K = 100$ users.

spread at the transmitter is small enough, making this approach suitable to wireless systems with elevated base station such as outdoor cellular networks.

## 3.7 Conclusions

In this chapter, the problem of joint linear beamforming and scheduling for MIMO broadcast channels has been presented. In such systems, transmission techniques and user selection algorithms with reasonable complexity are desired. In order to illustrate this fact, low-complexity solutions have been proposed both in scenarios with full and partial CSIT. In the following chapters, we focus on the optimization of different elements present in such communication systems. While assuming simple scheduling algorithms, similar to the ones here presented, we would like to identify what type of feedback and beamforming techniques are most appropriate in limited feedback scenarios, for the purpose of sum-rate maximization.

# APPENDIX

## 3.A Computation of Multiuser Interference Bounds

Using the definition of $\mathbf{\Psi}_k(\mathcal{S})$, the interference over the normalized channel for user $k$ and index set $\mathcal{S}$, denoted as $\overline{I}_k(\mathcal{S})$, can be expressed as

$$\overline{I}_k(\mathcal{S}) = \sum_{i\in\mathcal{S}, i\neq k} \left|\overline{\mathbf{h}}_k^H \mathbf{w}_i\right|^2 = \sum_{i\in\mathcal{S}, i\neq k} \overline{\mathbf{h}}_k^H \mathbf{w}_i \mathbf{w}_i^H \overline{\mathbf{h}}_k = \overline{\mathbf{h}}_k^H \mathbf{\Psi}_k(\mathcal{S}) \overline{\mathbf{h}}_k. \tag{3.35}$$

The normalized channel $\overline{\mathbf{h}}_k$ can be expressed as a linear combination of orthonormal basis vectors. Using Lemma 3.1, all possible unit-norm $\overline{\mathbf{h}}_k$ vectors with $\left|\overline{\mathbf{h}}_k^H \mathbf{w}_k\right| = \rho_k$ can be written as follows

$$\overline{\mathbf{h}}_k = \rho_k e^{j\alpha_k} \mathbf{w}_k + \sqrt{1-\rho_k^2}\mathbf{U}_k \mathbf{B}_k \mathbf{e}_k \tag{3.36}$$

where $\mathbf{B}_k$ is a diagonal matrix with entries $e^{j\beta_i}, i = 1, \ldots, M-1$ and $\mathbf{e}_k$ is an arbitrary unit-norm vector in $\mathbb{C}^{(M-1)\times 1}$. The complex phases $\beta_i$ and $\alpha_k$ are unknown and lie in $[0, 2\pi]$. Substituting (3.36) into (3.35) we get

$$\begin{aligned} \overline{I}_k(\mathcal{S}) &= \rho_k^2\ \mathbf{w}_k^H \mathbf{\Psi}_k(\mathcal{S}) \mathbf{w}_k \\ (a) \qquad &+ (1-\rho_k^2)\, \mathbf{e}_k^H \mathbf{B}_k^H \mathbf{U}_k^H \mathbf{\Psi}_k(\mathcal{S}) \mathbf{U}_k \mathbf{B}_k \mathbf{e}_k \\ (b) \qquad &+ \rho_k \sqrt{1-\rho_k^2}\, [e^{-j\alpha_k} \mathbf{w}_k^H \mathbf{\Psi}_k(\mathcal{S}) \mathbf{U}_k \mathbf{B}_k \mathbf{e}_k \\ &\qquad + \mathbf{e}_k^H \mathbf{B}_k^H \mathbf{U}_k^H \mathbf{\Psi}_k(\mathcal{S}) \mathbf{w}_k e^{j\alpha_k}]. \end{aligned} \tag{3.37}$$

Since the first term in (3.37) is perfectly known, the upper bound on $\overline{I}_k(\mathcal{S})$ is found by joint maximization of the summands (a) and (b) with respect to $\alpha_k$, $\mathbf{B}_k$ and $\mathbf{e}_k$. We use a simpler optimization method, which consists of bounding separately each term.
(a) Defining $\mathbf{A}_k(\mathcal{S}) = \mathbf{U}_k^H \mathbf{\Psi}_k(\mathcal{S}) \mathbf{U}_k$ for clarity of exposition, the second term can be bounded as follows

$$\begin{aligned} &\max_{\mathbf{B}_k, \mathbf{e}_k} \left(1-\rho_k^2\right) \mathbf{e}_k^H \mathbf{B}_k^H \mathbf{A}_k(\mathcal{S}) \mathbf{B}_k \mathbf{e}_k = \left(1-\rho_k^2\right) \lambda_{max}\{\mathbf{A}_k(\mathcal{S})\} \\ &s.t.\ \|\mathbf{e}_k\| = 1 \end{aligned} \tag{3.38}$$

where the operator $\lambda_{max}\{\cdot\}$ returns the largest eigenvalue. The maximum in (3.38) is obtained when the vector $\mathbf{B}_k\mathbf{e}_k$ equals the principal eigenvector of the matrix $\mathbf{A}_k(\mathcal{S})$.
(b) Defining $\mathbf{q}_k = \mathbf{B}_k^H\mathbf{U}_k^H\mathbf{\Psi}_k(\mathcal{S})\mathbf{w}_k e^{j\alpha_k}$ and noting that the matrix $\mathbf{\Psi}_k(\mathcal{S})$ is Hermitian by construction, the bound on the third term in (3.37) can be written as follows

$$\max_{\mathbf{q}_k,\mathbf{e}_k} \rho_k\sqrt{1-\rho_k^2}\left[\mathbf{q}_k^H\mathbf{e}_k + \mathbf{e}_k^H\mathbf{q}_k\right] = \max_{\mathbf{q}_k} 2\rho_k\sqrt{1-\rho_k^2}\,\|\mathbf{q}_k\|$$

$$s.t.\ \|\mathbf{e}_k\| = 1 \tag{3.39}$$

The equality follows from the fact that the left hand side is maximized for $\mathbf{e}_k = \frac{\mathbf{q}_k}{\|\mathbf{q}_k\|}$, which satisfies the unit-norm constraint. The solution is given by

$$\begin{aligned}\max_{\mathbf{q}_k} 2\rho_k\sqrt{1-\rho_k^2}\,\|\mathbf{q}_k\| &= \max_{\mathbf{B}_{k,\alpha_k}} 2\rho_k\sqrt{1-\rho_k^2}\left\|\mathbf{B}_k^H\mathbf{U}_k^H\mathbf{\Psi}_k(S)\mathbf{w}_k e^{j\alpha_k}\right\| \\ &= 2\rho_k\sqrt{1-\rho_k^2}\,\left\|\mathbf{U}_k^H\mathbf{\Psi}_k(S)\mathbf{w}_k\right\|.\end{aligned} \tag{3.40}$$

Finally, incorporating into (3.37) the bounds obtained in (3.38) and (3.40) we obtain the desired bound.

# Chapter 4

# A Design Framework for Scalar Feedback

*In this chapter, joint linear beamforming and scheduling is performed in a system where limited feedback is present at the transmitter side. The feedback conveyed by each user to the base station consists of channel direction information (CDI) based on a predetermined codebook and a scalar metric with channel quality information (CQI) used to perform user scheduling. In this chapter, we present a design framework for scalar feedback in MIMO broadcast channels with limited feedback. An approximation on the sum rate is provided for the proposed family of metrics, which is validated through simulations. For a given number of active users and average SNR conditions, the base station is able to update certain transmission parameters in order to maximize the sum-rate function. On the other hand, the proposed sum-rate function provides a means of simple comparison between transmission schemes and scalar feedback techniques. Particularly, the sum-rate of SDMA and TDMA is compared in the following extreme regimes: large number of users, high SNR and low SNR. Simulations are provided to illustrate the performance of various scalar feedback techniques based on the proposed design framework. In addition, the effect of scalar feedback quantization is studied, introducing the tradeoff between multiuser diversity and multiplexing gain that arises in systems with a sum rate feedback constraint.*

## 4.1 Introduction

The challenge of designing high performance schemes for MIMO broadcast channels based on joint linear beamforming and multiuser scheduling has been a focus of interest over the past years. In limited feedback scenarios, the linear beamformers, scheduling algorithms and feedback strategies need to be jointly design in order to provide high system sum rates. In this chapter, we consider limited feedback scenarios in which each user conveys channel quality information (CQI) to the base station for the purpose of user scheduling along with channel direction information (CDI).

In [2], an SDMA extension of opportunistic beamforming [63] using partial CSIT in the form of individual SINR is proposed, achieving optimum capacity scaling for large number of users. A simple scheme for joint scheduling and beamforming with limited feedback is proposed in [28], [60]. The receivers compute and feed back a scalar metric that can be interpreted as an upper bound on the SINR. Assuming certain orthogonality constraints between beamforming vectors, a lower bound on the instantaneous or average SINR can be computed as scalar feedback, as shown in [25] and [27] respectively. The total amount of feedback overhead in the system can be reduced by appropriately setting minimum desired SINR thresholds while controlling each user's quality of service (QoS). Design of feedback thresholds for general scheduling metrics have been proposed in [67].

In this chapter we present a design framework for scalar feedback in MIMO broadcast channels, which generalizes previously proposed techniques. A family of metrics is presented based on individual SINRs, which are computed at the receivers and fed back to the base station as channel quality information. The framework here presented can be applied to any system in which codebooks are employed for channel direction quantization. Moreover, additional orthogonality constraints between beamforming vectors may be considered with the purpose of simplifying the task of user scheduling and controlling the amount of multiuser interference.

An approximation on the ergodic sum rate is provided for the proposed family of metrics. The resulting sum-rate function fits well the simulated sum rate as shown through simulations, even in cells with reduced number of active users. This function, as we show, can be a powerful design tool and at the same time it greatly simplifies system analysis. On the one hand, we can envisage a cellular system in which, given certain average SNR conditions and number of active users, the base station sets the different parameters

so as to maximize the sum-rate function. On the other hand, as shown in the analysis, the sum-rate function provides a means of simple comparison between different transmission schemes and scalar feedback techniques in extreme regimes, without the need of extreme value theory. Particularly, we compare the sum-rate of SDMA and TDMA approaches in scenarios with large number of users, high SNR and low SNR regimes. Simulations are provided to illustrate the performance of different scalar feedback techniques based on the proposed design framework. Furthermore, the effect of quantizing the scalar metrics is studied in a system with finite sum rate feedback, identifying the existing tradeoff between multiuser diversity and multiplexing gain.

## 4.2 System Model

We consider a multiple antenna broadcast channel consisting of $M$ antennas at the transmitter and $K \geq M$ single-antenna receivers. The system model is equivalent to the one presented in Section 3.2, with some particularities. The received signal $y_k$ of the $k$-th user is mathematically described as

$$y_k = \mathbf{h}_k^H \mathbf{x} + n_k, \qquad k = 1, \ldots, K \tag{4.1}$$

where $\mathbf{x} \in \mathbb{C}^{M \times 1}$ is the transmitted signal, $\mathbf{h}_k \in \mathbb{C}^{M \times 1}$ is an i.i.d. Rayleigh flat fading channel vector, and $n_k$ is additive white Gaussian noise at receiver $k$ with zero mean and variance $\sigma^2$. We assume that each of the receivers has perfect and instantaneous knowledge of its own channel $\mathbf{h}_k$. Let $\mathcal{S}$ denote the set of users selected for transmission at a given time slot, with cardinality $|\mathcal{S}| = M_o$, $1 \leq M_o \leq M$. Let $\mathbf{w}_k$ be the unit-norm beamforming vector for user $k$. Assuming equal power allocation to the $M_o$ scheduled users, the received signal at the $k$-th mobile is given by

$$y_k = \sqrt{\frac{P}{M_o}} \sum_{i \in \mathcal{S}} \mathbf{h}_k^H \mathbf{w}_i s_i + n_k, \qquad k = 1, \ldots, K. \tag{4.2}$$

Hence, the SINR of user $k$ is

$$SINR_k = \frac{|\mathbf{h}_k^H \mathbf{w}_k|^2}{\sum_{i \in \mathcal{S}, i \neq k} |\mathbf{h}_k^H \mathbf{w}_i|^2 + \frac{M_o \sigma^2}{P}}. \tag{4.3}$$

We focus on the ergodic sum rate (SR) which, assuming Gaussian inputs, is equal to

$$SR = \mathbb{E}\left\{\sum_{k\in\mathcal{S}} \log\left[1 + SINR_k\right]\right\}. \tag{4.4}$$

## 4.3 Linear Beamforming with Limited Feedback

Joint linear beamforming and scheduling is performed in a system where limited feedback is present at the transmitter side. The feedback conveyed by each user to the base station consists of channel direction information based on a predetermined codebook and a scalar metric with channel quality information used to perform user scheduling.

In such systems, the design of appropriate scalar metrics in scenarios with realistic number of users and average SNR values remains a challenge. These metrics must contain information of the users' channel gains as well as channel quantization errors, as discussed in Section 3.6. If the users have additional knowledge of the beamforming technique used at the transmitter side, an estimate on the multiuser interference at the receiver can be computed. This information can be encapsulated together with the channel gain, quantization error and average noise power into a scalar metric $\xi$, which consists of an estimate on the SINR. In our work, we consider such scalar feedback strategies, as discussed in detail in next section. User selection is carried out based on these metrics and the users' spatial properties, obtained from channel quantizations.

As simple transmission technique we consider transmit matched filtering (TxMF), which consists of using as normalized beamforming vectors the quantized channel directions of users scheduled for transmission. The normalized channel vector of user $k$ to be quantized is $\overline{\mathbf{h}}_k = \mathbf{h}_k / \|\mathbf{h}_k\|$, which corresponds to the channel direction. A $B$-bit quantization codebook $\mathcal{V}_k$ is considered, containing $2^B$ unit norm vectors in $\mathbb{C}^{M\times M}$, which is assumed to be known to both the receiver and the transmitter. Similarly to [48], [49], we assume that each receiver quantizes its channel to the vector that maximizes the inner product

$$\mathbf{w}_k = \arg\max_{\mathbf{w}\in\mathcal{V}_k} |\overline{\mathbf{h}}_k^H \mathbf{w}|^2 = \arg\max_{\mathbf{w}\in\mathcal{V}_k} \cos^2(\angle(\overline{\mathbf{h}}_k, \mathbf{w})) \tag{4.5}$$

Each user sends the corresponding quantization index back to the transmitter through an error-free and zero-delay feedback channel using $B$ bits. Note that this model is equivalent to the finite rate feedback model proposed by [48], [51].

The optimal vector quantizer is difficult to find and the solution to this problem is not yet known. In this chapter, we focus on scalar feedback feedback design rather than on the design of quantization codebooks. This issue is treated in the next chapter. Therefore, we adopt a simple geometrical framework presented in [49]. The resulting quantization error is defined as $\sin^2\theta_k = \sin^2(\angle(\bar{\mathbf{h}}_k, \mathbf{w}_k)) = 1 - \left|\bar{\mathbf{h}}_k^H \mathbf{w}_k\right|^2$ [49], [50], where $\mathbf{w}_k$ is the quantized channel direction of user $k$. Note that, when using the quantized channel as beamforming vector, then $\rho_k^2 = \left|\bar{\mathbf{h}}_k^H \mathbf{w}_k\right|^2$ as described in Section 3.6, and thus $\sin^2\theta_k = 1 - \rho_k^2$. Using this framework, the cumulative distribution function (cdf) of the quantization error is given by [49], [50]

$$F_{\sin^2\theta_k}(x) = \begin{cases} \delta^{1-M} x^{M-1}, & 0 \le x \le \delta \\ 1, & x > \delta \end{cases} \tag{4.6}$$

where $\delta = 2^{-B/(M-1)}$.

Let the orthogonality factor $\epsilon$ denote the maximum degree of non orthogonality between two unit-norm vectors. The columns of the normalized beamforming matrix $\mathbf{W}(\mathcal{S})$ are constrained to be $\epsilon$-orthogonal and thus

$$\left|\mathbf{w}_i^H \mathbf{w}_j\right| \le \epsilon \quad \forall\, i, j \in \mathcal{S},\ i \ne j. \tag{4.7}$$

An outline of the proposed scheduling algorithm is shown in Table 4.1. In case $M_o$ users with $\epsilon$-orthogonality can not be found, the algorithm stops and distributes the power equally among the scheduled users, setting $M_o = |\mathcal{S}|$. Note that this greedy algorithm is equivalent to the one proposed in [15], [16], [68]. The first user is selected from the set $\mathcal{Q}^0 = \{1, \ldots, K\}$ as the one having the highest channel quality, i.e., $k_1 = \arg\max_{k \in \mathcal{Q}^0} \xi_k$. For $i = 1, \ldots, M_o - 1$, the $(i+1)$-th user is selected as $k_{i+1} = \arg\max_{k \in \mathcal{Q}^i} \xi_k$ among the user set $\mathcal{Q}^i = \left\{1 \le k \le K : |\mathbf{w}_k^H \mathbf{w}_{k_j}| \le \epsilon, 1 \le j \le i\right\}$.

The number of active beams for transmission $M_o$ and orthogonality factor $\epsilon$ are system parameters fixed by the base station that can be adapted in order to maximize the system sum rate.

Table 4.1: Outline of Scheduling Algorithm with Variable Number of Active Beams

**MS**

**Compute & Feedback** $\xi_k$

quantization index $i \in \{1, \ldots, 2^B\}$

**BS**

**Initialize** Set $\mathcal{S} = \emptyset$

**Loop** For $i : 1 \ldots M_o$ repeat

**Set** $\xi^i_{max} = 0$

**Loop** For $k : 1 \ldots K, k \notin \mathcal{S}$ repeat

If $\xi_k > \xi^i_{max}$ and $\left|\mathbf{w}_k^H \mathbf{w}_j\right| \leq \epsilon \;\; \forall\, j \in \mathcal{S}$

$\xi_k \rightarrow \xi^i_{max}$ and $k_i = k$

**Select** $k_i \rightarrow \mathcal{S}$

## 4.4 Scalar Feedback Design

In this section, we present design guidelines for scalar metrics based on signal-to-interference-plus-noise ratios, which are computed at the receivers and fed back to the base station as channel quality information. Complemented with channel quantizations as CDI, user scheduling at the base station of a MIMO broadcast channel is performed. The design framework for scalar feedback here presented can be applied to any system in which codebooks are employed for channel quantization, known both to the base station and mobile users.

These metrics must contain information of different nature in order to exploit the multiuser diversity of the MIMO broadcast channel. Moreover, additional information on the orthogonality constraints between beamforming vectors can be taken into account, thus providing a QoS estimate at the receiver side. The total amount of feedback overhead can be reduced by appropriately setting minimum desired SINR thresholds. Hence, in a practical system each user may send feedback to the base station only if a minimal QoS can be guaranteed.

Besides signal and noise power, the following information may be encapsulated by each user in such scalar metrics

- Channel power gain: $\|\mathbf{h}_k\|^2$
- Quantization error: $\sin^2\theta_k$
- Orthogonality factor: $\epsilon$
- Number of active beams: $M_o$

As shown in [22], channel power gain and quantization error information are necessary in order to exploit the available multiuser diversity. The quantization error is a function of the number of codebook bits, as shown in the previous section. By increasing the codebook size, the multiplexing gain of the system can be increased (better resolution) and at the same time the multiuser diversity gets increased, due to lower quantization error. The orthogonality factor $\epsilon$ can be used to bound the amount of expected multiuser interference, which in turn can be used to compute a lower bound on the SINR. In our work, we assume that the number of active beams (non-zero power) is a parameter appropriately set by the base station to maximize the system sum-rate.

### Multiuser Interference

For user $k$ and index set $\mathcal{S}$, the multiuser interference can be expressed as $I_k(\mathcal{S}) = \sum_{i\in\mathcal{S},i\neq k}\frac{P}{M_o}|\mathbf{h}_k^H\mathbf{v}_i|^2 = \frac{P}{M_o}\|\mathbf{h}_k\|^2\overline{I}_k(\mathcal{S})$, where $\overline{I}_k(\mathcal{S})$ denotes the interference over the normalized channel $\overline{\mathbf{h}}_k$. Let $\mathbf{U}_k \in \mathbb{C}^{M\times(M-1)}$ be an orthonormal basis spanning the null space of $\mathbf{v}_k^H$ and define the matrix $\Psi_k\mathcal{S} = \sum_{i\in S,i\neq k}\mathbf{v}_i\mathbf{v}_i^H$ and the operator $\lambda_{max}\{\cdot\}$, which returns the largest eigenvalue. Define $\overline{I}_{UB_k}$ as the upper bound on $\overline{I}_k$ and $\theta_k = \angle(\overline{\mathbf{h}}_k, \mathbf{w}_k)$. As shown in Theorem 3.1 in the previous chapter for systems with arbitrary orthogonality between beamforming vectors, the multiuser interference of user $k$ and set $\mathcal{S}$ can be bounded as follows

$$\overline{I}_{UB_k}(\mathcal{S}) = \alpha_k(\mathcal{S})\cos^2\theta_k + \beta_k(\mathcal{S})\sin^2\theta_k + 2\gamma_k(\mathcal{S})\sin\theta_k\cos\theta_k \tag{4.8}$$

where $\alpha_k(\mathcal{S})$, $\beta_k(\mathcal{S})$ and $\gamma_k(\mathcal{S})$ are given in (3.32).

### Family of Metrics

In the proposed design framework, any scalar feedback metric can be described as follows

$$\xi = \frac{\|\mathbf{h}_k\|^2 \cos^2\theta_k}{\|\mathbf{h}_k\|^2 \left(\alpha\cos^2\theta_k + \beta\sin^2\theta_k + 2\gamma\sin\theta_k\cos\theta_k\right) + \frac{M_o\sigma^2}{P}}. \tag{4.9}$$

The numerator in the expression above reflects the effective received power in a system with channel quantization. On the other hand, the denominator accounts for the noise power and provides a measure of the interference experienced by the user, for instance an upper or lower bound, by exploiting the structure of the beamforming matrix. By choosing different values for the parameters $\alpha$, $\beta$, $\gamma$ and $M_o$, the meaning of the proposed metric is modified, yielding different SINR measures. In next section, a sum-rate function is derived based on this metric structure, for arbitrary values of these parameters. When setting $\alpha = \alpha_k(\mathcal{S})$, $\beta = \beta_k(\mathcal{S})$ and $\gamma = \gamma_k(\mathcal{S})$ as in (3.32), the metric $\xi$ becomes a lower bound for the SINR described in (4.3). In Section 3.6, these values were computed at the base station, where the beamforming vectors for the scheduled users are perfectly known. However, in the current scenario, $\alpha$, $\beta$ and $\gamma$ are computed at the receiver side, and thus the beamforming vectors assigned to interfering users are not known. Instead, these values can be bounded by exploiting the fact that the beamforming vectors are constrained to form an $\epsilon$-orthogonal set. Note that, even though $\epsilon$-orthogonality beamformers are imposed at the transmitter, we may choose not to include this information in the scalar feedback metric. In addition, even though $M_o$ is in principle a parameter that may be modified by the base station, a simplified case with $M_o = M$ may be considered for feedback design.

In the remainder of this section we present several scalar metrics complying with this structure.

#### Metric I

Let $\mathbf{u}_{jk}$ be the $j$-th column vector of the matrix $\mathbf{U}_k$. The vector $\mathbf{u}_{jk}$ is isotropically distributed over an $M-1$ dimensional hyperplane orthogonal to $\mathbf{w}_k$, under the assumption that $\mathbf{w}_k$ is isotropically distributed over the unit norm hypersphere. Given a fixed unit-norm vector $\mathbf{w}_i$ in $\mathbb{C}^M$, the random variable $\left|\mathbf{w}_i^H\mathbf{u}_{jk}\right|^2$ follows a beta distribution with parameters $(1, M-2)$ [69]. The mean value of this random variable is $\frac{1}{M-1}$, and thus we have that

$\mathbb{E}\left[\sum_{i=1,i\neq k}^{M_o} |\mathbf{v}_i^H \mathbf{u}_{jk}|^2\right] = \frac{M_o-1}{M-1}$. Using this result in (3.32) and the fact that non-orthogonality between pairs of beamforming vectors is upper bounded by $\epsilon$, we propose the following values for this metric

$$\alpha = \frac{(M_o-1)^2}{M-1}\epsilon^2$$

$$\beta = \frac{(M_o-1)}{M-1}\left[1 + (M_o - 2)\epsilon\right]$$

$$\gamma = \frac{(M_o-1)^2}{M-1}\epsilon$$

and

$$1 \leq M_o \leq M.$$

Note that averaging the inverse of the resulting metric yields an upper bound on the average of the inverse SINR. Hence, the average value of this metric tends to be a lower bound on the average SINR.

**Metric II**

As a particular case, we consider $\epsilon = 0$ in the metric computation and thus

$$\alpha = 0$$
$$\beta = 1$$
$$\gamma = 0$$

and

$$M_o = M.$$

This metric can be interpreted as an upper bound on the SINR when exactly $M_o = M$ beams are used for transmission and equal power allocation is performed. Note that this metric was proposed in [28], [60].

**Metric III**

Another option consists of computing a lower bound on the instantaneous SINR [25]. As opposed to Metric I, no averaging over the distribution of $\left|\mathbf{w}_k^H \mathbf{u}_{ik}\right|$ is performed and thus this lower bound is less tight in average. The

metric parameters are given by

$$\alpha = (M_o - 1)\epsilon^2$$
$$\beta = \begin{cases} 0, & if \quad M_o = 1 \\ 1 + (M_o - 2)\epsilon, & otherwise \end{cases}$$
$$\gamma = (M_o - 1)\epsilon$$

and

$$1 \leq M_o \leq M.$$

Taking into account $\epsilon$ in the SINR computation may mask the contribution of the channel power gains in the SINR expression, hence reducing the benefits of multiuser diversity. However, this approach offers the advantage of avoiding outage events in the communication link.

**Metric IV**

A straightforward improvement of Metric II can be done by setting a variable number of active beams $1 \leq M_o \leq M$, keeping the same values for $\alpha$, $\beta$ and $\gamma$.

Note that, for a given scenario and feedback metric, there is an optimal pair of system parameters $\epsilon$ and $M_o$ that maximizes the sum rate. Increasing the value of $\epsilon$ relaxes the $\epsilon$-orthogonality constraint and thus more users are taken into account for scheduling, increasing the multiuser diversity benefit. However, as $\epsilon$ increases, so does the multiuser interference. On the other hand, increasing the number of active beams $M_o$ exploits the spatial multiplexing gain, at the expense of increasing the interference. Hence, for a given average SNR and number of active users $K$ in the cell, the base station must appropriately set $\epsilon$ and $M_o$ in order to balance the multiuser diversity and multiplexing gains and to maximize the system sum rate. In practice, this may be carried out by storing lookup tables at the base station, so that $\epsilon$ and $M_o$ can be quickly adapted whenever the average SNR or the number of active users changes. If the system parameters need to be updated, the base station broadcasts the new values to the users, which are used to compute the feedback metrics.

In Figure 4.1, an approximated lower bound on the system sum rate is plotted as a function of the alignment $\cos\theta_k$, computed as $SR \approx M_o \log(1 + \xi_k^I)$, where $\xi_k^I$ denotes the feedback Metric I of user $k$. This approximation

assumes that the $M_o$ scheduled users have the same $\xi_k^I$ value and thus the same estimated lower bound on the achievable rate. The system under consideration is assumed to have $M = 4$ antennas, $\epsilon = 0.1$ and an average SNR of 10 dB. The sum rate is evaluated for different number of active beams to observe the impact of appropriately choosing $M_o$. Note that the case of $M_o = 1$ corresponds to TDMA, whereas $M_o > 1$ corresponds to SDMA. The system with $M_o = 1$ exhibits better performance for low and intermediate values of $\cos\theta_k$, i.e. TDMA provides higher rates than SDMA in most cases. Only for large values of $\cos\theta_k$, $M_o > 1$ provides higher rates, which in practice occurs for large number of quantization bits $B$ or large number of users $K$. Since the amount of bits $B$ is generally low due to bandwidth limitations, SDMA will be chosen over TDMA when $M_o > 1$ users with small quantization errors can be found, with higher probability as the number of users in the cell increases. As the parameter $\epsilon$ increases, the crossing points of the curves in Figure 4.1 shift to the right and thus the range for which TDMA performs better also increases. This is due to the fact that the bound in $\xi_k^I$ becomes looser for increasing $\epsilon$ values. As shown in this example, for $\epsilon > 0$ there exist $M$ possible modes of transmission, i.e. $M_o = 1, \ldots, M$. However, for the case of $\epsilon = 0$ and varying $M_o$ as considered in Metric IV, it can be proven that the modes of transmission exhibiting higher rates are reduced to 2, namely $M_o = 1, M$.

## 4.5 Sum-Rate Function

In this section we derive a function to approximate the ergodic sum rate that a system with linear beamforming and limited feedback can provide, given knowledge of each user's SINR metric. A general and simple solution is derived based on the generic metric representation of $\xi$, given in (4.9). Note that the different metrics described in the previous section follow as particular cases of $\xi$ by setting accordingly the values of $\alpha$, $\beta$, $\gamma$ and $M_o$. The sum-rate function we provide is a tool that enables simple analysis and comparison of SDMA and TDMA approaches. Moreover, as shown in the simulations, it approximates well the system number even when the number of users in the cell is small. In our analysis we are interested in the actual sum rate that can be achieved. Hence, the metric takes on the meaning of either an upper or lower SINR bound as needed in order to compare SDMA and TDMA in the extreme regimes under study.

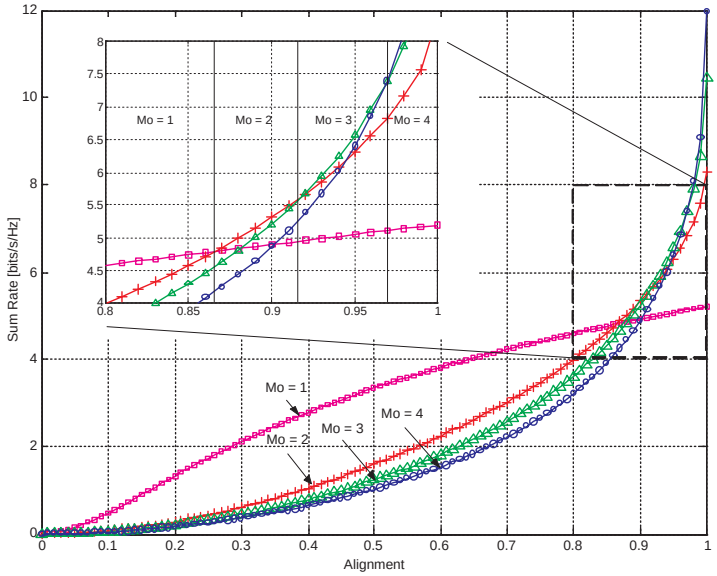


Figure 4.1: Approximated lower bound on the sum rate using Metric I versus the alignment ($\cos\theta_k$) for $M = 4$ antennas, variable number of active beams $M_o$, orthogonality factor $\epsilon = 0.1$ and SNR $= 10$ dB.

First, an approximation on the cdf of $\xi$ is derived, using mathematical tools from [70].

**Proposition 4.1** In the low-resolution regime (small $B$), the cdf of $\xi$ can be approximated as follows

$$F_\xi(s) \approx 1 - \frac{e^{\frac{-M_o\sigma^2 s}{P(1-\alpha s)}}}{\delta^{M-1}\left(1+m\right)^{M-1}} \tag{4.10}$$

where $m = \frac{2\gamma s\left[\gamma s+\sqrt{\gamma^2 s^2+(1-\alpha s)\beta s}\right]+(1-\alpha s)\beta s}{(1-\alpha s)^2}$.

*Proof.* See Appendix 4.A. □

Note that the above cdf is a generalization for arbitrary $\epsilon$ and $M_o$ of the cdf derived in [28]. Also, the result provided in [2] follows as a particular case by selecting $\epsilon = 0$, $M_o = M$ and $B = 0$.

Let the ordered variate $s_{i:K}$ denote the $i$-th largest among $K$ i.i.d. random variables. From known results of order statistics [71], we have that the cdf of $s_1 = \max_{1\leq i\leq K} s_{i:K}$ is $F_{s_1} = (F_\xi(s))^K$. According to the proposed user selection algorithm, the SINR of the first selected user is the maximum SINR over $K$ i.i.d. random variables. However, at the $i$-th selection step ($i$-th beam) the search space gets reduced since the $\epsilon$-orthogonality condition needs to be satisfied. Hence, the $i$-th user is selected over $K_i$ i.i.d. random variables yielding a cdf for the maximum SINR given by $F_{s_i} = (F_\xi(s))^{K_i}$. Since $\xi$ is upper bounded by $\frac{1}{\alpha}$, its mean value is given by

$$\mathbb{E}(s_i) = \int_0^{1/\alpha} 1 - (F_\xi(s))^{K_i} ds. \tag{4.11}$$

An approximation of $K_i$ can be calculated through the probability that a random vector in $\mathbb{C}^{M\times 1}$ is $\epsilon$-orthogonal to a set with $i-1$ vectors in $\mathbb{C}^{M\times 1}$, which is equal to $I_{\epsilon^2}(i-1, M-i+1)$ [15], $I_x(a,b)$ being the regularized incomplete beta function. By using the law of large numbers [68], we can find the following approximation:

$$K_i \approx K I_{\epsilon^2}(i-1, M-i+1). \tag{4.12}$$

The average sum rate in a system with $M_o$ active beams can be bounded as follows by using Jensen's inequality

$$SR = \sum_{i\in\mathcal{S}} \mathbb{E}\left[\log_2\left(1+s_i\right)\right] \leq \sum_{i\in\mathcal{S}} \log_2\left[1+\mathbb{E}\left(s_i\right)\right]. \tag{4.13}$$

Using (4.13) and solving the integral in (4.11) for the cdf of $\xi$ described in (4.10), we obtain the following theorem after some approximations.

**Theorem 4.1** Given $\epsilon$-orthogonal transmission in a system with $M_o$ active beams, the sum rate is approximated as follows

$$R_{M_o} \approx \sum_{i=1}^{M_o} \log_2\left[1 + \frac{1}{\alpha}\sum_{n=1}^{K_i} \mathcal{B}_n \mathcal{K}_{i,n} \mathcal{P}_n\right] \tag{4.14}$$

where

$$\begin{aligned} &\mathcal{B}_n = \tfrac{(-1)^{n-1}}{\delta^{n(M-1)}} \\ &\mathcal{K}_{i,n} = \tbinom{K_i}{n} \\ &\mathcal{P}_n = 1 + \tfrac{Cn}{\alpha} e^{\frac{Cn}{\alpha}} E_i\left(-\tfrac{Cn}{\alpha}\right) \end{aligned} \tag{4.15}$$

and $C = \frac{M_o\sigma^2}{P} + (M-1)\beta$. The exponential integral function is defined as $E_i(x) = -\int_{-x}^{\infty} \frac{e^{-t}}{t} dt$.

*Proof.* See Appendix 4.B. □

Note that the term $\mathcal{B}_n$ reflects the influence of the codebook design, $\mathcal{K}_{i,n}$ together with the summation upper limit $K_i$ inside the logarithm capture the amount of multiuser diversity exploited by the system and $\mathcal{P}_n$ accounts for the dependency of the sum rate on the power.

Note that, as a particular case of the equation above, a simpler expression can be derived for $M_o = 1$, given by

$$R_1 \approx \log_2 \left[ 1 + \sum_{n=1}^{K} \mathcal{B}_n \mathcal{K}_{1,n} \frac{P}{\sigma^2 n} \right] \tag{4.16}$$

Another case of interest is the case in which $\alpha = 0$. As $\alpha$ approaches zero, we have

$$\lim_{\alpha \to 0} \frac{1}{\alpha} \left[ 1 + \frac{Cn}{\alpha} e^{\frac{Cn}{\alpha}} E_i \left( -\frac{Cn}{\alpha} \right) \right] = \frac{1}{Cn} \tag{4.17}$$

and thus the sum-rate function in this case becomes

$$\lim_{\alpha \to 0} R_{M_o} = \sum_{i=1}^{M_o} \log_2 \left[ 1 + \sum_{n=1}^{K_i} \mathcal{B}_n \mathcal{K}_{i,n} \frac{1}{Cn} \right]. \tag{4.18}$$

In Figure 4.2, the sum-rate function in (4.14) is plotted as a function of the number of active beams $M_o$ and orthogonality factor $\epsilon$, using the values for $\alpha$, $\beta$ and $\gamma$ as described in Metric I. In this simulation, a system with $K = 35$ users has been considered, an average SNR of 10 dB and a simple codebook with $B = 1$ bit. Note that, in this particular scenario, SDMA can not guarantee better rates than TDMA regardless of the value of $\epsilon$. In this context, the number of users is low, hence there is low probability of obtaining large values of $\cos\theta_k$. Thus, TDMA transmission is favored, which is consistent with the results obtained in the previous section.

In order to validate the obtained sum-rate function, we consider a simple scenario with $M = 2$ antennas and a system in which $M_o = 2$ if 2 $\epsilon$-orthogonal users can be found in a given time slot and $M_o = 1$ otherwise. The probability of not finding 2 $\epsilon$-orthogonal users is given by $p = [1 - \epsilon^2]^{K-1}$. Hence, the approximated rate in this simplified scenario is given by

$$R \approx pR_1 + (1-p)R_2 \tag{4.19}$$

where $R_1$ and $R_2$ ($R_{M_o}$ with $M_o = 2$) are as described in (4.14) and (4.16) respectively. Figure 4.3 shows a comparison of analytical and simulated lower bounds on the sum rate in such a system, with $M = 2$ antennas, $K = 15$ users and SNR = 10 dB. The values for $\alpha$, $\beta$ and $\gamma$ used are those of Metric III, given in (4.10). Each user has a simple codebook designed as described in the previous section with $B = 1$ bit, different from user to user. Note that the jitter in the analytical curve is due to the rounding effect of $K_i$.

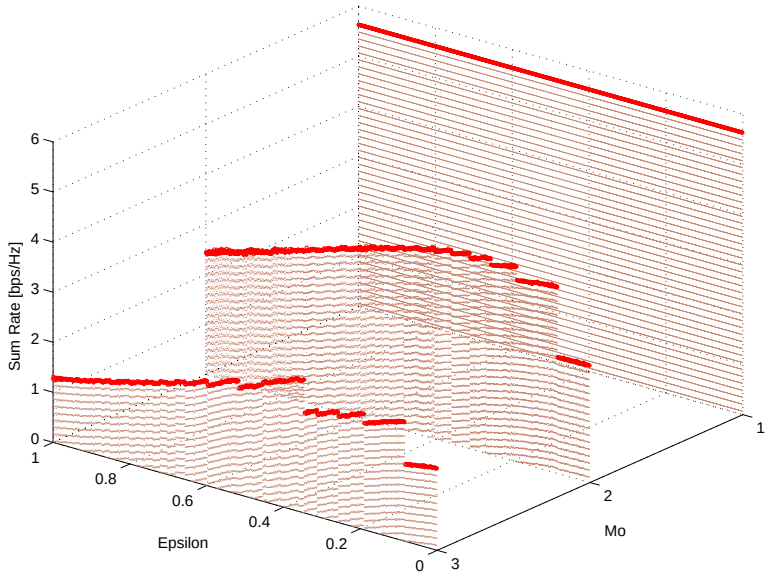


Figure 4.2: Sum-rate function using Metric I versus orthogonality factor $\epsilon$ and number of active beams $M_o$, for $K = 35$ users, SNR = 10 dB and $B = 1$ bit.

## 4.6 Study of Extreme Regimes

In this section we analyze several extreme regimes, namely scenarios with large number of users, high SNR and low SNR regime. The results intuitively clarify the cases in which SDMA is better than TDMA and the role of $\epsilon$ in the comparison of both techniques. Previous works in the literature focus on the study of the asymptotic scaling with $P$ or $K$ by using results from extreme value theory, as shown in [2], [28]. Here, we base our study on simpler mathematical tools. The ratios between the sum rates provided by

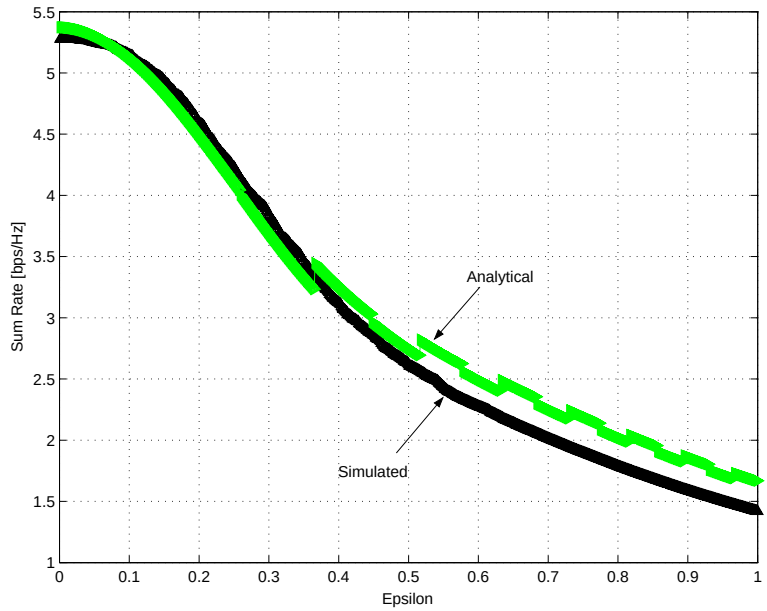


Figure 4.3: Comparison of analytical and simulated lower bounds on the sum rate using Metric III, for $M = 2$ antennas, $K = 15$ users, SNR $= 10$ dB and $B = 1$ bit.

SDMA and TDMA are computed in different limiting cases, by using the sum-rate functions derived in the previous section.

### 4.6.1 Large Number of Users

In this subsection we provide asymptotical results showing that SDMA can provide higher rates than TDMA in near-orthogonal MIMO systems as the number of users increases, which is consistent with the work presented in [13]. First, note that the number of available users at the $i$-th step can be bounded as $K_i \geq K\epsilon^{2(M-1)}$ as shown in [15]. For finite SNR, we can easily obtain from (4.14) and (4.16) the following result

**Theorem 4.2** Given an arbitrary $\epsilon$, SDMA outperforms TDMA asymptotically with the number of users

$$\lim_{K\to\infty} \frac{R_{M_o}}{R_1} = M_o. \tag{4.20}$$

*Proof.* As shown in Figure 4.3, it can be seen from (4.14) that $R_{M_o}$, as function of $\epsilon$, is lower bounded by $R_{M_o}|_{\epsilon=1}$. Thus, here we focus on a lower bound on the SINR, as described by Metric III, in order to provide a lower bound on the actual sum rate. The value $\epsilon = 1$ results in a pessimistic SINR lower bound. Setting $\epsilon = 1$, we obtain that in each selection step $K_i = K - i + 1, i = 1, \ldots, M_o$ and thus

$$R_{M_o} \geq \sum_{i=1}^{M_o} \log_2 \left[ 1 + \frac{1}{\bar{\alpha}} \sum_{n=1}^{K-i+1} \mathcal{B}_n \mathcal{K}_{1,n} \overline{\mathcal{P}}_n \right] \tag{4.21}$$

where $\overline{\mathcal{P}}_n = 1 + \frac{\bar{C}n}{\bar{\alpha}} e^{\frac{\bar{C}n}{\bar{\alpha}}} E_i \left( -\frac{\bar{C}n}{\bar{\alpha}} \right)$, $\bar{C} = C|_{\epsilon=1}$ and $\bar{\alpha} = \alpha|_{\epsilon=1}$. Therefore, we get the following lower bound on the ratio between $R_{M_o}$ and $R_1$

$$\begin{aligned} \lim_{K\to\infty} \frac{R_{M_o}}{R_1} &\geq \lim_{K\to\infty} \frac{R_{M_o}|_{\epsilon=1}}{R_1} \\ &\overset{(a)}{=} \lim_{K\to\infty} \frac{\sum_{i=1}^{M_o} \log_2 \left[ \binom{K-i+1}{(K-i+1)/2} \frac{1}{\bar{\alpha}} \mathcal{B}_{(K-i+1)/2} \overline{\mathcal{P}}_{(K-i+1)/2} \right]}{\log_2 \left[ \binom{K}{K/2} \mathcal{B}_{K/2} \frac{P}{\sigma^2 K/2} \right]} \\ &\overset{(b)}{=} \lim_{K\to\infty} \frac{\sum_{i=1}^{M_o} \log_2 \binom{K-i+1}{(K-i+1)/2}}{\log_2 \binom{K}{K/2}} \overset{(c)}{=} M_o \end{aligned} \tag{4.22}$$

where $(a)$ follows from selecting the highest exponent terms of $K$ in the numerator and denominator and $(b)$ from applying the logarithm property $\log(xy) = \log(x) + \log(y)$, keeping the relevant terms for the computation of the limit; (c) follows by realizing that $\lim_{K\to\infty} \frac{\log_2 \binom{K-a}{(K-a)/2}}{\log_2 \binom{K}{K/2}} = 1$ for any finite integer $a$.

Similarly to the lower bound obtained on $\frac{R_{M_o}}{R_1}$, it can be shown that $\lim_{K\to\infty} \frac{R_{M_o}}{R_1} \leq M_o$ by assuming an upper bound on the SINR as metric with $1 \leq M_o \leq M$, which corresponds to the case of using Metric IV. Setting $K_i = K - i + 1, i = 1 \ldots M_o$ and using the sum-rate function for the particular case of $\alpha = 0$, given in (4.18), yields the desired result. □

### 4.6.2 High SNR Regime

This scenario corresponds to the interference-limited region, in which the multiuser interference limits the system performance rather than the average

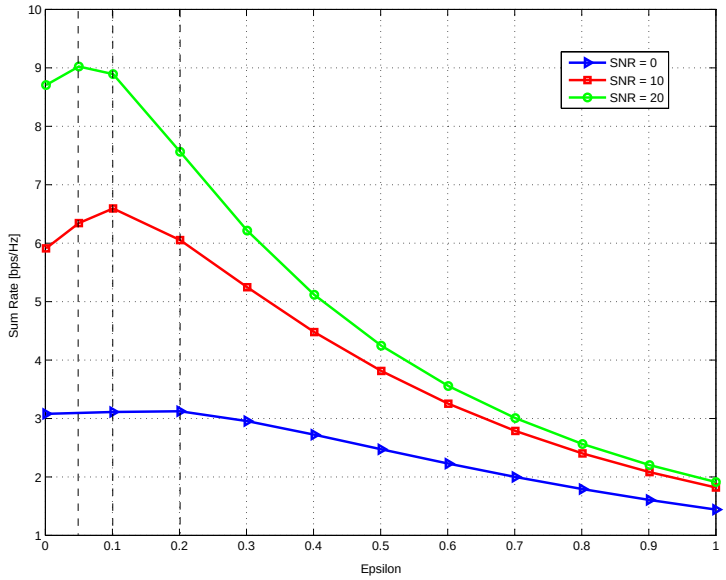


Figure 4.4: Simulated lower bound on the sum rate using Metric III as a function of the orthogonality factor $\epsilon$ for large $K$.

SNR. The number of users $K$ is considered to be finite in the analysis of this regime. For the sake of clarity, in the remainder of this chapter we consider that the noise power $\sigma^2$ is normalized, and thus $P$ takes on the meaning of average SNR.

**Theorem 4.3** Given an arbitrary $\epsilon$, TDMA outperforms SDMA in the high SNR regime

$$\lim_{P\to\infty} \frac{R_{M_o}}{R_1} = 0. \tag{4.23}$$

*Proof.* The bounded behavior of SDMA as function of the power $P$ is intuitively reflected in the proposed rate function. It suffices to realize that the power dependent part of $R_{M_o}$ can be upper bounded as follows

$$\mathcal{P}_n \leq 1. \tag{4.24}$$

In order to provide a proof for the theorem, we focus here on Metric IV, which yields an upper bound on the SDMA sum rate with variable number

of active beams. Since in this case we have that $\alpha = 0$, the sum rate is described by (4.18). The power dependent part is bounded by the following constant

$$\lim_{P\to\infty} \frac{1}{C} = \lim_{P\to\infty} \frac{P}{M_o + (M-1)\beta P} = \frac{1}{(M-1)\beta}. \tag{4.25}$$

Hence, when transmitting $M_o > 1$ active beams, the sum rate is bounded regardless of the transmitted power. Thus we have that

$$\lim_{P\to\infty} \frac{R_{M_o}}{R_1} \leq \lim_{P\to\infty} \frac{\sum_{i=1}^{M_o} \log_2 \left[1 + \sum_{n=1}^{K_i} \mathcal{B}_n \mathcal{K}_{i,n} \frac{1}{Cn}\right]}{\log_2 \left[1 + \sum_{n=1}^{K} \mathcal{B}_n \mathcal{K}_{1,n} \frac{P}{n}\right]} = 0 \tag{4.26}$$

where the inequality follows from the fact that an upper bound on the SDMA sum rate is used, based on Metric IV with $\alpha = 0$. The equality comes from the fact that when taking the limit, the numerator is not a function of $P$ as shown in (4.25). Since both $R_{M_o}$ and $R_1$ are greater than or equal to zero, we obtain the desired result. □

Note that the above result is consistent with the work in [51], in which the interference-limited behavior of MIMO broadcast channels is studied in a system where limited feedback is available in the form of channel direction information.

### 4.6.3 Low SNR Regime

This scenario corresponds to the noise-limited region. In this regime, the choice of $\epsilon$ has an impact on the optimal choice of transmission technique, i.e. SDMA or TDMA. In Figure 4.4 we show the evolution of the optimal value of $\epsilon$ for varying SNR in a cell with large number of users, $K = 1000$, $M = 2$ antennas and a codebook of $B = 1$ bit. The simulated system adapts the optimal number of active beams as a function of $\epsilon$ so that the lower bound on the sum-rate, computed on the basis of Metric III. Fixing $\epsilon = 0$ implies that the system forces a TDMA solution, since there is zero probability of finding two quantized random channels perfectly orthogonal, assuming different quantization codebooks for each user. A shift to the right in the position of the maximum implies that the number of $\epsilon$-orthogonal

users found at the second step ($K_2$) also increases, hence using 2 beams for transmission and thus exploiting the benefits of SDMA rather than TDMA. Therefore, Figure 4.4 shows that as the SNR decreases, a system based on near-orthogonal transmission tends to select SDMA over TDMA.

However, if the system parameter $\epsilon$ is set independently of the average SNR value (or equivalently the power $P$ for normalized noise power), we obtain the following theorem for finite number of users.

**Theorem 4.4** Given an arbitrary $\epsilon$, set independently of SNR, TDMA provides the same or better performance than SDMA in the low SNR regime.

$$\lim_{P\to 0}\frac{R_{M_o}}{R_1} \leq 1. \tag{4.27}$$

*Proof.* In order to proof the theorem, we first proof the following asymptotic relation between SDMA and TDMA in 2 extreme cases

$$0 \leq \lim_{P\to 0}\frac{R_{M_o}}{R_1} \leq \frac{1}{M_o}, \qquad if\ \epsilon = 0 \tag{4.28}$$

$$0 \leq \lim_{P\to 0}\frac{R_{M_o}}{R_1} \leq 1, \qquad if\ \epsilon = 1 \tag{4.29}$$

First, we note that the relation $\lim_{P\to 0}\frac{R_{M_o}}{R_1} \geq 0$ follows from the fact that both $R_{M_o}$ and $R_1$ are greater than zero for positive $P$. In order to proof the upper bound on $\lim_{P\to 0}\frac{R_{M_o}}{R_1}$ for $\epsilon = \{0, 1\}$, we consider an upper bound on the sum rate, provided by using Metric IV. Since in this case $\alpha = 0$, we use the sum-rate function given in (4.18). We obtain the following result

$$\begin{aligned}
\lim_{P\to 0}\frac{R_{M_o}}{R_1} &\leq \lim_{P\to 0}\frac{\sum_{i=1}^{M_o}\log_2\left[1+\sum_{n=1}^{K_i}\mathcal{B}_n\mathcal{K}_{i,n}\frac{1}{Cn}\right]}{\log_2\left[1+\sum_{n=1}^{K}\mathcal{B}_n\mathcal{K}_{1,n}\frac{P}{n}\right]} \\
&\overset{(a)}{=} \lim_{P\to 0}\left(\sum_{i=1}^{M_o}\frac{\sum_{n=1}^{K_i}\frac{\mathcal{B}_n\mathcal{K}_{i,n}}{n}(\frac{1}{C})'}{1+\sum_{n=1}^{K_i}\mathcal{B}_n\mathcal{K}_{i,n}\frac{1}{Cn}}\right)\left(\frac{1+\sum_{n=1}^{K}\mathcal{B}_n\mathcal{K}_{1,n}\frac{P}{n}}{\sum_{n=1}^{K}\frac{\mathcal{B}_n\mathcal{K}_{1,n}}{n}}\right) \\
&\overset{(b)}{=} \frac{1}{M_o}\frac{\sum_{i=1}^{M_o}\sum_{n=1}^{K_i}\frac{\mathcal{B}_n\mathcal{K}_{i,n}}{n}}{\sum_{n=1}^{K}\frac{\mathcal{B}_n\mathcal{K}_{1,n}}{n}}
\end{aligned} \tag{4.30}$$

where $(a)$ follows from applying L'Hôpital's rule, with $(\frac{1}{C})'$ given by

$$(\frac{1}{C})' = \frac{\partial \frac{1}{C}}{\partial P} = \frac{M_o}{[M_o + (M-1)\beta P]^2} \tag{4.31}$$

and $(b)$ follows from $\lim_{P\to 0}(\frac{1}{C})' = \frac{1}{M_o}$. For the case $\epsilon = 0$, we have that $K_1 = K$, and $K_i = 0$ for $i \geq 2$. Hence, it can be seen from (4.30) that the ratio becomes $\frac{1}{M_o}$, thus yielding (4.28). For the case $\epsilon = 1$, we get $K_i = K-i+1, i = 1, \ldots, M_o$. For simplicity, we provide a looser upper bound by considering $K_i = K, i = 1, \ldots, M_o$, which yields the result described in (4.29). Since intermediate values of $\epsilon$ independent of the SNR will yield values for (4.30) in the range $\left(\frac{1}{M_o}, 1\right)$, we obtain the desired result. □

## 4.7 Multiuser Diversity - Multiplexing Tradeoff

In this section, we consider a slightly different setting that applies to more realistic scenarios. We explore the effect of quantizing the scalar feedback studied in this chapter, in a scenario where the total amount of feedback bits for CDI and CQI is limited. In MIMO point-to-point systems, it has been shown in [6] that there exists a tradeoff between spatial multiplexing gain and diversity gain, defined in (1.1) and (1.2), respectively. This tradeoff is due to the fact that there is a certain number of degrees of freedom in the MIMO channel that need to be shared in order to achieve diversity or increase the transmission rate. In MIMO broadcast channels with user scheduling, there is in addition multiuser diversity gain

$$m = \lim_{K\to\infty} \frac{\mathcal{R}(P,K)}{r \log\log K}. \tag{4.32}$$

The multiuser diversity differs from single-user diversity in the sense that the latter refers to the ability for the multiple antennas to receive the same information across different paths, while in multiuser systems, different information is transmitted and received by different users. The multiuser diversity gain increases with the number of active users in the cell, while the available multiplexing gain remains $\min(M, K)$, regardless of the value of $K$. Hence,

with full CSIT both multiuser diversity and multiplexing gain can be attained since they scale with different magnitudes, $K$ and SNR respectively. The tradeoff appears when we consider a system with limited feedback rate, in which each mobile is allowed to feed back a finite number of bits.

In point-to-point MIMO systems, the effect of limited feedback on the system rate is less severe than in MIMO broadcast channels. It has been shown in [72] that even a few feedback bits can provide performance close to that with full CSIT, achieving full multiplexing gain. However, as it has been recently shown in [51], the level of CSIT critically affects the multiplexing gain of the MIMO broadcast channel. In order to achieve full multiplexing gain, the feedback load per user must increase approximately linearly with the number of transmit antennas and the number of feedback bits per mobile must increase linearly with the SNR (in dB). Hence, appropriate feedback load scaling in terms of channel directional information is needed to achieve full multiplexing gain. On the other hand, CDI can not exploit multiuser diversity gain in a multiuser context with $K \geq M$. In this situation, channel quality information at the transmitter becomes necessary in order to perform efficient user selection. However, since the available feedback rate is finite, the amount of bits used for CSIT quantization has to be shared for both CDI and CQI quantization. While CDI quantization incurs in loss of multiplexing gain, CQI quantization leads to a degradation of the multiuser diversity benefit, an thus a tradeoff arises between multiuser diversity and multiplexing gain in MIMO broadcast channels with limited feedback. The problem of feedback splitting for channel directional information and channel quality information is treated in this section, and useful feedback design guidelines are provided.

### 4.7.1 Finite Sum Rate Feedback Model

In the context considered in this section, each receiver $k$ is constrained to have a limited total number of feedback bits $B_{tot}$. From this total amount of bits, $B_1$ bits are used to quantize the CDI $\bar{\mathbf{h}} = \mathbf{h}/\left\|\mathbf{h}\right\|$ based on a predetermined codebook, and $B_2$ bits are used for scalar quantization of real-valued CQI. This model is depicted in Figure 4.5.

Channel directional information can be used to achieve full multiplexing gain when the feedback load $B_1$ scales appropriately [51]. In a multiuser context with $K > M$, CDI does not provide any information on users' channel gains, thus not being sufficient for efficient user selection failing to exploit

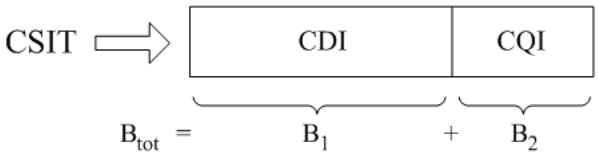


Figure 4.5: Finite sum rate feedback model.

multiuser diversity gain. Hence, additional instantaneous low-rate channel gain information is required as an indicator of the channel quality. The goal is to reveal the interplay between $K$, average SNR and feedback load $B_1$ and $B_2$, in order to exploit in the best possible way the degrees of freedom available in a multiuser MIMO downlink, i.e., the spatial multiplexing and multiuser diversity gain. The sum feedback rate constraint per user ($B_{tot}$) results to a tradeoff between multiuser diversity and multiplexing gain, and we focus on characterizing it by identifying the optimal feedback rate allocation (split) in order to exploit both gains. Plainly speaking, we intend to determine how many feedback bits are CDI and CQI worth.

### Channel Direction Quantization

We consider a quantization codebook $\mathcal{V}_k$ containing $2^{B_1}$ unit norm vectors in $\mathbb{C}^{M\times 1}$, which is assumed to be known to both the $k$-th receiver and the transmitter. In the most general case, the mobile terminals can have different codebooks, generated through random unitary rotation of a common, general codebook $\mathcal{V}_g$ known at both ends of the link. Based on the channel realization, the receiver selects its 'best' vector from the codebook, i.e. the codeword that optimizes a certain cost function. Here, we assume that each receiver quantizes its channel as described in (4.5). Each user sends the corresponding quantization index $n$ back to the transmitter through an error-free, and zero-delay feedback channel using $B_1$ bits.

### Channel Quality Quantization

As channel quality indicator, we consider instantaneous scalar feedback, denoted as $\xi_k$, which can take on various forms as described in this chapter and is evidently a certain function of the current channel realization $\mathbf{h}_k$ (i.e., $\xi_k = f(\mathbf{h}_k)$). We assume that $\xi_k$ are i.i.d. random variables with pdf $f_\xi(\xi)$.

Let $\xi$ and $\mathcal{Q}(\xi)$ denote the input and the output values of quantizer $\mathcal{Q}(\cdot)$. Let $\mathcal{X} = \{q_0 < q_1 < \ldots < q_{2^{B_2}}\}$ be the input decision levels and let $\mathcal{Y} = \left\{\xi_{q_0} < \xi_{q_1} < \ldots < \xi_{q_{2^{B_2}-1}}\right\}$ be the output representative levels (reconstruction values) of an $2^{B_2}$-level quantizer $\mathcal{Q}(\cdot)$ defined as:

$$\mathcal{Q}(\xi) = \xi_{q_i} \quad \text{if } q_i \leq \xi < q_{i+1} \;\; 0 \leq i \leq 2^{B_2} - 1 \tag{4.33}$$

with $q_0 = 0$ and $q_{2^{B_2}} = \infty$. A partition region (quantization level) is defined as $Q_i = [q_i, q_{i+1}), 0 \leq i \leq 2^{B_2} - 1$. Each user sends the corresponding quantization level index $i$ back to the transmitter using $B_2$ bits. In order to minimize the outage probability, we assume the following conservative but reliable quantization rule $\xi_{q_i} = q_i$.

### 4.7.2 Problem Formulation

Our objective is to dynamically allocate bits to CDI and CQI feedback (as shown in Figure 4.5) given a total amount of feedback bits $B_{tot}$, so that the capacity of the multiuser MIMO downlink $\mathcal{C}(B_1, B_2)$ is maximized. In the described finite sum rate feedback model, the optimal feedback rate allocation that maximizes the capacity can be formulated in the following constrained optimization problem:

$$\left.\begin{array}{c} \max\limits_{B_1, B_2} \mathcal{C}(B_1, B_2) \\ s.t. \;\; B_1 + B_2 = B_{tot} \end{array}\right\} \tag{4.34}$$

Let $\mathcal{W}$ be the event that a user $k$ is selected for transmission among $K$ users. Using the analysis of [73], we calculate the probability of the above event conditioned on the fact that $\xi$ falls into the quantization level $Q_j$

$$\Pr\left(\mathcal{W} | \xi \in Q_j\right) = \sum_{m=0}^{K} \frac{1}{m+1} \cdot \left( \begin{array}{c} K-1 \\ m \end{array} \right) \cdot \mathcal{P}_1 \cdot \mathcal{P}_2 \tag{4.35}$$

where

$$\mathcal{P}_1 = \Pr\left\{m \text{ users other than user } k \in Q_j\right\} = \left(\Pr\left(\xi \in Q_j\right)\right)^m \tag{4.36}$$

and

$$\mathcal{P}_2 = \Pr\left\{(K - m - 1) \text{ users other than user } k \in Q_n, n < j\right\}$$

$$= \left( \Pr \left( \xi \in \bigcup_{n<j} Q_n \right) \right)^{K-m-1} \tag{4.37}$$

We assume here that if more than one user lie in $Q_j$, a random user is scheduled for transmission. Using that $(\Pr(\xi \in Q_j)) = F_\xi(q_{j+1}) - F_\xi(q_j)$, and after some manipulations, one can show that

$$\Pr(\mathcal{W}|\xi \in Q_j) = \frac{[F_\xi(q_{j+1})]^K - [F_\xi(q_j)]^K}{K\left(F_\xi(q_{j+1}) - F_\xi(q_j)\right)} \tag{4.38}$$

where $F_\xi(\cdot)$ is the cdf of the CQI.

In a system with joint downlink scheduling and beamforming with limited feedback, beamforming is performed based on quantized channel directions. Let us now assume that the quality indicator $\xi$ is a function of each user's SINR. In that case, the effect of CDI quantization will be reflected on the distribution of $\xi$. Hence, the CQI contains information both on channel gain and CDI quantization error. For instance, the value $\xi$ can be a lower/upper bound on the achievable SINR or even the achievable SINR value itself. Suppose now that the metric $\xi$ is a lower bound on the SINR, as described by Metric III. Then, the rate of the selected user $k$, $\mathcal{R}_k$ is given by

$$\mathcal{R}_k \geq \sum_{j=0}^{2^{B_2}-1} \int_{\xi \in Q_j} \Pr(\mathcal{W}|\xi \in Q_j) \log_2(1+\xi) f_\xi(\xi) d\xi \tag{4.39}$$

$$= \sum_{j=0}^{2^{B_2}-1} \int_{Q_j} \log_2(1+\xi) \cdot \frac{[F_\xi(q_{j+1})]^K - [F_\xi(q_j)]^K}{K\left(F_\xi(q_{j+1}) - F_\xi(q_j)\right)} \cdot f_\xi(\xi) d\xi \tag{4.40}$$

Let $\mathcal{S}$ be a set of scheduled users with cardinality $|\mathcal{S}| = M$. The system capacity $\mathcal{C}(B_1, B_2)$ can be lower bounded by

$$\mathcal{C}(B_1, B_2) = \sum_{k \in \mathcal{S}} \mathcal{R}_k \geq \tag{4.41}$$

$$\sum_{k \in \mathcal{S}} \sum_{j=0}^{2^{B_2}-1} \int_{Q_j} \log_2(1+\xi) \frac{[F_\xi(q_{j+1})]^K - [F_\xi(q_j)]^K}{K\left(F_\xi(q_{j+1}) - F_\xi(q_j)\right)} f_\xi(\xi) d\xi \tag{4.42}$$

where $B_1$ is contained both in $F_\xi(\xi)$ and $f_\xi(\xi)$.

From the above analysis, it can be seen that the optimization problem in (4.34) has no closed-form solution. Additionally, the solution depends on the quantization levels $q_i, 0 \leq i \leq 2^{B_2} - 1$ to be considered, thus different CQI quantization strategies will yield different solutions. To circumvent the complexity of numerical brute force optimization and the non-linearity of this optimization problem, numerical algorithms relying on dynamic programming and providing a global optimum can be used.

### 4.7.3 Simplified Approach: Decoupled Feedback Optimization

A particular case is studied here based on zero-forcing beamforming, in order to illustrate the importance of the multiuser diversity vs. multiplexing tradeoff. Instead of determining jointly the optimal feedback bit split, an approach of reduced complexity consists of decomposing the problem in a two-step procedure: we first find the optimal number of CDI bits required to guarantee full multiplexing gain, implying that the feedback load that is allocated to CQI is $B_2 = (B_{tot} - B_1)$, and optimizing the $2^{B_2}$ quantization levels by using (4.42).

We apply the finite sum rate feedback model in a scheme that performs zero-forcing beamforming on the channel quantizations available at the transmitter as a multiuser transmission strategy. We assume here that all users feed back a quantized version of Metric II as CQI, and that $M_o = M$ users are scheduled in every time slot. Once $M$ $\epsilon$-orthogonal users have been selected, the zero-forcing beamforming is applied based on the channel quantizations of the users selected for transmission.

Based on the asymptotic growth of Metric II for large $K$ given in [55], we derive the scaling of CDI feedback load, which in turn determines the remaining CQI feedback bits. We define the power gap (per user) between the SINR of the above scheme, $SINR_I$, and that of zero-forcing with perfect CSI, $SINR_{ZF}$ as the ratio $\zeta = \frac{SINR_I}{SINR_{ZF}}$. Note that this power gap is translated to a rate gap. In order to achieve full multiplexing gain for finite $K$, the number of CDI bits $B_1$ per receiver $k$ should scale according to:

$$B_1 = (M-1)\log_2(P/M) - (1-\zeta)\log_2 K - \log_2 \kappa_{i-1} \tag{4.43}$$

where $\kappa_{i-1} = \mathcal{K}_i/K$ is a constant capturing the multiuser diversity reduction at each step $i$ of the user selection algorithm (the number of users $\mathcal{K}_i$ from

which $\xi_k$ is chosen is reduced at each step), due to the $\epsilon$-orthogonality constraint between scheduled users. As $\zeta < 1$, having more users in the cell, a smaller number of feedback bits $B_1$ per user is required in order to achieve full multiplexing gain. For a system with $M = 4$ antennas, $K = 30$ users and SNR = 10 dB, when a 3-dB SINR gap is considered, each user needs to feed back at least $B_1 = 9$ bits.

### Scaling of CDI feedback bits at high SNR regime

The high SNR regime corresponds to the interference-limited region, where the role of CDI is more critical due to the effect of quantization error [51]. As $P \to \infty$, the CQI becomes $\xi_k = \cot^2 \phi_k$, and based on asymptotic results of [55], we can show that for fixed $K$, the feedback load should scale as

$$B_1 = (M-1)\log_2 P - \log_2 K. \tag{4.44}$$

For instance, for a system with $M = 4$ antennas, SNR = 20 dB and $K = 60$ users, $B_1 = 14$ bits are required to guarantee full multiplexing gain. As it was intuitively expected, the feedback load $B_1$ at high SNR is larger than that of (4.43). Thus, it is more beneficial to use more feedback bits on the quantization of channel direction ($B_1$) at high SNR, and assign less bits for CQI ($B_2$).

## 4.8 Numerical Results

Figure 4.6 shows a performance comparison in terms of sum rate versus orthogonality factor $\epsilon$ for various levels of CSIT. The simulated system performs TxMF, has $M = 2$ antennas and a simple codebook of $B = 1$ bits. The number of active users is $K = 10$ and the average SNR = 20 dB. The upper curve corresponds to the sum rate obtained with TxMF, perfect CSIT and exhaustive user search. Hence, its average rate is not a function of the orthogonality factor. The lower curve corresponds to the sum rate that the system can guarantee when the CSIT consists of quantized channel directions and Metric III as scalar feedback (equivalent to Metric I for $M = 2$). Thus, this curve corresponds to a lower bound on the actual sum rate that the system can achieve. Finally, the third curve corresponds to the sum rate of a system with second step of full CSIT feedback, which means that given

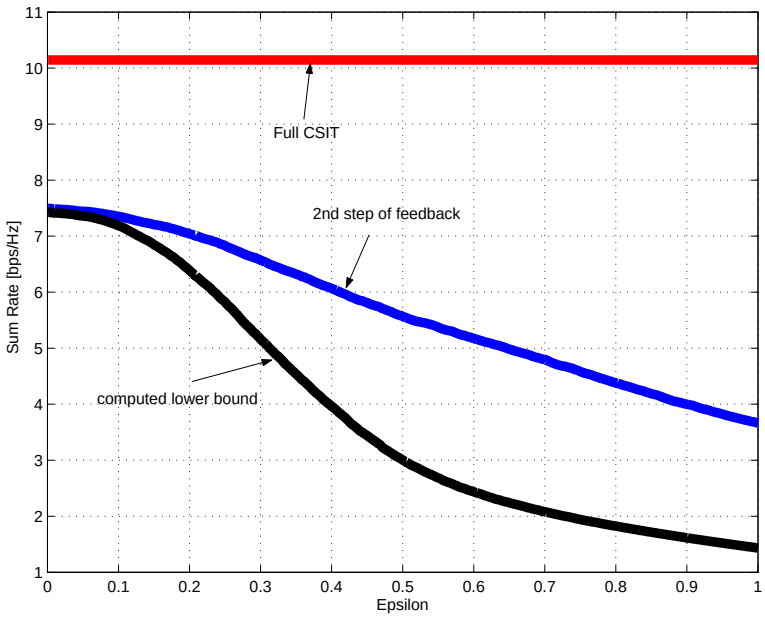


Figure 4.6: Comparison of simulated lower bound on the sum rate using Metric III, and actual sum rates obtained with second step of feedback and full CSIT. $M = 2$ antennas, $K = 10$ users, SNR $= 20$ dB and $B = 1$ bit.

a set of users selected for transmission by using Metric III, the BS requests full channel information from those users to perform transmit matched filtering. We can see that the bound becomes looser as $\epsilon$ increases, since the bound on the SINR becomes more pessimistic. In the simulated system with $K = 10$ users, the maximum average sum rate occurs when the system sets orthogonality $\epsilon = 0$. This means that the system forces that at each time slot only one beam will be active, since there is zero probability of finding two quantized random channels perfectly orthogonal, assuming different quantization codebooks for each user. Thus, in the simulated scenario with reduced number of users, TDMA (one active beam per time slot) is the optimal transmission technique while in systems with large number of users SDMA is optimal as shown in previous section.

In Figures 4.7 and 4.8, we compare the actual sum rate achieved by systems based on TxMF and different scalar feedback: metrics I, II, III and IV, for $M = 3$ antennas and $B = 9$ bits. For comparison, the performances of random beamforming (RBF) [2] and TxMF with perfect CSIT and

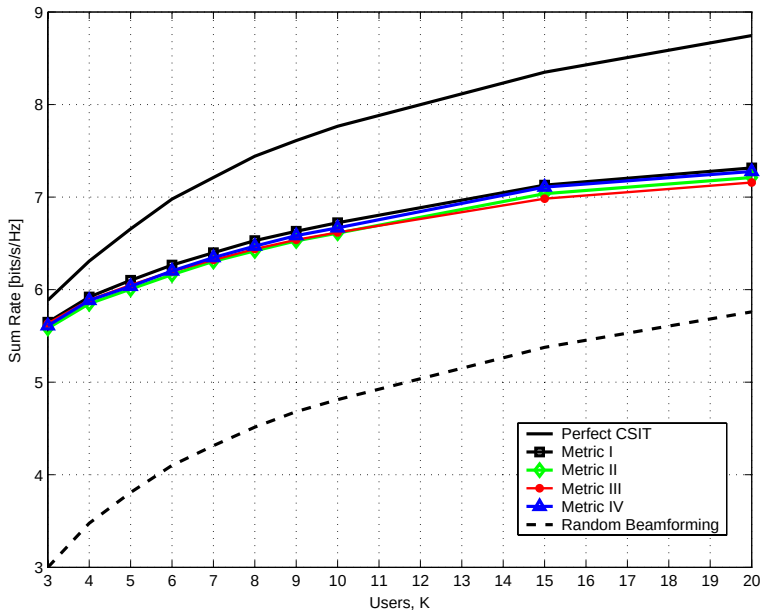


Figure 4.7: Sum rate achieved by different feedback approaches as a function of the number of users, for $B = 9$ bits, $M = 3$ transmit antennas and average SNR = 10 dB.

exhaustive-search user selection are provided. The systems using metrics I,II and IV are assumed to appropriately set $M_o$ and $\epsilon$ both for transmission and metric computation, maximizing the sum rate for each $K$ and SNR pair. On the other hand, the scheme with Metric II uses optimal $\epsilon$ values in each scenario.

Figure 4.7 shows a performance comparison in terms of sum rate versus number of users for SNR = 10 dB, in a cell with realistic number of active users. The scheme based on Metric I provides slightly better performance than the other schemes. The scheme based on Metric III exhibits worse scaling with the number of users, thus exploiting less effectively the multiuser diversity. Note that all schemes exhibit slightly worse scaling than RBF and the perfect CSIT solution. This is due to the fact that a simple transmission technique has been used, TxMF, since beamforming design is not the main focus of this chapter. In order to restore the optimal scaling with $K$, ZFBF can be performed at the transmitter based on the available channel

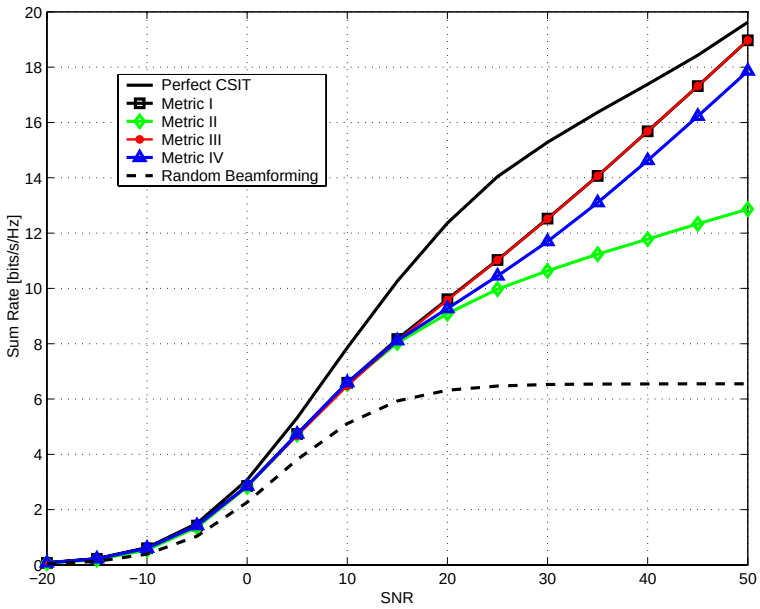


Figure 4.8: Sum rate achieved by different feedback approaches versus average SNR, for $B = 9$ bits, $M = 3$ transmit antennas and $K = 10$ users.

quantizations, as discussed in [28].

Figure 4.8 depicts the performances of different schemes in the low-mid SNR region, in a setting with $K = 10$ users. As the average SNR in the system increases, the sum rate of schemes using metrics I and III for feedback converges to the same value. They exhibit linear increase in the high SNR region as expected, which corresponds to a TDMA solution. The scheme that uses Metric IV for scheduling also benefits from a variable number of active beams, although providing worse performance than the systems using metrics I and III. Since in the simulated system the number of codebook bits $B$ is not increased proportionally to the average SNR, as discussed in [51], the scheme using Metric II ($M_o = M$) exhibits an interference-limited behavior, flattening out at high SNR.

### 4.8.1 Effect of Scalar Feedback Quantization

In the reminder of this section, we provide simulation results for the simplified approach described in Section 4.7, considering scalar feedback quantization

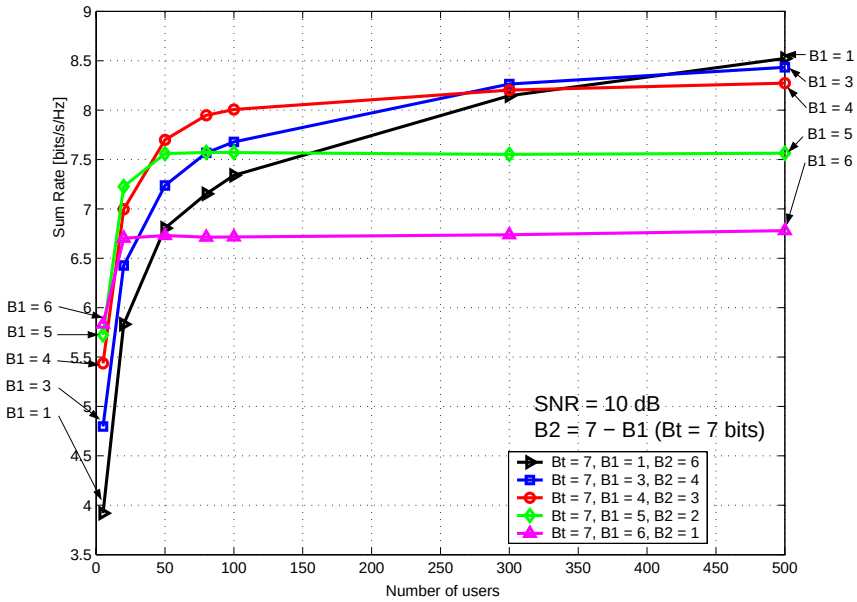


Figure 4.9: Sum rate vs. number of users for $M = 2$ and SNR = 10 dB.

and ZFBF at the transmitter side. We evaluate through simulations the sum rate performance in a system with $M = 2$ transmit antennas and $\epsilon = 0.4$. The total number of available feedback bits is $B_{tot} = 7$ bits. CQI quantization is performed through Lloyd's algorithm. Once both the input quantization levels $q_i$ and output representative levels $\xi_{q_i}$ are found, the quantizer sets $\xi_{q_i} = q_i$, $0 \leq i \leq 2^{B_2} - 1$ in order to avoid outage events as discussed in Section 4.7.1.

Figure 4.9 and 4.10 show the sum rate as a function of the number of users for SNR = 10 dB and SNR = 20 dB respectively for different CDI and CQI feedback bit split. As expected, it is more beneficial to allocate more bits on channel direction quantization in a system with low number of active users. On the other hand, as the number of users increases, it becomes more beneficial to allocate bits on CQI quantization instead. The black curve $B_1 = 1$ bit corresponds to the random unitary beamforming for $M = 2$ transmit antennas proposed in [2]. In a system with optimal quantization, i.e. matched to the pdf of the maximum CQI value among $K$ users, the amount of necessary quantization levels is reduced as the number of users in the cell increases. Thus, less amount of feedback bits is needed for CQI quantization in order to capture the multiuser diversity.

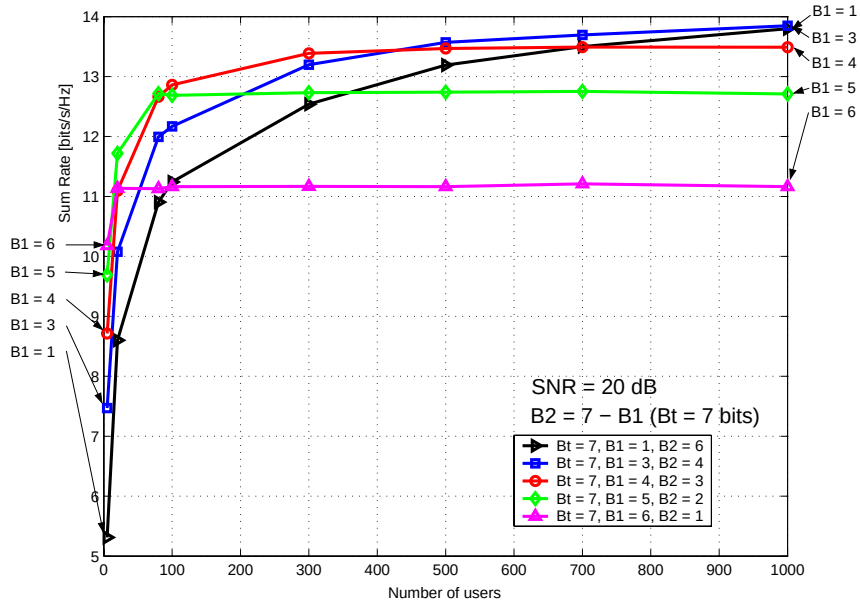


Figure 4.10: Sum rate vs. number of users for $M = 2$ and SNR = 20 dB.

In Figure 4.11, the envelope of the curves in the two previous figures is shown, which corresponds to a system that chooses the best $B_1/B_2$ balance for each average SNR and $K$ pair. In this figure, we compare how this best pair of $(B_1,\ B_2)$ changes as the system average SNR increases. Both curves are divided in different regions, according to the optimal $(B_1,\ B_2)$ pair in each region. It can be seen that the optimal threshold for switching from $B_1 \rightarrow B_1 - 1$ bits (and thus $B_2 \rightarrow B_2 + 1$) is shifted to the right for higher average SNR values (upper curve). This means that as the average SNR increases, more bits should be allocated on channel direction information. Summarizing, given a pair of average SNR and $K$ values, there exists an optimal compromise of $B_1$ and $B_2$, given that $B_{tot} = B_1 + B_2$.

## 4.9 Conclusions

A design framework for scalar feedback in MIMO broadcast channels with limited feedback has been presented. In order to perform user scheduling, these metrics may contain information such as channel power gain, quantization error, orthogonality factor between beamforming vectors and/or number

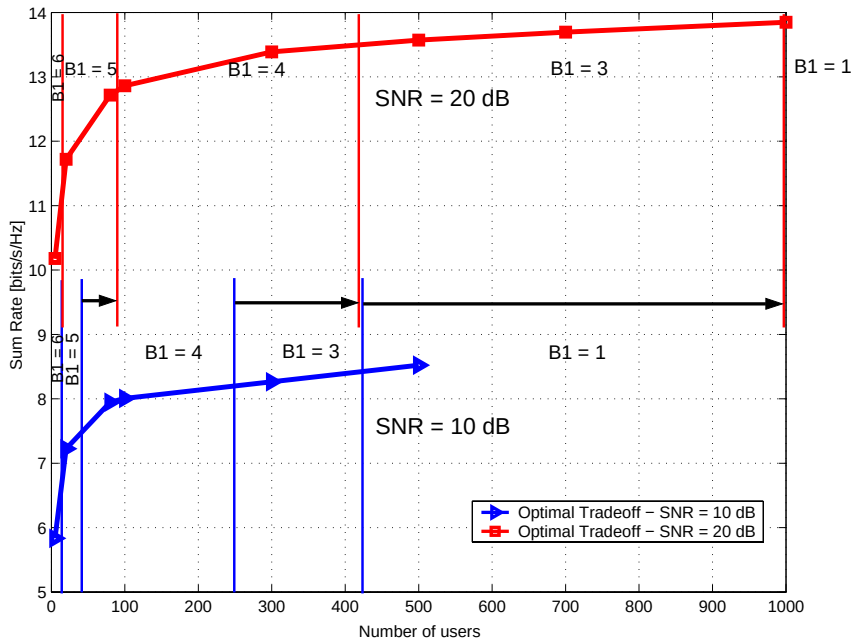


Figure 4.11: Sum rate vs. number of users in a system with optimal $B_1/B_2$ balancing for different SNR values.

of active beams. An approximation on the sum-rate has been provided for the proposed family of metrics, which has been validated through simulations.

As it has been shown, the proposed sum-rate function is a powerful design tool and enables simple analysis. A sum-rate comparison between SDMA and TDMA has been provided in several extreme regimes. Particularly, SDMA outperforms TDMA as the number of users becomes large. TDMA provides better rates than SDMA in the high SNR regime (interference-limited region). Moreover, the importance of optimizing the orthogonality factor $\epsilon$ in the low SNR regime has been highlighted. Several metrics have been presented based on the proposed design framework, illustrating their performances through numerical simulations. The system sum-rate can be drastically improved by considering a variable number of active beams adapted to each scenario. In addition, scalar metrics based on SINR lower bounds can provide benefits from a point of view of QoS and feedback reduction.

We have also formulated the problem of optimal feedback balancing in order to exploit spatial multiplexing gain and multiuser diversity gain under

a sum feedback rate constraint. A low complexity approach has been introduced to illustrate the performance improvement of systems with optimally balanced feedback. The scaling of CDI feedback load in order to achieve full multiplexing gain is also provided, revealing an interesting interplay between the number of users, the average SNR and the number of feedback bits.

# APPENDIX

## 4.A Proof of Proposition 4.1

Define the following changes of variables

$$\begin{array}{ll} \psi := \sin^2\theta_k & x := \frac{1}{\delta}\phi(1-\psi) \\ \phi := \|\mathbf{h}_k\|^2 & y := \frac{1}{\delta}\phi\psi. \end{array} \tag{4.45}$$

Then, the metric in (4.9) can be expressed as

$$\xi = \frac{x}{\alpha x + \beta y + 2\gamma\sqrt{xy} + \lambda} \tag{4.46}$$

where $\lambda = \frac{\delta M_o \sigma^2}{P}$ Note that $\xi \leq \frac{1}{\alpha}$, with equality for $P \to \infty$. The Jacobian of the transformation $x = f(\phi, \psi)$, $y = g(\phi, \psi)$ described in (4.45) is given by

$$J(\phi, \psi) = \begin{vmatrix} \frac{\partial x}{\partial \phi} & \frac{\partial x}{\partial \psi} \\ \frac{\partial y}{\partial \phi} & \frac{\partial y}{\partial \psi} \end{vmatrix} = \frac{\phi}{\delta^2}. \tag{4.47}$$

Expressing $\phi$ and $\psi$ as a function of $x$ and $y$, we have $\phi = \delta(x+y)$ and $\psi = \frac{y}{x+y}$. Substituting in the Jacobian, we get $J(x,y) = \frac{(x+y)}{\delta}$. Since $\phi$ and $\psi$ are independent random variables for i.i.d. channels, the joint pdf of $x$ and $y$ is obtained from $f_{xy}(x,y) = \frac{1}{J(x,y)} f_\phi\left[\delta(x+y)\right] f_\psi\left[\frac{y}{x+y}\right]$. The pdf of $\phi$ is

$$f_\phi(\phi) = \frac{\phi^{M-1}}{\Gamma(M)} e^{-\phi} \tag{4.48}$$

where $\Gamma(M) = (M-1)!$ is the complete gamma function. The pdf $f_\psi$ is obtained from the cdf of $\psi$ given in (4.6). Hence, we get the joint density

$$f_{xy}(x,y) = \frac{\delta}{\Gamma(M-1)} e^{-\delta(x+y)} y^{M-2}. \tag{4.49}$$

The cdf of the proposed SINR metric is found by solving the integral

$$F_\xi(s) = \iint_{x,y \in D_s} f_{xy}(x,y)\, dx\, dy. \tag{4.50}$$

The bounded region $D_s$ in the $xy$-plane represents the region where the inequality $\frac{x}{\alpha x+\beta y+2\gamma\sqrt{xy}+\lambda} \leq s$ holds. Isolating $x$ on the left side of the inequality, $D_s$ can be equivalently described as $x \leq g(y)$, with $g(y)$ given by

$$g(y) = \frac{(2\gamma^2 s^2+\beta s(1-\alpha s))y+2\gamma s\sqrt{(\gamma^2 s^2+\beta s(1-\alpha s))y^2+\lambda s(1-\alpha s)y}}{(1-\alpha s)^2} + \varphi(s) \quad (4.51)$$

where $\varphi(s) = \frac{\lambda s}{1-\alpha s}$. Since using $g(y)$ in the integration limits yields difficult integrals, we use the following linear approximation

$$g(y) \approx m(s)y + \varphi(s) \quad (4.52)$$

where the slope $m(s)$ corresponds to the oblique asymptote of $g(y)$

$$m(s) = \lim_{y\to\infty} \frac{\partial g(y)}{\partial y} = \frac{2\gamma s(\gamma s + \sqrt{\gamma^2 s^2 + \beta s(1-\alpha s)}) + \beta s(1-\alpha s)}{(1-\alpha s)^2}. \quad (4.53)$$

Note that, since $0 \leq s \leq \frac{1}{\alpha}$, then $m(s) \geq 0\, \forall s$. In addition, since the domain of $\psi$ is $D_\psi = [0, \delta]$, we also obtain the inequalities $\frac{y}{x+y} \geq 0$, $\frac{y}{x+y} \leq \delta$ and thus $x \geq \frac{1-\delta}{\delta} y$. Hence, $F_\xi(s)$ is obtained by integrating $f_{xy}(x, y)$ over the first quadrant of the $xy$-plane, in the region defined by $x \leq g(y)$ and $x \geq \frac{1-\delta}{\delta} y$. Depending on the slopes of these linear boundaries, the integral in (4.50) is carried out over different regions

$$F_\xi(s) \approx \begin{cases} \int_0^\infty \int_{\frac{1-\delta}{\delta}y}^{my+\varphi} f_{xy}(x, y)\, dx\, dy, & m \geq \frac{1-\delta}{\delta} \\ \int_0^{y_c} \int_{\frac{1-\delta}{\delta}y}^{my+\varphi} f_{xy}(x, y)\, dx\, dy, & 0 \leq m < \frac{1-\delta}{\delta}. \end{cases} \quad (4.54)$$

The upper integration limit $y_c$ along the $y$ axis in the region $0 \leq m < \frac{1-\delta}{\delta}$ corresponds to the value of $y$ in which the linear boundaries intersect

$$y_c = \frac{\lambda s(1-\alpha s)\delta}{(1-\alpha s)^2(1-\delta) - \beta s(1-\alpha s)\delta - 2\gamma s(\gamma s + \sqrt{\beta s(1-\alpha s) + \gamma^2 s^2})\delta}. \quad (4.55)$$

Expressing the regions of the domain of $F_\xi(s)$ as function of $s_c$, defined as the crossing point between $m(s)$ and $\frac{1-\delta}{\delta}$, and substituting (4.49) into (4.54), the cdf of $\xi$ is found from the following integrals

$$F_\xi(s) \approx \begin{cases} \frac{\delta}{\Gamma(M-1)} \int_0^\infty e^{-\delta y} y^{M-2} \int_{\frac{1-\delta}{\delta}y}^{my+\varphi} e^{-\delta x}\, dx\, dy, & s_c \leq s < \frac{1}{\alpha} \\ \frac{\delta}{\Gamma(M-1)} \int_0^{y_c} e^{-\delta y} y^{M-2} \int_{\frac{1-\delta}{\delta}y}^{my+\varphi} e^{-\delta x}\, dx\, dy, & 0 \leq s < s_c \end{cases} \quad (4.56)$$

where $s_c$ is given by

$$s_c = \frac{\alpha(1-\delta)^2 + \beta(1-\delta)\delta - 2\sqrt{\gamma^2(1-\delta)^3\delta}}{\alpha^2(1-\delta)^2 + 2\alpha\beta(1-\delta)\delta + \delta(\beta^2\delta - 4\gamma^2(1-\delta))}. \tag{4.57}$$

Solving the integrals in (4.56), the resulting cdf becomes

$$F_\xi\,(x) = \begin{cases} 1 - \frac{e^{\frac{-M_o\sigma^2 s}{P(1-\alpha s)}}}{\delta^{M-1}(1+m)^{M-1}}, & s_c \leq s < \frac{1}{\alpha} \\ \\ 1 - \frac{e^{\frac{-M_o\sigma^2 s}{P(1-\alpha s)}}}{\delta^{M-1}(1+m)^{M-1}} + \Phi(s), & 0 \leq s < s_c \end{cases} \tag{4.58}$$

where $\Phi(s) = \frac{1}{\Gamma(M-1)}\left[\frac{e^{-M_o\sigma^2 s/P(1-\alpha s)}}{\delta^{M-1}(1+m)^{M-1}}\Gamma(M-1, \delta(s+1)y_c) - \Gamma(M-1, y_c)\right]$ and $\Gamma(a,x) = \int_x^\infty t^{a-1}e^{-t}dt$ is the (upper) incomplete gamma function.

Note that this is a generalization of previous results in the literature. In the particular case of $B = 0$, then $\delta = 1$ and thus $s_c$ becomes 0, yielding the cdf derived in [2] for random beamforming. If the metric refers to an upper bound on the SINR, with $\epsilon = 0$, then $s_c = \frac{1-\delta}{\delta}$. If in addition $M_o = M$ is considered as in Metric II, the cdf of (4.58) becomes the one provided in [28].

In order to obtain a tractable expression for $F_\xi(s)$, we assume that $s_c$ is small so that $F_\xi(s)$ can be approximated as described in (4.10). Note that a small $s_c$ value corresponds to a low value of $B$ and thus the obtained cdf approximates better the low resolution regime.

## 4.B Proof of Theorem 4.1

Given $M_o$ beams active for transmission, using (4.13) we approximate the rate as

$$SR \approx \sum_{i=1}^{M_o} \log_2\left[1 + \mathbb{E}\left(s_i\right)\right]. \tag{4.59}$$

From (4.11), $\mathbb{E}\left(s_i\right)$ is computed as follows

$$\mathbb{E}(s_i) = \int_0^{1/\alpha} 1 - \left[1 - \frac{e^{\frac{-M_o\sigma^2 s}{P(1-\alpha s)}}}{\delta^{M-1}\left(1+m\right)^{M-1}}\right]^{K_i} ds. \tag{4.60}$$

Expanding the binomial in the integral, we get

$$\mathbb{E}(s_i) = \sum_{i=1}^{M_o} \frac{(-1)^{n-1}}{\delta^{n(M-1)}} \binom{K_i}{n} \int_0^{1/\alpha} \left[ \frac{e^{\frac{-M_o\sigma^2 s}{P(1-\alpha s)}}}{\delta^{M-1}\,(1+m)^{M-1}} \right]^n ds. \tag{4.61}$$

A closed-form solution for the integral in the above equation can not be found, and thus we use the Bernouilli inequality to obtain an approximation

$$\int_0^{1/\alpha} \left[ \frac{e^{\frac{-M_o\sigma^2 s}{P(1-\alpha s)}}}{\delta^{M-1}\,(1+m)^{M-1}} \right]^n ds \geq \int_0^{1/\alpha} e^{\left[\frac{-M_o\sigma^2 s}{P(1-\alpha s)} + (M-1)m\right] n}. \tag{4.62}$$

Note that the integral above is also difficult to solve, since $m$ is a nonlinear function of $s$, as shown in Proposition 4.1. In order to provide good sum rates, $\epsilon$ will take in general small values. Under this assumption, the following approximation can be made

$$m \approx \frac{\beta s}{1-\alpha s}. \tag{4.63}$$

Let $C = \frac{M_o\sigma^2}{P} + (M-1)\beta$, then the integral in (4.61) is approximated by the following integral

$$\int_0^{1/\alpha} e^{\frac{-Cns}{1-\alpha s}} = \frac{1}{\alpha}\left[1 + \frac{Cn}{\alpha} e^{\frac{Cn}{\alpha}} E_i\left(-\frac{Cn}{\alpha}\right)\right] \tag{4.64}$$

where $E_i(x)$ is the exponential integral function, defined as $E_i(x) = -\int_{-x}^{\infty} \frac{e^{-t}}{t} dt$. By substituting the approximated value of the integral found above into (4.61), and using the definitions of $\mathcal{B}_n$, $\mathcal{K}_{i,n}$ and $\mathcal{P}_n$ given in Theorem 4.1, we obtain the desired approximation for the sum rate.

# Chapter 5

# Optimization of Channel Quantization Codebooks

*The design of channel quantization codebooks for MIMO broadcast channels with limited feedback is addressed. Rather than separating CQI and CDI feedback, we consider a simple scenario in which each user quantizes directly its vector channel. Our goal consists of finding simple quantization codebooks which, in scenarios with spatial or temporal correlation, provide performance gains over classical quantization techniques. In addition, as we show, our optimized codebooks outperform existing techniques that rely on separate CDI and CQI feedback, in systems with a sum-rate feedback constraint. A design criterion that effectively exploits the spatial correlations in the cell is proposed, based on minimizing the average sum-rate distortion in a system with joint linear beamforming and multiuser scheduling. Moreover, we show how to apply Predictive Vector Quantization (PVQ) to quantize time-correlated broadcast channels. PVQ exploits the temporal correlation to reduce the quantization error, and thus to improve the sum rate of the system. In this chapter we show how the corresponding codebooks can be designed, and we present a prediction strategy. Numerical results are provided, which illustrate the benefits of effectively designing quantization codebooks in MIMO broadcast channels with spatial or temporal correlations.*

## 5.1 Introduction

MIMO systems can significantly increase the spectral efficiency by exploiting the spatial degrees of freedom created by multiple antennas [74]. As discussed in previous chapters, due to the complexity and need for accurate CSIT, linear beamforming techniques relying on limited feedback are a good alternative to DPC, the capacity achieving technique. In this chapter, we consider a limited feedback framework different from the one discussed in Chapter 3. Rather than separating CQI and CDI feedback, we consider a simpler system in which each user quantizes directly its vector channel. Our goal is to find simple quantization codebooks which, in scenarios with spatial or temporal correlation, provide performance gains over classical quantization techniques.

Codebook designs for MIMO broadcast channels with limited feedback follow in simple design criteria, that aim at simplifying codebook generation and system analysis. Random beamforming has been proposed in [2] as an SDMA extension of opportunistic beamforming [63], in which feedback from the users to the base station is conveyed in the form of a beamforming vector index and an individual SINR value. An extension of RBF is proposed in [3], coined as opportunistic SDMA with limited feedback (LF-OSDMA), in which the transmitter has a codebook containing an arbitrary number of unitary bases. In that approach, the users quantize the channel direction (channel shape) to the closest codeword in the codebook, feeding back the quantization index and the expected SINR. Multiuser scheduling is performed based on the available feedback, using the unitary basis in the codebook that maximizes the system sum rate as a beamforming matrix. Other schemes for MIMO broadcast channels, like the approach described in [51], propose to use simple Random Vector Quantization (RVQ) [75] for quantizing the user vector channels. A simple geometrical framework for codebook design is proposed in [49], which divides the unit sphere in quantization cells with equal surface area. This framework is also used for channel direction quantization in [28], where feedback to the base station consists of a quantization index along with a channel quality indicator for user selection. These codebook designs take neither spatial nor temporal correlations present in the system into account. Taking them into account could yield better quantization codebooks and in turn better sum-rate performance.

The gains of adaptive cell sectorization have been studied in [76] in the context of CDMA networks and single antenna communications, with the

aim of minimizing the total transmit power in the uplink of a system with non-uniform user distribution over the cell. This situation is analogous to a system with multiple transmit antennas in which beamforming is performed, adapting its beams to uneven user distributions. In a scenario with limited feedback available, adaptation of quantization codebooks can be performed instead, in order to improve the system performance. In [77], an approach for exploiting long term channel state information in the downlink of multiuser MIMO systems is proposed. A flat-fading multipath channel model is assumed, with no line of sight (NLOS) between the base station and user terminals. Each user can be reached through a finite number of multipath components with a certain mean angle of departure (AoD) from the antenna broadside and a certain angle spread. The mean of the angles of departure are fixed and thus no user mobility is considered.

In this chapter, we highlight the importance of cell statistics for codebook design in MIMO broadcast channels with limited feedback. Firstly, the importance of exploiting spatial correlations is addressed. The average sum-rate distortion in a system with joint linear beamforming and multiuser scheduling is minimized, exploiting the information on the macroscopic nature of the underlying channel. In this first part, a non-geometrical stochastic channel model is considered, in which each user can be reached in different spatial directions and with different angle spread. Based on this model, comparisons with limited feedback approaches relying on random codebooks are provided in order to illustrate the importance of matching the codebook design to the cell statistics.

Secondly, we address the problem of exploiting the temporal correlations in the system. We present a scheme that uses Predictive Vector Quantization (PVQ) [78] to exploit the correlation between successive channel realizations in order to improve the quantization, and thus to improve the sum rate of the system. Further, our scheme does not make any assumptions on the scheduling function and on the transmission strategy, thus providing a high flexibility.

Numerical results illustrate the benefits of effectively designing quantization codebooks in MIMO broadcast channels with spatial or temporal correlations. The proposed optimized codebooks outperform existing techniques that rely on separate CDI and CQI feedback, in a system with a sum-rate feedback constraint.

## 5.2 System Description

We consider a multiple antenna broadcast channel consisting of $M$ antennas at the transmitter and $K \geq M$ single-antenna receivers in a single cell scenario. The system model is equivalent to the one described in (3.1). Let $\mathcal{S}$ denote an arbitrary set of users with cardinality $|\mathcal{S}| = M$. Given a set of $M$ users scheduled for transmission, the signal received at the $k$-th user terminal is given by

$$y_k = \mathbf{h}_k^H \mathbf{w}_k s_k + \sum_{i \in \mathcal{S}, i \neq k} \mathbf{h}_k^H \mathbf{w}_i s_i + n_k \tag{5.1}$$

where $\mathbf{h}_k \in \mathbb{C}^{M \times 1}$, $\mathbf{w}_k \in \mathbb{C}^{M \times 1}$, $s_k$ and $n_k$ are the channel vector, beamforming vector, transmitted signal and additive white Gaussian noise at receiver $k$, respectively. The first term in the above equation is the useful signal, while the second term corresponds to the interference. We assume that the variance of the transmitted signal $s_k$ is normalized to one and $n_k$ is independent and identically distributed (i.i.d.) circularly symmetric complex Gaussian random variable with zero mean and variance $\sigma^2$. We assume that the receivers have achieved perfect CSI through the use of pilots. The users then quantize the channel to an element of a common codebook $\mathcal{V}$, and feed back the corresponding index to the base station. The base station then decides, based on the received feedback, which set of users to serve, and forms the appropriate beamforming vector. The data is transmitted in a block-wise fashion. We assume a data-rate limited feedback link that can send back $B$ bits at the beginning of each block. Further, the feedback is assumed to be instantaneous and error-free.

### 5.2.1 Linear Beamforming

Let $\mathbf{W}$ denote the beamforming matrix obtained by concatenating the beamforming vectors. The matrix $\mathbf{W}$ is computed on the basis of the matrix $\widehat{\mathbf{H}}$, whose rows are the conjugate transpose quantized user channels $\widehat{\mathbf{h}}_k^H$, $k \in \mathcal{S}$. Different linear beamforming techniques may be considered, as discussed in Section 3.3.

Commonly applied low-complexity linear beamforming techniques are TxMF and ZFBF [15] (or channel inversion). TxMF uses the normalized columns of $\widehat{\mathbf{H}}^H$ as beamforming vectors. ZFBF uses the normalized columns of the pseudo-inverse of $\widehat{\mathbf{H}}$.

### 5.2.2 User Selection

Since the base station has no access to perfect channel state information, the following SINR estimate is computed for the user set $\mathcal{S}$ and $k$-th user

$$\widehat{SINR}_k = \frac{|\widehat{\mathbf{h}}_k^H \mathbf{w}_k|^2}{\sum\limits_{i \in \mathcal{S}, i \neq k} |\widehat{\mathbf{h}}_k^H \mathbf{w}_i|^2 + \sigma^2}. \tag{5.2}$$

Let $\mathcal{G}$ be the set of all possible user subsets of cardinality $M$ with disjoint indices in $\{1, \ldots, K\}$. The set of users scheduled for transmission at each time slot corresponds to the one that maximizes the estimated sum rate over all possible user sets

$$\widehat{\mathcal{S}^*} = \arg\max_{\mathcal{S} \in \mathcal{G}} \sum_{k \in \mathcal{S}} \log_2(1 + \widehat{SINR}_k) \tag{5.3}$$

## 5.3 Exploiting Spatial Correlations

### 5.3.1 Channel Model

In this section we present the model considered both for the user vector channels and the cell statistics. A non-geometrical stochastic channel is assumed, in which the channel physical parameters are described by probability density functions assuming an underlying geometry. It is mainly based on the work in [79], extended to multiuser scenarios. We consider an outdoor environment with NLOS between transmitter and receivers, in which local scatterers, randomly distributed around each mobile user, produce a clustering effect. The multipath components (MPC) arrive in clusters in both space and time. For the sake of simplicity, we consider flat fading and hence all paths are assumed to arrive at zero delay. Furthermore, we assume that each user sees MPCs incoming from surrounding scatterers that are grouped into one cluster.

Each user is reached with a different mean angle of departure (AoD) $\overline{\theta}_k$. The AoDs associated to the multipath components are distributed around the mean according to a certain power angular spectrum (PAS), which depends on the spatial distribution of scatterers. In practice, we only consider the azimuth directions (angle of propagation with respect to the antenna array broadside) since the elevation angle spread is generally small compared to

Table 5.1: Parameters of Broadcast Channel Model

| | |
|---|---|
| $M$ | number of transmit antennas at the BS |
| $K$ | number of active users in the cell |
| $L$ | number of multipath components per user channel |
| $PAS$ | power angular spectrum around mean AoD |
| $\sigma_\theta$ | angular spread, second order moment of $PAS$ |
| $\lambda$ | wavelength |
| $d$ | antenna spacing at the BS |
| *AoD Range* | effective range of mean AoDs in the cell |

the azimuthal angle. Different probability density functions are considered in the literature, such as Gaussian, uniform or Laplacian [80]. A summary of the model parameters is given in Table 5.1.

### User Vector Channels

The signals from the base station arrive at each user terminal (UT) through a finite number of $L$ paths, which have different angles of departure with respect to the antenna array broadside but arrive at the receiver with the same delay. The AoD for the $k$-th user and $l$-th path can be expressed as $\theta_{kl} = \overline{\theta}_k + \Delta\theta_{kl}$, where $\overline{\theta}_k$ is the mean AoD for user $k$ and $\Delta\theta_{kl}$ is the angle offset for the $l$-th multipath component. The multipath components have complex Gaussian distributed gains $\gamma_{kl}$ with zero mean and unit variance. The channel of user $k$ is given by

$$\mathbf{h}_k = \frac{1}{\sqrt{L}} \sum_{l=1}^{L} \gamma_{kl} \mathbf{a}(\theta_{kl}) \tag{5.4}$$

where $\mathbf{a}(\theta_{kl})$ are the steering vectors. An omnidirectional uniform linear array is considered (ULA) although the proposed technique can benefit from any array configuration. The steering vectors $\mathbf{a}(\theta_{kl})$ of a ULA are given by

$$\mathbf{a}(\theta_{kl}) = \left[1, e^{-j2\pi\frac{d\sin\theta_{kl}}{\lambda}}, \ldots, e^{-j2\pi\frac{(M-1)d\sin\theta_{kl}}{\lambda}}\right]^T. \tag{5.5}$$

The distribution of the angles around the mean AoD is assumed to have a double-sided Laplacian pdf, given by

$$f(\Delta\theta_{kl}) = \frac{1}{\sqrt{2}\sigma_\theta} \exp(-|\sqrt{2}\Delta\theta_{kl}/\sigma_\theta|) \tag{5.6}$$

where $\sigma_\theta$ is the angular standard deviation, $\sigma_\theta = \sqrt{E[|\Delta\theta_{kl}|^2]}$. Under the assumption of using a ULA at the base station, the cross-correlation coefficients of each user's vector channel can be computed in closed form given the PAS, as shown in [81].

### Spatial Cell Statistics

Most papers based on the above mentioned stochastic models assume that mean AoDs are uniformly distributed between 0 and $2\pi$. In indoor scenarios, the relative cluster AoD is indeed uniformly distributed over $[0, 2\pi]$, as it has been seen from channel measurements [81], since the location of cluster centers is uniformly distributed over the cell. However, as noted in [81], this is not realistic in outdoor scenarios where the base station is elevated and the mobile stations are often surrounded by local scatterers. In these cases, the mean AoD is very dependent on the macroscopic characteristics of each particular scenario: topology, user distribution, mobility pattern, distribution of scatterers, etc. Hence, the mean angles of departure for each user, $\overline{\theta}_k$, do not need to be uniformly distributed over the interval $[0, 2\pi]$. In our model, they are considered to be uniformly distributed over an arbitrary range of angles $\bigcup_i [\overline{\theta}_{min_i}, \overline{\theta}_{max_i}]$. A graphical representation of the broadcast channel model is depicted in Figure 5.1.

## 5.3.2 Codebook Design

A design criterion and an optimization procedure is proposed for generating channel quantization codebooks for a given scenario, with the purpose of exploiting the spatial correlation in MIMO broadcast channels.

As discussed in Chapter 3, most techniques relying on limited quantized channel state information consider separate feedback bits (and thus separate quantization) for CDI and CQI. Since the amount of feedback is limited, a tradeoff arises between the amount of bits used for CDI quantization, which has an impact on the multiplexing gain, and the amount of bits used for CQI

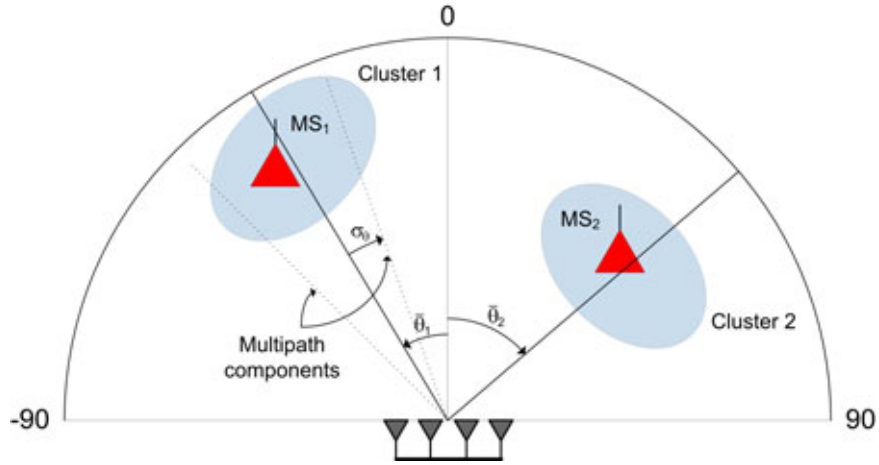


Figure 5.1: Broadcast channel model with mobile stations (MS) surrounded by local scatterers grouped in clusters, located in different mean angles of departure (AoD) with respect to uniform linear array (ULA) broadside.

quantization, which has an impact on the multiuser diversity gain achieved from user selection. In this chapter, we consider joint quantization of CDI and CQI information. Channel quantization is done directly over the user vector channels rather than quantizing the norm and channel direction separately, thus providing better granularity. Hence, since the proposed channel quantization is adapted to the cell statistics, including the average SNR conditions and the number of active users, the tradeoff between multiplexing gain and multiuser diversity is implicitly optimized.

The proposed approach consists of designing a channel quantization codebook valid for all users in the cell by minimizing the average sum-rate distortion of the scheduled users. Since scheduling and beamforming are performed jointly at each time slot, the distortion measure needs to account for both jointly. Hence, different linear beamforming techniques will result in different optimized codebooks. This criterion yields quantization codebooks that are statistically matched to the users that maximize the estimated sum rate, selected according to equation (5.3). The quantization codebook is optimized during an initial training period, after which the codebook is fixed and broadcasted to the users.

Given a codebook $\mathcal{V}$ with $2^B$ codewords, the optimized design is found

by solving the following optimization problem

$$\min_{\mathcal{V}} E[d(\mathcal{H}, \widehat{\mathcal{H}})] \tag{5.7}$$

where $d(\mathcal{H}, \widehat{\mathcal{H}})$ is the distortion measure between the input matrix of concatenated user channels $\mathcal{H} = [\mathbf{h}_1, \ldots, \mathbf{h}_K]$ and the matrix $\widehat{\mathcal{H}} = \left[\widehat{\mathbf{h}}_1, \ldots, \widehat{\mathbf{h}}_K\right]$ of concatenated quantized user channels. The vector quantizer maps each of the columns of $\mathcal{H}$ to the codeword in $\mathcal{V}$ with the smallest Euclidean distance as described by

$$\widehat{\mathbf{h}}_k = \arg\min_{\mathbf{v} \in \mathcal{V}} \|\mathbf{h}_k - \mathbf{v}\|^2 . \tag{5.8}$$

### 5.3.3 Distortion Measure

The proposed distortion measure is the sum-rate distortion for the scheduled users given an arbitrary linear beamforming technique. Thus, the distortion measure can be described as

$$d(\mathcal{H}, \widehat{\mathcal{H}}) = SR(\mathcal{H}) - SR(\widehat{\mathcal{H}}). \tag{5.9}$$

The first term in the equation above corresponds to the maximum sum rate that can be achieved with the chosen linear beamforming technique and perfect channel state information, given by

$$SR(\mathcal{H}) = \max_{\mathcal{S} \in \mathcal{G}} \sum_{k \in \mathcal{S}} \log_2(1 + SINR_k). \tag{5.10}$$

The beamforming vectors and user selection obtained in the case of perfect channel state information are in general different than the ones obtained on the basis of quantized channel information for a given time slot. The second term in (5.9) corresponds to the actual sum rate achieved by the system. The beamforming vectors are computed on the basis of the quantized channels and the users scheduled for transmission are selected as described in (5.3). Hence, the achieved sum rate is given by

$$SR(\widehat{\mathcal{H}}) = \sum_{k \in \widehat{\mathcal{S}^*}} \log_2(1 + SINR_k). \tag{5.11}$$

Note that, as opposed to the estimated SINR values employed for user selection, the above equation computes the effective SINR experienced by each of the users in the scheduled set $\widehat{\mathcal{S}^*}$.

### 5.3.4 Optimization Procedure

A simple optimization procedure is performed to find the quantization codebook $\mathcal{V}$ in (5.7). For a given scenario, a large number $N_c$ of random codebooks, with the same distribution as the channel, is generated. The selected codebook corresponds to the one that minimizes the long term sample average distortion.

An alternative procedure consists of using the generalized Lloyd algorithm to iteratively find the optimizing codebook and partition cells. The proposed algorithm avoids convergence to local minima exhibited by Lloyd's algorithm and provides good performances for large $N_c$, as we show later on.

### 5.3.5 Practical Considerations

The proposed technique for codebook design is expected to perform better in scenarios with strong spatial correlations. Different linear beamforming techniques will achieve different performances, since quantization errors affect them differently. For instance, while the performance of ZF beamforming is very sensitive to channel quantization errors, optimized unitary beamforming proves to be very robust, as it will be shown in Chapter 6.

Since the statistics of the best $M$ users govern the design, the quantization codebooks may favor certain spatial locations or directions that provide good sum rates, favoring the users in those particular locations. In a system with low mobility and slow variations, this situation may lead to a fairness issue. This behavior may be accentuated when incorporating shadowing and pathloss to the channel model. Its effect can be attenuated by performing proportional fair scheduling (PFS) [82], which would yield an average distortion function based on a weighted sum rate, penalizing the users that have already been scheduled.

Instead of simply generating the quantization codebooks during a training period, the base station may slowly adapt the codebook to changes in the environment: temperature, changes in traffic and mobility patterns, changes of scatterers, etc. Each time a user enters the system or in case there is a codebook update, the base station would send the updated codebook to the users, which in general changes from cell to cell.

In addition, similarly to the work presented in [83] for single user MIMO communications, the amount of feedback can be reduced by exploiting temporal correlations in the system. In the following section, we present an algorithm to exploit temporal correlations in MIMO broadcast channels.

## 5.4 Exploiting Temporal Correlations

In this section we present a scheme that uses PVQ to exploit the correlation between successive channel realizations in order to improve the quantization, and thus to improve the sum rate of the system. Further, our scheme does not make any assumptions on the scheduling function and on the transmission strategy, thus providing a high flexibility.

### 5.4.1 Channel Model

Although the proposed methods work for more general channel models, we assume stationarity (in the time domain) and a separable channel correlation in space and time

$$\mathbf{R}_m = E(\mathbf{h}_k[n]\mathbf{h}_k^H[n-m]) = \mathbf{R}\rho_m \tag{5.12}$$

where $\mathbf{R}$ is the spatial correlation matrix, and $\rho_m$ is the time-correlation function. In this section, we mainly concentrate on the time-correlation.

The performance of the vector quantization (VQ) step can be improved by taking the time correlation of the channel into account. Vector quantizers with memory allow to quantize the actual channel more efficiently, i.e., the quantization error of VQ with memory is smaller than the quantization error of VQ without memory for the same amount of feedback. Even though there exists a large number of VQs with memory [84], we focus here solely on the so-called PVQ since its simplicity makes it a good candidate for practical systems. It allows to exploit the correlation of the channel by considering a variable number of previous channels, without resulting in an exponential increase of the storage requirements for the codebooks as is the case for finite-state vector quantizers.

### 5.4.2 Predictive Vector Quantization

We provide here an overview of PVQ and its application to channel quantization of broadcast channels. In the remainder of this section, we omit the

user index for the sake of clarity.

PVQ starts by estimating the current channel $\mathbf{h}[n]$ based on the $m$ previously quantized channels $\widehat{\mathbf{h}}[n-i], i = 1 \ldots m$, at both the base station and the users, resulting in

$$\tilde{\mathbf{h}}[n] = P(\widehat{\mathbf{h}}[n-1], \widehat{\mathbf{h}}[n-2], \ldots, \widehat{\mathbf{h}}[n-m]) \tag{5.13}$$

where $P(\cdot)$ denotes the prediction function. The users, who have full CSI knowledge, then calculate the true error $\mathbf{e}[n]$ between the estimated channel $\tilde{\mathbf{h}}[n]$ and the true channel $\mathbf{h}[n]$

$$\mathbf{e}[n] = \mathbf{h}[n] - \tilde{\mathbf{h}}[n]. \tag{5.14}$$

The error is quantized by finding the entry in the quantization codebook $\mathcal{V}$ with the smallest Euclidean distance to the true error

$$\mathbf{e}_Q[n] = \arg\min_{\mathbf{v}\in\mathcal{V}} \|\mathbf{e}[n] - \mathbf{v}\|^2. \tag{5.15}$$

The quantized error $\mathbf{e}_Q[n]$ is fed back to the base station, which computes the quantized channel at time instant $n$ as

$$\widehat{\mathbf{h}}[n] = \tilde{\mathbf{h}}[n] + \mathbf{e}_Q[n]. \tag{5.16}$$

Note that the prediction function $P(\cdot)$ is common to both the base station and the users. Hence, both ends compute the same $\tilde{\mathbf{h}}[n]$, which is based on the previously quantized channels, $\widehat{\mathbf{h}}[n-i], i = 1 \ldots m$, also available at the base station and user ends.

The challenge of PVQ is to design the codebook and the prediction function.

### 5.4.3 Codebook Design

A popular approach to design a codebook for PVQ is the open-loop approach [84]. It does not have an iterative nature, and it relies on the assumption that the quantized channels are a good approximation of the real channels. The codebook design assumes that the prediction function is known, and it uses regular VQ without memory on a training set $\mathcal{T}$, where the different elements of the training set $\mathcal{T}$ are the ideal prediction errors calculated as

$$\mathbf{e}_{\text{ideal}}[n] = \mathbf{h}[n] - P(\mathbf{h}[n-1], \mathbf{h}[n-2], \ldots, \mathbf{h}[n-m]). \tag{5.17}$$

The application of a memoryless VQ is possible since the prediction step in (5.17) removes, in the ideal case, the time correlation between the channels at different time instances.

Note that the ideal prediction error $\mathbf{e}_{\text{ideal}}[n]$ differs from the true error $\mathbf{e}[n]$ in (5.14). The true error is calculated as a function of the previously quantized channels, and thus depends on the quantization codebook. Using the ideal prediction error to design the codebooks removes this dependence, hence the name open-loop approach. Iterative designs, i.e., closed-loop approaches [78], only provide a minor gain.

The most common algorithm to design codebooks is the generalized Lloyd algorithm (GLA) [85]. It is a descent algorithm [84], i.e., it reduces the average distortion of the codebook with every iteration. However, the GLA is not guaranteed to find the global optimal codebook for non-convex distortion functions [86], since it may get trapped in a local minimum.

A more robust approach to find good codebooks is a Monte-Carlo based codebook design, such as the one proposed in the previous section for spatially correlated channels. As it has been shown, the optimal design aims at finding a codebook that maximizes the overall sum rate of the system. However, this design objective is computationally complex, and it depends on all the components of the system, e.g., the number of users, the selected beamforming strategy, the selection function. In this section, in order to reduce the computational complexity, we focus instead on codebooks which minimize the average Euclidean distance between the ideal prediction error and the quantized prediction error

$$\mathcal{V}^* = \arg\min_{\mathcal{V}} E(\|\mathbf{e}_{\text{ideal}}[n] - \mathbf{e}_{\text{ideal},Q}[n]\|^2) \tag{5.18}$$

with

$$\mathbf{e}_{\text{ideal},Q}[n] = \arg\min_{\mathbf{v}\in\mathcal{V}} \|\mathbf{e}_{\text{ideal}}[n] - \mathbf{v}\|^2. \tag{5.19}$$

### 5.4.4 Prediction Function

The other crucial part in designing the PVQ is the prediction function. A common technique for PVQ is vector linear prediction [87].

Based on the previous $m$ known channel vectors we want to predict the

vector $\mathbf{h}[n]$ using the coefficient matrices $\mathbf{A}_j$ as follows

$$\widetilde{\mathbf{h}}[n] = -\sum_{j=1}^{m} \mathbf{A}_j \mathbf{h}[n-j]. \tag{5.20}$$

The goal is to minimize the average mean square prediction error. Using the orthogonality principle, the coefficient matrices can be derived from

$$\mathbf{R}_{0j} = -\sum_{\mu=1}^{m} \mathbf{A}_\mu \mathbf{R}_{\mu j} \quad j = 1, \ldots, m \tag{5.21}$$

where $\mathbf{R}_{ij}$ is the channel correlation matrix

$$\mathbf{R}_{ij} = E(\mathbf{h}[n-i]\mathbf{h}[n-j]^H). \tag{5.22}$$

Stacking (5.21) in matrix form as

$$\begin{bmatrix} \mathbf{R}_{11} & \mathbf{R}_{12} & \ldots & \mathbf{R}_{1m} \\ \mathbf{R}_{21} & \mathbf{R}_{22} & \ldots & \mathbf{R}_{2m} \\ \vdots & \vdots & \ddots & \vdots \\ \mathbf{R}_{m1} & \mathbf{R}_{m2} & \ldots & \mathbf{R}_{mm} \end{bmatrix} \begin{bmatrix} \mathbf{A}_1^H \\ \mathbf{A}_2^H \\ \vdots \\ \mathbf{A}_m^H \end{bmatrix} = - \begin{bmatrix} \mathbf{R}_{10} \\ \mathbf{R}_{20} \\ \vdots \\ \mathbf{R}_{m0} \end{bmatrix} \tag{5.23}$$

the coefficient matrices $\mathbf{A}_j$ can now be found through simple matrix inversion.

For the channel model defined in (5.12), we have that $\mathbf{R}_{ij} = \mathbf{R}_{j-i} = \mathbf{R}\rho_{j-i}$. In that case, (5.23) becomes

$$\begin{bmatrix} \rho_0 & \rho_{-1} & \cdots & \rho_{-m} \\ \rho_1 & \rho_0 & \cdots & \rho_{-m+1} \\ \vdots & \vdots & \ddots & \vdots \\ \rho_m & \rho_{m-1} & \cdots & \rho_0 \end{bmatrix} \otimes \mathbf{R} \begin{bmatrix} \mathbf{A}_1^H \\ \mathbf{A}_2^H \\ \vdots \\ \mathbf{A}_m^H \end{bmatrix} = - \begin{bmatrix} \rho_{-1} \\ \rho_{-2} \\ \vdots \\ \rho_{-m} \end{bmatrix} \otimes \mathbf{R}. \tag{5.24}$$

If $\mathbf{R}$ is assumed diagonal, it is clear that this equation can be solved for every channel entry separately.

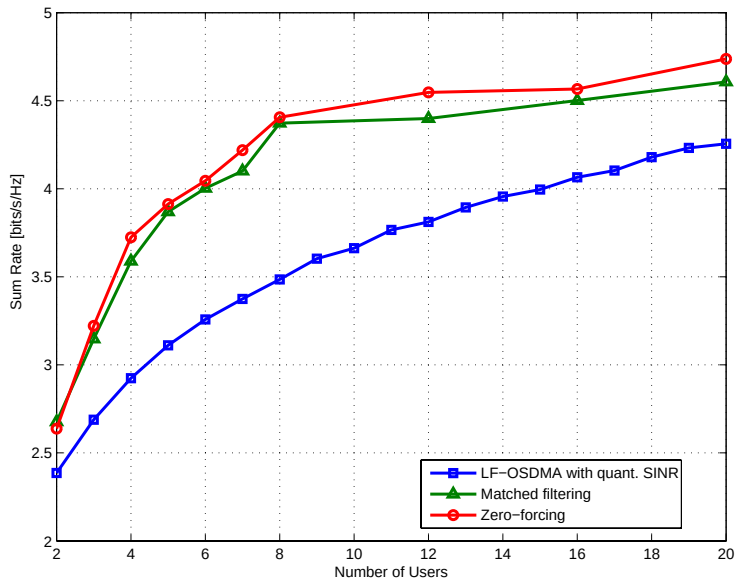


Figure 5.2: Sum rate for different number of users in a spatially correlated channel, $M = 2$ transmit antennas and SNR = 10 dB.

## 5.5 Numerical Results

We compare the performance of linear beamforming with quantized CSI feedback to LF-OSDMA, which generalizes RBF to CDI codebooks of size larger than $\log_2 M$. The linear beamforming strategies that we use are ZFBF and TxMF. We assume single-antenna users and a base station with $M = 2$ antennas. The data rate on the feedback link is limited to $B = 3$ bits/transmission. In order to make a fair comparison between the schemes, the SINR feedback of the LF-OSDMA algorithm is also quantized. Thus, the LF-OSDMA algorithm has to share the available 3 bits between the CDI, i.e., the index of the preferred beamforming vector, and the CQI, i.e., the SINR of the preferred beamforming vector. We simulate the performance of all possible CDI/CQI bit allocations, and finally select the allocation that results in the highest sum rate. This is equivalent to choosing the configuration that maximizes the multiuser diversity - multiplexing tradeoff, as discussed in 4.7. The codebook to quantize the scalar CQI is designed with the generalized Lloyd algorithm [84], using the mean square error as distortion function.

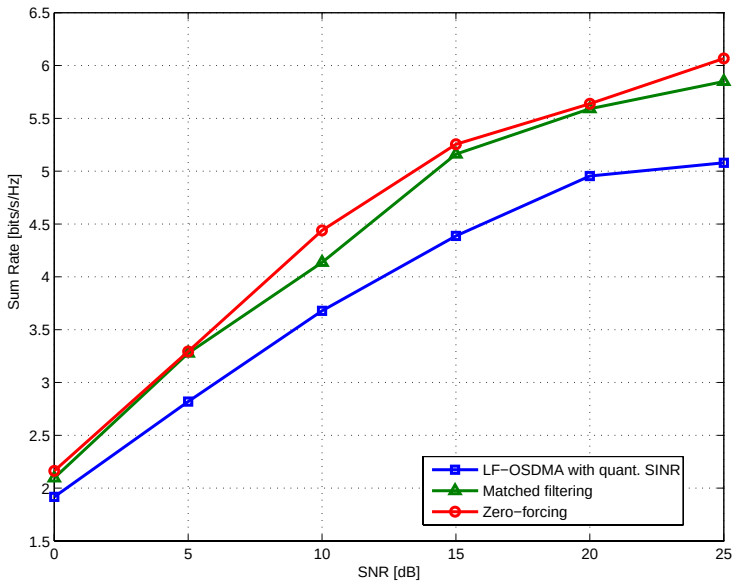


Figure 5.3: Sum rate for different SNR values in a spatially correlated channel, $M = 2$ transmit antennas and $K = 10$ users.

### 5.5.1 Spatially Correlated Channels

First, we study the benefits of codebook design in a system with spatial correlation and no temporal correlation. Following the channel model described in 5.3.1, a 2-GHz system is considered with an antenna spacing at the base station of $d = 0.4\lambda \approx 15$ cm. Each user channel is modeled with $L = 10$ multipath components. The mean AoD of the different users is uniformly distributed over the interval $[-30°, 30°]$, and the angular spread is fixed to $\sigma_\theta = 30°$.

Figure 5.2 depicts the performance for different numbers of users with a fixed SNR of 10 dB. We see that ZF and TxMF with quantized CSI outperform LF-OSDMA with quantized SINR feedback.

The same result can be seen in Figure 5.3 for different SNR values and $K = 10$ users. We see how the sum rate of the different schemes saturates at high SNR, where the performance is limited by the quantization error.

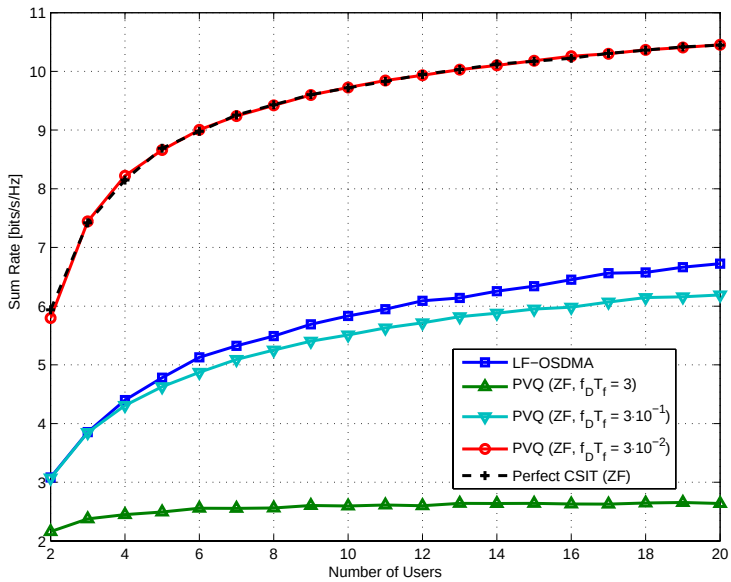


Figure 5.4: Sum rate for different number of users in a temporally correlated channel, $M = 2$ transmit antennas and SNR = 10 dB.

### 5.5.2 Temporally Correlated Channels

We focus here our attention on exploitation of temporal correlations. In this case, the users are assumed to be distributed in the cell in such way that the different channel vectors are spatially i.i.d., and thus $\mathbf{R} = \mathbf{I}_M$. The channel is modeled through (5.12) with $\rho_m = J_0(2\pi f_D T_f m)$ where $J_0$ is the Bessel function of zeroth-order, $f_D$ the Doppler spread, and $T_f$ the frame length (Jakes' model [88]). The algorithm predicts the channel based on the last $m = 3$ channels.

Figure 5.4 depicts the sum rate of PVQ with ZFBF, and of LF-OSDMA. We assume each user has an average SNR = 10 dB, and simulate different $f_D T_f$ products. The initial channels are assumed to be known perfectly, which can be approximated by starting the algorithm with a high-resolution memoryless VQ. We see in Figure 5.4 how the performance of PVQ with ZF improves for lower $f_D T_f$ values, i.e., for scenarios with a higher time correlation between the channels.

## 5.6 Conclusions

The problem of designing channel quantization codebooks for MIMO broadcast channels with limited feedback has been addressed, in systems where joint linear beamforming and multiuser scheduling is performed. Rather than considering a framework with separate CQI and CDI feedback, as studied in the previous chapter, a simpler framework is considered in which each user directly quantizes its channel vector, or the prediction error in temporally correlated channels. The tradeoff between multiuser diversity and multiplexing gain introduced in the previous chapter is implicitly optimized in the proposed approaches, at the expense of feedback overhead during the initial training period in which the codebooks are optimized. The numerical results provided have shown the benefits of using quantization codebooks optimized according to the cell statistics.

When designing codebooks adapted to the spatial correlation present in the system, the proposed technique performs well in scenarios with reduced angular spread and effective range of mean angles of departure. This makes the proposed approach particularly interesting in outdoor systems with non uniform user distribution. In addition, we depicted through numerical simulations the benefits of using PVQ for time-correlated channels. PVQ uses a simple prediction step to remove the correlation between the channel to be quantized and the previous channels. This allows to improve the performance of the quantization step, as shown in our simulations.

# Chapter 6

# Linear Beamforming Design

*In this chapter, the problem of linear beamforming design in MIMO broadcast channels is addressed. An iterative optimization method for unitary beamforming is proposed, based on successive optimization of Givens rotations. Under the assumption of perfect CSIT and for practical average SNR values, the proposed technique provides higher sum rates than ZF beamforming while performing close to MMSE beamforming. Moreover, it is shown to achieve linear sum-rate growth with the number of transmit antennas. Interestingly, the proposed unitary beamforming approach proves to be very robust to channel estimation errors, providing better sum rates than ZF beamforming and even MMSE beamforming as the variance of the estimation error increases. When combined with simple vector quantization techniques for CSI feedback in systems with multiuser scheduling, the proposed technique proves to be well suited for limited feedback scenarios with practical number of users, exhibiting performance gains over existing techniques.*

## 6.1 Introduction

Unitary beamforming (UBF) techniques have recently become a focus of interest in MIMO broadcast channels, especially in scenarios where the amount of feedback available at the base station is limited. Particularly, RBF [2] has been proposed as a simple technique that achieves optimal capacity scaling in MIMO broadcast channels. In [3], LF-OSDMA is proposed as a transmission technique in which the transmitter has a codebook containing an arbitrary number of unitary bases. In this approach, the users quantize the channel shape (channel direction) to the closest codeword in the codebook, feeding back the quantization index and expected SINR. Multiuser scheduling is performed based on the available feedback, using as beamforming matrix the unitary basis in the codebook that maximizes the system sum rate. An extension to scenarios with a sum feedback rate constraint is provided in [57], coined as orthogonal SDMA with threshold feedback (TF-OSDMA). Codebook-based unitary precoding is a solid candidate for MIMO downlink transmission in future mobile communication standards, currently under study in 3GPP [89], [90], [91]. Similarly to the work reported in [3], feedback from the mobile users in the form of a quantization index and channel quality indicator are used for user scheduling and beamforming design. Simple codebooks containing unitary bases have been considered so far, generated either randomly or from phase rotations of a DFT matrix. An advantage of DFT matrices is that multiplication with vectors can be done efficiently in reduced time. In addition, unitary beamforming yields smooth switching between single user point-to-point MIMO operation and multiuser SDMA.

In order to obtain good sum rates, the precoding matrices, quantization codebooks and feedback strategies need to be jointly designed. When constraining the precoding matrices to be unitary, the performance of suboptimal schemes should be evaluated by comparison with optimal unitary beamforming in order to measure the degree of suboptimality introduced. Conversely, limited feedback schemes relying on unitary beamforming should be designed with low complexity and reduced feedback, while approaching the performance of the optimal unitary beamforming solution. However, optimal unitary beamforming in MIMO broadcast channels - in the sense of system sum-rate maximization - is not yet known. Thus, most limited feedback schemes with unitary beamforming use low complexity as main design criterion, evaluating their performances through simulations. Multiuser MIMO schemes based on full channel knowledge at the transmitter and unitary

beamforming have been proposed in [21], exhibiting performance gains over ZF beamforming approaches particularly at low SNR. However, the beamforming matrices in [21] are generated by following low-complexity design criteria with the aim of simplifying the scheduling algorithms in scenarios where the number of users is larger than the number of transmit antennas.

In this chapter, an iterative optimization method for unitary beamforming in MIMO broadcast channels is proposed, based on successive optimization of Givens rotations. Initially, we consider a system with perfect CSIT side. As we show, the proposed technique provides higher sum rates than ZF beamforming while performing close to MMSE beamforming for practical average SNR values. However, as the average SNR becomes large, the slope of the sum-rate versus SNR curve converges to that of a system with TDMA that selects the best user, thus incurring a loss of multiplexing gain. Moreover, it is shown to achieve linear sum-rate growth with the number of transmit antennas. The main advantage of the proposed unitary beamforming approach is its robustness to channel estimation errors. As shown through numerical simulations, it provides better sum rates than ZF beamforming and even MMSE beamforming as the variance of the estimation error increases. Hence, the proposed beamforming technique can be seen as an interesting alternative to other existing linear beamforming schemes, such as ZF and MMSE. In the last part of this chapter, the proposed technique is investigated in MIMO broadcast channels with multiuser scheduling and limited feedback, evaluating the performance of unitary beamforming approaches with limited feedback, namely RBF and LF-OSDMA. A simple vector quantization technique is used, based on random vector quantization (RVQ) with pruning. Our results highlight the importance of linear beamforming optimization in MIMO broadcast channels with limited feedback.

## 6.2 System Model

In this section, the system models for the different scenarios under study are presented. Initially, we introduce the general model for a system in which the user terminals have multiple receive antennas, followed by the single antenna case. A simple model for the imperfect CSIT case is also introduced, which will be used later on for testing the proposed linear beamforming algorithm in more realistic scenarios.

### 6.2.1 Multi-antenna Receivers

We consider a multiple antenna broadcast channel consisting of a transmitter equipped with $M$ antennas and $K$ multi-antenna receivers. The $k$-th receiver has $N_k$ antennas, and the system satisfies $\sum_{k=1}^{K} N_k \geq M$. Given a set $\mathcal{S}$ of users scheduled for transmission with $\sum_{k\in\mathcal{S}} N_k = M$, the signal received at the $k$-th mobile is given by

$$\mathbf{y}_k = \sqrt{\frac{P}{M}}\mathbf{H}_k^H\mathbf{W}_k\mathbf{s}_k + \sqrt{\frac{P}{M}}\sum_{i\in\mathcal{S},i\neq k}\mathbf{H}_k^H\mathbf{W}_i\mathbf{s}_i + \mathbf{n}_k \tag{6.1}$$

where $\mathbf{H}_k \in \mathbb{C}^{M\times N_k}$, $\mathbf{W}_k \in \mathbb{C}^{M\times N_k}$, $\mathbf{s}_k \in \mathbb{C}^{M\times 1}$, $\mathbf{n}_k \in \mathbb{C}^{M\times 1}$ and $P$ are the channel matrix, beamforming matrix, transmitted signal vector, additive Gaussian noise vector at receiver $k$ and transmit power, respectively. The first term in the above equation is the useful signal, while the second term corresponds to the interference. We assume that the channels are i.i.d. block Rayleigh flat fading, the covariance of the transmitted signal $\mathbf{s_k}$ is $\mathbf{I}_{N_k}$ and $\mathbf{n}_k$ is circularly symmetric complex Gaussian with zero mean and covariance $\sigma^2\mathbf{I}_{N_k}$. A unitary beamforming matrix $\mathbf{W} \in \mathbb{C}^{M\times M}$ is considered at the transmitter, obtained by concatenating horizontally (along the row dimension) the beamforming matrices of the scheduled users $\mathbf{W}_k$, $\forall k \in \mathcal{S}$. The average transmitted power is equal to $P$. In order to design the beamforming matrix, perfect knowledge of the user channels will be assumed at the transmitter unless stated otherwise.

### 6.2.2 Single-antenna Receivers

In the particular case of interest $N_k = 1\ \forall k$, given a set of $M$ users scheduled for transmission, the signal model in (6.1) can be simplified as follows

$$y_k = \sqrt{\frac{P}{M}}\mathbf{h}_k^H\mathbf{w}_k s_k + \sqrt{\frac{P}{M}}\sum_{i=1,i\neq k}^{M}\mathbf{h}_k^H\mathbf{w}_i s_i + n_k \tag{6.2}$$

where $\mathbf{h}_k \in \mathbb{C}^{M\times 1}$, $\mathbf{w}_k \in \mathbb{C}^{M\times 1}$, $s_k$ and $n_k$ are the channel vector, beamforming vector, transmitted signal and additive Gaussian noise of user $k$. This signal model is equivalent to the one described in Section 3.2, with equal power allocation per transmit beam. The unitary beamforming matrix contains the beamforming vectors of the users scheduled for transmission $\mathbf{W} = [\mathbf{w}_1\ \mathbf{w}_2 \ldots \mathbf{w}_M] \in \mathbb{C}^{M\times M}$.

### 6.2.3 Imperfect CSIT Model

The robustness of the proposed approach to channel estimation errors is studied through numerical simulations. When imperfect knowledge of the user channel vectors is available at the transmitter side, the estimation error is modeled as an additive spatially white complex Gaussian noise. Hence, the channel estimate of user $k$ is given by

$$\widehat{\mathbf{H}}_k = \mathbf{H}_k + \widetilde{\mathbf{H}}_k \tag{6.3}$$

where $\widetilde{\mathbf{H}}_k$ has a distribution $\mathcal{CN}(0, \sigma_e^2\mathbf{I})$. Imperfect CSIT can be the result of a combination of channel estimation noise, quantization errors, prediction errors, etc.

## 6.3 Problem Formulation

### 6.3.1 Multi-antenna Receivers

In the general case of an arbitrary number of receive antennas per user, the optimization criterion considered in our problem is sum capacity maximization, constrained to using linear unitary beamforming at the transmitter. Hence, the optimization problem can be formulated as follows

$$\begin{aligned} &\max_{\mathbf{W}} \sum_{k\in\mathcal{S}} C_k(\mathbf{H}_k, \mathbf{W}_k) \\ &s.t. \quad \mathbf{W}^H\mathbf{W} = \mathbf{I}_M \end{aligned} \tag{6.4}$$

where $C_k$ corresponds to the mutual information between vectors $\mathbf{s}_k$ and $\mathbf{y}_k$, given by $C_k = I(\mathbf{s}_k, \mathbf{y}_k) = H(\mathbf{y}_k) - H(\mathbf{y}_k|\mathbf{s}_k)$, $H$ being the differential entropy. Gaussian inputs and perfect CSIR are assumed. Following the steps in [5] for the derivation of the capacity of the MIMO channel, due to independence between the signal vectors $\mathbf{s}_k$ transmitted to different users, and between the signal and noise vectors, $C_k$ can be expressed as follows

$$C_k = H(\mathbf{y}_k) - H(\mathbf{x}_k) \tag{6.5}$$

where $\mathbf{x}_k$ is the interference plus noise vector, given by

$$\mathbf{x}_k = \sqrt{\frac{P}{M}} \sum_{i\in\mathcal{S}, i\neq k} \mathbf{H}_k^H \mathbf{W}_i \mathbf{s}_i + \mathbf{n}_k. \tag{6.6}$$

The differential entropy of $\mathbf{x}_k$ is given by

$$H(\mathbf{x}_k) = \log_2 |\pi e \mathbf{R}_{x_k}| \tag{6.7}$$

where $\mathbf{R}_{x_k}$ is the covariance matrix of $\mathbf{x}_k$, given by

$$\mathbf{R}_{x_k} = \frac{P}{M} \sum_{i \in \mathcal{S}, i \neq k} \mathbf{H}_k^H \mathbf{W}_i \mathbf{W}_i^H \mathbf{H}_k + \sigma^2 \mathbf{I}_{N_k}. \tag{6.8}$$

As defined in the previous section, the matrix $\mathbf{W}$ is the concatenation of the $\mathbf{W}_k$ matrices. Since $\mathbf{W}$ is constrained to be unitary, we have that

$$\mathbf{W} = \sum_{k \in \mathcal{S}} \mathbf{W}_k \mathbf{W}_k^H = \mathbf{I}_M \tag{6.9}$$

and thus (6.8) becomes

$$\mathbf{R}_{x_k} = \frac{P}{M} \mathbf{H}_k^H \left( \mathbf{I}_M - \mathbf{W}_k \mathbf{W}_k^H \right) \mathbf{H}_k + \sigma^2 \mathbf{I}_{N_k}. \tag{6.10}$$

The differential entropy of $\mathbf{y}_k$ is given by

$$H(\mathbf{y}_k) = \log_2 |\pi e \mathbf{R}_{y_k}| \tag{6.11}$$

where $\mathbf{R}_{y_k}$, using again the result in (6.8), is given by

$$\mathbf{R}_{y_k} = \frac{P}{M} \mathbf{H}_k^H \mathbf{H}_k + \sigma^2 \mathbf{I}_{N_k}. \tag{6.12}$$

Given two arbitrary squared matrices $\mathbf{A}$, $\mathbf{B}$, we recall the folowing properties of the determinant: $\det(\mathbf{A}^{-1}) = \frac{1}{det(\mathbf{A})}$ and $\det(\mathbf{AB}) = \det(\mathbf{A})\det(\mathbf{B})$. Using these properties and the results obtained in (6.10) and (6.12), the expression for $C_k$ in (6.5) becomes

$$C_k = \log_2 \left| \mathbf{I}_{N_k} + \frac{P}{M} \mathbf{H}_k^H \mathbf{W}_k \mathbf{W}_k^H \mathbf{H}_k \left[ \frac{P}{M} \mathbf{H}_k^H \left( \mathbf{I}_M - \mathbf{W}_k \mathbf{W}_k^H \right) \mathbf{H}_k + \sigma^2 \mathbf{I}_{N_k} \right]^{-1} \right|. \tag{6.13}$$

Hence, $C_k$ is a function of $\mathbf{H}_k$ and the beamforming vectors for the $k$-th user, $\mathbf{W}_k$. Thus, due to the use of unitary beamforming, a user $k$ is able to compute $C_k$ without knowledge of the beamforming vectors intended to other users. In multiuser scenarios with limited feedback, this value can be used as scalar

feedback to exploit multiuser diversity through user scheduling at the base station. This expression can be considered an extension to multiple-antenna receivers of Metric II, presented in Chapter 4. In this work, single-antenna users feed back an estimated SINR value rather than a rate value, which is achieved when using unitary beamforming. However, scalar feedback design for multi-antenna receivers is beyond the scope of this thesis.

Note also that $P_{W_k} = \mathbf{W}_k\mathbf{W}_k^H$ is a projection matrix whose range is the subspace spanned by the columns of $\mathbf{W}_k$, and $P_{W_k}^{\perp} = \mathbf{I}_M - \mathbf{W}_k\mathbf{W}_k^H$ is the complementary projection. Thus, maximizing the contribution of the numerator to the determinant in (6.13) by appropriately setting $\mathbf{W}_k$ is equivalent to minimizing the contribution of the denominator to the determinant. Define the singular value decomposition $\mathbf{H}_k = \mathbf{U}_k\Lambda_k\mathbf{V}_k^H$. If $C_k$ was to be maximized without any constraints on the structure of $\mathbf{W}_k$, the solution would be given by setting $\mathbf{W}_k = \mathbf{V}_k(1:N_k)$, i.e., by matching the beamforming vectors to the $N_k$ input singular vectors associated with the $N_k$ largest singular values. However, in our case, the concatenated beamforming matrices $\mathbf{W}_k$ form a unitary matrix, which complicates the optimization problem presented in (6.4). Note also that, in the particular case of $N_k = M$, we have that $\mathbf{W}_k\mathbf{W}_k^H = \mathbf{I}_M$ and $C_k$ simply becomes the capacity of the MIMO channel without CSIT, and thus the design of a unitary beamforming matrix has no impact on the system performance.

In the remainder of this chapter, we focus our interest on single-antenna receivers. Besides being a case of particular interest in current cellular networks, a simple algorithm can be proposed to optimize the design of the corresponding linear beamforming matrix.

### 6.3.2 Single-antenna Receivers

In this case, the optimization criterion considered in our problem is sum rate maximization, constrained to using linear unitary beamforming at the transmitter. Hence, the optimization problem can be formulated as follows

$$\begin{aligned} &\max_{\mathbf{W}} \sum_{k=1}^{M} \log_2\left(1 + SINR_k\right) \\ &s.t. \quad \mathbf{W}^H\mathbf{W} = \mathbf{I}_M \end{aligned} \tag{6.14}$$

where $\log_2\left(1 + SINR_k\right)$ corresponds to $C_k$ for the particular case of $N_k = 1$. This optimization problem is rather difficult to solve using this formulation, since the problem is nonconvex and the constraints are nonlinear. The

problem can be reformulated by exploiting the particularities of the $SINR_k$ expression when unitary beamforming is used. Let $\rho_k$ be the alignment between the $k$-th user instantaneous normalized channel vector $\overline{\mathbf{h}}_k = \frac{\mathbf{h}_k}{\|\mathbf{h}_k\|}$ (channel direction) and the corresponding beamforming vector $\mathbf{w}_k$, defined as $\rho_k = \left|\overline{\mathbf{h}}_k^H \mathbf{w}_k\right|$. Using these definitions and particularizing the result obtained in (6.13) to the case of $N_k = 1$, we get

$$SINR_k = \frac{\|\mathbf{h}_k\|^2 \rho_k^2}{\|\mathbf{h}_k\|^2 (1-\rho_k^2) + \frac{M\sigma^2}{P}} \tag{6.15}$$

which is equivalent to the SINR scheduling metric described in (3.11). Define the vector $\boldsymbol{\rho} = [\rho_1\, \rho_2 \ldots \rho_M]$. Note that, when subtituting the $SINR_k$ expression shown in (6.15) into equation (6.14), the $k$-th term in the sum of logarithms becomes only a function of the variable $\rho_k$. The difficulty now lies in determining the feasible set of solutions for $\boldsymbol{\rho}$, i.e. the set of values for which a $\mathbf{W}$ matrix exists given that the user channels are known and fixed. This can be done by incorporating the geometrical structure of the problem into new constraints on $\boldsymbol{\rho}$, which is also a difficult task. Instead, in next section, we propose a simple method to iteratively improve $\boldsymbol{\rho}$, while ensuring its feasibility by algorithm construction.

Another way to simplify the constrained optimization problem in equation (6.14) is to transform it into an unconstrained problem. Define the initial matrix $\mathbf{W}^0$ as an arbitrary unitary matrix. Let $\mathbf{R}_{mn}$ be the Givens rotation matrix in the $(\mathbf{w}_m, \mathbf{w}_n)$-plane, which performs an orthogonal rotation of the $m$-th and $n$-th columns of a unitary matrix while keeping the others fixed, thus preserving unitarity. Assume without loss of generality $n > m$. The Givens rotation matrix in the $(\mathbf{w}_m, \mathbf{w}_n)$-plane is given by

$$\mathbf{R}_{mn}(\alpha,\delta) = \begin{bmatrix} 1 & \cdots & 0 & \cdots & 0 & \cdots & 0 \\ \vdots & \ddots & \vdots & & \vdots & & \vdots \\ 0 & \cdots & \cos\alpha & \cdots & \sin\alpha e^{j\delta} & \cdots & 0 \\ \vdots & & \vdots & \ddots & \vdots & & \vdots \\ 0 & \cdots & -\sin\alpha e^{-j\delta} & \cdots & \cos\alpha & \cdots & 0 \\ \vdots & & \vdots & & \vdots & \ddots & \vdots \\ 0 & \cdots & 0 & \cdots & 0 & \cdots & 1 \end{bmatrix} \tag{6.16}$$

where the non trivial entries appear at the intersections of $m$-th and $n$-th rows and columns. Hence, any unitary matrix $\mathbf{W}$ can be expressed using the

Table 6.1: Outline of the Unitary Beamforming Optimization Procedure

**Initialization**

- Initialize the UBF matrix $\mathbf{W}^0$

**$i$-th iteration step**, $i = 1, \ldots, N_{PR}$

- Select an index pair $\{m, n\}$ from $\mathcal{G}$
- Find optimal rotation parameters for the $(\mathbf{w}_m, \mathbf{w}_n)$-plane
$$\{\alpha^*, \delta^*\} = \arg\min_{\alpha,\delta} F_{mn}(\alpha, \delta)$$
- Update UBF matrix $\mathbf{W}^i = \mathbf{W}^{i-1}\mathbf{R}_{mn}(\alpha^*, \delta^*)$

following parameterization

$$\mathbf{W} = \mathbf{W}^0 \prod_{m=1}^{M} \prod_{n=m+1}^{M} \mathbf{R}_{mn} \tag{6.17}$$

up to a global $e^{j\theta}$ factor. Note that such global factor has no importance for transmission purposes. Each rotation matrix $\mathbf{R}_{mn}$ in (6.17) is function of 2 rotation parameters, $\alpha$ and $\delta$. Hence, by imposing this structure, the optimization problem in equation (6.14) becomes unconstrained and it boils down to finding the optimal $2\binom{M}{2}$ rotation parameters of the corresponding $\binom{M}{2}$ rotation matrices. Since the resulting $\rho_k$ values, $k = 1, \ldots, M$, are complicated non-linear functions of the rotation parameters, we propose an iterative algorithm to compute the optimal rotation matrix for a given plane, iterating along different planes until convergence is reached. Hence, the algorithm we propose is based on a divide-and-conquer type of approach. The matrix $\mathbf{W}$ is divided into smaller instances that are solved recursively in order to provide a solution to the optimization problem in (6.14). However, convergence to a global optimum can not be ensured for an arbitrary channel.

## 6.4 Algorithm Description

The proposed unitary beamformer is designed on the basis of the available user channels $\mathbf{h}_k, k = 1, \ldots, M$ and balances the amount of power and interference received by each user. Given an initial unitary beamforming matrix $\mathbf{W}^0$ available at the transmitter, we propose an iterative algorithm which

consists of rotating the beamforming matrix by performing successive optimization of Givens rotations until convergence is reached. At the $i$-th iteration, a refined unitary beamforming matrix is computed by rotating the matrix $\mathbf{W}^{i-1}$ - computed at the previous iteration - in the plane defined by the complex vectors $(\mathbf{w}_m, \mathbf{w}_n)$, performing right multiplication with the rotation matrix defined in equation (6.16). For each plane rotation, the optimal $\alpha^*$ and $\delta^*$ rotation parameters are found. Let $\mathcal{G}$ be the set of all possible index pairs among the complete index set $\{1, \ldots, M\}$, in which each $\{m, n\}$ index pair satisfies $n > m$. Define $N_{PR}$ as the total number of plane rotations performed by the proposed approach. An outline of the proposed algorithm is provided in Table 6.1.

It can be seen from the structure of the matrix in (6.16) that rotation in the $(\mathbf{w}_m, \mathbf{w}_n)$-plane does not change the directions of the remaining beamforming vectors. Equivalently, since $SINR_k$ is only function of $\rho_k = \left|\overline{\mathbf{h}}_k^H \mathbf{w}_k\right|$, a rotation in the $(\mathbf{w}_m, \mathbf{w}_n)$-plane only modifies $SINR_m$ and $SINR_n$. Hence, the optimal rotation parameters are found by solving the following optimization problem

$$\{\alpha^*, \delta^*\} = \arg\max_{\alpha,\delta} \left\{ \log_2 \left( 1 + \frac{\|\mathbf{h}_m\|^2 \rho_m^2(\alpha,\delta)}{\|\mathbf{h}_m\|^2 (1-\rho_m^2(\alpha,\delta)) + \frac{M\sigma^2}{P}} \right) \right.$$
$$\left. + \log_2 \left( 1 + \frac{\|\mathbf{h}_n\|^2 \rho_n^2(\alpha,\delta)}{\|\mathbf{h}_n\|^2 (1-\rho_n^2(\alpha,\delta)) + \frac{M\sigma^2}{P}} \right) \right\} \tag{6.18}$$

where $\rho_m(\alpha,\delta), \rho_n(\alpha,\delta)$ are the modified alignments between channels and beamfoming vectors after rotation, given by

$$\rho_m(\alpha,\delta) = \left|\overline{\mathbf{h}}_m^H \left(\mathbf{w}_m \cos\alpha - \mathbf{w}_n \sin\alpha e^{-j\delta}\right)\right| \tag{6.19}$$
$$\rho_n(\alpha,\delta) = \left|\overline{\mathbf{h}}_n^H \left(\mathbf{w}_m \sin\alpha e^{j\delta} + \mathbf{w}_n \cos\alpha\right)\right|.$$

Defining the following variables

$$\begin{aligned} r_{mm} &= \left|\overline{\mathbf{h}}_m^H \mathbf{w}_m\right| & r_{mn} &= \left|\overline{\mathbf{h}}_m^H \mathbf{w}_n\right| \\ r_{nm} &= \left|\overline{\mathbf{h}}_n^H \mathbf{w}_m\right| & r_{nn} &= \left|\overline{\mathbf{h}}_n^H \mathbf{w}_n\right| \\ \Delta_{mn} &= \angle\overline{\mathbf{h}}_m^H \mathbf{w}_m - \angle\overline{\mathbf{h}}_m^H \mathbf{w}_n & \Delta_{nm} &= \angle\overline{\mathbf{h}}_n^H \mathbf{w}_n - \angle\overline{\mathbf{h}}_n^H \mathbf{w}_m \end{aligned} \tag{6.20}$$

we have that

$$\rho_m^2(\alpha,\delta) = r_{mm}^2 \cos^2\alpha + r_{mn}^2 \sin^2\alpha - r_{mm} r_{mn} \cos(\Delta_{mn}+\delta) \sin 2\alpha$$

$$\rho_n^2(\alpha,\delta) = r_{nm}^2 \sin^2\alpha + r_{nn}^2 \cos^2\alpha + r_{nm} r_{nn} \cos(\delta-\Delta_{nm}) \sin 2\alpha. \tag{6.21}$$

Define the parameter $\beta_k = \frac{M\sigma^2}{P\|\mathbf{h}_k\|^2}, k = m, n$. Since the logarithm is a monotonically increasing function, the optimization problem in equation (6.18) can be transformed into

$$\{\alpha^*, \delta^*\} = \arg\min_{\alpha,\delta} F_{mn}(\alpha,\delta) \tag{6.22}$$

where the function $F_{mn}$ is defined as follows

$$F_{mn}(\alpha,\delta) = \left(1 - \rho_m^2(\alpha,\delta) + \beta_m\right)\left(1 - \rho_n^2(\alpha,\delta) + \beta_n\right). \tag{6.23}$$

The solution is found by equating the gradient of $F_{mn}$ to zero

$$\frac{\partial F_{mn}(\alpha,\delta)}{\partial \alpha} = 0 \tag{6.24}$$

$$\frac{\partial F_{mn}(\alpha,\delta)}{\partial \delta} = 0 \tag{6.25}$$

In order to solve the above equations, we introduce the change of variable $t = \tan\alpha$ to solve equation (6.24) and $s = \tan\delta/2$ to solve equation (6.25). After some algebraic manipulations the problem is reduced to finding the roots of polynomials of the form

$$P_\alpha(t) = f_4 t^4 + f_3 t^3 + f_2 t^2 + f_1 t + f_0 \tag{6.26}$$

$$P_\delta(s) = g_4 s^4 + g_3 s^3 + g_2 s^2 + g_1 s + g_0 \tag{6.27}$$

where $f_i, g_i, i = 0, \ldots, 4$ are real coefficients involving simple arithmetic and trigonometric operations, defined in Appendix 6.A. The roots of these 4-th degree polynomials can be found by solving the respective quartic equations, for which closed form solutions exist [92]. Once the real roots are found, we invert the changes of variable introduced. The roots of $P_\alpha$ correspond to the extremes of the function $F_{mn}(\alpha,\delta)$ for fixed $\delta$, while those of $P_\delta$ are the extremes of $F_{mn}(\alpha,\delta)$ for fixed $\alpha$. Since up to 4 real roots may be found, the function $F_{mn}(\alpha,\delta)$ needs to be evaluated in the obtained roots in order to find the minimizing value $\alpha^*$. An equivalent operation is performed for obtaining $\delta^*$. Since computing $\alpha^*$ requires a constant value for $\delta$ and

computing $\delta^*$ requires a constant value for $\alpha$, the optimal values are found iteratively. Hence, $\alpha^*$ is computed initially by considering a certain initial value for $\delta$ (e.g. $\delta = 0$) and the resulting $\alpha^*$ is kept constant for computation of $\delta^*$. This operation is iterated $I_R$ times until convergence, which in practice occurs after 1 or 2 iterations.

Hence, although the unconstrained optimization problem in (6.18) is non-convex, it can be solved by finding the roots of the polynomials $P_\alpha$ and $P_\delta$, selecting among these roots the maximizing values $\alpha^*$ and $\delta^*$.

### 6.4.1 Practical Considerations

Although closed form solutions exist for quartic equations, fast converging algorithms can be applied involving much lower complexity. Since only real roots are sought, the quotient-difference (QD) algorithm can be used to identify the roots followed by a fast converging algorithm like Newton-Raphson (NR) [93]. The initial unitary beamforming matrix $\mathbf{W}^0$ can be generated randomly, although more complex initializations may yield faster convergence. For instance, $\mathbf{W}^0$ can be constrained to have one of its vectors well aligned with the user channel that has the largest channel norm, as proposed in Section 3.5 as a suboptimal beamforming approach. In practice, this can be implemented by storing a number of unitary matrices (codebook), selecting the most appropriate one for initialization at each slot. For simplicity, in the remainder of the chapter, we consider that the proposed algorithm is initialized by choosing $\mathbf{W}^0$ randomly unless stated otherwise. Note that the proposed algorithm provides computational flexibility, since the number of plane rotations $N_{PR}$ can be modified. In the most general case, all possible combinations of plane rotations should be performed, i.e. $\binom{M}{2}$ combinations. Moreover, the order in which these plane rotations are performed has an impact on the convergence. Hence, the total number of plane rotations can be expressed as $N_{PR} = I_T\binom{M}{2}$, where $I_T$ is a natural number.

## 6.5 Convergence

When optimizing the rotation along the $(\mathbf{w}_m, \mathbf{w}_n)$-plane, the sum of the rates provided by the $m$-th and $n$-th beamforming vectors is maximized with respect to the rotation parameters. Thus, defining $SR_{mn} = \log_2(1 + SINR_m) + \log_2(1 + SINR_n)$, at each plane rotation optimization we have

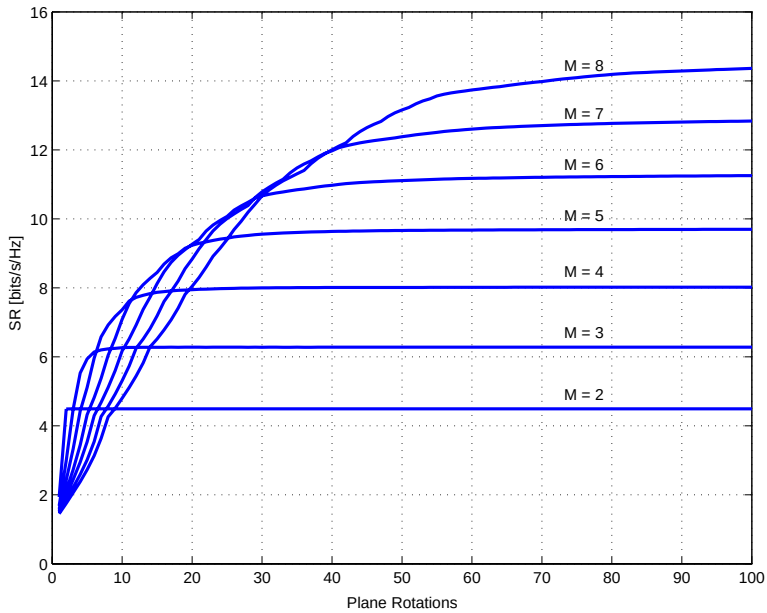


Figure 6.1: Sum rate as a function of the number of plane rotations (algorithm iterations) for different number of transmit antennas, $K = M$ users and average SNR = 10 dB.

that $SR_{mn}(\alpha^*, \delta^*) \geq SR_{m,n}(\alpha, \delta)$. In addition, as discussed in the previous section, the SINR values associated to the remaining beamforming vectors do not change. Hence, at each iteration the resulting sum rate does not decrease, i.e. $SR(\mathbf{W}^i) \geq SR(\mathbf{W}^{i-1})$. On the other hand, since the transmitted power is finite, the sum rate - which is the objective function that the algorithm tries to maximize - is bounded from above. Thus, local convergence is guaranteed in the proposed optimization problem. In practice, given arbitrary channel realizations, simulations have shown that the proposed algorithm always converges to the same beamforming matrix regardless of the algorithm initialization. Thus, experiments seem to indicate that the proposed algorithm converges to a global optimum. The convergence behavior of the proposed iterative algorithm is exemplified in Figure 6.1 for different number of transmit antennas. In this simulation, Givens rotations are performed in all possible $(\mathbf{w}_m, \mathbf{w}_n)$-planes, and a large number of plane rotations $N_{PR} \rightarrow \infty$ is considered.

In order to better illustrate the convergence speed of the proposed algo-

rithm for different number of transmit antennas, we study a simple case in the remainder of this section for which the optimal solution is known. Let $\mathbf{H}$ be the concatenation of the user channels $\mathbf{H} = [\mathbf{h}_1 \dots \mathbf{h}_M]^H$. Consider a simple channel model in which the concatenated channel can be factorized as $\mathbf{H} = \mathbf{\Lambda}\mathbf{V}^H$, where $\mathbf{\Lambda}$ is a diagonal matrix with real entries ordered in descending order and $\mathbf{V}$ is a unitary matrix. This is equivalent to a point-to-point MIMO channel $\overline{\mathbf{H}}$ in which, given its singular value decomposition $\overline{\mathbf{H}} = \mathbf{U}\mathbf{\Lambda}\mathbf{V}^H$, the receiver filters the received signal with the matrix $\mathbf{U}^H$. If perfect channel state information is available at the transmitter and equal power allocation per beam is assumed, the optimal linear beamformer is known to be $\mathbf{W} = \mathbf{V}$, yielding $M$ virtual parallel channels [4], [5]. In order to evaluate the convergence of the proposed algorithm to the optimal solution, we compute the following Frobenius distance at each iteration

$$d(\mathbf{W}, \mathbf{V}) = \left\| \mathbf{W}^H \mathbf{V} - \mathbf{I} \right\|_F . \tag{6.28}$$

Figure 6.2 shows the convergence behavior of the proposed algorithm for different number of transmit antennas. In this scenario, the proposed algorithm converges iteratively to the optimal solution. Note that for each value of $M$ there are 2 differentiated regions with different convergence speed. The 1-st part converges faster, which corresponds to the 1-st $\binom{M}{2}$ iterations while the 2-nd part converges slower. This is due to the fact that the order in which plane rotations are performed matters, becoming more important as the size of the unitary beamforming matrix increases.

## 6.6 Complexity Analysis

In this section, the complexity of the proposed algorithm is studied in terms of the number of real arithmetic operations (ops) performed. Assuming QD and NR iterative root-finding algorithms are used, with $I_{QD}$ and $I_{NR}$ iterations respectively, the average complexity of the proposed algorithm is

$$\mathcal{C}_{UBF} = N_{PR} \{52M + 15 + I_R[28I_{QD} + 32I_{NR} + 7(\overline{r}_\alpha + \overline{r}_\delta) + 69]\}$$

where $\overline{r}_\alpha$ and $\overline{r}_\delta$ are the average number of real roots in $P_\alpha$ and $P_\delta$ , respectively.

In order to compare UBF with commonly applied beamforming techniques, we provide a complexity analysis of ZF and MMSE beamforming (refer to Section 3.3 for an overview). In our complexity analysis, we consider

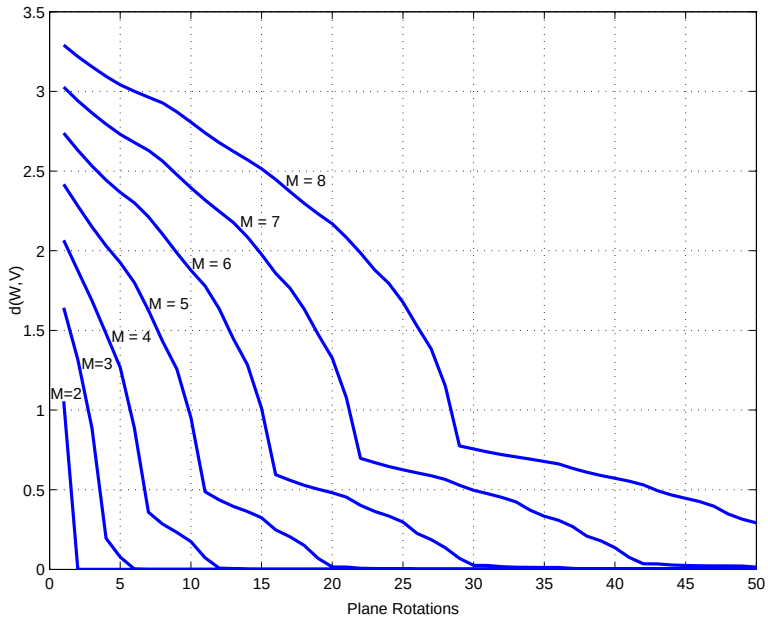


Figure 6.2: Convergence of unitary beamforming matrix for different number of transmit antennas.

that channel inversions are computed by using Lower-Upper (LU) matrix factorizations. The resulting complexities are

$$\mathcal{C}_{ZF} = \frac{80}{3}M^3 - 4M^2 - \frac{11}{3}M - 1 \tag{6.29}$$

$$\mathcal{C}_{MMSE} = \frac{104}{3}M^3 - 6M^2 - \frac{8}{3}M - 1 \tag{6.30}$$

which implies that computation of ZF and MMSE beamformers has $O(M^3)$ complexity order.

Note that the complexity order of the proposed algorithm strongly depends on the number of plane rotations $N_{PR}$. If $\binom{M}{2}$ Givens rotations are performed, then the complexity order becomes $O(M^3)$, equivalent to the complexity order of ZF and MMSE beamforming as discussed. However, thanks to the flexibility of the proposed approach, the algorithmic complexity can be reduced by considering a reduced number of plane rotations.

## 6.7 Performance Evaluation

In this section, we evaluate the performance of the proposed unitary beamforming approach and compare it to other existing approaches. The proposed algorithm is initialized by choosing $\mathbf{W}^0$ randomly. Plane rotations are performed in all possible combinations, resulting in $N_{PR} = I_T\binom{M}{2}$ rotations, with $I_T = 3$. In the simulated scenarios, the algorithm approximately converges for this choice. The MATLAB function *roots* is used to compute the polynomial roots, which involves computing the eigenvalues of the companion matrix for each polynomial. In Subsections 6.7.1 and 6.7.2, a system with $K = M$ is studied, hence assuming a given set of $M$ users has been scheduled for transmission. While in 6.7.1 perfect CSIT is assumed to be available, a system with imperfect CSIT is considered in 6.7.2. In the last subsection, a system with multiuser scheduling is considered, comparing the proposed approach to limited feedback techniques based on unitary beamforming.

### 6.7.1 Case $K = M$, Perfect CSIT

The performances of the proposed unitary beamforming technique, ZF beamforming and MMSE beamforming are compared in a system in which perfect CSIT is available, given a set of $K = M$ users scheduled for transmission. In addition, the performance of a system that performs TDMA is also plotted for reference, selecting the user with largest channel norm out of $M$ available users.

Figure 6.3 shows a performance comparison in terms of sum rate versus number of transmit antennas $M$, for SNR = 10 dB. As expected, the MMSE solution provides linear sum-rate growth with the number of transmit antennas, while ZF beamforming flattens out [59]. The proposed algorithm also provides linear growth with $M$, performing close to MMSE beamforming.

In Figure 6.4, we compare the sum rate as function of the average SNR in a system with $M = 8$ transmit antennas. As the SNR increases, the MMSE solution converges to ZF, removing all multi-user interference. The proposed technique provides considerable gains over ZF in the regular SNR range, performing close to the MMSE solution. On the other hand, the proposed algorithm does not completely eliminate interference, since instead it balances the useful power and undesired interference in the SINR expression. Suboptimal techniques based on unitary beamforming have shown to become interference limited at high SNR, thus providing zero multiplexing gain [2],

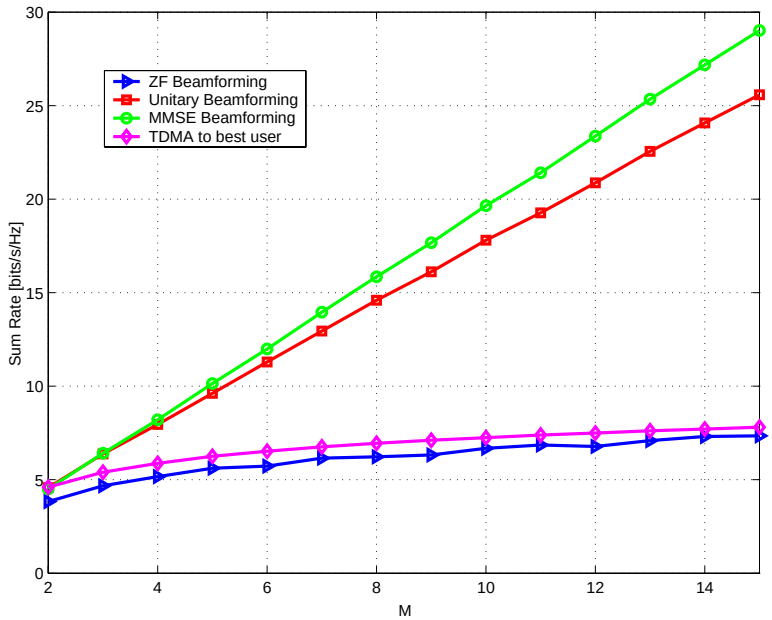


Figure 6.3: Sum rate as a function of the number of antennas $M$ for $K = M$ users and average SNR = 10 dB.

[3]. The multiplexing gain is defined as follows

$$m = \lim_{P \to \infty} \frac{\sum_{k=1}^{M} \mathbb{E}\left[\log_2\left(1 + SINR_k\right)\right]}{log_2(P)}. \tag{6.31}$$

However, as it can be observed from Figure 6.4, the multiplexing gain of the proposed scheme converges to the one of TDMA (same slope). A particular case of the proposed approach corresponds to the case in which one of the unitary beamforming vectors is aligned with the channel vector that has largest norm. In that case, at least one of the users does not see any interference from the other users and hence at least $m = 1$ is achieved. Thus, for the proposed approach we obtain

$$m^{UBF} \geq \lim_{P \to \infty} \frac{\mathbb{E}\left[\log_2\left(1 + \frac{P}{M\sigma^2} \max_{i \in 1,\ldots,M} \|\mathbf{h}_i\|^2\right)\right]}{log_2(P)} + \frac{\sum_{k=1, k \neq i}^{M} \mathbb{E}\left[\log_2\left(1 + SINR_k\right)\right]}{log_2(P)} \geq 1 \tag{6.32}$$

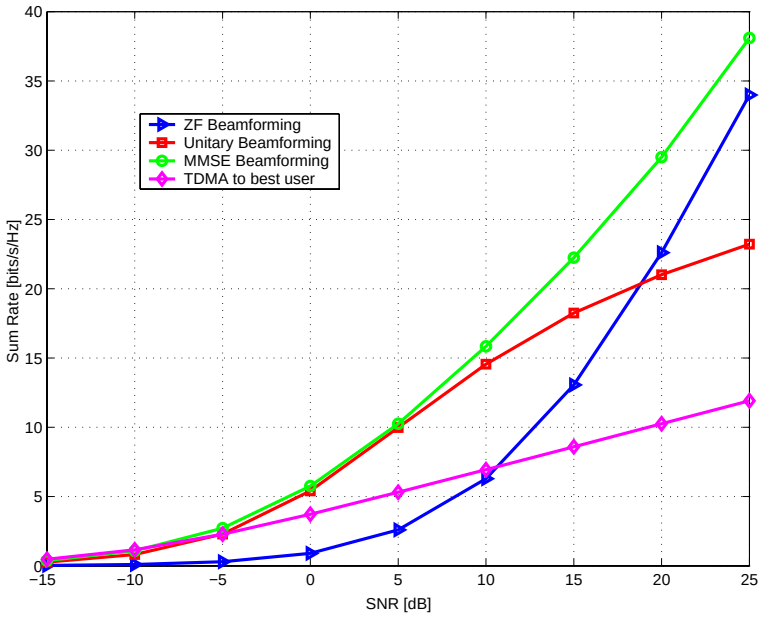


Figure 6.4: Sum rate as a function of the average SNR for $M = 8$ transmit antennas and $K = M$ users.

where the first term in the summation corresponds to aligning a unit-norm beamforming vector along the channel direction of the user with largest channel gain and the second term corresponds to the remaining $M-1$ beamforming vectors. The second inequality in the above equation follows from the fact that if none of the $M-1$ beamforming vectors in the second term is aligned with the remaining $M-1$ channels, they exhibit zero multiplexing gain.

### 6.7.2 Case $K = M$, Imperfect CSIT

The impact of imperfect channel knowledge at the transmitter in a system with $K = M$ users is investigated. The beamforming matrices are computed on the basis of noisy channel estimates, modeled as described in equation (6.3), which produces a performance degradation in terms of system sum rate. Figure 6.5 shows a sum-rate comparison between the proposed approach, ZF beamforming, MMSE beamforming and TDMA as a function of the variance of the channel estimation error, for $M = 4, 8$ antennas and average SNR of 10

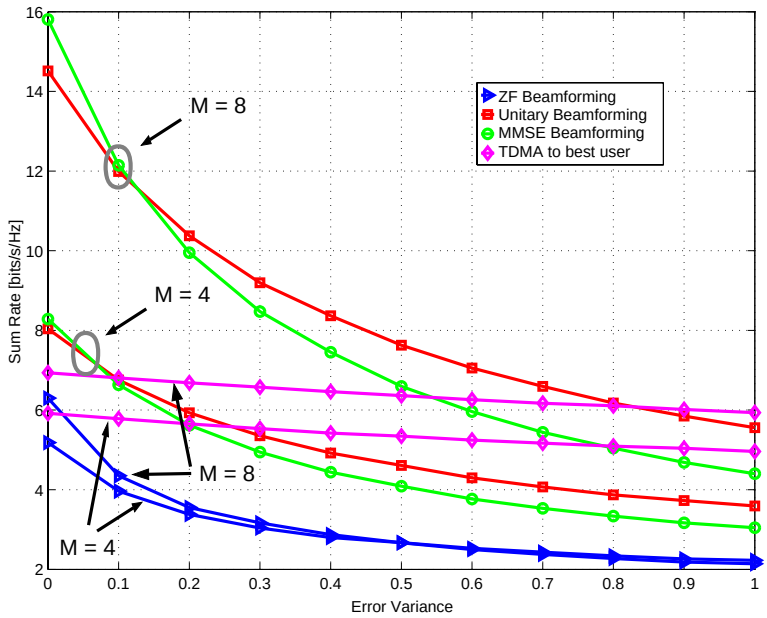


Figure 6.5: Sum rate as a function of the channel estimation error variance for $M = 4, 8$ transmit antennas, $K = M$ users and average SNR = 10 dB.

dB. The proposed unitary beamforming approach proves to be more robust to CSIT errors than ZF or MMSE beamforming. Indeed, a small error variance suffices for unitary beamforming to outperform MMSE beamforming, even for large number of transmit antennas. However, TDMA provides higher rates in scenarios with reduced number of transmit antennas and very low quality of CSIT.

### 6.7.3 Case $K \geq M$, Limited Feedback

The proposed technique is evaluated in a MIMO broadcast channel where limited feedback is available from the user terminals to the base station. Most existing techniques with joint linear beamforming and multiuser scheduling designed for limited feedback scenarios are based on simple beamforming designs. While the design of feedback measures is carefully taken into account, suboptimal beamforming techniques are often considered, such as the well known RBF [2] and LF-OSDMA [3] techniques. In these techniques, the base station has precise SINR information from the users, but on the

other hand, random linear beamformers are used. In the remainder of this section, we highlight the importance of beamforming design in limited feedback scenarios. By exploiting the robustness to channel estimation errors exhibited by the proposed approach, we show that optimization of the linear beamformers is crucial in MIMO broadcast channels with imperfect CSIT.

A scenario with $K \geq M$ is considered and thus the need for multiuser scheduling arises. For simplicity, exhaustive user search is performed, i.e. the base station evaluates the estimated sum rate of all possible user sets with cardinality $M$ and selects the one that provides higher estimated sum rate. Thus, the user set scheduled for transmission is found as described in (5.3), based on the SINR estimates computed at the base station.

In the proposed scheme, each user quantizes its channel vector based on a quantization codebook $\mathcal{V}$ that is common to all users in the system. The vector quantizer maps the user channel to the codeword in $\mathcal{V}$ with the smallest Euclidean distance. A random vector quantization (RVQ) codebook is considered, complemented with simple codeword pruning as described in [84, pp. 359]. Pruning consists of starting with an initial training set of candidate codewords (randomly generated), and selectively eliminating (pruning) training vectors until obtaining a final set of $2^B$ vectors. The codebook is generated recursively, adding a new codeword to the codebook at each step. When a codeword is added, it must satisfy that the distortion measure - in our case given by the Euclidean distance - between the newly added codeword and the nearest neighbor in the codebook is greater than some threshold. In our case, this threshold has been set empirically in order to provide good performances.

The limited feedback approaches we consider for comparison are RBF and LF-OSDMA. As discussed in the previous chapter, in LF-OSDMA a codebook with $N$ random unitary matrices is generated (each with $M$ unit-norm vectors), known both to the base station and mobile users. In the original LF-OSDMA scheme proposed in [3], the users feed back a codeword index using $B = log_2(MN)$ bits together with the expected SINR, which in the case of unitary beamforming can be precisely determined without knowledge of the beamforming vectors intended to other users. In the scenario under study, the data rate on the feedback link is limited to $B = 10$ bits/transmission. In order to make a fair comparison between the schemes, the SINR feedback of the LF-OSDMA algorithm is also quantized. Thus, the LF-OSDMA algorithm has to share the available $B$ bits between the CDI, i.e., the index of the preferred beamforming vector, and the CQI, i.e., the SINR of the preferred

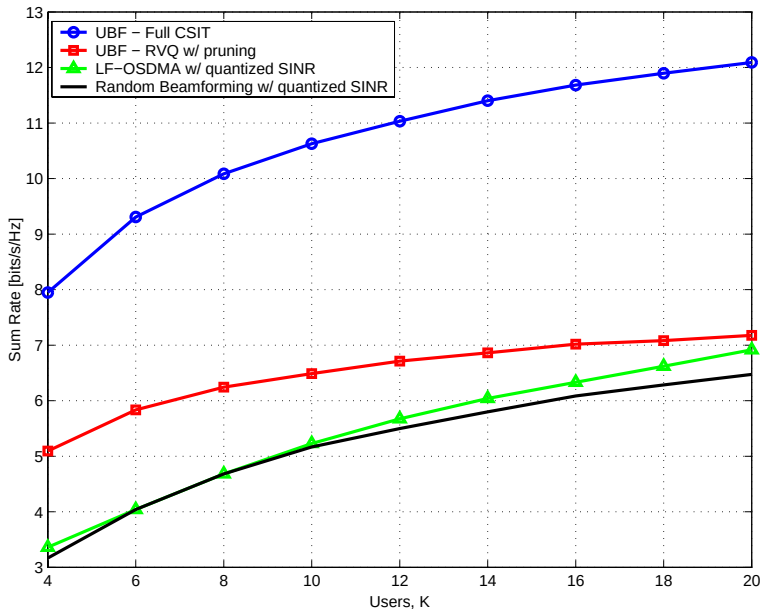


Figure 6.6: Sum rate as a function of the number of users in a system with joint beamforming and user scheduling, $M = 4$ transmit antennas, SNR = 10 dB, and $B = 10$ feedback bits.

beamforming vector. This setting is equivalent to the finite sum rate feedback model presented in Section 4.7, where a tradeoff between multiuser diversity and multiplexing gain has been presented. In our simulations, we simulate the performance of all possible CDI/CQI bit allocations, and finally select the allocation that results in the highest sum rate. The codebook to quantize the scalar CQI is designed with the generalized Lloyd algorithm [84], using the mean square error as distortion function. In the case of RBF, the amount of bits for CDI feedback is given by $\log_2 M$, since only a single beamforming matrix is generated at each time slot. The remaining bits are used for SINR quantization, following the same quantization criterion as for LF-OSDMA.

Figure 6.6 depicts the performance for different numbers of users with a fixed SNR of 10 dB, in a system with $M = 4$ transmit antennas and $B = 10$ bits available for feedback. The performance of the proposed UBF approach with perfect CSIT is also provided for comparison. The proposed approach combined with simple RVQ and pruning outperforms RBF and LF-OSDMA, especially in systems with reduced number of users, providing

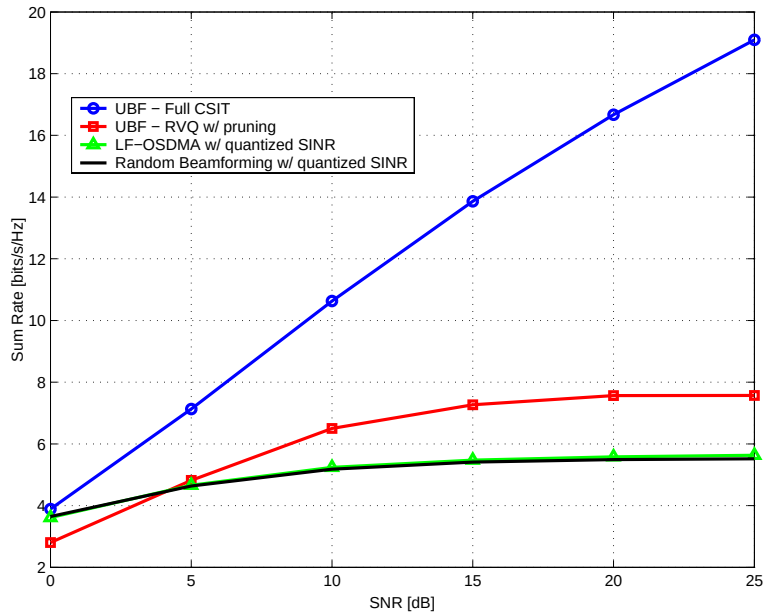


Figure 6.7: Sum rate as a function of the average SNR in a system with joint beamforming and user scheduling, $M = 4$ transmit antennas, $K = 10$ users, and $B = 10$ feedback bits.

sum-rate gains over 1.5 bps/Hz. Note that the performance of RBF, which was shown to achieve the optimal capacity scaling in [2], is a pessimistic lower bound on the performance of LF-OSDMA. As the number of users increases, the simplicity of the quantization codebook used in the proposed unitary beamforming approach does not allow to capture all multiuser diversity gain and the sum rate curve flattens out. On the other hand, LF-OSDMA exhibits optimal sum-rate growth in the simulated range, thanks to an optimal bit allocation for CDI/CQI information.

In Figure 6.7, a sum-rate comparison as function of the average SNR is shown in a system with $M = 4$ transmit antennas, $K = 10$ users and $B = 10$ bits. As expected, the limited feedback approaches become interference limited at high SNR. In the simulated scenario, the proposed technique provides performance gains of up 2-bps/Hz over RBF and LF-OSDMA for a given SNR. Note that the simulation parameters here used reflect realistic scenarios of practical importance, often encountered in indoor wireless systems.

## 6.8 Conclusions

An iterative optimization method for unitary beamforming in MIMO broadcast channels has been proposed, based on successive optimization of Givens rotations. In a scenario with perfect CSIT and for practical average SNR values, the proposed technique provides higher sum rates than ZF beamforming and performs close to MMSE beamforming, achieving linear sum-rate growth with the number of transmit antennas. The proposed unitary beamforming approach exhibits robustness to channel estimation errors, providing better sum rates than ZF beamforming and even MMSE beamforming as the variance of the estimation error increases. In addition, the proposed technique has been evaluated in scenarios with multiuser scheduling and limited feedback. As simulations have shown, our approach provides gains when compared to other existing techniques based on unitary beamforming and the same amount of feedback. A simple vector quantization technique has been used, based on RVQ with pruning. Hence, our work highlights the importance of linear beamforming optimization in limited feedback scenarios. While the random beamforming technique introduced in [2] enables perfect SINR knowledge of all users at the base station, the generation of the beamforming vectors is clearly suboptimal. Instead, as we have shown in this chapter, the system performance can be improved by performing simpler feedback design through direct channel vector quantization and optimization of the linear beamformers.

# APPENDIX

## 6.A Computation of Polynomial Coefficients

This appendix describes a procedure to obtain the coefficients of the polynomials $P_\alpha$ and $P_\delta$ of equations (6.26) and (6.27), respectively. Although the procedure to obtain these coefficients can be described in different ways, here we present it in a simple and sequential fashion for straightforward software implementation. For each plane rotation, the auxiliary variables defined in Table 6.2 are computed and used for the computation of the coefficients of both $P_\alpha$ and $P_\delta$. These auxiliary variables are functions of $r_{mm}$, $r_{mn}$, $r_{nm}$, $r_{nn}$, $\Delta_{mn}$, $\Delta_{nm}$, which are given in equation (6.20), and the parameter $\beta_k$.

**Computation of the polynomial coefficients of $P_\alpha$**

The coefficients of $P_\alpha$ are functions of the rotation parameter $\delta$. For clarity of exposition, the following functions are defined

$$\begin{aligned} \phi_1(\delta) &= d_1 \cos(\Delta_{mn} + \delta) \\ \phi_2(\delta) &= -d_2 \cos(\delta - \Delta_{nm}) \end{aligned} \tag{6.33}$$

The coefficients of the polynomial $P_\alpha$ are given by

$$\begin{aligned} f_4 &= -2\phi_1(\delta)(e_3 - e_4) - 2\phi_2(\delta)(e_2 - e_5) \\ f_3 &= -2\phi_1(\delta)\phi_2(\delta) + e_1 - e_6 \\ f_2 &= -12\left[\phi_1(\delta)e_4 + \phi_2(\delta)e_5\right] \\ f_1 &= 2\phi_1(\delta)\phi_2(\delta) - e_1 - e_6 \\ f_0 &= 2\phi_1(\delta)(e_3 + e_4) + 2\phi_2(\delta)(e_2 + e_5) \end{aligned} \tag{6.34}$$

**Computation of the polynomial coefficients of $P_\delta$**

The coefficients of $P_\delta$ are functions of the rotation parameter $\alpha$. The following functions are defined

$$\begin{aligned} \varphi_1(\alpha) &= e_2 \sin 2\alpha + \tfrac{e_5 \sin 4\alpha}{2} \\ \varphi_2(\alpha) &= e_3 \sin 2\alpha + \tfrac{e_4 \sin 4\alpha}{2} \\ \varphi_3(\alpha) &= \tfrac{1-\cos 4\alpha}{4} \end{aligned} \tag{6.35}$$

Table 6.2: Auxiliary Variables for the Computation of Polynomial Coefficients

| | |
|---|---|
| $b_{mn} = -(r_{mm}^2 + r_{mn}^2)$ | $b_{nm} = -(r_{nn}^2 + r_{nm}^2)$ |
| $c_{mn} = -(r_{mm}^2 - r_{mn}^2)$ | $c_{nm} = -(r_{nn}^2 - r_{nm}^2)$ |
| $d_1 = 2r_{mm}r_{mn}$ | $a_m = 1 + \beta_m$ |
| $d_2 = 2r_{nm}r_{nn}$ | $a_n = 1 + \beta_n$ |
| $d_3 = -2d_1d_2\cos(\Delta_{nm} - \Delta_{mn})$ | $e_1 = 2c_{mn}c_{nm}$ |
| $d_4 = -\frac{d_1d_2}{2}\sin(\Delta_{nm} - \Delta_{mn})$ | $e_2 = \frac{a_m}{2} + \frac{b_{mn}}{4}$ |
| $d_5 = 2d_1\cos\Delta_{mn}$ | $e_3 = \frac{a_n}{2} + \frac{b_{nm}}{4}$ |
| $d_6 = d_1\sin\Delta_{mn}$ | $e_4 = \frac{c_{nm}}{4}$ |
| $d_7 = 2d_2\cos\Delta_{nm}$ | $e_5 = \frac{c_{mn}}{4}$ |
| $d_8 = -d_2\sin\Delta_{nm}$ | $e_6 = 4(c_{nm}e_2 + c_{mn}e_3)$ |

The coefficients of the polynomial $P_\delta$ are given by

$$\begin{aligned}
g_4 &= -d_8\varphi_1(\alpha) + d_6\varphi_2(\alpha) + d_4\varphi_3(\alpha) \\
g_3 &= d_7\varphi_1(\alpha) - d_5\varphi_2(\alpha) + d_3\varphi_3(\alpha) \\
g_2 &= -6d_4\varphi_3(\alpha) \\
g_1 &= d_7\varphi_1(\alpha) - d_5\varphi_2(\alpha) - d_3\varphi_3(\alpha) \\
g_0 &= d_8\varphi_1(\alpha) - d_6\varphi_2(\alpha) + d_4\varphi_3(\alpha)
\end{aligned} \tag{6.36}$$

# General Conclusion

In this thesis, we have focused on the performance optimization of MIMO wireless systems with partial CSIT. On the one hand, the problem of obtaining and designing partial CSIT in single user and multiuser scenarios has been investigated, providing insights into the most relevant sources of information that are needed at the transmitter side. On the other hand, this thesis has addressed the issue of how to efficiently exploit the available CSIT in order to enhance the system performance.

In the first part of this thesis, point-to-point MIMO channels have been considered, highlighting the importance of statistical CSIT for the design of linear precoding techniques. As we have shown, the error rate of an ST coded MIMO system can be significantly improved through a linear precoder that exploits mean and covariance information. In order to provide a clear intuition of how mean and covariance must be combined to achieve good performances, different MIMO channel models have been considered.

The second part of this thesis has been devoted to sum-rate performance optimization in MIMO broadcast channels with limited feedback. We have mainly considered systems in which a base station communicates with a set of single-antenna users by means of SDMA. With the aim of designing practical low-complexity techniques, we have focused on systems with joint linear beamforming and multiuser scheduling with limited feedback. In our work, we have shown the importance of cross-layer design at PHY-MAC level, optimizing the following elements of a multiuser MIMO downlink: linear beamforming techniques, scheduling algorithms, feedback strategies and feedback quantization techniques.

In Chapter 3, the design challenges of MIMO systems with joint linear beamforming and multiuser scheduling have been presented. In such systems, transmission techniques and user selection algorithms with reasonable complexity are desired. In order to illustrate this fact, low-complexity solutions

have been proposed both in scenarios with full and partial CSIT. In the full CSIT case, a multiuser scheduling algorithm for systems with orthonormal beamforming vectors has been proposed. In a spatially correlated MIMO setting with limited feedback, the importance of combining statistical and instantaneous information has been highlighted through a low-complexity approach. A bound on the multiuser interference of practical relevance has been proposed, which can be used for designing multiuser scheduling metrics.

In Chapter 4, a design framework for scalar feedback design in MIMO broadcast channels has been introduced. A scenario with separate feedback for CDI and CQI has been considered. In such systems, the users need to estimate the amount of multiuser interference, which is a difficult task since the users can not cooperate. This information is embedded in the proposed scalar feedback as channel quality information for the purpose of multiuser scheduling, together with other measures of interest, such as the channel gain, the quantization error, the orthogonality constraints between beamformers and the number of active beams. A comparative study between SDMA and TDMA has been provided in different asymptotic regimes, showing the cases in which SDMA becomes more beneficial than TDMA in terms of sum-rate performance and viceversa. Particularly, SDMA outperforms TDMA as the number of users becomes large. TDMA provides better rates than SDMA in the high SNR regime (interference-limited region). Moreover, the importance of optimizing the orthogonality factor in the low SNR regime has been highlighted. In addition, a more realistic system has been considered in which each user has a sum rate feedback constraint. In this scenario, the existing tradeoff between multiuser diversity and multiplexing gain has been identified, arising from the fact that the available feedback bits need to be shared for CDI and CQI quantization. The problem of optimizing the feedback balance has been addressed, revealing an interesting interplay between the number of users, the average SNR and the number of feedback bits. While most bits should be allocated to CDI in systems with low number of users, it becomes more beneficial to allocate bits to CQI for increasing number of users. On the other hand, as the average SNR increases, more bits should be allocated to channel direction information.

In Chapter 5, the problem of designing channel quantization codebooks for MIMO broadcast channels with limited feedback has been addressed, in systems where joint linear beamforming and multiuser scheduling is performed. Rather than considering a framework with separate CQI and CDI feedback, as studied in Chapter 4, a simpler framework is considered in which

each user directly quantizes its channel vector or the prediction error. Codebook generation techniques have been proposed, based on matching the channel quantization codebooks to the channel statistics - exploiting temporal and spatial correlations - following a Monte-Carlo based approach. Our results have shown the performance gains that can be achieved when using quantization codebooks optimized according to the cell statistics.

The design of linear beamforming techniques has been addressed in Chapter 6. An iterative optimization method for unitary beamforming in MIMO broadcast channels has been proposed, based on successive optimization of Givens rotations. The proposed technique is shown to achieve linear sum-rate growth with the number of transmit antennas if perfect CSIT is available. In addition, it exhibits robustness to channel estimation errors, providing better sum rates than ZF beamforming and even MMSE beamforming as the variance of the estimation error increases. The proposed unitary beamforming approach has been evaluated in scenarios with multiuser scheduling and limited feedback. As our simulations show, it outperforms other existing techniques based on unitary beamforming and the same amount of feedback. A simple vector quantization technique has been used, based on random vector quantization with pruning. Our work highlights the importance of linear beamforming optimization in limited feedback scenarios. Rather than designing sophisticated feedback schemes and relying on simple linear beamforming techniques, the system performance can be improved by using simple (traditional) channel quantization strategies combined with optimized linear beamforming techniques robust to CSIT errors.

Throughout this dissertation, we have stressed the fact that joint optimization of different parts of MIMO wireless communication systems is needed in order to provide good performances, while keeping the amount of information on the feedback link low. In our designs, some aspects of interest in such communication systems have been optimized, targetting mostly realistic scenarios with practical number of users, reasonable number of transmit antennas and common average SNR conditions. Obtaining CSIT in current wireless systems is expensive, since the available resources on the uplink are limited. Thus, any source of CSIT, instantaneous or statistical, must be exploited at the transmitter side in order to enhance the system performance.

### Future Research

As a result of the work presented in this dissertation, we list in the following lines several areas that require further research and understanding.

The core of this dissertation has focused on sum-rate optimization in MIMO broadcast channels. In general, fairness issues have not been taken into account, being beyond the scope of the work here presented. Different fairness mechanisms could be incorporated, in order to provide good performances while satisfying certain QoS constraints. For instance, maximum delay tolerance for real-time applications could be considered.

Further investigation is required in MIMO broadcast channels with multi-antenna receivers. A simple way to extend the work presented in this thesis to multi-antenna receivers is to consider as effective channel the concatenation of the MIMO channel and a spatial linear receiver. However, we believe that simple approaches achieving better performance can be designed, not necessarily limiting the system to a single data stream per user. On the other hand, treating each receive antenna independently - as proposed by some authors in the literature - seems too simplistic. The challenge is to design feedback measures with a feedback rate that does not grow linearly with the number of receive antennas and that provides good performances. The solution to this problem could be along the lines of the estimated user capacity provided in Section 6.3.1.

Another important issue is to quantify the benefits provided by feedback in real cellular networks. While the proposed techniques can increase the data rates in the downlink, there is also an increase of complexity, and also feedback, control and training overhead in the system. Hence, it is of great importance to compare the performance gains and associated overhead in real systems.

Extensions of the multiuser MIMO downlink problem with limited feedback to wideband systems and multicell scenarios are also problems of timely relevance that require further research.

# Bibliography


[1] M. H. M. Costa, "Writing on dirty paper," *IEEE Trans. on Inform. Theory*, vol. 29, no. 3, pp. 439–441, May 1983.

[2] M. Sharif and B. Hassibi, "On the capacity of MIMO broadcast channel with partial side information," *IEEE Trans. on Inform. Theory*, vol. 51, no. 2, pp. 506–522, Feb. 2005.

[3] K. Huang, J. G. Andrews, and R. W. Heath, Jr., "Orthogonal beamforming for SDMA downlink with limited feedback," in *Proc. IEEE Int. Conf. Acoust., Speech and Sig. Proc. (ICASSP'07)*, Honolulu, HI, USA, Apr. 2007.

[4] G. J. Foschini and M. J. Gans, "On limits of wireless communication in fading environment when using multiple antennas," *Wireless Personal Communication*, vol. 6, pp. 311–335, Mar. 1998.

[5] I. E. Telatar, "Capacity of multi-antenna Gaussian channels," *Europ. Trans. on Telecom.*, vol. 10, pp. 585–595, Nov. 1999.

[6] L. Zheng and D. N. Tse, "Diversity and multiplexing: A fundamental tradeoff in multiple antenna channels," *IEEE Trans. on Inform. Theory*, vol. 49, no. 5, pp. 1073–1096, May 2003.

[7] S.M. Alamouti, "A simple transmit diversity technique for wireless communications," *IEEE J. Select. Areas Commun.*, vol. 16, pp. 1451–1458, Oct. 1998.

[8] V. Tarokh, H. Jafarkhami, and A. R. Calderbank, "Space-time block codes from orthogonal designs," *IEEE Trans. on Inform. Theory*, vol. 45, pp. 1456–1467, July 1999.

[9] J.-C. Belfiore, G. Rekaya, and E. Viterbo, "The Golden code: A 2x2 full-rate space-time code with non-vanishing determinants," in *Proc. of IEEE Int. Symp. Inform. Theory (ISIT'04)*, Chicago, Illinois, USA, June 2004.

[10] G. Caire and S. Shamai (Shitz), "On the achievable throughput of a multi-antenna Gaussian broadcast channel," *IEEE Trans. on Inform. Theory*, vol. 49, no. 7, pp. 1691–1706, July 2003.

[11] N. Jindal and A. Goldsmith, "Dirty paper coding vs. TDMA for MIMO broadcast channels," *IEEE Trans. on Inform. Theory*, vol. 51, no. 5, pp. 1783–1794, May 2005.

[12] H. Weigarten, Y. Steinberg, and S. Shamai, "Capacity region of the degraded MIMO broadcast channel," *IEEE Trans. on Inform. Theory*, vol. 52, no. 9, pp. 3936–3964, Sept. 2006.

[13] M. Sharif and B. Hassibi, "A comparison of time-sharing, DPC, and beamforming for MIMO broadcast channels with many users," *IEEE Trans. on Commun.*, vol. 55, no. 1, pp. 11–15, Jan. 2007.

[14] H. Viswanathan, S. Venkatesan, and H. Huang, "Downlink capacity evaluation of cellular networks with known-interference cancellation," *IEEE J. Select. Areas Commun.*, vol. 21, no. 5, pp. 802–811, June 2003.

[15] T. Yoo and A. Goldsmith, "On the optimality of multiantenna broadcast scheduling using zero-forcing beamforming," *IEEE J. Select. Areas Commun.*, vol. 24, no. 3, pp. 528–541, Mar. 2006.

[16] G. Dimić and N. D. Sidiropoulos, "On downlink beamforming with greedy user selection: performance analysis and a simple new algorithm," *IEEE Trans. on Signal Proc.*, vol. 53, no. 10, pp. 3857–3868, Oct. 2005.

[17] R. Knopp and P. Humblet, "Information capacity and power control in single cell multiuser communications," in *Proc. IEEE Int. Conf. on Communications (ICC'95)*, Seattle, June 1995, pp. 331–335.

[18] R. de Francisco and D. T. M. Slock, "Bayesian approaches for combining noisy mean and covariance channel information," in *Proc. IEEE Sig. Proc. Adv. on Wir. Commun. (SPAWC'05)*, New York, USA, June 2005.

[19] R. de Francisco and D. T. M. Slock, "Spatial transmit prefiltering for frequency-flat MIMO transmission with mean and covariance information," in *Proc. of 39th IEEE Asilomar Conf. on Signals, Systems, and Computers*, Pacific Grove, CA, USA, Nov. 2005.

[20] G. Jongren, M. Skoglund, and B. Ottersten, "Combining beamforming and orthogonal space-time block coding," *IEEE Trans. on Inform. Theory*, vol. 48, no. 3, pp. 611–627, Mar. 2002.

[21] R. de Francisco, M. Kountouris, D. T. M. Slock, and D. Gesbert, "Orthogonal linear beamforming in MIMO broadcast channels," in *Proc. IEEE Wireless Commun. and Networking Conf. (WCNC'07)*, Hong Kong, Mar. 2007.

[22] M. Kountouris, R. de Francisco, D. Gesbert, D. T. M. Slock, and T. Sälzer, "Low complexity scheduling and beamforming for multiuser MIMO systems," in *Proc. IEEE Sig. Proc. Adv. on Wir. Commun. (SPAWC'06)*, Cannes, France, July 2006.

[23] R. de Francisco and D. T. M. Slock, "A design framework for scalar feedback in MIMO broadcast channels," *EURASIP Journal on Aplied Signal Processing, Special Issue on MIMO Transmission with Limited Feedback*, vol. 2008, Article ID 574784, 12 pages, 2008.

[24] M. Kountouris, R. de Francisco, D. Gesbert, D. T. M. Slock, and T. Sälzer, "Exploiting multiuser diversity in MIMO broadcast channels with limited feedback," *submitted to IEEE Trans. Signal Proc.*

[25] R. de Francisco, D. T. M. Slock, and Y-C. Liang, "Balance of multiuser diversity and multiplexing gain in near-orthogonal MIMO systems with limited feedback," in *Proc. IEEE Wireless Commun. and Networking Conf. (WCNC'07)*, Hong Kong, Mar. 2007.

[26] M. Kountouris, R. de Francisco, D. Gesbert, D. T. M. Slock, and T. Sälzer, "Efficient metrics for scheduling in MIMO broadcast channels with limited feedback," in *Proc. IEEE Int. Conf. Acoust., Speech and Sig. Proc. (ICASSP'07)*, Honolulu, HI, USA, Apr. 2007.

[27] R. de Francisco and D. T. M. Slock, "On the design of scalar feedback techniques for MIMO broadcast scheduling," in *Proc. IEEE Sig. Proc. Adv. on Wir. Commun. (SPAWC'07)*, Helsinki, Finland, June 2007.

[28] T. Yoo, N. Jindal, and A. Goldsmith, "Finite-rate feedback MIMO broadcast channels with a large number of users," in *Proc. of IEEE Int. Symp. Inform. Theory (ISIT'06)*, Seattle, Washington, USA, July 2006, pp. 1214–1218.

[29] M. Kountouris, R. de Francisco, D. Gesbert, D. T. M. Slock, and T. Sälzer, "Multiuser diversity - multiplexing tradeoff in MIMO broadcast channels with limited feedback," in *Proc. of 40th IEEE Asilomar Conf. on Signals, Systems, and Computers*, Pacific Grove, CA, USA (invited paper), Oct. 2006.

[30] C. Simon, R. de Francisco, D. T. M. Slock, and G. Leus, "Feedback compression for correlated broadcast channels," in *Proc. IEEE Symp. on Commun. and Vehic. Tech. in the Benelux (SCVT'07)*, Delft, The Netherlands, Nov. 2007.

[31] R. de Francisco and D. T. M. Slock, "An optimized unitary beamforming technique for MIMO broadcast channels," *submitted to IEEE Trans. Wireless Commun.*

[32] R. de Francisco and D. T. M. Slock, "An iterative optimization method for unitary beamforming in MIMO broadcast channels," in *Proc. of 45th Allerton Conf. on Commun., Control and Comput.*, Monticello, IL, USA, Sept. 2007.

[33] R. de Francisco and D. T. M. Slock, "Linear precoding for MIMO transmission with partial CSIT," in *Proc. IEEE Sig. Proc. Adv. on Wir. Commun. (SPAWC'05)*, New York, USA, June 2005.

[34] R. de Francisco, D. T. M. Slock, D. Nussbaum, A. Kountouris, and F. Marx, "Adaptive complexity equalization for the downlink in WCDMA systems," in *Proc. IEEE Vehic. Tech. Conf. (VTC'06-Fall)*, Montreal, Canada, Sept. 2006.

[35] D. Gesbert, "Robust linear MIMO receivers: A minimum error-rate approach," *IEEE Trans. on Signal Proc.*, vol. 51, no. 11, pp. 2863–2871, Nov. 2003.

[36] C. Brunner, J. Hammerschmidt, and J. Nosek, "Downlink eigenbeamforming in WCDMA," in *Proc. European Wireless (EW'00)*, Dresden, Germany, Sept. 2000.

[37] H. Sampath and A. Paulraj, "Linear precoding for space-time coded systems with known fading correlations," *IEEE Commun. Letters*, vol. 6, no. 6, June 2002.

[38] S. A. Jafar and A. Goldsmith, "Transmitter optimization and optimality of beamforming for multiple antenna systems," *IEEE Trans. on Wireless Commun.*, vol. 3, no. 4, pp. 1165–1175, July 2004.

[39] M. Vu and A. Paulraj, "Optimal linear precoders for MIMO wireless correlated channels with nonzero mean in space-time coded systems," *IEEE Trans. on Signal Proc.*, vol. 54, no. 6, pp. 2318–2332, June 2006.

[40] A. Pascual-Iserte, M. Payaró, A. I. Pérez-Neira, and M. A. Lagunas, "Impact of a line-of-sight component on the performance of a MIMO system designed under statistical channel knowledge," in *Proc. IEEE Sig. Proc. Adv. on Wir. Commun. (SPAWC'06)*, Cannes, France, July 2006.

[41] A. Paulraj, R. Nabar, and D. Gore, *Introduction to Space-Time Wireless Communications*, Cambridge University Press, 2003.

[42] A. Medles and D. T. M. Slock, "Linear convolutive space-time precoding for spatial multiplexing MIMO systems," in *Proc. of 39th Allerton Conf. on Commun., Control and Comput.*, Monticello, IL, USA, Oct. 2001.

[43] H. Weingarten, Y. Steinberg, and S. Shamai (Shitz), "The capacity region of the Gaussian MIMO broadcast channel," in *Proc. 38th Conf. Inform. Sciences and Systems (CISS'04)*, Princeton, NJ, USA, Mar. 2004.

[44] Q. H. Spencer, A. L. Swindlehurst, and M. Haardt, "Zero-forcing methods for downlink spatial multiplexing in multiuser MIMO channels," *IEEE Trans. on Signal Proc.*, vol. 51, no. 2, pp. 506–522, Feb. 2005.

[45] A. Lapidoth and S. Shamai (Shitz), "Collapse of degrees of freedom in MIMO broadcast with finite precision CSI," in *Proc. of 43rd Allerton Conf. on Commun., Control and Comput.*, Monticello, Illinois, USA, Sept. 2005.

[46] S. A. Jafar and A. Goldsmith, "Isotropic fading vector broadcast channels: The scalar upper bound and loss in degrees of freedom," *IEEE Trans. on Inform. Theory*, vol. 51, no. 3, pp. 848–857, Mar. 2005.

[47] A. Narula, M. J. Lopez, M. D. Trott, and G. W. Wornell, "Efficient use of side information in multiple-antenna data transmission over fading channels," *IEEE J. Select. Areas Commun.*, vol. 16, no. 8, pp. 1423–1436, Oct. 1998.

[48] D. Love, R. W. Heath, Jr., and T. Strohmer, "Grassmannian beamforming for multiple-input multiple-output wireless systems," *IEEE Trans. on Inform. Theory*, vol. 49, no. 10, pp. 2735–2747, Oct. 2003.

[49] K. Mukkavilli, A. Sabharwal, E. Erkip, and B. Aazhang, "On beamforming with finite rate feedback in multiple-antenna systems," *IEEE Trans. on Inform. Theory*, vol. 49, no. 10, pp. 2562–2579, Oct. 2003.

[50] S. Zhou, Z. Wang, and G. B. Giannakis, "Quantifying the power loss when transmit beamforming relies on finite rate feedback," *IEEE Trans. on Wireless Commun.*, vol. 4, no. 4, pp. 1948–1957, July 2005.

[51] N. Jindal, "MIMO broadcast channels with finite-rate feedback," *IEEE Trans. on Inform. Theory*, vol. 52, no. 11, pp. 5045–5060, Nov. 2006.

[52] P. Ding, D. Love, and M. Zoltowski, "Multiple antenna broadcast channels with shape feedback and limited feedback," *IEEE Trans. on Signal Proc.*, vol. 55, no. 7, pp. 3417–3428, July 2007.

[53] K. Huang, J.G. Andrews, and R. W. Heath, Jr., "Orthogonal beamforming for SDMA downlink with limited feedback," in *Proc. IEEE Int. Conf. Acoust., Speech and Sig. Proc. (ICASSP'07)*, Honolulu, HI, USA, Apr. 2007.

[54] C. Swannack, G. Wornell, and E. Uysal-Biyikoglu, "MIMO broadcast scheduling with quantized channel state information," in *Proc. of IEEE Int. Symp. Inform. Theory (ISIT'06)*, Seattle, Washington, USA, July 2006, pp. 1788–1792.

[55] T.Yoo, N. Jindal, and A. Goldsmith, "Multi-antenna broadcast channels with limited feedback and user selection," *IEEE J. Select. Areas Commun.*, vol. 25, no. 7, pp. 1478–1491, Sept. 2007.

[56] M. Trivellato, F. Boccardi, and F. Tosato, "User selection schemes for MIMO broadcast channels with limited feedback," in *Proc. IEEE Vehic. Tech. Conf. (VTC'07-Spring)*, Dublin, Ireland, Apr. 2007.

[57] K. Huang, R. W. Heath, Jr., and J. G. Andrews, "Space division multiple access with a sum feedback rate constraint," in *Proc. IEEE Int. Conf. Acoust., Speech and Sig. Proc. (ICASSP'07)*, Hawaii, USA, Apr. 2007.

[58] T. Haustein, C. von Helmolt, E. Jorswieck, V. Jungnickel, and V. Pohl, "Performance of MIMO systems with channel inversion," in *Proc. IEEE Vehic. Tech. Conf. (VTC'07-Spring)*, Birmingham, AL, US, May 2002, vol. 1, pp. 35–39.

[59] C. B. Peel, B. M. Hochwald, and A. L. Swindlehurst, "A vector-perturbation technique for near-capacity multiantenna multiuser comunication - Part I," *IEEE Trans. on Commun.*, vol. 53, no. 1, pp. 195–202, Jan. 2005.

[60] N. Jindal, "Finite rate feedback MIMO broadcast channels," in *Workshop on Inform. Theory and its Applications (ITA'06)*, UC San Diego, USA (invited paper), Feb. 2006.

[61] G. H. Golub and C. F. van Loan, *Matrix Computations, 2nd edition*, The John Hopkins University Press, Baltimore, 1989.

[62] S. Verdú, "Spectral efficiency in the wideband regime," *IEEE Trans. on Inform. Theory*, vol. 48, no. 6, pp. 1319–1343, June 2002.

[63] P. Viswanath, D. N. Tse, and R. Laroia, "Opportunistic beamforming using dumb antennas," *IEEE Trans. on Inform. Theory*, vol. 48, pp. 1277–1294, June 2002.

[64] D. Samuelsson, M. Bengtsson, and B. Ottersten, "Improved multiuser diversity using smart antennas with limited feedback," in *Proc. Eur. Sig. Proc. Conf. (EUSIPCO'05)*, Antalya, Turkey, 2005.

[65] D. Gesbert, L. Pittman, and M. Kountouris, "Transmit correlation-aided scheduling in multiuser MIMO networks," in *Proc. IEEE Int. Conf. Acoust., Speech and Sig. Proc. (ICASSP'06)*, Toulouse, France, May 2006.

[66] S. Jafar, S. Viswanath, and A. Goldsmith, "Channel capacity and beamforming for multiple transmit and multiple receive antennas with covariance feedback," in *Proc. of IEEE Int. Conf. on Communications (ICC'01)*, Helsinki, Finland, June 2001.

[67] V. Hassel, M.-S. Alouini, D. Gesbert, and G. E. Øien, "A threshold-based channel state feedback algorithm for modern cellular systems," *IEEE Trans. on Wireless Commun.*, vol. 6, no. 7, pp. 2422–2426, July 2007.

[68] T. Yoo and A. Goldsmith, "Sum-rate optimal multi-antenna downlink beamforming strategy based on clique search," in *Proc. IEEE Global Tel. Conf. (GLOBECOM'05)*, St. Louis, MO, USA, Dec. 2005, pp. 1510–1514.

[69] J. C. Roh and B. D. Rao, "Transmit beamforming in multiple-antenna systems with finite rate feedback: A VQ-based approach," *IEEE Trans. on Inform. Theory*, vol. 52, no. 3, pp. 1101–1112, Mar. 2006.

[70] A. Papoulis and S. U. Pillai, *Probability, Random Variables, and Stochastic Processes, 4th Edition*, McGraw-Hill, Boston, 2002.

[71] H. A. David and H. N. Nagaraja, *Order Statistics, 3rd edition*, John Wiley and Sons, Inc, New York, 2003.

[72] D. J. Love, R. W. Heath, W. Santipach, and M. L. Honig, "What is the value of limited feedback for MIMO channels?," *IEEE Comm. Magazine*, vol. 42, no. 10, pp. 54–59, Oct. 2004.

[73] F. Floren, O. Edfors, and B-A. Molin, "The effect of feedback quantization on the throughput of a multiuser diversity scheme," in *Proc. IEEE Global Telec. Conf. (GLOBECOM'03)*, San Francisco, CA, USA, Dec. 2003, pp. 497–501.

[74] H. Bölcskei, D. Gesbert, C. B. Papadias, and A-J. van der Veen, Eds., *Space-Time Wireless Systems*, Cambridge University Press, 2006.

[75] W. Santipach and M. Honig, "Asymptotic capacity of beamforming with limited feedback," in *Proc. of IEEE Int. Symp. Inform. Theory (ISIT'04)*, Chicago, IL, USA, July 2004, p. 290.

[76] C. Oh and A. Yener, "Adaptive CDMA cell sectorization with linear multiuser detection," in *Proc. IEEE Vehic. Tech. Conf. (VTC'03 - Fall)*, Orlando, FL, USA, Oct. 2003.

[77] M. T. Ivrlac, R. L-U. Choi, R. D. Murch, and J. A. Nossek, "Effective use of long-term transmit channel state information in multi-user MIMO communication systems," in *Proc. IEEE Vehic. Tech. Conf. (VTC'03-Fall)*, Orlando, FL, USA, Oct. 2003, pp. 409–413.

[78] A. Gersho and V. Cuperman, "Vector quantization: A pattern-matching technique for speech coding," *IEEE Comm. Magazine*, vol. 21, no. 9, pp. 15–21, Dec. 1983.

[79] J. W. Wallace and M. A. Jensen, "Statistical characteristics of measured MIMO wireless channel data and comparison to conventional models," in *Proc. IEEE Vehic. Tech. Conf. (VTC'01-Fall)*, Atlantic City, NJ, USA, Oct. 2001, vol. 2, pp. 1078–1082.

[80] J. Fuhl, A.F. Molisch, and E. Bonek, "Unified channel model for mobile radio systems with smart antennas," *IEE Proc. Radar, Sonar and Navigation*, vol. 145, no. 1, pp. 32–41, 1998.

[81] V. Erceg et al., "TGn channel models," *IEEE 802.11-03/940r4*, May 2004.

[82] F. Kelly, "Charging and rate control for elastic traffic," *European Trans. on Telecommun.*, vol. 8, pp. 33–37, 1997.

[83] G. Leus and C. Simon, "Quantized feedback and feedback reduction for precoded spatial multiplexing MIMO systems," in *Proc. Int. Symp. on Signal Process. and its Applicat. (ISSPA'07)*, Feb. 2007.

[84] A. Gersho and R. M. Gray, *Vector Quantization and Signal Compressing*, Kluwer Academic Publishers, 1995.

[85] Y. Linde, A. Buzo, and R. M. Gray, "An algorithm for vector quantizer design," *IEEE Trans. on Commun.*, vol. 28, no. 1, pp. 84–95, Jan. 1980.

[86] M. J. Sabin and R. M. Gray, "Global convergence and empirical consistency of the generalized Lloyd algorithm," *IEEE Trans. on Inform. Theory*, vol. 32, no. 2, pp. 148–155, Mar. 1986.

[87] J. Makhoul, "Linear prediction: A tutorial review," *Proc. IEEE*, vol. 63, no. 4, pp. 561–580, Apr. 1975.

[88] William C. Jakes Jr., *Microwave Mobile Communications*, John Wiley and Sons, Inc, 1974.

[89] R1-051353 Samsung, "Downlink MIMO for EUTRA," in *3GPP TSG RAN WG1 Meeting 43*, Seoul, SK, Nov. 2005.

[90] R1-051353 Huawei, "Precoding and multiuser-MIMO," in *3GPP TSG RAN WG1 Meeting 44bis*, Athens, Greece, Mar. 2006.

[91] R1-063130 Ericsson, "System level comparison between MU- and SU-MIMO for downlink precoding systems with four transmit antennas," in *3GPP TSG RAN WG1 Meeting 47*, Riga, Latvia, Nov. 2006.

[92] M. Abramowitz and I. A. Stegun, *Handbook of Mathematical Functions with Formulas, Graphs, and Mathematical tables, 10th Edition*, Government Printing Office, New York, 1972.

[93] C. J. Small and J. Wang, *Numerical Methods for Nonlinear Estimating Equations, 1st Edition*, Oxford University Press, Oxford, 2003.